Antonio Barletta

Routes to Absolute Instability in Porous Media

Springer

Routes to Absolute Instability in Porous Media

Antonio Barletta

Routes to Absolute Instability in Porous Media

Springer

Antonio Barletta
Department of Industrial Engineering
Alma Mater Studiorum Università
di Bologna
Bologna, Italy

ISBN 978-3-030-06193-7 ISBN 978-3-030-06194-4 (eBook)
https://doi.org/10.1007/978-3-030-06194-4

Library of Congress Control Number: 2018964933

This Springer imprint is published by the registered company Springer Nature Switzerland AG
The registered company address is: Gewerbestrasse 11, 6330 Cham, Switzerland

What we cannot speak about we must pass over in silence.

Ludwig Wittgenstein

Foreword

Stability theory has an old and venerable history in the context of fluid mechanics: much is known and much remains to be discovered. In our desire to model accurately our highly nonlinear world, it is quite natural to begin slowly by determining first the flow field for small values of a parameter such as the Reynolds, Rayleigh, Taylor or Görtler numbers. In such cases, the flow is slow and nonlinear effects are barely felt. Perhaps it is unsurprising then that such flows are stable, not that we have yet defined this word. One potential definition of stability might be that the flow is unique, but this idea is unsatisfactory because it mentions neither the presence of nor the rôle played by disturbances of any kind. Consideration of these matters is central to stability theory and is essential before pressing on to fully numerical simulations and the transition to turbulence.

We all have an intuitive idea of what the words *stable* and *unstable* mean because they may be related to many aspects of human life and experience: nitroglycerine is unstable; a cyclist in motion is stable; a poorly constructed building is unstable; a person may be said to have a stable character. Each of these examples gives a hint as to what stability might mean in the context of fluid mechanics. A small disturbance of the form of an impact applied to nitroglycerine will cause it to explode. Even a poorly constructed building will collapse only when the magnitude of an earthquake exceeds a certain value. An experienced cyclist who has spent a lifetime successfully negotiating difficult terrain may be destabilised (i.e. floored) by the sudden but unwelcome presence of a squirrel in the wrong place. People with highly stable characters are able to manage to cope with the usual pressures of life, but when a large disturbance arises (I am thinking here of chronic job stresses, domestic issues, a bereavement, a mugging and so on), then a breakdown of some kind could follow and life changes subsequently. All four of these examples may be interpreted in terms of how the nature and the magnitude of the disturbances can alter forever the original state.

Returning to fluid mechanics, it is well known that some flows, which we may call basic states, will be destabilised by the presence of infinitesimally sized disturbances, and that the value of the governing parameter above which this happens may be minimised by the appropriate selection of the shape of the disturbance.

The analysis which determines the critical value of the parameter is termed a linear stability theory since the temporal growth of the disturbance satisfies a linear evolution equation at least initially. A growing small-amplitude disturbance will eventually saturate; the new flow will have a different appearance from that of the basic state, and it also has fewer symmetries. On the other hand, other basic states may resist small disturbances at a given value of the governing parameter but are nevertheless helpless to resist the effect of larger ones. This, then, is the realm of the energy stability analysis which may also be used to determine the critical parameter below which nonlinear flow does not exist. Weakly nonlinear theory may also be used to further the understanding of the full behind-the-scene behaviour of the system being studied, and this includes pattern selection and bifurcations.

These different types of analysis, followed by comprehensive nonlinear simulations of the governing equations, form the backbone of stability theory in general. They have been described in detail both in monographs and in a bewilderingly large number of journal papers over the last 100 years or so. This remains true even when one restricts attention to convection in porous media. The fact that different basic flows have a multitude of potentially different routes towards turbulence makes stability theory a very interesting, challenging and rewarding topic to study even if one does not consider its utility.

The present book is devoted to the concepts of absolute instability and convective instability, a topic which is very new in the field of porous medium convection. When a flow is absolutely unstable, a disturbance placed in one locality will continue to grow within that locality. This does not preclude it spreading or diffusing into formerly undisturbed regions as time passes. On the other hand, a convective instability will correspond to a disturbance which also grows in time, but where the background flow field is sufficiently strong that the disturbance will eventually decay within the region where it was introduced. In other words, the growing disturbance leaves the scene of the crime! The word, *convective*, when used in this way, refers to the carrying away of the disturbance, an idea which reflects the Latin etymology of the word. However, there is a potential confusion between the use of the term, *convective instability*, to describe such a moving instability mechanism and its use when talking about systems such as Bénard convection which is a buoyancy-induced instability. Generally, the context will be unambiguous, but the careful author might need to state something like the following in order to guarantee clarity: *the present thermoconvective instability is a convective instability as opposed to being an absolute instability.*

Professor Barletta has crafted a monograph which describes with great clarity how to determine whether an instability is absolute or convective. To do this, he has set the scene in the earlier chapters by introducing the reader to the Fourier and Laplace transforms and, in particular, to their role in the study of the evolution and movement of wave packets. These are illustrated using simplified systems of partial differential equations which display unstable behaviour of the kind which shows a transition between convective instability and absolute instability. Part II brings the reader an introduction to flows and convection in porous media, and a whole chapter is devoted to the porous medium analogue of the Rayleigh–Bénard

problem, often called the Darcy–Bénard problem or the Horton–Rogers–Lapwood problem. Then, in Part III, the Prats variant of the Darcy–Bénard problem is considered where an externally applied pressure gradient drives a horizontal basic flow. This is analysed in detail using all the theoretical concepts developed earlier, and the transition from convective to absolute instability is studied. The analysis is also extended to the equivalent vertical layer with sidewall heating and with fixed pressure profiles at the surfaces. The final chapter and two appendices complete the work, and these describe ancillary matters.

The present book fills an important gap in the market because it has been written specifically to introduce the reader to the relatively recent topic of convective and absolute instabilities but within the context of convection in porous media where these ideas are unknown to all but a select few.

Finally, I would like to say a few words about the author. I count him as a very good friend indeed and occasional confidante. Antonio and I have collaborated in the publication of many journal and conference papers in the last 10 years, and I look forward to very many more. The present book represents, in a way, a distillation of an alternative life of his, one that I do not know and have not been part of, where he has collaborated with others, and I have thoroughly enjoyed reading it from end to end. I now know much more about the angst that the writing of a book can induce, but this experience has not destabilised him! Rather, the book displays well his clear thinking, erudite style and teaching ability. I have learned some new tricks, and I hope that very many others do the same.

Bath, UK
October 2018

D. Andrew S. Rees
University of Bath

Preface

It is an impression of this author that there is a disproportion between the plethora of studies regarding the convective instability in porous media and those where the analysis is pushed forward to investigate the transition to absolute instability. The possible reason is that this concept is hardly recognised among the shared knowledge within the porous media community. This is the main motivation behind this book. In fact, this book is aimed to provide all the information necessary for approaching an analysis of absolute instability for applications to flow and heat transfer in fluid-saturated porous media.

This book is for those who study convection heat transfer at a graduate level and have a specific interest for porous media applications. Another possible target is those who are familiar with the topic of mechanical instability and aim to enter the research topic of fluid mechanics and heat transfer in porous media. In both cases, this book is meant to be a pedagogical guide that can be employed in a class on thermal instability in porous media, or even as a self-learning tool.

All the mathematics needed to understand the topics of convective and absolute instabilities is provided in Part I of this book. Chapters 2 and 3 provide a self-contained introduction to the basic mathematical methods employed for the assessment of instability in flow systems, namely the Fourier transform and calculus with complex variables. Chapter 4 introduces the concept of instability in a mechanical system with a finite number of degrees of freedom extending this concept to a continuous system whose evolution is described by a partial differential equation. This chapter provides formal definitions of convective and absolute instabilities.

An introduction to the essential elements of fluid mechanics and convection heat transfer is provided in Part II, where Chap. 5 contains the description of the mathematical model of fluid flow, Chap. 6 discusses the basic ideas behind the theory of fluid mechanics in porous media, while Chap. 7 contains a discussion of the thermal instability through the classical case study of the Rayleigh–Bénard problem and its variants. Among them, the applications to saturated porous media are investigated, starting from the Horton–Rogers–Lapwood problem.

Part III has its focus on the transition from convective to absolute instability in porous media. Chapter 8 contains a discussion of Prats problem including a variant formulation where the effects of the form-drag effect are taken into account. In Chap. 9, cases where the analysis of convective and absolute instabilities is approached numerically are presented. Finally, Chap. 10 offers a detailed description of a numerical method for the solution of stability eigenvalue problems for the convective or the absolute instability.

What is not present in this book is the nonlinear approach to instability. This choice has been made to keep the mathematical difficulties at their lowest and because the linear approach is in itself sufficiently wide and diversified as to provide a very large amount of information. More than aiming for completeness in the presentation of convective and absolute instabilities, it has been chosen to follow the pedagogical way: discuss less, but be as detailed and comprehensible as you can be.

Bologna, Italy
October 2018

Antonio Barletta

Acknowledgements

I am very grateful to Leonardo Alves and Najib Ouarzazi for having introduced me to the importance of the analysis of absolute instability and its potential applications in the area of porous media. Many interesting and fruitful discussions with them were so important to focus the appropriate mathematical formalism for the presentation of this topic. Many thanks go also to Don Nield. I had the honour to collaborate with him in many papers. His experience and advice have been an invaluable help. So many other colleagues shared my research path during the years. I thank all of them as they gave me new perspectives, viewpoints and ideas that enriched my work.

Special thanks go to Andrew Rees, as I first started my work on instability in porous media by collaborating with him. His deep competence and mathematical rigour always guide my research. Andrew Rees offered me many insightful suggestions on reading the manuscript. His invaluable help in the final revision of the chapters has been of paramount importance. I am and always will be deeply indebted to him.

Contents

Chapter 1
Introduction

There exist several industrial and environmental applications where heat transfer and fluid flow in porous media happen to be of paramount importance. Such applications span civil engineering with all that regards insulation materials in buildings and their permeability to air and water vapour. Quite important is also the investigation of groundwater flow in rocks and sands, and the study of geothermal reservoirs where underground heating conditions occur.

In his pioneering study on the Rayleigh–Bénard instability of a boundary layer in a porous medium, Wooding [12] had in mind the geothermal region of Wairakei, in the North Island of New Zealand, where groundwater is driven by an upward convective force due to the high underground temperature. In his classical paper, Wooding cites a previous paper by Lapwood [5] regarding the onset of convection cells in a horizontal porous layer. Lapwood meant to extend the classical study by Rayleigh [7] on the instability in a horizontal fluid layer with a vertical, downward-oriented, temperature gradient to the case where the fluid saturates a porous medium. Even though disregarded in Lapwood's paper, there is a previously published study by Horton and Rogers Jr [3] that discusses the same topic of thermal instability induced by heating from below in a horizontal porous layer. This is the reason why it is nowadays a common stance calling Horton–Rogers–Lapwood problem, the mathematical formulation of the thermal instability phenomenon caused by a vertical temperature gradient in a horizontal porous layer. An alternative name is Darcy–Bénard problem which acknowledges both the well-known experiments regarding convection cells in a fluid by Henri Claude Bénard [4] and the classical law of momentum transfer in a fluid-saturated porous medium formulated by Henry Philibert Gaspard Darcy [1].

The Rayleigh–Bénard instability is activated by a vertical temperature gradient causing the fluid to be heated from below and cooled from above. Such a condition promotes a buoyancy drift of the hotter fluid to the upper region and a downward drift of the cooler fluid. This circumstance results in the emergence of structures called convection cells. The observational fact is that no convection cells are produced when the driving temperature gradient is not sufficiently intense or, in other terms, if the temperature difference across the fluid region is not sufficiently large. The minimal conditions leading to the formation of convection cells can be predicted theoretically,

A. Barletta, *Routes to Absolute Instability in Porous Media*,
https://doi.org/10.1007/978-3-030-06194-4_1

and, generally speaking, they can be formulated so that a dimensionless parameter, the Rayleigh number, exceeds a critical value. Such a critical value depends on the environment surrounding the fluid layer or the fluid-saturated porous layer. In mathematical terms, it depends on the boundary conditions constraining the fluid flow and heat transfer.

The model generally followed to assess the onset conditions of convection cells is one of the stability analyses, carried out on the partial differential equations governing the phenomenon of convection. In a stability analysis, we devise a basic state prior to the emergence of the cells. In the Horton–Rogers–Lapwood problem, this basic state is a situation where the fluid is at rest and a temperature gap across the fluid region creates an externally impressed thermal forcing. Seeking the critical conditions for the emergence of convection cells means, in this framework, establishing the neutral stability condition or the transition from linear stability to convective instability. In fact, the approach widespread across the literature is based on a presumption of small-amplitude perturbations acting on the basic state. Under this scheme, the partial differential equations governing the dynamics of the perturbations and the heat transfer process are linearised by neglecting terms of order higher than the first in the perturbation amplitude.

Most stability analyses available in the literature, regarding the Horton–Rogers–Lapwood problem, are relative to linear perturbations. However, there are many adopting a nonlinear approach where the assumption of small perturbations is relaxed. An important investigation scheme in the nonlinear domain is based on the so-called energy method. For a discussion of this method, we refer the reader to the excellent books by Straughan [9, 10]. For a widespread analysis of convective instability in porous media, authoritative reviews can be found in Nield and Bejan [6] and Rees [8].

Within this framework, one may question about the role of this book. In fact, there are many treatises and reviews regarding the onset of linear instability, and hence of convection cells, in a porous layer. However, all of them are focussed on the concept of convective instability happening when the value of the Rayleigh number exceeds its critical threshold. If this focus is the central one in many cases where the transition to instability has a linear nature, this is not so in general. Even in a purely linear approach, the threshold to convective instability involves the dynamics of pure Fourier modes with given wave numbers. However, the naturally emerging perturbations are not necessarily Fourier modes, but they can be thought of as superposition of Fourier modes, or wave packets. The linear dynamics of wave packets is peculiar as, even if the superposition includes unstable Fourier modes, the wave packet may well display a stable behaviour at large times, meaning that its amplitude is ultimately damped in time. This mathematical concept is hard to grasp with purely heuristic arguments, but its impact is of uttermost importance. It means that, even if the critical value of the Rayleigh number for the onset of the convective instability is exceeded, a wave packet perturbation may still display a stable behaviour. This automatically brings us to the quest of an upper parametric threshold in the supercritical domain where all wave packet perturbations are unstable. Such a threshold marks the transition to the absolute instability.

The terminology, absolute instability, the concept and its applications are well settled in the area of fluid dynamics. They started with studies regarding plasma physics in the 1950s as reported, for instance, by Swanson [11]. Very soon, the idea of absolute instability was extended to the fluid mechanics of internal flows and boundary layers. Finally, studies of absolute instability appeared within the area of convection in porous media. Among the earliest studies of absolute instability in porous media, it must be mentioned the paper by Dufour and Néel [2]. Many others followed, but not as many as the importance of this topic would deserve.

Notation

We will denote by $\mathbb{R}$ the set of real numbers, by $\mathbb{C}$ the set of complex numbers, by $\mathbb{Z}$ the set of integer numbers, by $\mathbb{N}$ the set of natural numbers and by $\mathbb{N}_0$ the set of natural numbers including zero. The imaginary unit is $\mathrm{i} = \sqrt{-1}$, while the real and imaginary parts of a complex number z are denoted by $\Re(z)$ and $\Im(z)$. The complex conjugate of z is denoted by $\bar{z}$.

The partial derivatives will be denoted by the standard notation, $\partial/\partial x$ or $\partial/\partial t$. The ordinary derivatives of a function f will be denoted either by, say, $\mathrm{d}f/\mathrm{d}x$ or by a prime, f'. Higher-order ordinary derivatives of f will be also written as f'', f''', f'''' and $f^{(n)}$, where $n \geqslant 5$ is the order of the derivative.

References

1. Bear J (1988) Dynamics of fluids in porous media. Dover, New York
2. Dufour F, Néel MC (1998) Numerical study of instability in a horizontal porous channel with bottom heating and forced horizontal flow. Phys Fluids 10:2198–2207
3. Horton CW, Rogers FT Jr (1945) Convection currents in a porous medium. J Appl Phys 16:367–370
4. Koschmieder EL (1993) Bénard cells and Taylor vortices. Cambridge University Press, Cambridge
5. Lapwood ER (1948) Convection of a fluid in a porous medium. Math Proc Camb Philos Soc 44:508–521
6. Nield DA, Bejan A (2017) Convection in porous media, 5th edn. Springer, New York
7. Rayleigh L (1916) On convection currents in a horizontal layer of fluid, when the higher temperature is on the under side. Lond Edinb Dublin Philos Mag J Sci 32:529–546
8. Rees DAS (2000) The stability of Darcy-Bénard convection. In: Vafai K (ed) Handbook of porous media, vol 1. Marcel Dekker, New York, pp 521–588
9. Straughan B (2004) The energy method, stability, and nonlinear convection. Springer, New York
10. Straughan B (2008) Stability and wave motion in porous media. Springer, New York
11. Swanson DG (2003) Plasma waves. CRC Press, Boca Raton
12. Wooding RA (1960) Rayleigh instability of a thermal boundary layer in flow through a porous medium. J Fluid Mech 9:183–192

Part I
Mathematical Models of Flow Instability

The basic mathematical tools behind the concepts of convective and absolute instability in flow systems are introduced. These include the method of Fourier transform and the dynamics of wave packets. Such tools will be introduced here from scratch. The application of Fourier transform to the analysis of the linear behaviour of perturbations acting on an intrinsically nonlinear flow system is analysed by considering specific mathematical models. Despite their scarce utility in the description of real-world applications, these mathematical models have the great advantage of being simple. As such, they are excellent arenas within which to start one's practice in the study of convective and absolute instability.

Chapter 2
Fourier Transform and Wave Packets

2.1 Integral Transforms

In several different conditions encountered in engineering and in physics, one may find it useful to define the *integral transform* of a given function $f(t)$, namely

$$\tilde{f}(k) = \int_a^b f(t)\, K(t,k)\, \mathrm{d}\, t, \tag{2.1}$$

where $K(t,k)$ expresses the *kernel* of the integral transform. Typically, different integral transforms correspond to different choices of the kernel function $K(t,k)$ and of the integration interval (a,b). The purpose in defining an integral transform is to set a rule for linking a function of "time", $f(t)$, to a transformed function, $\tilde{f}(k)$, of the independent variable, k. This independent variable can be physically interpreted either as the "frequency" or the "wave number". On the other hand, depending on the type of transform and on its applications, t can be either intended as time or as a spatial Cartesian coordinate. In this case, it is replaced by x.

Examples of integral transforms are:

- the Fourier transform,

$$K(t,k) = \frac{\mathrm{e}^{-\mathrm{i}\,kt}}{\sqrt{2\pi}}\,, \quad (a,b) = (-\infty,\infty)\,, \quad k \in \mathbb{R}\,;$$

- the Laplace transform,

$$K(t,k) = \mathrm{e}^{-kt}\,, \quad (a,b) = (0,\infty)\,, \quad k \in \mathbb{C}\,;$$

- the Hankel, or Fourier–Bessel, transform,

$$K(t,k) = t\, J_n(kt)\,, \quad (a,b) = (0,\infty)\,, \quad k \in \mathbb{R}\,,$$

A. Barletta, *Routes to Absolute Instability in Porous Media*,
https://doi.org/10.1007/978-3-030-06194-4_2

where J_n denotes the Bessel function of first kind and order $n \in \mathbb{N}_0$;
- the Mellin transform,

$$K(t,k) = t^{k-1} \ , \quad (a,b) = (0,\infty) \ , \quad k \in \mathbb{R} \ .$$

In the following, we will focus on the Fourier transform as it is definitely the most important within the stability analysis of flow systems.

2.2 The Fourier Transform

The aim of this section is not providing an exhaustive and mathematically rigorous survey of the Fourier transform and its properties. In fact, there exist several monographs devoted to the study of integral transforms, more or less mathematically oriented [1–3, 6].

2.2.1 Definition

Hereafter, we will choose to define and study the Fourier transform of functions of x, intended as a coordinate. Thus, we interpret k as a wave number along the x-direction. This choice, which at this stage is just a matter of notation, will turn out to be appropriate for the stability analysis applications.

Given a function $f(x)$, the *Fourier transform* is defined as

$$\mathfrak{F}\{f(x)\}(k) = \tilde{f}(k) = \frac{1}{\sqrt{2\pi}} \int_{-\infty}^{\infty} f(x)\, \mathrm{e}^{-\mathrm{i}kx}\, \mathrm{d}x \ . \tag{2.2}$$

The conditions for this transform to be well defined are:

- $f(x)$ is piecewise continuously differentiable;
- $f(x)$ is absolutely integrable on $\mathbb{R}$, namely

$$\int_{-\infty}^{\infty} |f(x)|\, \mathrm{d}x < \infty \ . \tag{2.3}$$

2.2.2 Inversion of the Fourier Transform

The possibility to determine function $f(x)$, if one knows its Fourier transform $\tilde{f}(k)$, arises from *Fourier's integral formula*,

$$f(x) = \frac{1}{2\pi} \int_{-\infty}^{\infty} \left[\int_{-\infty}^{\infty} f(s)\, \mathrm{e}^{-\mathrm{i}ks}\, \mathrm{d}\, s \right] \mathrm{e}^{\mathrm{i}kx}\, \mathrm{d}\, k \ . \tag{2.4}$$

If x represents a finite discontinuity of $f(x)$, then Eq. (2.4) must be modified as follows:

$$\frac{1}{2}\left[f(x+0) + f(x-0)\right] = \frac{1}{2\pi} \int_{-\infty}^{\infty} \left[\int_{-\infty}^{\infty} f(s)\, \mathrm{e}^{-\mathrm{i}ks}\, \mathrm{d}\, s \right] \mathrm{e}^{\mathrm{i}kx}\, \mathrm{d}\, k \ , \tag{2.5}$$

where $x + 0$ and $x - 0$ indicate the limits where x is approached from the right and from the left. From Eqs. (2.2) and (2.4), one may obtain the so-called inversion of the Fourier transform

$$f(x) = \mathfrak{F}^{-1}\{\tilde{f}(k)\}(x) = \frac{1}{\sqrt{2\pi}} \int_{-\infty}^{\infty} \tilde{f}(k)\, \mathrm{e}^{\mathrm{i}kx}\, \mathrm{d}\, k \ . \tag{2.6}$$

Equation (2.6) is the *inversion formula of the Fourier transform*. We note that the conditions for the existence of the Fourier transform pose some strong restrictions on the function $f(x)$. These restrictions can be relaxed if one goes beyond the usual concept of function and introduces the *generalised functions* or *distributions*. A rigorous theory of distributions was first introduced by Laurent Schwartz (1915–2002). This French mathematician was awarded in 1950 with the Fields medal for his work on the theory of distributions. We will not describe the details of this mathematical topic here, and we refer the reader to the book by Schwartz [5].

The most important distribution is *Dirac's delta function*, $\delta(x - x_0)$. Dirac's delta function is such that $\delta(x - x_0) = 0$ for every $x \neq x_0$, and it is defined through the relationship

$$\int_{-\infty}^{\infty} \varphi(x)\, \delta(x - x_0)\, dx = \varphi(x_0) \ , \tag{2.7}$$

where $\varphi(x)$ is any test function picked up from a properly defined functional space. Without any attempt to be rigorous, we merely mention that a typical choice is the space of the smooth functions on $(-\infty, \infty)$ with a compact support, i.e. functions that vanish outside a bounded open interval in $\mathbb{R}$ [5]. The typical role of Dirac's delta function in the mathematical models of physical systems is for expressing the density of a point-like object. Such a quantity is the result of a limit where it gets an infinite value at a point, x_0, and it is zero everywhere else.

If we evaluate the Fourier transform of Dirac's delta function through Eq. (2.2), and we employ Eq. (2.7), then we obtain

$$f(x) = \delta(x - x_0) \ ,$$
$$\tilde{f}(k) = \frac{1}{\sqrt{2\pi}} \int_{-\infty}^{\infty} \delta(x - x_0)\, \mathrm{e}^{-\mathrm{i}\,kx}\, \mathrm{d}\,x = \frac{\mathrm{e}^{-\mathrm{i}\,kx_0}}{\sqrt{2\pi}} \ . \tag{2.8}$$

Conversely, one may note that the Fourier transform of function

$$f(x) = \mathrm{e}^{\mathrm{i}\,ax} \ , \tag{2.9}$$

where a is a constant, is given by

$$\tilde{f}(k) = \sqrt{2\pi}\, \delta(k - a) \ . \tag{2.10}$$

This result is easily proved by employing the inversion formula of Fourier transform, Eqs. (2.6), and (2.7). Obviously, function $f(x)$ defined by Eq. (2.9) is not absolutely integrable on $\mathbb{R}$, that is, it does not satisfy Eq. (2.3). In fact, its Fourier transform exists only in the extended sense of the theory of distributions.

2.2.3 *Some Properties of the Fourier Transform*

The Fourier transform has several important properties. Most of them are straightforward consequences of its definition (2.2). A list of some properties of the Fourier transform is the following:

- *Linearity*

$$\mathfrak{F}\{a\, f(x) + b\, g(x)\}(k) = a\, \tilde{f}(k) + b\, \tilde{g}(k) \ , \quad \forall a, b \in \mathbb{R} \ . \tag{2.11}$$

- *Scaling*

$$\mathfrak{F}\{f(ax)\}(k) = \frac{1}{|a|}\, \tilde{f}\left(\frac{k}{a}\right), \quad \forall a \in \mathbb{R} \ , \quad a \neq 0 \ . \tag{2.12}$$

- *Shifting*

$$\mathfrak{F}\{f(x - x_0)\}(k) = \mathrm{e}^{-\mathrm{i}\,kx_0}\, \tilde{f}(k), \quad \forall x_0 \in \mathbb{R} \ . \tag{2.13}$$

- *Translation*

$$\mathfrak{F}\{\mathrm{e}^{\mathrm{i}\,k_0 x} f(x)\}(k) = \tilde{f}(k - k_0), \quad \forall k_0 \in \mathbb{R} \ . \tag{2.14}$$

- *Derivative*

$$\mathfrak{F}\{f'(x)\}(k) = \mathrm{i}\,k\, \tilde{f}(k) \ , \tag{2.15}$$

$$\mathfrak{F}\{f^{(n)}(x)\}(k) = (\mathrm{i}\,k)^n\, \tilde{f}(k) \ , \quad \forall n \in \mathbb{N} \ . \tag{2.16}$$

- *Partial derivative*

$$\mathfrak{F}\left\{\frac{\partial}{\partial x} f(x,t)\right\}(k) = \mathrm{i}\,k\,\tilde{f}(k,t)\ , \quad \mathfrak{F}\left\{\frac{\partial}{\partial t} f(x,t)\right\}(k) = \frac{\partial}{\partial t}\tilde{f}(k,t)\ , \tag{2.17}$$

$$\mathfrak{F}\left\{\frac{\partial^m}{\partial x^m}\frac{\partial^n}{\partial t^n} f(x,t)\right\}(k) = (\mathrm{i}\,k)^m\,\frac{\partial^n}{\partial t^n}\tilde{f}(k,t)\ , \quad \forall m,n \in \mathbb{N}_0\ , \tag{2.18}$$

  where, conventionally, $\partial^0/\partial x^0 = 1$ and $\partial^0/\partial t^0 = 1$.
- *Convolution*
  The convolution of two functions $f(x)$ and $g(x)$ is defined as

$$f(x)*g(x) = \frac{1}{\sqrt{2\pi}}\int_{-\infty}^{\infty} f(x-\hat{x})g(\hat{x})\,\mathrm{d}\,\hat{x}\ . \tag{2.19}$$

  Hence, another important property of the Fourier transform is the following:

$$\mathfrak{F}\{f(x)*g(x)\}(k) = \tilde{f}(k)\ \tilde{g}(k)\ . \tag{2.20}$$

  We mention that the convolution between two functions has the usual properties of a product, namely

$$\begin{aligned} &\text{commutative :} && f*g = g*f\ ; \\ &\text{associative :} && f*(g*h) = (f*g)*h\ ; \\ &\text{distributive :} && f*(g+h) = f*g + f*h\ . \end{aligned} \tag{2.21}$$

  Dirac's delta function plays the role of the neutral element for the convolution,

$$f*\delta = \delta*f = f\ . \tag{2.22}$$

2.2.4 Solution of the One-Dimensional Wave Equation

We aim to solve the partial differential equation

$$\frac{\partial^2\psi(x,t)}{\partial t^2} = c^2\,\frac{\partial^2\psi(x,t)}{\partial x^2}\ , \tag{2.23}$$

for $x \in (-\infty,\infty)$ and $t \in [0,\infty)$ with the initial conditions

$$\psi(x,0) = f(x), \quad \left.\frac{\partial\psi(x,t)}{\partial t}\right|_{t=0} = c\,g'(x)\ . \tag{2.24}$$

Here, $f(x)$ and $g(x)$ are functions known a priori, while c is the *phase velocity* of the wave, k is the *wave number*, and $\omega = ck$ is the *angular frequency*. We apply the Fourier transform operator to both sides of the wave equation and we employ Eq. (2.18), so that we obtain

$$\frac{\partial^2 \tilde{\psi}(k,t)}{\partial t^2} + c^2 k^2 \tilde{\psi}(k,t) = 0 \; . \tag{2.25}$$

By the same method, the initial conditions can be rewritten as

$$\tilde{\psi}(k,0) = \tilde{f}(k), \quad \left.\frac{\partial \tilde{\psi}(k,t)}{\partial t}\right|_{t=0} = \mathrm{i}\, ck\, \tilde{g}(k) \; . \tag{2.26}$$

Therefore, we have just to solve an ordinary differential problem where t is the independent variable and k is a parameter. The general solution of Eq. (2.25) is

$$\tilde{\psi}(k,t) = \tilde{a}(k)\, \mathrm{e}^{\mathrm{i}\, ckt} + \tilde{b}(k)\, \mathrm{e}^{-\mathrm{i}\, ckt} \; . \tag{2.27}$$

The integration constants $\tilde{a}(k)$ and $\tilde{b}(k)$ can be determined from the initial conditions, namely

$$\tilde{a}(k) + \tilde{b}(k) = \tilde{f}(k) \; , \quad \tilde{a}(k) - \tilde{b}(k) = \tilde{g}(k) \; , \tag{2.28}$$

so that we obtain

$$\tilde{a}(k) = \frac{1}{2}\left[\tilde{f}(k) + \tilde{g}(k)\right] \; , \quad \tilde{b}(k) = \frac{1}{2}\left[\tilde{f}(k) - \tilde{g}(k)\right] \; . \tag{2.29}$$

Hence, the Fourier transform of our solution is given by

$$\tilde{\psi}(k,t) = \frac{1}{2}\, \tilde{f}(k) \left(\mathrm{e}^{\mathrm{i}\, ckt} + \mathrm{e}^{-\mathrm{i}\, ckt}\right) + \frac{1}{2}\, \tilde{g}(k) \left(\mathrm{e}^{\mathrm{i}\, ckt} - \mathrm{e}^{-\mathrm{i}\, ckt}\right) \; . \tag{2.30}$$

On account of the shifting property, Eq. (2.13), we have

$$\mathfrak{F}^{-1}\left\{\tilde{f}(k)\, \mathrm{e}^{\mathrm{i}\, ckt}\right\} = f(x+ct), \quad \mathfrak{F}^{-1}\left\{\tilde{f}(k)\, \mathrm{e}^{-\mathrm{i}\, ckt}\right\} = f(x-ct) \; , \tag{2.31}$$

$$\mathfrak{F}^{-1}\left\{\tilde{g}(k)\, \mathrm{e}^{\mathrm{i}\, ckt}\right\} = g(x+ct), \quad \mathfrak{F}^{-1}\left\{\tilde{g}(k)\, \mathrm{e}^{-\mathrm{i}\, ckt}\right\} = g(x-ct) \; . \tag{2.32}$$

The solution of our problem is

$$\psi(x,t) = \frac{1}{2}\left[f(x+ct) + f(x-ct)\right] + \frac{1}{2}\left[g(x+ct) - g(x-ct)\right] \; . \tag{2.33}$$

It is easily verified that, if we introduce $G(x) = g'(x)$, then we have

$$\psi(x,t) = \frac{1}{2}\left[f(x+ct) + f(x-ct)\right] + \frac{1}{2}\int_{x-ct}^{x+ct} G(s)\,\mathrm{d}s \ . \tag{2.34}$$

2.2.5 Solution of the One-Dimensional Diffusion Equation

Let us now solve the partial differential equation,

$$\frac{\partial\psi(x,t)}{\partial t} = \alpha\,\frac{\partial^2\psi(x,t)}{\partial x^2} \ , \tag{2.35}$$

for $x \in (-\infty, \infty)$ and $t \in [0, \infty)$ with the initial condition

$$\psi(x,0) = f(x) \ . \tag{2.36}$$

Here, α is the diffusion coefficient, or the thermal diffusivity in the case of the heat conduction equation for a solid.

On applying the Fourier transform operator to both sides of the diffusion equation and employing Eqs. (2.17) and (2.18), we obtain

$$\frac{\partial\tilde{\psi}(k,t)}{\partial t} + \alpha k^2\tilde{\psi}(k,t) = 0 \ . \tag{2.37}$$

The initial condition can be rewritten as

$$\tilde{\psi}(k,0) = \tilde{f}(k) \ . \tag{2.38}$$

Again, we have to solve an ordinary differential problem where t is the independent variable and k is a parameter. The general solution is

$$\tilde{\psi}(k,t) = \tilde{a}(k)\,\mathrm{e}^{-\alpha k^2 t} \ . \tag{2.39}$$

The integration constant $\tilde{a}(k)$ is easily determined from the initial condition, namely

$$\tilde{a}(k) = \tilde{f}(k) \ . \tag{2.40}$$

Therefore, the Fourier transform of our solution is given by

$$\tilde{\psi}(k,t) = \tilde{f}(k)\,\mathrm{e}^{-\alpha k^2 t} \ . \tag{2.41}$$

If we denote $\mathrm{e}^{-\alpha k^2 t}$ as $\tilde{g}(k,t)$, then we may write

$$\tilde{\psi}(k,t) = \tilde{f}(k)\,\tilde{g}(k,t)\ , \tag{2.42}$$

and invoke the convolution property, Eq. (2.20), for expressing the solution as

$$\psi(x,t) = \frac{1}{\sqrt{2\pi}} \int_{-\infty}^{\infty} f(\hat{x}) g(x-\hat{x},t)\,\mathrm{d}\,\hat{x}\ . \tag{2.43}$$

We have just to evaluate the inverse Fourier transform of $\tilde{g}(k)$ by employing Eq. (2.6),

$$g(x,t) = \mathfrak{F}^{-1}\{\mathrm{e}^{-\alpha k^2 t}\}(x) = \frac{1}{\sqrt{2\pi}} \int_{-\infty}^{\infty} \mathrm{e}^{-\alpha k^2 t + \mathrm{i}\,kx}\,\mathrm{d}\,k\ . \tag{2.44}$$

The integral can be evaluated as follows:

$$\begin{aligned} -\alpha k^2 t + \mathrm{i}\,kx &= -\left(k\sqrt{\alpha t} - \frac{\mathrm{i}\,x}{2\sqrt{\alpha t}}\right)^2 - \frac{x^2}{4\alpha t}\ , \\ w = k\sqrt{\alpha t} - \frac{\mathrm{i}\,x}{2\alpha\sqrt{t}}\ ,\quad \mathrm{d}\,w &= \sqrt{\alpha t}\,\mathrm{d}\,k\ ,\quad \mathrm{d}\,k = \frac{\mathrm{d}\,w}{\sqrt{\alpha t}}\ , \\ g(x,t) = \frac{\mathrm{e}^{-x^2/(4\alpha t)}}{\sqrt{2\pi\alpha t}} \int_{-\infty}^{\infty} \mathrm{e}^{-w^2}\,\mathrm{d}\,w &= \frac{\mathrm{e}^{-x^2/(4\alpha t)}}{\sqrt{2\pi\alpha t}}\,\sqrt{\pi} = \frac{\mathrm{e}^{-x^2/(4\alpha t)}}{\sqrt{2\alpha t}}\ . \end{aligned} \tag{2.45}$$

To conclude, the solution can be expressed as

$$\psi(x,t) = \frac{1}{2\sqrt{\pi\alpha t}} \int_{-\infty}^{\infty} f(\hat{x})\,\mathrm{e}^{-(x-\hat{x})^2/(4\alpha t)}\,\mathrm{d}\,\hat{x}\ . \tag{2.46}$$

Equation (2.46) allows one to infer that, when the initial condition (2.38) involves a point-like source at $x = 0$,

$$\psi(x,0) = f(x) = \delta(x)\ , \tag{2.47}$$

Equations (2.43) and (2.45) yield

$$\psi(x,t) = \frac{g(x,t)}{\sqrt{2\pi}} = \frac{\mathrm{e}^{-x^2/(4\alpha t)}}{2\sqrt{\pi\alpha t}}\ . \tag{2.48}$$

This means that the initial point-like distribution gradually spreads over the real axis with Gaussian trend as time t increases. In fact, Eqs. (2.47) and (2.48) suggest one of the many limit formula that lead to Dirac's delta, namely

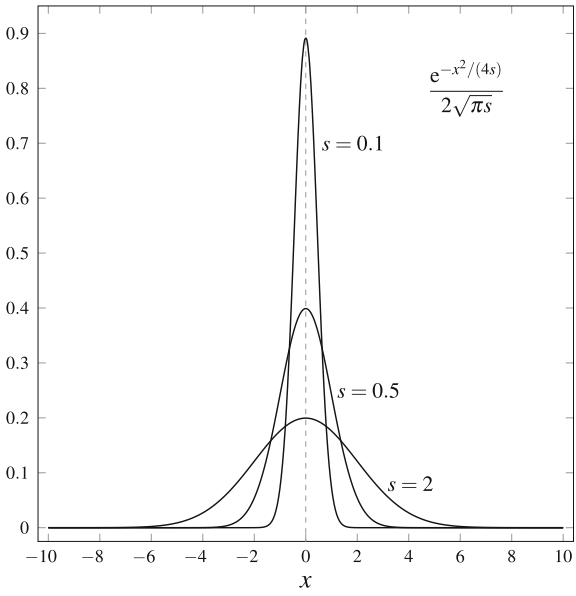

Fig. 2.1 Illustration of the limit in Eq. (2.49)

$$\lim_{s\to 0^+} \frac{e^{-x^2/(4s)}}{2\sqrt{\pi s}} = \delta(x) \; . \tag{2.49}$$

A sketch of how the Gaussian function becomes more and more peaked as $s \to 0^+$ resembling more and more a distribution with point-like support and infinite strength, viz. Dirac's delta function, is shown in Fig. 2.1.

2.2.6 *Solution of the One-Dimensional Advection–Diffusion Equation*

The advection–diffusion equation is an extension of the diffusion equation discussed in Sect. 2.2.5,

$$\frac{\partial \psi(x,t)}{\partial t} + U_0 \frac{\partial \psi(x,t)}{\partial x} = \alpha \frac{\partial^2 \psi(x,t)}{\partial x^2} \; , \tag{2.50}$$

for $x \in (-\infty, \infty)$ and $t \in [0, \infty)$ with the initial condition

$$\psi(x,0) = f(x) \; . \tag{2.51}$$

The constant U_0 defines an imposed flow that drives the diffusion along the x-axis.

By evaluating the Fourier transform of both sides of the advection equation and by using Eqs. (2.17) and (2.18), we get

$$\frac{\partial \tilde{\psi}(k,t)}{\partial t} + (\alpha k^2 + \mathrm{i}\, k U_0)\, \tilde{\psi}(k,t) = 0 \,. \tag{2.52}$$

The initial condition (2.51) yields

$$\tilde{\psi}(k,0) = \tilde{f}(k) \,. \tag{2.53}$$

Equations (2.52) and (2.53) define an ordinary differential problem where t is the independent variable and k is a parameter. The general solution is

$$\tilde{\psi}(k,t) = \tilde{a}(k)\, \mathrm{e}^{-(\alpha k^2 + \mathrm{i}\, k U_0)t} \,. \tag{2.54}$$

The integration constant $\tilde{a}(k)$ is evaluated from the initial condition, namely

$$\tilde{a}(k) = \tilde{f}(k) \,. \tag{2.55}$$

The Fourier transform of $\psi(x,t)$ is expressed as

$$\tilde{\psi}(k,t) = \tilde{f}(k)\, \mathrm{e}^{-(\alpha k^2 + \mathrm{i}\, k U_0)t} \,. \tag{2.56}$$

On writing $\mathrm{e}^{-(\alpha k^2 + \mathrm{i}\, k U_0)t}$ as $\tilde{g}(k,t)$, then we obtain

$$\tilde{\psi}(k,t) = \tilde{f}(k)\, \tilde{g}(k,t) \,. \tag{2.57}$$

We now employ the convolution property, Eq. (2.20), and express $\psi(x,t)$ as

$$\psi(x,t) = \frac{1}{\sqrt{2\pi}} \int_{-\infty}^{\infty} f(\hat{x}) g(x - \hat{x}, t)\, \mathrm{d}\, \hat{x} \,. \tag{2.58}$$

We evaluate the inverse Fourier transform of $\tilde{g}(k,t)$ by employing Eq. (2.6),

$$g(x,t) = \mathfrak{F}^{-1}\{\mathrm{e}^{-(\alpha k^2 + \mathrm{i}\, k U_0)t}\}(x) = \frac{1}{\sqrt{2\pi}} \int_{-\infty}^{\infty} \mathrm{e}^{-\alpha k^2 t + \mathrm{i}\, k(x - U_0 t)}\, \mathrm{d}\, k \,. \tag{2.59}$$

The evaluation of the integral in Eq. (2.59) yields

$$\begin{gathered} -\alpha k^2 t + \mathrm{i}\, k(x - U_0 t) = -\left[k\sqrt{\alpha t} - \frac{\mathrm{i}\,(x - U_0 t)}{2\sqrt{\alpha t}}\right]^2 - \frac{(x - U_0 t)^2}{4\alpha t} \,, \\ w = k\sqrt{\alpha t} - \frac{\mathrm{i}\,(x - U_0 t)}{2\alpha\sqrt{t}} \,, \quad \mathrm{d}\, w = \sqrt{\alpha t}\, \mathrm{d}\, k \,, \quad \mathrm{d}\, k = \frac{\mathrm{d}\, w}{\sqrt{\alpha t}} \,, \\ g(x,t) = \frac{\mathrm{e}^{-(x - U_0 t)^2/(4\alpha t)}}{\sqrt{2\pi\alpha t}} \int_{-\infty}^{\infty} \mathrm{e}^{-w^2}\, \mathrm{d}\, w = \frac{\mathrm{e}^{-(x - U_0 t)^2/(4\alpha t)}}{\sqrt{2\alpha t}} \,. \end{gathered} \tag{2.60}$$

The final expression of $\psi(x,t)$ can be written as

$$\psi(x,t) = \frac{1}{2\sqrt{\pi\alpha t}} \int_{-\infty}^{\infty} f(\hat{x})\, \mathrm{e}^{-(x-\hat{x}-U_0 t)^2/(4\alpha t)}\, \mathrm{d}\,\hat{x}\ . \tag{2.61}$$

With a reasoning similar to that presented in Sect. 2.2.5, Eq. (2.61) implies that, when the initial condition (2.51) describes a point-like source at $x = 0$,

$$f(x) = \delta(x)\ , \tag{2.62}$$

Equations (2.43) and (2.60) lead to

$$\psi(x,t) = \frac{g(x,t)}{\sqrt{2\pi}} = \frac{\mathrm{e}^{-(x-U_0 t)^2/(4\alpha t)}}{2\sqrt{\pi\alpha t}}\ . \tag{2.63}$$

Equation (2.63) describes a situation where the initial condition, given by a point-like distribution at $x = 0$, gradually spreads over the real axis as time t increases, while the maximum of this Gaussian signal travels along the x-direction with constant velocity U_0.

2.2.7 *Solution of the One-Dimensional Schrödinger Equation*

The Schrödinger equation for the one-dimensional quantum evolution of a free particle reads [4],

$$\mathrm{i}\,\hbar\,\frac{\partial\psi(x,t)}{\partial t} = \mathsf{H}\,\psi(x,t)\ , \tag{2.64}$$

where $\hbar = 1.05457 \times 10^{-34}$ J s is the reduced Planck's constant, $\psi(x,t)$ is the wave function of the particle, and H is the Hamiltonian operator. For a one-dimensional free particle, H is given by

$$\mathsf{H} = -\frac{\hbar^2}{2m}\frac{\partial^2}{\partial x^2}\ , \tag{2.65}$$

where m is the particle mass. Thus, Eq. (2.64) can be rewritten as

$$\frac{\partial\psi(x,t)}{\partial t} = \frac{\mathrm{i}\,\hbar}{2m}\frac{\partial^2\psi(x,t)}{\partial x^2}\ . \tag{2.66}$$

Mathematically speaking, Eq. (2.66) is nothing but a diffusion equation (2.35) with an imaginary diffusion coefficient,

$$\alpha = \frac{\mathrm{i}\,\hbar}{2m}. \tag{2.67}$$

This information is what is strictly needed to deduce from Eq. (2.46) the evolution formula, at a given time t, of an initial wave function $\psi(x, 0) = f(x)$, namely

$$\psi(x,t) = \sqrt{\frac{m}{2\pi \mathrm{i}\,\hbar t}} \int_{-\infty}^{\infty} f(\hat{x})\, \mathrm{e}^{\mathrm{i}\, m\,(x-\hat{x})^2/(2\hbar t)}\, \mathrm{d}\,\hat{x}\ . \tag{2.68}$$

2.3 Plane Waves and Wave Packets

In general, we will call *plane wave* a function defined as

$$\psi(x,t) = A\, \mathrm{e}^{\mathrm{i}\,(kx-\omega t)}\ . \tag{2.69}$$

Here, A is the *amplitude* of the wave, while k and ω are the wave number and the angular frequency, respectively. With A, k and ω considered as constants, plane waves are typical solutions of the wave equation (2.23), provided that

$$\omega = \pm\, ck\ . \tag{2.70}$$

This is a special case, as c is a characteristic positive constant of governing equation (2.23) and, hence, it is independent of k or, equivalently, $\omega = \pm\, ck$ just means that ω depends linearly on k. Such a situation defines a *non-dispersive wave* propagation. On the other hand, *dispersive waves* occur when ω is a function of k and $\mathrm{d}^2\omega/\mathrm{d}\,k^2$ is not identically zero. We also mention that A is not, in general, a constant as it can be time-dependent.

A linear combination of several plane waves yields a *wave packet*, namely

$$\psi(x,t) = \sum_k B(k,t)\, \mathrm{e}^{\mathrm{i}\,[kx-\omega(k)\,t]}\ , \tag{2.71}$$

where $B(k, t)$ is the product of the coefficients of the linear combination and the amplitude of each plane wave. An alternative name for the plane waves is *normal modes*.[1]

Hence, a wave packet is often devised as a superposition of several normal modes. Such a superposition may involve a continuously varying k over a given real interval or, possibly, over all real axis. In that case, the sum in Eq. (2.71) is rather an integral over all real values of k. For the continuum limit to be mathematically coherent, $B(k, t)$ becomes infinitesimal, namely $B(k, t) = b(k, t)\,\mathrm{d}\,k$, so that Eq. (2.71) is rewritten as

[1] It should be noted that a superposition of plane waves as described by Eq. (2.71) needs a time-independent $B(k, t)$ to provide a solution of the wave equation (2.23). On the other hand, other partial differential equations allow the possibility that $B(k, t)$ actually depends on time.

$$\psi(x,t) = \int_{-\infty}^{\infty} b(k,t)\, \mathrm{e}^{\mathrm{i}\,[kx-\omega(k)\,t]}\, \mathrm{d}\,k\ . \tag{2.72}$$

By comparing Eq. (2.6) with Eq. (2.72), one can immediately recognise that the Fourier transform of $\psi(x,t)$ is given by

$$\tilde{\psi}(k,t) = \sqrt{2\pi}\, b(k,t)\, \mathrm{e}^{-\mathrm{i}\,\omega(k)\,t}\ . \tag{2.73}$$

On the basis of Eq. (2.73), every function $\psi(x,t)$ that admits a Fourier transform can be considered as a wave packet.

The main features of wave packets are illustrated in the following Sects. 2.3.1 and 2.3.2. This discussion follows that presented by [4] in Chap. 2 of his book, on illustrating the wave–particle duality of quantum mechanics. Such a method applies well beyond the domain of quantum theory and is extremely illuminating for general wave phenomena.

2.3.1 *Stationary Waves in x-Space and k-Space*

Stationary wave packets are given by Eq. (2.72) when $\omega(k) = 0$ and $b(k,t)$ is time-independent, namely

$$\psi_{\mathrm{s}}(x) = \int_{-\infty}^{\infty} b_{\mathrm{s}}(k)\, \mathrm{e}^{\mathrm{i}\,kx}\, \mathrm{d}\,k\ . \tag{2.74}$$

Equation (2.74) defines $\psi_{\mathrm{s}}(x)$ as a linear superposition of infinite standing plane waves with wavelength $\lambda = 2\pi/k$. This means that, say, two neighbouring maxima of the real and imaginary parts of $\mathrm{e}^{\mathrm{i}\,kx}$ are separated by a distance $2\pi/k$. Each stationary wave, $\mathrm{e}^{\mathrm{i}\,kx}$, is weighted by the coefficient function $b_{\mathrm{s}}(k)$.
One may consider a Gaussian weight function

$$b_{\mathrm{s}}(k) = \mathrm{e}^{-\gamma(k-k_0)^2}\ , \tag{2.75}$$

where $\gamma > 0$ is a constant parameter. One can substitute Eq. (2.75) into (2.74) and evaluate the integral on the right-hand side of Eq. (2.74),

$$\begin{aligned}\psi_{\mathrm{s}}(x) = \int_{-\infty}^{\infty} \mathrm{e}^{-\gamma(k-k_0)^2}\, \mathrm{e}^{\mathrm{i}\,kx}\, \mathrm{d}\,k = \mathrm{e}^{\mathrm{i}\,k_0 x} \int_{-\infty}^{\infty} \mathrm{e}^{-\gamma\kappa^2}\, \mathrm{e}^{\mathrm{i}\,\kappa x}\, \mathrm{d}\kappa \\ = \mathrm{e}^{\mathrm{i}\,k_0 x} \sqrt{\frac{\pi}{\gamma}}\, \mathrm{e}^{-x^2/(4\gamma)}\ .\end{aligned} \tag{2.76}$$

Here, the change of variable $\kappa = k - k_0$ has been done. On considering the square modulus of $b_{\rm s}(k)$ and the square modulus of $\psi_{\rm s}(x)$,

$$|b_{\rm s}(k)|^2 = {\rm e}^{-2\gamma(k-k_0)^2}, \qquad |\psi_{\rm s}(x)|^2 = \frac{\pi}{\gamma}\,{\rm e}^{-x^2/(2\gamma)}\,, \tag{2.77}$$

one realises that we have a Gaussian signal both in k-space and in x-space. We may easily check that, when $k = k_0 \pm \Delta k/2$, where $\Delta k = 2/\sqrt{2\gamma}$, the Gaussian signal in k-space drops to ${\rm e}^{-1}$ times its peak value. When $x = \pm\Delta x/2$, where $\Delta x = 2\sqrt{2\gamma}$, the Gaussian signal in x-space drops to ${\rm e}^{-1}$ times its peak value (a qualitative sketch is given in Fig. 2.2). If γ becomes smaller and smaller, the signal in k-space increases its width Δk, while the signal in x-space decreases its width Δx. One may easily check that

$$\Delta k\ \Delta x = 4\,. \tag{2.78}$$

The precise numerical value of the product is not important. What is important is that the product $\Delta k\ \Delta x$ is finite and independent of γ. A highly localised Gaussian

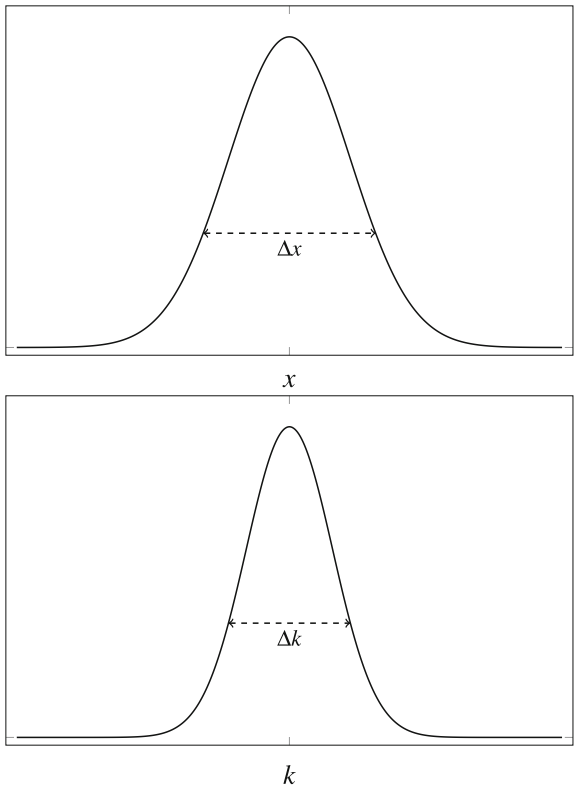

Fig. 2.2 Gaussian signals in x-space and in k-space

distribution in k-space, i.e. one with a small Δk, means a poorly localised Gaussian distribution in x-space, i.e. one with a large Δx, and vice versa.

It is not possible to reduce the width of the Gaussian signal both in k-space and in x-space. This feature is a statement of the Heisenberg *uncertainty principle* relative to general wave phenomena [4].

2.3.2 Travelling Wave Packets

Let us now consider a non-stationary wave packet given by Eq. (2.72). The simplest case is that of non-dispersive waves, with $\omega = ck$, where c is a constant. In this case, Eq. (2.72) describes a superposition of plane waves having a constant phase velocity c. Then, a comparison between Eqs. (2.72) and (2.74), allows one to write

$$\psi(x, t) = \psi_s(x - ct) \ . \tag{2.79}$$

The effect of the standing waves being replaced by travelling waves is just a rigid translational motion of the wave packet with a velocity c. No distortion of the wave packet is caused by the time evolution. This is the typical behaviour of the solutions of Eq. (2.23) as it can be inferred from Eq. (2.33).

With dispersive waves, ω is not simply proportional to k. We are, therefore, interested in assuming a general relationship $\omega = \omega(k)$, where $\omega(k)/k$ is not a constant. We assume a wave packet strongly localised in k-space, with $b(k, t) = b_s(k)$ given by Eq. (2.75) and a marked peak at $k = k_0$, namely a *quasi-monochromatic* wave packet. This means that γ in Eq. (2.75) is assumed to have a large value.

The strong localisation in k-space suggests that one may express $\omega(k)$ as a Taylor expansion around $k = k_0$ truncated to second order,

$$\omega(k) \approx \omega(k_0) + \left.\frac{\mathrm{d}\,\omega}{\mathrm{d}\,k}\right|_{k=k_0} (k - k_0) + \frac{1}{2} \left.\frac{\mathrm{d}^2\omega}{\mathrm{d}\,k^2}\right|_{k=k_0} (k - k_0)^2 \ . \tag{2.80}$$

We use the notations

$$\omega_0 = \omega(k_0) \ , \qquad c_g = \left.\frac{\mathrm{d}\,\omega}{\mathrm{d}\,k}\right|_{k=k_0} \ , \qquad \sigma = \frac{1}{2} \left.\frac{\mathrm{d}^2\omega}{\mathrm{d}\,k^2}\right|_{k=k_0} \ , \tag{2.81}$$

where c_g is called the *group velocity*.

We now substitute Eqs. (2.75), (2.80) and (2.81) in Eq. (2.72) and we obtain

$$\begin{aligned}\psi(x,t) &= \int_{-\infty}^{\infty} \mathrm{e}^{-\gamma(k-k_0)^2}\mathrm{e}^{\mathrm{i}\{kx-[\omega_0+(k-k_0)c_\mathrm{g}+(k-k_0)^2\sigma]t\}}\,\mathrm{d}\,k \\ &= \int_{-\infty}^{\infty} \mathrm{e}^{-\gamma\kappa^2}\mathrm{e}^{\mathrm{i}\{(k_0+\kappa)x-[\omega_0+\kappa c_\mathrm{g}+\kappa^2\sigma]t\}}\,\mathrm{d}\kappa \\ &= \mathrm{e}^{\mathrm{i}(k_0x-\omega_0t)}\int_{-\infty}^{\infty} \mathrm{e}^{-(\gamma+\mathrm{i}\,\sigma t)\kappa^2}\mathrm{e}^{\mathrm{i}\,\kappa\left(x-c_\mathrm{g}t\right)}\,\mathrm{d}\kappa \\ &= \mathrm{e}^{\mathrm{i}(k_0x-\omega_0t)}\int_{-\infty}^{\infty} \mathrm{e}^{-\gamma^*\kappa^2}\mathrm{e}^{\mathrm{i}\,\kappa x^*}\,\mathrm{d}\kappa\,,\end{aligned} \tag{2.82}$$

where $\gamma^* = \gamma + \mathrm{i}\,\sigma t$ and $x^* = x - c_\mathrm{g}t$. We note that the integral appearing in Eq. (2.82) is just the same as that evaluated in Eq. (2.76), with γ replaced by γ^* and x replaced by x^*. Thus, we may write

$$\begin{aligned}\psi(x,t) &= \mathrm{e}^{\mathrm{i}(k_0x-\omega_0t)}\int_{-\infty}^{\infty} \mathrm{e}^{-\gamma^*\kappa^2}\mathrm{e}^{\mathrm{i}\,\kappa x^*}\,\mathrm{d}\kappa \\ &= \mathrm{e}^{\mathrm{i}(k_0x-\omega_0t)}\sqrt{\frac{\pi}{\gamma+i\sigma t}}\,\exp\left[-\frac{\left(x-c_\mathrm{g}t\right)^2}{4\left(\gamma+i\sigma t\right)}\right]\,.\end{aligned} \tag{2.83}$$

Again, we consider the square moduli of $b(k,t)$ and of $\psi(x,t)$ as in Eq. (2.77),

$$\begin{aligned}|b(k,t)|^2 &= \mathrm{e}^{-2\gamma(k-k_0)^2}\,, \\ |\psi(x,t)|^2 &= \frac{\pi}{\sqrt{\gamma^2+\sigma^2t^2}}\,\exp\left[-\frac{\gamma\left(x-c_\mathrm{g}t\right)^2}{2\left(\gamma^2+\sigma^2t^2\right)}\right]\,.\end{aligned} \tag{2.84}$$

One recognises Gaussian signals both in k-space and in x-space. The peak of the Gaussian signal in x-space is located at $x = c_\mathrm{g}t$, and thus, it travels in the x-direction with the constant group velocity, c_g.

The width of the Gaussian signal in k-space is still defined as in Sect. 2.3.1 and it is given by $\Delta k = 2/\sqrt{2\gamma}$. The width of the Gaussian signal in x-space, also defined as in Sect. 2.3.1, is now a function of time,

$$\Delta x = 2\sqrt{2\gamma}\,\sqrt{1+\frac{\sigma^2t^2}{\gamma^2}}\,. \tag{2.85}$$

Equation (2.85) shows that the width of the Gaussian signal in x-space increases in time. This means that the time evolution of the wave packet implies a spreading in x-space with a decreasing value at the peak position, $x = c_\mathrm{g}t$. The latter feature can be easily inferred from Eq. (2.84), and it is qualitatively sketched in Fig. 2.3.

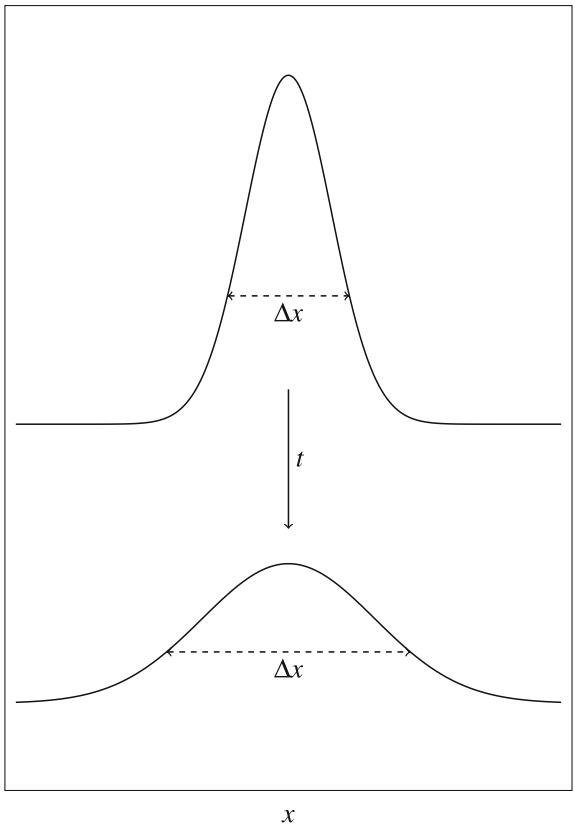

Fig. 2.3 Spreading of the Gaussian wave packet in x-space

2.4 Three-Dimensional Fourier Transform and Wave Packets

Up to this point, we have discussed cases where the symmetries existing in the physical system are such that the solution of the governing equation depends on just one Cartesian coordinate, x. In the general case, with a $f(\mathbf{x})$ where $\mathbf{x} = (x, y, z)$ is the *position vector*, we can define the *three-dimensional Fourier transform*, namely

$$\begin{aligned} \mathfrak{F}_3\{f(x, y, z)\}(k_x, k_y, k_z) &= \tilde{f}(k_x, k_y, k_z) \\ &= \frac{1}{(2\pi)^{3/2}} \int_{-\infty}^{\infty} \int_{-\infty}^{\infty} \int_{-\infty}^{\infty} f(x, y, z)\, \mathrm{e}^{-\mathrm{i}(k_x x + k_y y + k_z z)}\, \mathrm{d}\, x\, \mathrm{d}\, y\, \mathrm{d}\, z\ . \end{aligned} \tag{2.86}$$

Such definition extends Eq. (2.2). In Eq. (2.86), $\mathbf{k} = (k_x, k_y, k_z)$ is the *wave vector*. The wave number, k, is given by the modulus of vector $\mathbf{k}$, namely

$$k = |\mathbf{k}| = \sqrt{k_x^2 + k_y^2 + k_z^2} \, . \tag{2.87}$$

The inversion formula of Fourier transform, Eq. (2.6), can be extended to the three-dimensional case,

$$\begin{aligned} &\mathfrak{F}_3^{-1}\{\tilde{f}(k_x, k_y, k_z)\}(x, y, z) = f(x, y, z) \\ &= \frac{1}{(2\pi)^{3/2}} \int_{-\infty}^{\infty} \int_{-\infty}^{\infty} \int_{-\infty}^{\infty} \tilde{f}(k_x, k_y, k_z) \, \mathrm{e}^{\mathrm{i}(k_x x + k_y y + k_z z)} \, \mathrm{d}\, k_x \, \mathrm{d}\, k_y \, \mathrm{d}\, k_z \, . \end{aligned} \tag{2.88}$$

The main properties of the three-dimensional Fourier transform are quite similar to those reviewed in Sect. 2.2.3. In particular the transform of derivatives now reads

$$\begin{aligned} \mathfrak{F}_3\{\nabla f\} &= \mathrm{i}\, \mathbf{k}\, \tilde{f}(\mathbf{k}) \, , \\ \mathfrak{F}_3\{\nabla^2 f\} &= -k^2 \, \tilde{f}(\mathbf{k}) \, . \end{aligned} \tag{2.89}$$

The definition of three-dimensional transform is really useful when the physical domain is the whole real space $\mathbb{R}^3$. If, on the contrary, one or two coordinates have a limited range of variation, it is more appropriate to transform only the functional dependence on the unbounded coordinate or coordinates. For instance, if both $y \in [0, a]$ and $z \in [0, b]$, while $x \in \mathbb{R}$, one finds more useful a one-dimensional Fourier transform given by

$$\mathfrak{F}\{f(x, y, z)\}(k, y, z) = \tilde{f}(k, y, z) = \frac{1}{\sqrt{2\pi}} \int_{-\infty}^{\infty} f(x, y, z) \, \mathrm{e}^{-\mathrm{i}\, k x} \, \mathrm{d}\, x \, . \tag{2.90}$$

If $z \in [0, b]$, while $(x, y) \in \mathbb{R}^2$, one should rather employ a *two-dimensional Fourier transform*, given by

$$\begin{aligned} &\mathfrak{F}_2\{f(x, y, z)\}(k_x, k_y, z) = \tilde{f}(k_x, k_y, z) \\ &= \frac{1}{2\pi} \int_{-\infty}^{\infty} \int_{-\infty}^{\infty} f(x, y, z) \, \mathrm{e}^{-\mathrm{i}(k_x x + k_y y)} \, \mathrm{d}\, x \, \mathrm{d}\, y \, . \end{aligned} \tag{2.91}$$

In Eq. (2.91), the wave vector is just two-dimensional, $\mathbf{k} = (k_x, k_y)$. The inversion formula for $\mathfrak{F}_2$ reads

$$\begin{aligned} &\mathfrak{F}_2^{-1}\{\tilde{f}(k_x, k_y, z)\}(x, y, z) = f(x, y, z) \\ &= \frac{1}{2\pi} \int_{-\infty}^{\infty} \int_{-\infty}^{\infty} \tilde{f}(k_x, k_y, z) \, \mathrm{e}^{\mathrm{i}(k_x x + k_y y)} \, \mathrm{d}\, k_x \, \mathrm{d}\, k_y \, . \end{aligned} \tag{2.92}$$

A variant of Eq. (2.90) is appropriate for cylindrical systems where the polar coordinates (r, ϕ) are employed instead of (y, z). For instance, one may have $r \in [r_1, r_2]$ and $\phi \in [0, 2\pi]$ in the case of a cylindrical layer. In these cases, Eq. (2.90) is rather written as

$$\mathfrak{F}\{f(x, r, \phi)\}(k, r, \phi) = \tilde{f}(k, r, \phi) = \frac{1}{\sqrt{2\pi}} \int_{-\infty}^{\infty} f(x, r, \phi)\, \mathrm{e}^{-\mathrm{i}\, kx}\, \mathrm{d}\, x \ . \tag{2.93}$$

The three-dimensional wave equation is given by

$$\frac{\partial^2 \psi(\mathbf{x}, t)}{\partial t^2} = c^2\, \nabla^2 \psi(\mathbf{x}, t) \ . \tag{2.94}$$

Simple solutions of Eq. (2.94) are the plane waves,

$$\psi(\mathbf{x}, t) = A\, \mathrm{e}^{\mathrm{i}\, (\mathbf{k}\cdot\mathbf{x} - \omega t)} \ . \tag{2.95}$$

In fact, $\psi(\mathbf{x}, t)$ given by Eq. (2.95) is a solution of Eq. (2.94) provided that A is a constant and Eq. (2.70) is satisfied with $k = |\mathbf{k}|$. More general, dispersive, plane waves entail a function $\omega(\mathbf{k})$ not necessarily given by a linear function of k. Thus, a three-dimensional wave packet built by the superposition of plane waves with all possible wave vectors, $\mathbf{k} \in \mathbb{R}^3$, is expressed as

$$\psi(\mathbf{x}, t) = \int_{-\infty}^{\infty} \int_{-\infty}^{\infty} \int_{-\infty}^{\infty} b(\mathbf{k}, t)\, \mathrm{e}^{\mathrm{i}\, [\mathbf{k}\cdot\mathbf{x} - \omega(\mathbf{k})\, t]}\, \mathrm{d}\, k_x\, \mathrm{d}\, k_y\, \mathrm{d}\, k_z \ , \tag{2.96}$$

which is an extended form of Eq. (2.72). Comparison with Eq. (2.88) suggests that function $b(\mathbf{k}, t)$ is directly related to the Fourier transform of $\psi(\mathbf{x}, t)$, namely

$$b(\mathbf{k}, t) = \frac{1}{(2\pi)^{3/2}}\, \tilde{\psi}(\mathbf{k}, t)\, \mathrm{e}^{\mathrm{i}\, \omega(\mathbf{k})\, t} \ . \tag{2.97}$$

In three dimensions, there is much more that can be done in terms of wave packets. For instance, one can create a superposition of those plane waves whose wave vector is directed, say, along the x-axis, namely $\mathbf{k} = (k, 0, 0)$. In this case, one has

$$\psi(\mathbf{x}, t) = \int_{-\infty}^{\infty} b(k, y, z, t)\, \mathrm{e}^{\mathrm{i}\, [kx - \omega(k)\, t]}\, \mathrm{d}\, k \ . \tag{2.98}$$

Another possibility is that the linear combination of plane waves involves just those waves having a wave vector lying on the (x, y) plane, $\mathbf{k} = (k_x, k_y, 0)$, namely

$$\psi(\mathbf{x},t)=\int_{-\infty}^{\infty}\int_{-\infty}^{\infty}b(k_x,k_y,z,t)\,\mathrm{e}^{\mathrm{i}\,[k_x x+k_y y-\omega(\mathbf{k})\,t]}\,\mathrm{d}\,k_x\,\mathrm{d}\,k_y\ , \tag{2.99}$$

Clearly, Eqs. (2.98) and (2.99) are to be compared with the partial Fourier transforms in one and two dimensions as defined in Eqs. (2.90) and (2.91).

Other possibilities are allowed in three dimensions, for wave propagation, that expand the limited class of plane waves. For instance, a point-like source may generate spherical waves, invariant under general rotations around the origin. Such waves are solutions of the spherically symmetric wave equation, i.e. a special case of Eq. (2.94),

$$\frac{\partial^2\psi(r,t)}{\partial t^2}=\frac{c^2}{r^2}\,\frac{\partial}{\partial r}\left[r^2\,\frac{\partial\psi(r,t)}{\partial r}\right]\ , \tag{2.100}$$

where $r=|\mathbf{x}|$ is the spherical radial coordinate. Spherical normal modes are given by

$$\psi(r,t)=A\,\frac{\mathrm{e}^{\mathrm{i}(kr-\omega t)}}{r}\ , \tag{2.101}$$

and they solve Eq. (2.100) provided that $\omega=\pm kc$ and A is a constant. As for plane waves, given by Eqs. (2.69), (2.101) with a constant amplitude A defines the case of non-dispersive waves. Other partial differential equations might involve dispersive spherical waves, where A is time-dependent and ω is a nonlinear function of k. Wave packets can be built up from the superposition of these more general, dispersive, spherical waves, so that we can write the analogous of Eqs. (2.71) and (2.72),

$$\psi(r,t)=\frac{1}{r}\sum_k B(k,t)\,\mathrm{e}^{\mathrm{i}\,[kr-\omega(k)\,t]}\ , \tag{2.102}$$

and

$$\psi(r,t)=\frac{1}{r}\int_{-\infty}^{\infty}b(k,t)\,\mathrm{e}^{\mathrm{i}\,[kr-\omega(k)\,t]}\,\mathrm{d}\,k\ , \tag{2.103}$$

respectively, where Eq. (2.103) is relative to a case where k spans continuously the whole real axis.

References

1. Cotta RM (1993) Integral transforms in computational heat and fluid flow. CRC Press, Boca Raton
2. Davies B (2002) Integral transforms and their applications, 3rd edn. Springer, New York
3. Debnath L, Bhatta D (2015) Integral transforms and their applications, 3rd edn. CRC Press, Boca Raton

4. Gasiorowicz S (1974) Quantum physics. Wiley, New York
5. Schwartz L (2008) Mathematics for the physical sciences. Dover Publications, New York
6. Wolf K (2013) Integral transforms in science and engineering. Springer, New York

Chapter 3
Large-time Behaviour of Wave Packets

3.1 What is a Holomorphic Function?

The main elements of the theory of the functions of a complex variable can be found in many textbooks. Among these, the treatment presented in this section, as well as in Sects. 3.2 and 3.3, mainly follows the much more extended presentations of this topic available in Cartan [6], in Priestley [8], and in chapter 11 of Arfken et al. [4].

Let us recall the definition of set $\mathbb{C}$. The set $\mathbb{C}$ coincides with $\mathbb{R}^2$, in the sense that to every pair $(x, y) \in \mathbb{R}^2$ there corresponds one and only one complex number $z \in \mathbb{C}$ defined as

$$z = x + \mathrm{i}\, y \ . \tag{3.1}$$

The real number x is called the real part of z, while real number y is called the imaginary part of z,

$$x = \Re(z) \ , \quad y = \Im(z) \ . \tag{3.2}$$

The set $\mathbb{R}^2$ is also called the *complex plane*.

Unlike $\mathbb{R}^2$, the set $\mathbb{C}$ is structured as a field. This means that it has not only an inner operation of sum between any two elements, already present in $\mathbb{R}^2$, but also an operation of product, not present in $\mathbb{R}^2$. The product is defined as

$$\begin{cases} z_1 = x_1 + \mathrm{i}\, y_1 \ , \\ z_2 = x_2 + \mathrm{i}\, y_2 \ , \end{cases} \longmapsto z_1\, z_2 = x_1\, x_2 - y_1\, y_2 + \mathrm{i}\, (x_1\, y_2 + y_1\, x_2) \ . \tag{3.3}$$

A special element of $\mathbb{C}$ is i, called the *imaginary unit*. On account of the definition of product between any two complex numbers, given by Eq. (3.3), the product of the imaginary unit and itself, i^2, is equal to -1.

To every complex number z, there corresponds one and only one complex number $\overline{z}$, called the *complex conjugate* of z and defined as

$$z = x + \mathrm{i}\, y \ , \quad \longmapsto \quad \overline{z} = x - \mathrm{i}\, y \ . \tag{3.4}$$

A. Barletta, *Routes to Absolute Instability in Porous Media*,
https://doi.org/10.1007/978-3-030-06194-4_3

The product of z and $\overline{z}$ is a real number called the square modulus of z,

$$z = x + \mathrm{i}\, y \ , \quad \longmapsto \quad z\,\overline{z} = x^2 + y^2 \equiv |z|^2 \ . \tag{3.5}$$

The exponential of any $z \in \mathbb{C}$ is defined as the power series

$$\mathrm{e}^z = \sum_{n=0}^{\infty} \frac{z^n}{n!} \ . \tag{3.6}$$

The main property of the exponential function is

$$\mathrm{e}^z\, \mathrm{e}^w = \mathrm{e}^{z+w} \ , \quad \forall z, w \in \mathbb{C} \ . \tag{3.7}$$

The imaginary exponential function is an application $\mathbb{R} \to \mathbb{C}$ defined as $\theta \to e^{\mathrm{i}\,\theta}$. This function satisfies *Euler's formula*,

$$e^{\mathrm{i}\,\theta} = \cos\theta + \mathrm{i}\, \sin\theta \ , \quad \forall \theta \in \mathbb{R} \ . \tag{3.8}$$

Since $\sin^2\theta + \cos^2\theta = 1$, Eq. (3.8) allows one to express any complex number with modulus 1. Then,

$$\forall z \in \mathbb{C} \ , \quad \frac{z}{|z|} = \cos\theta + \mathrm{i}\, \sin\theta = e^{\mathrm{i}\,\theta} \ . \tag{3.9}$$

Equation (3.9) associates a real number θ to any complex number z. This real number is called the *argument* of z, i.e. $\theta = \arg(z)$. However, since the sine and cosine functions are periodic with period 2π, $\arg(z)$ is defined only up to integer multiples of 2π. Therefore, Eq. (3.9) gives rise to the so-called *polar representation* of a complex number,

$$\forall z \in \mathbb{C} \ , \quad z = |z|\, e^{\mathrm{i}\, \arg(z)} = |z| \Big\{ \cos[\arg(z)] + \mathrm{i}\, \sin[\arg(z)] \Big\} \ . \tag{3.10}$$

Since $\arg(z)$ is defined only up to integer multiples of $2\,\pi$, it is not strictly speaking an application $\mathbb{C} \to \mathbb{R}$, but a so-called multifunction, or *multivalued function*. In fact, for a given $z \in \mathbb{C}$, $\arg(z)$ can be a real number in the interval $[-\pi, \pi]$, and a real number in the interval $[\pi, 3\pi]$, and a real number in the interval $[-3\pi, -\pi]$, … . The terms of this infinite sequence of real numbers can be obtained by adding $2\pi k$, with $k \in \mathbb{Z}$, to the first real number (the value in the interval $[-\pi, \pi]$). The value in the interval $[-\pi, \pi]$ is called the *principal branch* of $\arg(z)$.

Another important multivalued function is the (natural) logarithm of z, defined as the inverse function of e^z. From Eq. (3.8), the main property of the logarithm is

$$\ln(z\, w) = \ln(z) + \ln(w) \ , \quad \forall z, w \in \mathbb{C} \ . \tag{3.11}$$

From Eqs. (3.10) and (3.11), one obtains

$$\ln(z) = \ln(|z|) + \mathrm{i}\ \arg(z)\ . \tag{3.12}$$

Equation (2.13) shows that the logarithm of z is a multivalued function $\mathbb{C} \to \mathbb{C}$. We have a principal branch of $\ln(z)$ defined by considering the principal branch of the argument of z, i.e. $\arg(z) \in [-\pi, \pi]$.

Example 3.1 In order to evaluate the logarithm of -1, we have just to recognise, from Eq. (3.8), that

$$-1 = \mathrm{e}^{\mathrm{i}\,(\pi + 2\pi k)}\ , \quad \forall k \in \mathbb{Z}\ . \tag{3.13}$$

Then, we deduce that

$$\ln(-1) = \mathrm{i}\,\pi + 2\mathrm{i}\,\pi k\ , \quad \forall k \in \mathbb{Z}\ . \tag{3.14}$$

The principal branch value of $\ln(-1)$ is $\mathrm{i}\,\pi$.

3.1.1 Derivative of a Complex-Valued Function

The metric structure in $\mathbb{C}$ defined by the distance $|z - w|$ between any two complex numbers z and w allows us to extend the notions of limit and continuity defined in the elementary analysis of real functions. These notions are formally identical to those of the real analysis. The same holds for the notions of derivative and differentiability. A function $f : \mathscr{D} \to \mathbb{C}$, where $\mathscr{D}$ is an open connected subset of $\mathbb{C}$, is said to be differentiable at a point $z_0 \in \mathscr{D}$ if

$$\lim_{\substack{z \to z_0 \\ z \in \mathscr{D}}} \frac{f(z) - f(z_0)}{z - z_0} = f'(z_0) \in \mathbb{C}\ . \tag{3.15}$$

This means that, on considering $f(z) = f(x, y)$ where $x = \Re(z)$ and $y = \Im(z)$, there exists the double limit

$$\lim_{\substack{h_1 \to 0, h_2 \to 0 \\ h_1, h_2 \in \mathbb{R}}} \frac{f(x_0 + h_1, y_0 + h_2) - f(x_0, y_0)}{h_1 + i\, h_2} = f'(z_0) \in \mathbb{C}\ , \tag{3.16}$$

where $x_0 = \Re(z_0)$ and $y_0 = \Im(z_0)$. Obviously, the real numbers h_1, h_2 must be chosen as sufficiently small so that $(x_0 + h_1) + \mathrm{i}\,(y_0 + h_2) \in \mathscr{D}$. For the limit in the left-hand side of Eq. (3.16) to exist, its value $f'(z_0)$ must be independent of the special way it is evaluated. For instance, one may evaluate the limit by keeping $h_2 = 0$, so that

$$f'(z_0) = \lim_{\substack{h_1 \to 0 \\ h_1 \in \mathbb{R}}} \frac{f(x_0 + h_1, y_0) - f(x_0, y_0)}{h_1} = \left.\frac{\partial f(x, y)}{\partial x}\right|_{(x,y)=(x_0,y_0)}\ . \tag{3.17}$$

Alternatively, one may evaluate the limit by keeping $h_1 = 0$, so that

$$\begin{aligned} f'(z_0) &= \lim_{\substack{h_2 \to 0 \\ h_2 \in \mathbb{R}}} \frac{f(x_0, y_0 + h_2) - f(x_0, y_0)}{\mathrm{i}\, h_2} \\ &= \frac{1}{\mathrm{i}} \left. \frac{\partial f(x, y)}{\partial y} \right|_{(x,y)=(x_0,y_0)} = -\,\mathrm{i} \left. \frac{\partial f(x, y)}{\partial y} \right|_{(x,y)=(x_0,y_0)} . \end{aligned} \tag{3.18}$$

From Eqs. (3.17) and (3.18), one may easily infer that, if $f(z) = f(x, y)$ is differentiable at $z_0 = x_0 + \mathrm{i}\, y_0 \in \mathscr{D}$, then

$$\left. \frac{\partial f(x, y)}{\partial x} \right|_{(x,y)=(x_0,y_0)} + \mathrm{i} \left. \frac{\partial f(x, y)}{\partial y} \right|_{(x,y)=(x_0,y_0)} = 0 . \tag{3.19}$$

Definition 3.1 If $\mathscr{D}$ is an open connected subset of $\mathbb{C}$, a function $f : \mathscr{D} \to \mathbb{C}$ is *holomorphic* in $\mathscr{D}$ if it is differentiable at every point $z_0 \in \mathscr{D}$.

We note that a holomorphic function $f(z)$ has a very important feature. Let $f(z) = f(x, y)$, with $z = x + \mathrm{i}\, y$, and let $f(x, y) = u(x, y) + \mathrm{i}\, v(x, y)$, where u and v are real-valued functions. Then, Eq. (3.19) implies that

$$\frac{\partial f(x, y)}{\partial x} + \mathrm{i}\, \frac{\partial f(x, y)}{\partial y} = 0 , \tag{3.20}$$

namely

$$\begin{aligned} &\frac{\partial}{\partial x} [u(x, y) + \mathrm{i}\, v(x, y)] + \mathrm{i}\, \frac{\partial}{\partial y} [u(x, y) + \mathrm{i}\, v(x, y)] = 0 , \\ &\frac{\partial u(x, y)}{\partial x} - \frac{\partial v(x, y)}{\partial y} + \mathrm{i} \left[\frac{\partial v(x, y)}{\partial x} + \frac{\partial u(x, y)}{\partial y} \right] = 0 . \end{aligned} \tag{3.21}$$

From Eq. (3.21), one easily proves the following theorem.

Theorem 3.1 (Cauchy–Riemann equations) *Let $\mathscr{D}$ be an open connected subset of $\mathbb{C}$, and $f : \mathscr{D} \to \mathbb{C}$ be holomorphic in $\mathscr{D}$ with $f(z) = f(x, y) = u(x, y) + \mathrm{i}\, v(x, y)$, where u and v are real-valued. Then, the Cauchy–Riemann equations hold,*

$$\frac{\partial u(x, y)}{\partial x} = \frac{\partial v(x, y)}{\partial y} , \quad \frac{\partial v(x, y)}{\partial x} = -\frac{\partial u(x, y)}{\partial y} . \tag{3.22}$$

Equation (3.22) reveals that a holomorphic function $f(z)$ is something more than the mere representation of a differentiable function $f(x, y)$ in an open subset of $\mathbb{R}^2$. On account of the definition of complex conjugation, we have

$$\begin{aligned} &z = x + \mathrm{i}\, y , \quad \overline{z} = x - \mathrm{i}\, y , \\ &x = \frac{z + \overline{z}}{2} , \quad y = \frac{z - \overline{z}}{2\,\mathrm{i}} , \end{aligned} \tag{3.23}$$

so that

$$\frac{\partial f(x,y)}{\partial \bar{z}} = \frac{\partial x}{\partial \bar{z}}\frac{\partial f(x,y)}{\partial x} + \frac{\partial y}{\partial \bar{z}}\frac{\partial f(x,y)}{\partial y}$$
$$= \frac{1}{2}\frac{\partial f(x,y)}{\partial x} - \frac{1}{2\,\mathrm{i}}\frac{\partial f(x,y)}{\partial y} = \frac{1}{2}\left[\frac{\partial f(x,y)}{\partial x} + \mathrm{i}\,\frac{\partial f(x,y)}{\partial y}\right]. \tag{3.24}$$

On account of Eqs. (3.20) and (3.24), we conclude that, when a differentiable function in an open subset of $\mathbb{R}^2$, $f(x,y)$, defines a holomorphic function in an open subset of $\mathbb{C}$, then $f(x,y)$ depends on z, but it cannot depend on the complex conjugate of z, namely

$$\frac{\partial f(x,y)}{\partial \bar{z}} = 0. \tag{3.25}$$

In a completely symmetric way, one can prove that if a differentiable function, $f(x,y)$, in an open subset of $\mathbb{R}^2$ defines a holomorphic function in an open subset of $\mathbb{C}$, then $f(x,y)$ can depend on $\bar{z}$, but it cannot depend on z.

Example 3.2 We can easily prove that $f : \mathbb{R}^2 \to \mathbb{R}^2$ such that $f(x,y) = (x^2 + y^2, 1 - x^2 - y^2)$ does not define a holomorphic function $f : \mathbb{C} \to \mathbb{C}$. In fact, $f(x,y) = (x^2 + y^2, 1 - x^2 - y^2)$ is differentiable in $\mathbb{R}^2$. However, $f : \mathbb{C} \to \mathbb{C}$ such that $f(z) = z\,\bar{z} + \mathrm{i}\,(1 - z\,\bar{z})$ cannot be a holomorphic function. In fact, f depends on both z and $\bar{z}$, so that, in particular, Eq. (3.25) is not satisfied.

Let us define a *harmonic function* as a twice differentiable function $f(x,y)$ with a vanishing Laplacian, namely

$$\frac{\partial^2 f(x,y)}{\partial x^2} + \frac{\partial^2 f(x,y)}{\partial y^2} = 0\,. \tag{3.26}$$

In other words, a harmonic function is any solution of Laplace's equation (3.26).

A general theorem can be proved.

Theorem 3.2 *A twice differentiable function $f(z,\bar{z})$ is harmonic if and only if it is the sum of a holomorphic function of z and a holomorphic function of $\bar{z}$.*

The proof of this theorem is as follows. Let us first assume that

$$f(z,\bar{z}) = F(z) + G(\bar{z})\,, \tag{3.27}$$

where $F(z)$ and $G(\bar{z})$ are differentiable. Then, from Eq. (3.23), we have

$$0 = \frac{\partial F}{\partial \bar{z}} = \frac{\partial F}{\partial x}\frac{\partial x}{\partial \bar{z}} + \frac{\partial F}{\partial y}\frac{\partial y}{\partial \bar{z}} = \frac{1}{2}\frac{\partial F}{\partial x} - \frac{1}{2\,\mathrm{i}}\frac{\partial F}{\partial y}\,. \tag{3.28}$$

Thus, we have

$$\frac{\partial F}{\partial x} = -\,\mathrm{i}\,\frac{\partial F}{\partial y}\,. \tag{3.29}$$

As a consequence,

$$\frac{\partial^2 F}{\partial x^2} + \frac{\partial^2 F}{\partial y^2} = -\mathrm{i}\,\frac{\partial^2 F}{\partial x\,\partial y} + \mathrm{i}\,\frac{\partial^2 F}{\partial y\,\partial x} = 0\,. \tag{3.30}$$

Moreover, we have

$$\frac{\partial G}{\partial z} = 0\,, \tag{3.31}$$

so that we obtain, by employing Eq. (3.23),

$$0 = \frac{\partial G}{\partial z} = \frac{\partial G}{\partial x}\frac{\partial x}{\partial z} + \frac{\partial G}{\partial y}\frac{\partial y}{\partial z} = \frac{1}{2}\frac{\partial G}{\partial x} + \frac{1}{2\,\mathrm{i}}\frac{\partial G}{\partial y}\,. \tag{3.32}$$

Thus, we can write

$$\frac{\partial G}{\partial x} = \mathrm{i}\,\frac{\partial G}{\partial y}\,. \tag{3.33}$$

As a consequence,

$$\frac{\partial^2 G}{\partial x^2} + \frac{\partial^2 G}{\partial y^2} = \mathrm{i}\,\frac{\partial^2 G}{\partial x\,\partial y} - \mathrm{i}\frac{\partial^2 G}{\partial y\,\partial x} = 0\,. \tag{3.34}$$

Therefore, we can conclude that $F(z) + G(\bar{z})$ is a harmonic function. Conversely, let us now assume that $f(z, \bar{z})$ is harmonic. Then, we can express

$$\begin{aligned}\frac{\partial^2 f}{\partial x^2} &= \frac{\partial}{\partial x}\frac{\partial f}{\partial x} = \frac{\partial}{\partial x}\left(\frac{\partial f}{\partial z}\frac{\partial z}{\partial x} + \frac{\partial f}{\partial \bar{z}}\frac{\partial \bar{z}}{\partial x}\right) = \frac{\partial}{\partial x}\left(\frac{\partial f}{\partial z} + \frac{\partial f}{\partial \bar{z}}\right)\\ &= \frac{\partial}{\partial z}\left(\frac{\partial f}{\partial z} + \frac{\partial f}{\partial \bar{z}}\right) + \frac{\partial}{\partial \bar{z}}\left(\frac{\partial f}{\partial z} + \frac{\partial f}{\partial \bar{z}}\right)\\ &= \frac{\partial^2 f}{\partial z^2} + \frac{\partial^2 f}{\partial \bar{z}^2} + 2\,\frac{\partial^2 f}{\partial z\,\partial \bar{z}}\,,\end{aligned} \tag{3.35}$$

and

$$\begin{aligned}\frac{\partial^2 f}{\partial y^2} &= \frac{\partial}{\partial y}\frac{\partial f}{\partial y} = \frac{\partial}{\partial y}\left(\frac{\partial f}{\partial z}\frac{\partial z}{\partial y} + \frac{\partial f}{\partial \bar{z}}\frac{\partial \bar{z}}{\partial y}\right) = \mathrm{i}\,\frac{\partial}{\partial y}\left(\frac{\partial f}{\partial z} - \frac{\partial f}{\partial \bar{z}}\right)\\ &= -\frac{\partial}{\partial z}\left(\frac{\partial f}{\partial z} - \frac{\partial f}{\partial \bar{z}}\right) + \frac{\partial}{\partial \bar{z}}\left(\frac{\partial f}{\partial z} - \frac{\partial f}{\partial \bar{z}}\right)\\ &= -\frac{\partial^2 f}{\partial z^2} - \frac{\partial^2 f}{\partial \bar{z}^2} + 2\,\frac{\partial^2 f}{\partial z\,\partial \bar{z}}\,.\end{aligned} \tag{3.36}$$

Therefore,

$$0 = \frac{\partial^2 f}{\partial x^2} + \frac{\partial^2 f}{\partial y^2} = 4\,\frac{\partial^2 f}{\partial z\,\partial \bar{z}}\,, \tag{3.37}$$

a condition which can be satisfied if and only if f is the sum of a function of z and a function of $\bar{z}$, namely

$$f(z, \bar{z}) = F(z) + G(\bar{z}) \ . \tag{3.38}$$

3.1.2 *Path Integration in* $\mathbb{C}$

A path or a contour in $\mathbb{C}$ is nothing but an oriented open or closed curve in the complex plane. Mathematically, a path in $\mathbb{C}$ is defined by a differentiable application $\gamma : [t_1, t_2] \to \mathbb{C}$, $\gamma = \gamma(t)$, where $[t_1, t_2] \subseteq \mathbb{R}$ is a real interval. Then, $\gamma(t)$ is the parametrisation of the path. For simplicity of notation, we will denote the path with the same symbol γ of its parametrisation. The *path integral* on γ of a function $f(z)$ is defined as

$$\int_\gamma f(z)\, \mathrm{d}\, z = \int_{t_1}^{t_2} f[\gamma(t)]\, \gamma'(t)\, \mathrm{d}\, t \ . \tag{3.39}$$

It may be objected that the result of a path integration on a given oriented curve in the complex plane may be dependent on the chosen parametrisation of that curve. In fact, it may be proved that, under suitable conditions, two different parametrisations yield the same contour integral. In the case of closed contours γ, the mentioned suitable conditions mainly depend on the so-called winding number of the contour.

Example 3.3 To illustrate this point, let us evaluate

$$\int_\gamma \frac{\mathrm{d}\, z}{z} \ , \tag{3.40}$$

where γ is the unit circle centred in $z = 0$ and oriented counterclockwise. A parametrisation of γ can be given by

$$\gamma(\theta) = \cos\theta + \mathrm{i}\, \sin\theta \ , \quad \theta \in [0, 2\pi] \ . \tag{3.41}$$

On account of Eq. (3.8), one may equivalently write

$$\gamma(\theta) = \mathrm{e}^{\mathrm{i}\,\theta}, \quad \theta \in [0, 2\pi] \ . \tag{3.42}$$

Then, on account of Eq. (3.39), one has

$$\int_\gamma \frac{\mathrm{d}\, z}{z} = \mathrm{i} \int_0^{2\pi} \frac{1}{\mathrm{e}^{\mathrm{i}\,\theta}}\, \mathrm{e}^{\mathrm{i}\,\theta}\, \mathrm{d}\, \theta = \mathrm{i} \int_0^{2\pi} \mathrm{d}\, \theta = 2\pi\, \mathrm{i} \ . \tag{3.43}$$

We note that one could have also employed other parametrisations of the unit circle, such as

$$\gamma(\theta) = \mathrm{e}^{\mathrm{i}\,\theta} = \cos\theta + \mathrm{i}\,\sin\theta, \quad \theta \in [0, 4\pi]\,, \tag{3.44}$$

or

$$\gamma(\theta) = \mathrm{e}^{\mathrm{i}\,\theta} = \cos\theta + \mathrm{i}\,\sin\theta, \quad \theta \in [0, 6\pi]\,. \tag{3.45}$$

The result of the integration would have been $4\pi\mathrm{i}$ in the first case and $6\pi\mathrm{i}$ in the second case. However, the *winding number* of the parametrisation defined on $[0, 4\pi]$ is 2, and the winding number of the parametrisation defined on $[0, 6\pi]$ is 3. This means that, in the first case, the point $z = \gamma(t)$ undergoes two complete turns around $z = 0$ and, in the second case, three complete counterclockwise turns around $z = 0$.

Incidentally, on relaxing the assumption of counterclockwise orientation of the path γ, one can devise both positive and negative winding numbers. The latter concept being relative to clockwise-oriented closed paths.

Here and in the following, if not differently specified, we will always assume that the winding number of a closed path is 1.

3.1.3 Homotopy

We consider an open connected subset $\mathscr{D} \subseteq \mathbb{C}$ and two closed paths γ_1 and γ_2 both oriented counterclockwise, or both oriented clockwise. If there exists a continuous map,

$$\Lambda : \mathscr{D} \times [0, 1] \to \mathscr{D}\,, \tag{3.46}$$

such that

$$\gamma_1(t) = \Lambda[\gamma_1(t), 0], \quad \gamma_2(t) = \Lambda[\gamma_1(t), 1]\,, \tag{3.47}$$

for every t, then γ_1 and γ_2 are homotopic. In other words, γ_1 and γ_2 are said to be homotopic in $\mathscr{D}$ if γ_1 can be continuously deformed into γ_2.

A special case is that of an oriented closed path γ which is homotopic in $\mathscr{D}$ to a point $z_0 \in \mathscr{D}$. In this case, γ can be continuously shrunk to a point z_0.

Theorem 3.3 *Let us consider an open connected subset $\mathscr{D} \subseteq \mathbb{C}$ and two closed paths $\gamma_1 \subseteq \mathscr{D}$ and $\gamma_2 \subseteq \mathscr{D}$ both oriented counterclockwise, or both oriented clockwise. If $f : \mathscr{D} \to \mathbb{C}$ is holomorphic, and if γ_1 and γ_2 are homotopic, then*

$$\int_{\gamma_1} f(z)\,\mathrm{d}\,z = \int_{\gamma_2} f(z)\,\mathrm{d}\,z\,. \tag{3.48}$$

Corollary 3.1 *Let us consider an open connected subset $\mathscr{D} \subseteq \mathbb{C}$ and a closed path $\gamma \subseteq \mathscr{D}$ homotopic to a point $z_0 \in \mathscr{D}$. If $f : \mathscr{D} \to \mathbb{C}$ is holomorphic, then*

$$\int_{\gamma} f(z)\,\mathrm{d}\,z = 0\,. \tag{3.49}$$

We note that the thesis of Corollary 3.1 is not incompatible with the result obtained working out the example regarding function $f(z) = 1/z$. In fact, in that exercise, the function $f(z) = 1/z$ is holomorphic in the punctured complex plane $\mathscr{D} = \mathbb{C} \setminus \{0\}$, due to the singularity in $z = 0$. Then, the unit circle centred in $z = 0$ is included in $\mathscr{D}$ while the point $z = 0$ is not. Thus, one cannot even question about the homotopy in $\mathscr{D}$ of the unit circle and the point $z = 0$.

If $\mathscr{D} \subseteq \mathbb{C}$ is open and connected, and if every closed path γ in $\mathscr{D}$ is homotopic to a point in $\mathscr{D}$, then $\mathscr{D}$ is called *simply connected*. Obviously, the punctured complex plane $\mathbb{C} \setminus \{0\}$ is not simply connected.

Corollary 3.2 *Let us consider a simply connected subset $\mathscr{D} \subseteq \mathbb{C}$ and a closed path $\gamma \subseteq \mathscr{D}$. If $f : \mathscr{D} \to \mathbb{C}$ is holomorphic, then*

$$\int_{\gamma} f(z)\,\mathrm{d}\,z = 0\,. \tag{3.50}$$

3.2 Laurent Expansions, Singular Points

Let us consider an annulus,

$$\mathscr{A} = \{z \in \mathbb{C} : R_1 < |z| < R_2\}\,. \tag{3.51}$$

A function $f : \mathscr{A} \to \mathbb{C}$ has a *Laurent expansion* in $\mathscr{A}$ if there exists a power series,

$$\begin{aligned}\sum_{n=-\infty}^{\infty} a_n\, z^n = \cdots + \frac{a_{-n}}{z^n} + \cdots + \frac{a_{-2}}{z^2} + \frac{a_{-1}}{z} + a_0 + a_1\, z \\ + a_2\, z^2 + \cdots + a_n\, z^n + \cdots\,,\end{aligned} \tag{3.52}$$

that converges in $\mathscr{A}$ and whose sum coincides with $f(z)$ for every $z \in \mathscr{A}$.

Theorem 3.4 *Any holomorphic function in an annulus $\mathscr{A}$, defined by Eq. (3.51), has one and only one Laurent expansion.*

An interesting special case is the limit $R_1 \to 0$, meaning a punctured disc

$$\mathscr{A}_0 = \{z \in \mathbb{C} : 0 < |z| < R\}\ . \tag{3.53}$$

Let us consider a holomorphic function $f(z)$ in the punctured disc $\mathscr{A}_0$. If $f(z)$ cannot be extended to a holomorphic function in the disc

$$\tilde{\mathscr{A}}_0 = \{z \in \mathbb{C} : |z| < R\} \ , \tag{3.54}$$

the origin $z = 0$ is an *isolated singularity* of $f(z)$. In other words, $z = 0$ is an isolated singularity of $f(z)$ unless the Laurent expansion of $f(z)$ is such that

$$a_{-n} = 0 \ , \quad \forall n \in \mathbb{N} \ . \tag{3.55}$$

From the analysis of the Laurent expansion of $f(z)$, there are two possible kinds of isolated singularities.

- *A pole* — If only a finite number of coefficients a_{-n}, with $n \in \mathbb{N}$, is nonzero, the isolated singularity is a pole. If N is the largest $N \in \mathbb{N}$ such that $a_{-N} \neq 0$, we say that the pole is *multiple* with order N. If the largest $N \in \mathbb{N}$ such that $a_{-N} \neq 0$ is $N = 1$, we say that the pole is *simple*.
- *An essential singularity* — If there is an infinite number of nonzero coefficients a_{-n}, with $n \in \mathbb{N}$, the isolated singularity is an essential singularity.

We note that, if $f(z)$ is a holomorphic function in the punctured disc $\mathscr{A}_0$, Eq. (3.53), with a multiple pole of order N, then $z^N f(z)$ is holomorphic in the disc $\tilde{\mathscr{A}}_0$, Eq. (2.31).

We note that

$$f(z) = \frac{1}{z} \tag{3.56}$$

has a simple pole at $z = 0$, while

$$f(z) = \mathrm{e}^{1/z} \tag{3.57}$$

has an essential singularity at $z = 0$.

So far, we discussed the singularities of a function $f(z)$. We know that there also exist multivalued functions, an example being the logarithm $\ln(z)$, Eq. (3.12). We know that there exist infinite branches of $\ln(z)$, each one determining a different value associated with a given z. Other multivalued functions can be defined with the fractional powers of z. An example is

$$f(z) = \sqrt{z} = \sqrt{|z|}\, \mathrm{e}^{\mathrm{i}\, \arg(z)/2} \ . \tag{3.58}$$

If we consider the first branch $\arg(z) \in [-\pi, \pi]$, we obtain values of $\sqrt{z}$ with a positive or zero real part. If we consider another branch, say $[\pi, 3\pi]$, we obtain values of $\sqrt{z}$ with a negative or zero real part. Both in the case of $\ln(z)$ and in the case of $\sqrt{z}$, the multivaluedness can be represented by a *branch cut* in the complex plane (see Fig. 3.1). The branch cut is the wavy line on the half-axis $\mathfrak{Re}(z) \leqslant 0$. Every time we cross the branch cut and we enter a new branch of the multivalued function. The origin of the branch cut, $z = 0$, is to be considered as a singularity of the multivalued function, even if in a sense different from the isolated singularities

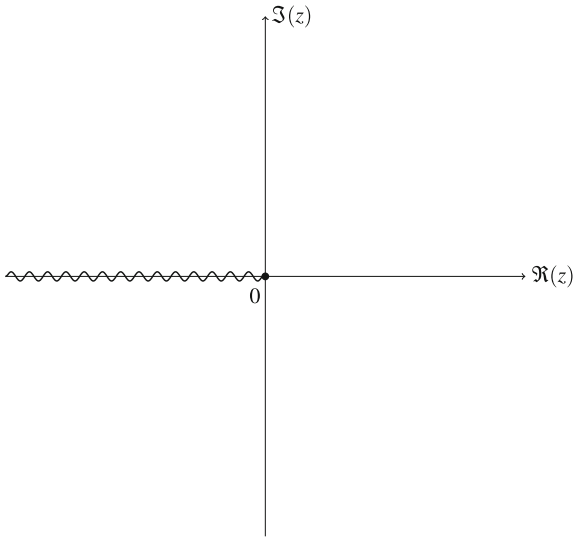

Fig. 3.1 Branch cut in the complex plane

of the functions discussed above. In fact, in this case we don't base our definition on the features of a Laurent series.

For the sake of simplicity, our definitions of Laurent series, isolated singularity, pole and essential singularity were relative to the origin. The same definitions may be relative to any other point $z = z_0 \in \mathbb{C}$ without any substantial difference. Indeed, we must consider an annulus,

$$\mathscr{A}_{z_0} = \{z \in \mathbb{C} : R_1 < |z - z_0| < R_2\}\,. \tag{3.59}$$

Then, a Laurent expansion of a function $f : \mathscr{A}_{z_0} \to \mathbb{C}$ exists if the power series,

$$\begin{aligned}\sum_{n=-\infty}^{\infty} a_n\,(z-z_0)^n = \cdots + \frac{a_{-n}}{(z-z_0)^n} + \cdots + \frac{a_{-2}}{(z-z_0)^2} + \frac{a_{-1}}{z-z_0} + a_0 \\ + a_1\,(z-z_0) + a_2\,(z-z_0)^2 + \cdots + a_n\,(z-z_0)^n + \cdots\,,\end{aligned} \tag{3.60}$$

converges to $f(z)$ for every $z \in \mathscr{A}_{z_0}$.

Let us consider an open connected subset $\mathscr{D} \subseteq \mathbb{C}$. If $f : \mathscr{D} \to \mathbb{C}$ is holomorphic in $\mathscr{D}$ except for a set of isolated singularities of $f(z)$ classified as poles, then $f(z)$ is said to be *meromorphic* in $\mathscr{D}$.

3.3 Residues

Let $f(z)$ be a holomorphic function in the punctured disc centred in $z = z_0$,

$$\mathscr{A}_{z_0} = \{z \in \mathbb{C} : 0 < |z - z_0| < R\} \ , \tag{3.61}$$

and let $z = z_0$ be a multiple pole of order N. Then, we may write the Laurent expansion

$$f(z) = \sum_{n=-N}^{\infty} a_n (z - z_0)^n \ , \quad \forall z \in \mathscr{A}_{z_0} \ . \tag{3.62}$$

The coefficient a_{-1} is called the *residue* of $f(z)$ at $z = z_0$,

$$\mathrm{Res}(f(z); z_0) = a_{-1} \ . \tag{3.63}$$

We can prove that, if $z = z_0$ is a simple pole of a holomorphic function $f(z)$ in the punctured disc $\mathscr{A}_{z_0}$, Eq. (3.61), then the residue of $f(z)$ at $z = z_0$ can be evaluated as

$$\mathrm{Res}(f(z); z_0) = \lim_{z \to z_0} (z - z_0) f(z) \ . \tag{3.64}$$

The proof is as follows. We express $f(z)$ through its Laurent expansion

$$f(z) = \frac{a_{-1}}{z - z_0} + a_0 + a_1 (z - z_0) + a_2 (z - z_0)^2 + \ \cdots \ . \tag{3.65}$$

Then,

$$(z - z_0) f(z) = a_{-1} + a_0 (z - z_0) + a_1 (z - z_0)^2 + a_2 (z - z_0)^3 + \ \cdots \ . \tag{3.66}$$

By taking the limit $z \to z_0$ at both sides of this equation, we obtain

$$\lim_{z \to z_0} (z - z_0) f(z) = a_{-1} = \mathrm{Res}(f(z); z_0) \ . \tag{3.67}$$

Furthermore, we can prove that, if $z = z_0$ is a multiple pole of order $N > 1$ of a holomorphic function $f(z)$ in the punctured disc $\mathscr{A}_{z_0}$, Eq. (3.61), then the residue of $f(z)$ at $z = z_0$ can be evaluated as

$$\mathrm{Res}(f(z); z_0) = \frac{1}{(N-1)!} \lim_{z \to z_0} \frac{\mathrm{d}^{N-1}}{\mathrm{d}\, z^{N-1}} \left[(z - z_0)^N f(z) \right] \ . \tag{3.68}$$

Equation (3.68) can be proved by expressing $f(z)$ through its Laurent expansion, so that we obtain

$$\begin{aligned} (z - z_0)^N f(z) = a_{-N} + a_{-(N-1)} (z - z_0) + \ \cdots \\ + a_{-1} (z - z_0)^{N-1} + a_0 (z - z_0)^N + a_1 (z - z_0)^{N+1} \ \ldots \ . \end{aligned} \tag{3.69}$$

One may easily verify that

$$\frac{\mathrm{d}^{N-1}}{\mathrm{d}\,z^{N-1}}\,(z-z_0)^n = 0\;,\quad 0 \leqslant n < N-1\;,$$

$$\frac{\mathrm{d}^{N-1}}{\mathrm{d}\,z^{N-1}}\,(z-z_0)^n = \frac{n!}{(n-N+1)!}\,(z-z_0)^{n-N+1}\;,\quad n \geqslant N-1\;. \tag{3.70}$$

Thus, by employing Eqs. (3.67)–(3.69), we obtain

$$\lim_{z\to z_0}\frac{\mathrm{d}^{N-1}}{\mathrm{d}\,z^{N-1}}\left[(z-z_0)^N f(z)\right] = a_{-1}\,(N-1)! = (N-1)!\,\mathrm{Res}(f(z);z_0)\;. \tag{3.71}$$

Theorem 3.5 (Cauchy's Residue Theorem) *Let us consider an open connected subset $\mathscr{D}\subseteq\mathbb{C}$ and a closed counterclockwise-oriented path $\gamma\subseteq\mathscr{D}$. Let $f(z)$ be a meromorphic function in $\mathscr{D}$ with a finite number of poles $z_1, z_2, \ldots, z_m$ inside the region bounded by γ, and such that γ does not pass through any singularities of $f(z)$. Then,*

$$\int_\gamma f(z)\,\mathrm{d}\,z = 2\pi\,\mathrm{i}\sum_{k=1}^{m}\mathrm{Res}(f(z);z_k)\;. \tag{3.72}$$

Cauchy's residue theorem is of paramount importance in the complex analysis, as it provides an extremely effective tool for the evaluation of integrals. For this purpose, Theorem 3.5 is completed by a useful lemma.

Lemma 3.1 *Let $f(z)$ be a meromorphic function in an open connected subset $\mathscr{D}\subseteq\mathbb{C}$ that includes the sector of the complex plane*

$$\mathscr{S} = \{z\in\mathbb{C} : \theta_1 < \arg(z) < \theta_2\}\;. \tag{3.73}$$

Let $\gamma_0(R;\theta_1,\theta_2)$ be the arc of the circle $|z|=R$ included in $\mathscr{S}$ and oriented counterclockwise. If

$$\forall z\in\mathscr{S},\quad \lim_{|z|\to\infty} z f(z) = 0\;, \tag{3.74}$$

then

$$\lim_{R\to\infty}\int_{\gamma_0(R;\theta_1,\theta_2)} f(z)\,\mathrm{d}\,z = 0\;. \tag{3.75}$$

3.3.1 Evaluation of Integrals

Let us consider a few examples, in order to see how Cauchy's residue theorem can be a very useful method for the evaluation of integrals.

Example 3.4 We want to evaluate the integral

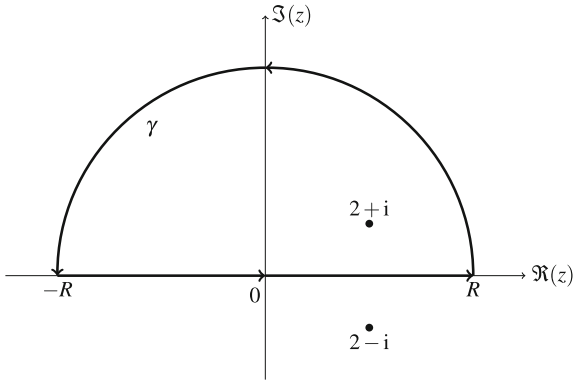

Fig. 3.2 Closed semicircular path used in Example 3.4

$$I = \int_{-\infty}^{\infty} \frac{\mathrm{d}\, x}{x^2 - 4x + 5} \,. \tag{3.76}$$

Obviously, I is given by the limit $R \to \infty$ of the integral

$$I_R = \int_{-R}^{R} \frac{\mathrm{d}\, x}{x^2 - 4x + 5} \,. \tag{3.77}$$

Function

$$f(z) = \frac{1}{z^2 - 4z + 5} = \frac{1}{(z - 2 + \mathrm{i})(z - 2 - \mathrm{i})} \tag{3.78}$$

is meromorphic in $\mathbb{C}$ with two simple poles in $z = 2 - \mathrm{i}$ and in $z = 2 + \mathrm{i}$.

If we consider the closed semicircular path γ sketched in Fig. 3.2, the pole $z = 2 + \mathrm{i}$ is contained in the region bounded by γ, provided that R is sufficiently large. The following identity holds

$$\int_{\gamma} \frac{\mathrm{d}\, z}{z^2 - 4z + 5} = I_R + \int_{\gamma_0(R;0,\pi)} \frac{\mathrm{d}\, z}{z^2 - 4z + 5} \,, \tag{3.79}$$

where

$$\gamma_0(R; 0, \pi) = \{z \in \mathbb{C} : |z| = R,\ \Im\mathrm{m}(z) > 0\} \,. \tag{3.80}$$

On account of Lemma 3.1, we can write

$$\lim_{R\to\infty} \int_{\gamma_0(R;0,\pi)} \frac{\mathrm{d}\, z}{z^2 - 4z + 5} = 0 \,. \tag{3.81}$$

Therefore, by invoking Cauchy's residue theorem, we may write

$$\begin{aligned} I &= \lim_{R\to\infty} \int_{\gamma} \frac{\mathrm{d}\, z}{z^2 - 4z + 5} \\ &= 2\pi\,\mathrm{i}\,\mathrm{Res}\left(\frac{1}{(z-2+\mathrm{i})(z-2-\mathrm{i})}; 2+\mathrm{i} \right) = 2\pi\,\mathrm{i}\,\frac{1}{2\,\mathrm{i}} = \pi \ , \end{aligned} \tag{3.82}$$

where Eq. (3.64) has been used for the evaluation of the residue.

Example 3.5 Let us consider the integral

$$I = \int_0^{2\pi} \frac{\mathrm{d}\, x}{\sin x + \cos x + 5} \ . \tag{3.83}$$

We note that a parametrisation of the unit circle,

$$\mathscr{C} = \{ z \in \mathbb{C} : |z| = 1 \} \ , \tag{3.84}$$

oriented counterclockwise, is

$$z = \mathrm{e}^{\mathrm{i}\, x} = \cos x + \mathrm{i}\, \sin x \ , \quad x \in [0, 2\pi] \ , \tag{3.85}$$

so that

$$\mathrm{d}\, z = \mathrm{i}\, \mathrm{e}^{\mathrm{i}\, x} \mathrm{d}\, x = \mathrm{i}\, z\, \mathrm{d}\, x \ , \quad \mathrm{d}\, x = -\,\mathrm{i}\, \frac{\mathrm{d}\, z}{z} \ . \tag{3.86}$$

Then, on the unit circle $\mathscr{C}$, we have

$$\frac{1}{z} = \mathrm{e}^{-\mathrm{i}\, x} = \cos x - \mathrm{i}\, \sin x \ , \quad x \in [0, 2\pi] \ . \tag{3.87}$$

As a consequence, we may write

$$\begin{aligned} &\cos x = \frac{1}{2}\left(z + \frac{1}{z} \right) , \quad \sin x = \frac{1}{2\,\mathrm{i}}\left(z - \frac{1}{z} \right) , \\ &\frac{\mathrm{d}\, x}{\sin x + \cos x + 5} = \frac{-\,2\mathrm{i}\, \mathrm{d}\, z}{(1-\mathrm{i})z^2 + 10z + (1+\mathrm{i})} \ . \end{aligned} \tag{3.88}$$

Therefore, we have

$$I = -\,2\,\mathrm{i} \int_{\mathscr{C}} \frac{\mathrm{d}\, z}{(1-\mathrm{i})z^2 + 10z + (1+\mathrm{i})} \ . \tag{3.89}$$

The function

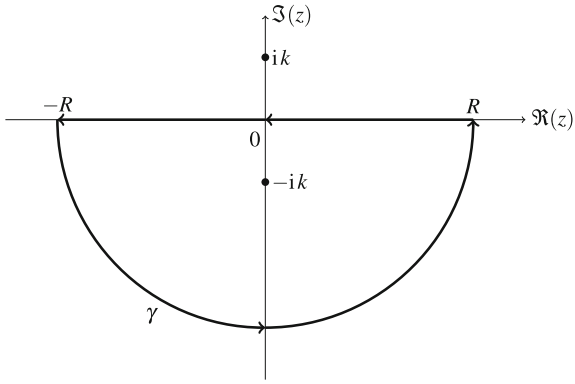

Fig. 3.3 Closed semicircular path used in Example 3.6

$$f(z) = \frac{1}{(1-\mathrm{i})z^2 + 10z + (1+\mathrm{i})} \tag{3.90}$$

has two simple poles at

$$z_1 = \frac{1+\mathrm{i}}{2}\left(\sqrt{23} - 5\right), \quad z_2 = -\frac{1+\mathrm{i}}{2}\left(\sqrt{23} + 5\right). \tag{3.91}$$

Only the pole z_1 is in the region bounded by $\mathscr{C}$, $|z_1| < 1$, while z_2 is outside this region, $|z_2| > 1$. Hence, on employing Cauchy's residue theorem, we obtain

$$I = 4\pi \ \mathrm{Res}(f(z); z_1) = \frac{2\pi}{\sqrt{23}} \, . \tag{3.92}$$

Example 3.6 We are now interested in evaluating the integrals

$$I_1 = \int_{-\infty}^{\infty} \frac{\cos(kx)}{x^2+1} \, \mathrm{d}x \, , \quad I_2 = \int_{-\infty}^{\infty} \frac{\sin(kx)}{x^2+1} \, \mathrm{d}x \, , \quad k > 0 \, . \tag{3.93}$$

We note that, on account of Euler's formula (3.8), we may write

$$I_1 = \Re(I) \, , \quad I_2 = -\Im(I) \, , \tag{3.94}$$

where

$$I = \int_{-\infty}^{\infty} \frac{\mathrm{e}^{-\mathrm{i}kx}}{x^2+1} \, \mathrm{d}x \, . \tag{3.95}$$

A comparison with the definition given by Eq. (2.2) leads us to the conclusion that I is the Fourier transform of function $F(x) = \sqrt{2\pi}/(1+x^2)$ for the range $k > 0$. Then, we can focus on the evaluation of I. We change the integration variable,

$$y = kx\ , \quad x = \frac{y}{k}\ , \quad \mathrm{d}\,x = \frac{\mathrm{d}\,y}{k}\ , \tag{3.96}$$

so that

$$I = k \int\limits_{-\infty}^{\infty} \frac{\mathrm{e}^{-\mathrm{i}\,y}}{y^2 + k^2}\,\mathrm{d}\,y\ . \tag{3.97}$$

On considering the closed semicircular path in Fig. 3.3, we write

$$\int\limits_{\gamma} \frac{\mathrm{e}^{-\mathrm{i}\,z}}{z^2 + k^2}\,\mathrm{d}\,z = -\int\limits_{-R}^{R} \frac{\mathrm{e}^{-\mathrm{i}\,y}}{y^2 + k^2}\,\mathrm{d}\,y + \int\limits_{\gamma_0(R,\pi,2\pi)} \frac{\mathrm{e}^{-\mathrm{i}\,z}}{z^2 + k^2}\,\mathrm{d}\,z\ , \tag{3.98}$$

where

$$\gamma_0(R;\pi,2\pi) = \{z \in \mathbb{C} : |z| = R,\ \Im(z) < 0\}\ . \tag{3.99}$$

Since $\Im(z) < 0$, we have

$$\lim_{|z|\to\infty} \frac{z\,\mathrm{e}^{-\mathrm{i}\,z}}{z^2 + k^2} = 0\ . \tag{3.100}$$

Therefore, as consequence of Lemma 3.1, we obtain

$$\lim_{R\to\infty} \int\limits_{\gamma_0(R,\pi,2\pi)} \frac{\mathrm{e}^{-\mathrm{i}\,z}}{z^2 + k^2}\,\mathrm{d}\,z = 0\ , \tag{3.101}$$

so that

$$I = -k \lim_{R\to\infty} \int\limits_{\gamma} \frac{\mathrm{e}^{-\mathrm{i}\,z}}{z^2 + k^2}\,\mathrm{d}\,z\ . \tag{3.102}$$

We employ Cauchy's residue theorem to evaluate

$$\int\limits_{\gamma} \frac{\mathrm{e}^{-\mathrm{i}\,z}}{z^2 + k^2}\,\mathrm{d}\,z\ . \tag{3.103}$$

Function

$$f(z) = \frac{\mathrm{e}^{-\mathrm{i}\,z}}{z^2 + k^2} = \frac{\mathrm{e}^{-\mathrm{i}\,z}}{(z - \mathrm{i}\,k)(z + \mathrm{i}\,k)} \tag{3.104}$$

has two simple poles $z_1 = \mathrm{i}\,k$ and $z_2 = -\mathrm{i}\,k$. The closed path γ encircles the pole z_2, but not z_1, provided that R is sufficiently large ($R > k$). Then, we have

$$I = -k \lim_{R\to\infty} \int_{\gamma} \frac{\mathrm{e}^{-\mathrm{i}\, z}}{z^2 + k^2}\, \mathrm{d}\, z = -2\pi k\, \mathrm{i}\, \mathrm{Res}(f(z); z_2)\ . \tag{3.105}$$

The residue is given by

$$\mathrm{Res}(f(z); z_2) = -\frac{\mathrm{e}^{-k}}{2\mathrm{i}\, k}\ . \tag{3.106}$$

Therefore, we conclude that

$$I = 2\pi k\, \mathrm{i}\, \frac{\mathrm{e}^{-k}}{2\mathrm{i}\, k} = \pi\, \mathrm{e}^{-k}\ . \tag{3.107}$$

This means that

$$I_1 = \pi\, \mathrm{e}^{-k}\ , \quad I_2 = 0\ . \tag{3.108}$$

3.4 The Laplace Transform

The Laplace transform of a function $f(t)$ is given by

$$\mathfrak{L}\{f(t)\}(s) = \tilde{f}(s) = \int_0^{\infty} f(t)\, \mathrm{e}^{-st}\, \mathrm{d}\, t\ . \tag{3.109}$$

The transform $\mathfrak{L}\{f(t)\}$ is defined in the complex half-plane $\Re(s) > a$ where a is a real constant such that the following condition holds:

$$|\, f(t)| < C\, \mathrm{e}^{at}, \quad \forall t \geqslant 0, \tag{3.110}$$

with a proper choice of a positive real constant C. A sketch of the domain where $\tilde{f}(s)$ is defined is given in Fig. 3.4.

3.4.1 Inversion of the Laplace Transform

If the Laplace transform of a function $f(t)$ is known, one may determine $f(t)$. To achieve this task, there exists a procedure for the inversion of the Laplace transform. The inversion formula of the Laplace transform is as follows:

$$f(t) = \mathfrak{L}^{-1}\{\tilde{f}(s)\}(t) = \frac{1}{2\pi\, \mathrm{i}} \int_{p-\mathrm{i}\,\infty}^{p+\mathrm{i}\,\infty} \tilde{f}(s)\, \mathrm{e}^{st}\, \mathrm{d}\, s\ , \tag{3.111}$$

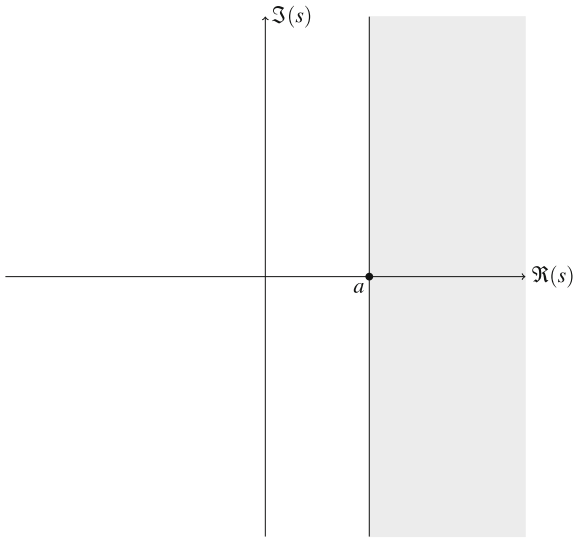

Fig. 3.4 Domain where the Laplace transform $\tilde{f}(s)$ is defined

for every real number $p > a$. The integration must be performed along a line path in the complex plane. This path is given by a vertical line that intersects the real axis, $\Im(s) = 0$, at $s = p$ (see Fig. 3.5).

Hence, the evaluation of the inverse Laplace transform implies the calculation of an integral in the complex plane. The theory of the integration in $\mathbb{C}$, and Cauchy's residue Theorem 3.5, is a strong basis for the inversion of the Laplace transform. In the simplest cases, one may utilise suitable tables where the pairs $[f(t), \tilde{f}(s)]$ are reported (see, for instance, Debnath and Bhatta [7]).

3.4.2 Main Properties of the Laplace Transform

Let $f(t)$ and $g(t)$ be any two functions satisfying Eq. (3.110). Among the main properties of the Laplace transform, we mention the following:

- *Linearity*
  For every pair of real constants (C_1, C_2), we have

$$\begin{aligned} \mathfrak{L}\{C_1 f(t) + C_2 g(t)\}(s) &= C_1 \mathfrak{L}\{f(t)\}(s) + C_2 \mathfrak{L}\{g(t)\}(s) \\ &= C_1 \tilde{f}(s) + C_2 \tilde{g}(s) . \end{aligned} \tag{3.112}$$

- *Derivative*
  On considering the first derivative of $f(t)$ and evaluating its Laplace transform, we obtain

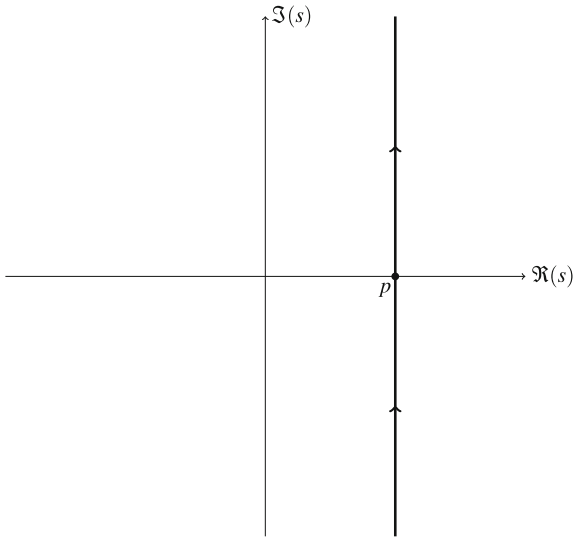

Fig. 3.5 Integration path for the inversion formula, Eq. (3.111)

$$\begin{aligned}\mathfrak{L}\left\{f'(t)\right\}(s) &= \int_0^\infty f'(t)\,\mathrm{e}^{-st}\,\mathrm{d}\,t = \left[f(t)\,\mathrm{e}^{-st}\right]_0^\infty + s\int_0^\infty f(t)\,\mathrm{e}^{-st}\,\mathrm{d}\,t \\ &= s\,\mathfrak{L}\{f(t)\}(s) - f(0) = s\,\tilde{f}(s) - f(0)\,.\end{aligned} \tag{3.113}$$

In a similar way, one may evaluate the Laplace transforms of higher-order derivatives,

$$\begin{aligned}\mathfrak{L}\left\{f''(t)\right\}(s) &= s^2\,\tilde{f}(s) - s\,f(0) - f'(0)\,, \\ \mathfrak{L}\left\{f^{(n)}(t)\right\}(s) &= s^n\,\tilde{f}(s) - s^{n-1}\,f(0) \\ &\quad - s^{n-2}\,f'(0) - \cdots - f^{(n-1)}(0)\,,\end{aligned} \tag{3.114}$$

where $n \geqslant 2$.

- *Translation*
  The Laplace transform of $f(t)\,\mathrm{e}^{bt}$, where $b \in \mathbb{R}$ and $b \leqslant a$ so that the condition expressed by Eq. (3.110) is satisfied by $f(t)\,\mathrm{e}^{bt}$, is given by

$$\mathfrak{L}\left\{f(t)\,\mathrm{e}^{bt}\right\}(s) = \int_0^\infty f(t)\,\mathrm{e}^{-(s-b)t}\,\mathrm{d}\,t = \tilde{f}(s-b)\,. \tag{3.115}$$

In the special case where $f(t) = 1$, we get

$$\mathfrak{L}\left\{\mathrm{e}^{bt}\right\}(s) = \int_0^\infty \mathrm{e}^{-(s-b)t}\,\mathrm{d}\,t = \frac{1}{s-b}\ . \tag{3.116}$$

- *Scaling*
  Let us consider the Laplace transform of $f(bt)$, where $b > 0$. One has

$$\begin{aligned}\mathfrak{L}\left\{f(bt)\right\}(s) &= \int_0^\infty f(bt)\,\mathrm{e}^{-st}\,\mathrm{d}\,t = \frac{1}{b}\int_0^\infty f(u)\,\mathrm{e}^{-su/b}\,\mathrm{d}\,u \\ &= \frac{1}{b}\,\tilde{f}\left(\frac{s}{b}\right)\ .\end{aligned} \tag{3.117}$$

- *Convolution*
  The Laplace transform of the *convolution* between two functions $f(t)$ and $g(t)$, $f(t)\star g(t)$, defined as

$$f(t)\star g(t) = \int_0^t f(\hat{t})\,g(t-\hat{t})\,\mathrm{d}\,\hat{t}\ , \tag{3.118}$$

  is given by the product of the Laplace transforms of $f(t)$ e $g(t)$,

$$\mathfrak{L}\{f(t)\star g(t)\}(s) = \mathfrak{L}\{f(t)\}(s)\,\mathfrak{L}\{g(t)\}(s) = \tilde{f}(s)\,\tilde{g}(s)\ . \tag{3.119}$$

  Although the definition of convolution given by Eq. (3.118) differs from the definition of convolution stated for the Fourier transform, Eq. (2.19), it shares the same properties,

$$commutative \quad \rightsquigarrow \quad f\star g = g\star f\ ; \tag{3.120}$$

$$associative \quad \rightsquigarrow \quad f\star(g\star h) = (f\star g)\star h\ ; \tag{3.121}$$

$$distributive \quad \rightsquigarrow \quad f\star(g+h) = f\star g + f\star h\ . \tag{3.122}$$

- *Ratio between two polynomials*
  Let us consider $\tilde{f}(s) = \tilde{G}(s)/\tilde{H}(s)$, where $\tilde{G}(s)$ and $\tilde{H}(s)$ are two polynomials such that the degree of $\tilde{H}(s)$ is greater than that of $\tilde{G}(s)$, and that $\tilde{H}(s)$ has only zeros with algebraic multiplicity 1. In that case, $\tilde{f}(s)$ can be expressed as the sum of partial fractions,

$$\tilde{f}(s) = \frac{c_1}{s-b_1} + \frac{c_2}{s-b_2} + \cdots + \frac{c_n}{s-b_n}\ , \tag{3.123}$$

  where $b_1, b_2, \ldots, b_n$ are the zeros of $\tilde{H}(s)$ and the coefficients c_i can be evaluated as

$$c_k = \lim_{s \to b_k} [(s - b_k)\, \tilde{f}(s)], \quad \forall k = 1, \ \ldots \ , n \ . \tag{3.124}$$

In other words, the coefficients c_k are the residues of $\tilde{f}(s)$ at the simple poles $s = b_k$. On account of the linearity and of the translation properties of the Laplace transform, we obtain

$$f(t) = c_1 \, \mathrm{e}^{b_1 t} + c_2 \, \mathrm{e}^{b_2 t} + \cdots + c_n \, \mathrm{e}^{b_n t} = \sum_{k=1}^{n} c_k \, \mathrm{e}^{b_k t} \ . \tag{3.125}$$

3.4.3 Meromorphic Functions

Let us assume that $\tilde{f}(s)$ has no essential singularities and that its poles $b_1, b_2, \ldots, b_n, \ldots$ are in the complex half-plane $\Re(s) < p$. The integral expressing the inverse Laplace transform of $\tilde{f}(s)$, Eq. (3.111), can be evaluated through a limit of the integral of

$$\tilde{f}(s) \, \mathrm{e}^{st} \tag{3.126}$$

evaluated on a closed path, γ, in the complex plane called the *Bromwich contour*,

$$f(t) = \lim_{R \to \infty} \left[\frac{1}{2\pi \, \mathrm{i}} \int_{\gamma} \tilde{f}(s) \, \mathrm{e}^{st} \, \mathrm{d}\, s \right] \ , \tag{3.127}$$

where R is the radius of the curved part of the Bromwich contour. A sketch of this contour in the complex plane is given in Fig. 3.6.

In the limit $R \to \infty$, the integral on the semicircular part of the Bromwich contour tends to zero provided that, on this semicircle, the following condition holds:

$$|\tilde{f}(s)| < \frac{M}{R^{\kappa}} \ , \tag{3.128}$$

where M and κ are positive constants [8, 9]. Moreover, in the limit $R \to \infty$, the integral along the vertical line of the Bromwich contour tends to coincide with the integral that appears in the inversion formula of the Laplace transform, Eq. (3.111). In the limit $R \to \infty$, the Bromwich contour encloses all the poles of $\tilde{f}(s)$. Hence, the inverse Laplace transform of $\tilde{f}(s)$ can be evaluated by employing Cauchy's residue Theorem 3.5,

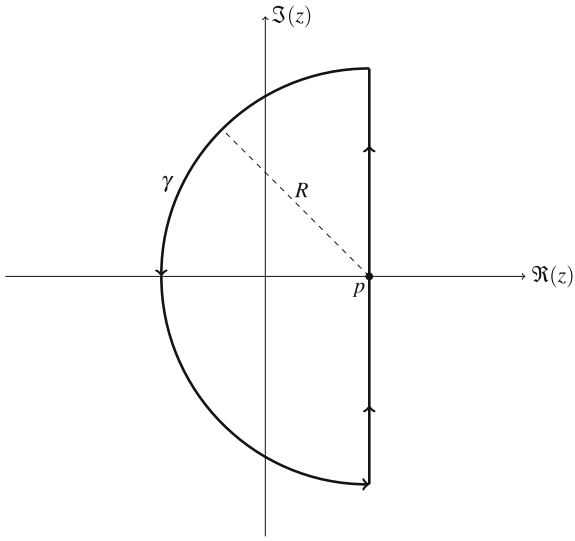

Fig. 3.6 Bromwich contour

$$f(t) = \frac{1}{2\pi\,\mathrm{i}} \int_{p-\mathrm{i}\,\infty}^{p+\mathrm{i}\,\infty} \tilde{f}(s)\,\mathrm{e}^{st}\,\mathrm{d}\,s = \lim_{R\to\infty} \left[\frac{1}{2\pi\,\mathrm{i}} \int_{\gamma} \tilde{f}(s)\,\mathrm{e}^{st}\,\mathrm{d}\,s \right] = \sum_{n} \mathrm{Res}\Big(\tilde{f}(s)\,\mathrm{e}^{st}; b_n \Big)\ , \tag{3.129}$$

where γ is the Bromwich contour.

Equation (3.129) is the basis for the evaluation of the inverse Laplace transform of $\tilde{f}(s)$ in all cases where $\tilde{f}(s)$ does not have either essential singularities or branch points.

3.5 Saddle Points

If $\mathscr{D}$ is an open connected subset of $\mathbb{C}$ and $\mathscr{D}^\circ$ its correspondent open connected subset of $\mathbb{R}^2$, a holomorphic function $f : \mathscr{D} \to \mathbb{C}$ can be rewritten as a function of two real variables, $f : \mathscr{D}^\circ \to \mathbb{R}^2$, by expressing $z = x + \mathrm{i}\,y$ and by evaluating the real and imaginary parts of $f(z)$. We have already pointed out that the resulting $f(x, y)$ is quite special on discussing the Cauchy–Riemann equations, Theorem 3.1. Other aspects of these special features are discussed in the following.

Let us denote by

$$u(x, y) = \Re(f(x + \mathrm{i}\,y))\ , \quad v(x, y) = \Im(f(x + \mathrm{i}\,y))\ , \tag{3.130}$$

the real and imaginary parts of a holomorphic function $f(z)$. Then, we can write

$$f(z) = u(x, y) + \mathrm{i}\, v(x, y) \,. \tag{3.131}$$

3.5.1 Stationary Point

Let us consider a point $z_0 = x_0 + \mathrm{i}\, y_0 \in \mathscr{D}$ such that $f'(z_0) = 0$. Since

$$x = \frac{z + \overline{z}}{2} \,, \quad y = \frac{z - \overline{z}}{2\mathrm{i}} \,, \tag{3.132}$$

we obtain

$$\begin{aligned} f'(z) &= \left[\frac{\partial u(x, y)}{\partial x}\,\frac{\partial x}{\partial z} + \frac{\partial u(x, y)}{\partial y}\,\frac{\partial y}{\partial z}\right] + \mathrm{i}\left[\frac{\partial v(x, y)}{\partial x}\,\frac{\partial x}{\partial z} + \frac{\partial v(x, y)}{\partial y}\,\frac{\partial y}{\partial z}\right] \\ &= \frac{1}{2}\left[\frac{\partial u(x, y)}{\partial x} - \mathrm{i}\,\frac{\partial u(x, y)}{\partial y}\right] + \frac{\mathrm{i}}{2}\left[\frac{\partial v(x, y)}{\partial x} - \mathrm{i}\,\frac{\partial v(x, y)}{\partial y}\right] \\ &= \frac{1}{2}\left[\frac{\partial u(x, y)}{\partial x} + \frac{\partial v(x, y)}{\partial y}\right] + \frac{\mathrm{i}}{2}\left[\frac{\partial v(x, y)}{\partial x} - \frac{\partial u(x, y)}{\partial y}\right] . \end{aligned} \tag{3.133}$$

The condition $f'(z_0) = 0$ implies that, at $(x, y) = (x_0, y_0)$, the following equations hold

$$\frac{\partial u}{\partial x} = -\frac{\partial v}{\partial y} \,, \qquad \frac{\partial v}{\partial x} = \frac{\partial u}{\partial y} \,. \tag{3.134}$$

By invoking the Cauchy–Riemann equations (3.22), one may conclude that Eqs. (3.22) and (3.134) can hold simultaneously at $(x, y) = (x_0, y_0)$ if and only if

$$\frac{\partial u}{\partial x} = 0 = \frac{\partial u}{\partial y} \,, \qquad \frac{\partial v}{\partial x} = 0 = \frac{\partial v}{\partial y} \,. \tag{3.135}$$

Equation (3.135) means that $(x, y) = (x_0, y_0)$, i.e. $z = z_0$, is a stationary point of both functions u and v.

The determinant of the Hessian matrix of either u or v may provide a characterisation of the stationary point [3]. We have to evaluate the second derivatives of $f(x, y)$,

$$\begin{aligned} \frac{\partial f(x, y)}{\partial x} &= f'(z)\,\frac{\partial z}{\partial x} = f'(z) \,, \quad \frac{\partial f(x, y)}{\partial y} = f'(z)\,\frac{\partial z}{\partial y} = \mathrm{i}\, f'(z) \,, \\ \frac{\partial^2 f(x, y)}{\partial x^2} &= f''(z) \,, \quad \frac{\partial^2 f(x, y)}{\partial y^2} = -\, f''(z) \,, \end{aligned} \tag{3.136}$$

so that we may conclude that $f(x, y)$ is a *harmonic function*, i.e. a solution of Laplace's equation,

$$\frac{\partial^2 f(x,y)}{\partial x^2} + \frac{\partial^2 f(x,y)}{\partial y^2} = 0\,. \tag{3.137}$$

This is also a consequence of Theorem 3.2. Since $f = u + \mathrm{i}\,v$, Eq. (3.137) yields

$$\frac{\partial^2 f(x,y)}{\partial x^2} + \frac{\partial^2 f(x,y)}{\partial y^2} = 0 \quad \Longrightarrow \quad \begin{cases} \dfrac{\partial^2 u(x,y)}{\partial x^2} + \dfrac{\partial^2 u(x,y)}{\partial y^2} = 0\,, \\ \dfrac{\partial^2 v(x,y)}{\partial x^2} + \dfrac{\partial^2 v(x,y)}{\partial y^2} = 0\,, \end{cases} \tag{3.138}$$

meaning that both $u(x,y)$ and $v(x,y)$ are harmonic functions. Equation (3.138) allows one to conclude that the Hessian matrix of $u(x,y)$ has a non-positive determinant at the stationary point (x_0, y_0), and likewise for $v(x,y)$,

$$\begin{vmatrix} \dfrac{\partial^2 u}{\partial x^2} & \dfrac{\partial^2 u}{\partial x\,\partial y} \\ \dfrac{\partial^2 u}{\partial y\,\partial x} & \dfrac{\partial^2 u}{\partial y^2} \end{vmatrix} = -\left(\frac{\partial^2 u}{\partial x^2}\right)^2 - \left(\frac{\partial^2 u}{\partial x\,\partial y}\right)^2 \leqslant 0\,. \tag{3.139}$$

As a consequence of Eq. (3.139), the eigenvalues of the Hessian matrix cannot be both positive or both negative, so that (x_0, y_0) can be neither a local maximum nor a local minimum. On the other hand, (x_0, y_0) can be a *saddle point* for $u(x,y)$ whenever the determinant of the Hessian matrix is strictly negative. With just the same argument, based on Eq. (3.138), this result can be achieved also for $v(x,y)$, namely

$$\begin{vmatrix} \dfrac{\partial^2 v}{\partial x^2} & \dfrac{\partial^2 v}{\partial x\,\partial y} \\ \dfrac{\partial^2 v}{\partial y\,\partial x} & \dfrac{\partial^2 v}{\partial y^2} \end{vmatrix} = -\left(\frac{\partial^2 v}{\partial x^2}\right)^2 - \left(\frac{\partial^2 v}{\partial x\,\partial y}\right)^2 \leqslant 0\,. \tag{3.140}$$

We note that the determinant of the Hessian matrix of either $u(x,y)$ or $v(x,y)$ is strictly negative at the stationary point $(x,y) = (x_0, y_0)$ when $f''(z_0) \neq 0$. In fact, by employing the Cauchy–Riemann equations (3.22), one obtains

$$\frac{\partial^2 u(x,y)}{\partial x^2} = \frac{\partial^2 v(x,y)}{\partial x\,\partial y}\,, \quad \frac{\partial^2 v(x,y)}{\partial x^2} = -\frac{\partial^2 u(x,y)}{\partial x\,\partial y}\,. \tag{3.141}$$

Thus, on account of Eqs. (3.136), (3.139), (3.140) and (3.141), one can infer that the determinant of the Hessian matrix of $u(x,y)$ at $(x,y) = (x_0, y_0)$ is given by

$$\begin{vmatrix} \dfrac{\partial^2 u}{\partial x^2} & \dfrac{\partial^2 u}{\partial x\,\partial y} \\ \dfrac{\partial^2 u}{\partial y\,\partial x} & \dfrac{\partial^2 u}{\partial y^2} \end{vmatrix} = -\left(\frac{\partial^2 u}{\partial x^2}\right)^2 - \left(\frac{\partial^2 v}{\partial x^2}\right)^2 = -\left|\frac{\partial^2 f}{\partial x^2}\right|^2 = -|f''(z_0)|^2 \leqslant 0\,. \tag{3.142}$$

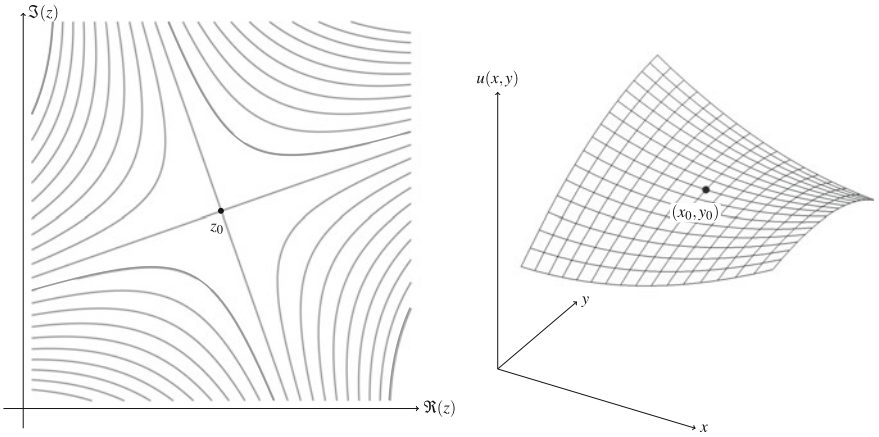

Fig. 3.7 Illustration of Theorem 3.6: contour lines of the real part of $f(z)$ around a saddle point $z_0 = x_0 + \mathrm{i}\, y_0$ and three-dimensional plot of $u(x, y) = \Re(f(x, y))$ at the saddle point

Likewise, for the determinant of the Hessian matrix of $v(x, y)$ at $(x, y) = (x_0, y_0)$, one obtains

$$\begin{vmatrix} \dfrac{\partial^2 v}{\partial x^2} & \dfrac{\partial^2 v}{\partial x\, \partial y} \\ \dfrac{\partial^2 v}{\partial y\, \partial x} & \dfrac{\partial^2 v}{\partial y^2} \end{vmatrix} = -\left(\frac{\partial^2 u}{\partial x^2}\right)^2 - \left(\frac{\partial^2 v}{\partial x^2}\right)^2 = -\left|\frac{\partial^2 f}{\partial x^2}\right|^2 = -|f''(z_0)|^2 \leqslant 0\,. \tag{3.143}$$

The conclusion of this reasoning can be stated in the form of a theorem.

Theorem 3.6 *Let $\mathscr{D}$ be an open connected subset of $\mathbb{C}$, and $f : \mathscr{D} \to \mathbb{C}$ be holomorphic in $\mathscr{D}$. If there exists $z_0 = x_0 + \mathrm{i}\, y_0 \in \mathscr{D}$ such that $f'(z_0) = 0$ and $f''(z_0) \neq 0$, then both the real and the imaginary parts of $f(x, y) = f(x + \mathrm{i}\, y)$ have a saddle point at $(x, y) = (x_0, y_0)$.*

The saddle-point concept as discussed in Theorem 3.6 is drawn qualitatively in Fig. 3.7. In the figure caption, it is mentioned the real part of $f(z)$, but there is no intrinsic difference in the graphical features if one deals with the imaginary part.

A comment on Theorem 3.6 can be useful. One may wonder what happens when $f''(z_0) = 0$. The answer is that, strictly speaking, one cannot employ the criterion based on the sign of the determinant of the Hessian matrix, as it becomes inconclusive when the determinant vanishes [3]. In fact, one may distinguish a case where all derivatives of $f(z)$ vanish at $z = z_0$, namely $f^{(n)}(z_0) = 0$ for all $n \geqslant 1$. In this case, a Taylor series expansion of $f(z)$ around $z = z_0$ is sufficient to prove that $f(z)$ is constant over the open connected subset of $\mathscr{D}$. A more interesting alternative is when there exists $n \geqslant 3$ such that $f^{(n)}(z_0) \neq 0$. In this case, strictly speaking, we do not have a saddle point at $z = z_0$. In fact, we are dealing with a saddle point in a generalised sense. A sketch of the geometrical features in a sample case with $n = 3$ is

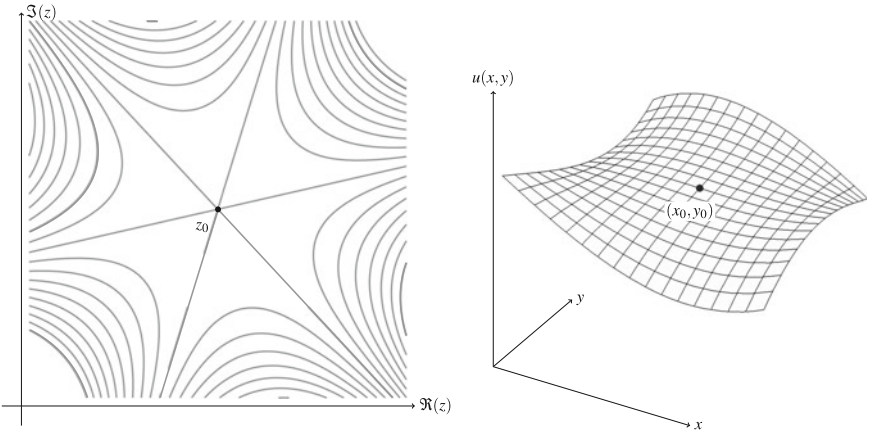

Fig. 3.8 Contour lines of the real part of $f(z)$ around a monkey saddle point $z_0 = x_0 + \mathrm{i}\, y_0$, where $f'(z_0) = f''(z_0) = 0$ with $f'''(z_0) \neq 0$, and three-dimensional plot of $u(x, y) = \Re(f(x, y))$ at the saddle point

presented in Fig. 3.8. This case is also called monkey saddle, as a saddle for monkeys should allow a place for the tail and not only for the legs. For the *generalised saddle points*, when the lowest n such that $f^{(n)}(z_0) \neq 0$ is greater than 2, we call n the *order* of the saddle point. A saddle point where $f''(z_0) \neq 0$ has order 2.

Whatever is the order of the saddle point, there exist ascending and descending paths that depart from z_0. This is clearly seen in the three-dimensional plots, reported in Figs. 3.7 and 3.8, displaying $\Re(f(z))$ versus (x, y). Among these ascending and descending paths, one may graphically detect those of *steepest ascent* and *steepest descent*. These paths are central in the formulation of the asymptotic approximation of wave packets at large times.

3.5.2 *Paths from a Saddle Point*

We consider an open connected subset of $\mathbb{C}$, namely $\mathscr{D}$, and a holomorphic function $f : \mathscr{D} \to \mathbb{C}$. Let $z_0 \in \mathscr{D}$ be a saddle point of order n.

In a small neighbourhood of z_0, one can express z as

$$z = z_0 + r\, \mathrm{e}^{\mathrm{i}\varphi} , \quad r \geqslant 0 , \quad \varphi \in [0, 2\pi] . \tag{3.144}$$

Moreover, one can write an approximate expression of $f(z)$ as a Taylor series centred in $z = z_0$ and truncated to the first two nonzero terms, namely

$$f(z) \approx f(z_0) + \frac{1}{n!} f^{(n)}(z_0)\, (z - z_0)^n . \tag{3.145}$$

Here, we are neglecting terms of order $|z - z_0|^{n+1}$, and we are assuming that all derivatives of $f(z)$ up to order $n-1$ are zero at $z = z_0$. We write $f^{(n)}(z_0)$ in its polar form as

$$f^{(n)}(z_0) = |f^{(n)}(z_0)|\, e^{\mathrm{i}\,\theta} \ , \tag{3.146}$$

where θ is the argument of $f^{(n)}(z_0)$. On substituting Eqs. (3.144) and (3.146) into (3.145), we obtain

$$\begin{aligned} f(z) &\approx f(z_0) + \frac{1}{n!}\,|f^{(n)}(z_0)|\, r^n\, e^{\mathrm{i}\,(\theta + n\,\varphi)} \\ &= f(z_0) + \frac{1}{n!}\,|f^{(n)}(z_0)|\, r^n \Big[\, \cos(\theta + n\,\varphi) + \mathrm{i}\, \sin(\theta + n\,\varphi) \Big] \ . \end{aligned} \tag{3.147}$$

On inspecting Eq. (3.147), one can conclude that the value of $\theta + n\,\varphi$ delineates if and how the real and imaginary parts of function $f(z)$ increase or decrease when z departs from the saddle point z_0 .

Let us consider $\Re(f(z))$. Equation (3.147) implies that $\Re(f(z))$ undergoes the steepest increase when z departs from z_0 if one chooses a path given by any line with $\cos(\theta + n\,\varphi) = 1$. Thus we define, for $\Re(f(z))$, the lines of *steepest ascent* from z_0 as those where

$$\begin{gathered} \theta + n\,\varphi = 2m\pi \quad \longmapsto \quad \varphi = \frac{2m}{n}\,\pi - \frac{\theta}{n} \ , \\ m = 0, 1, 2, \ \ldots \ , \ n-1 \ . \end{gathered} \tag{3.148}$$

Since there exist n different determinations of the angle φ, predicted by Eq. (3.148), there are n different paths of steepest ascent, for $\Re(f(z))$, departing from z_0. These paths can be easily detected in Figs. 3.7 and 3.8 and are explicitly displayed as thick dashed lines in Fig. 3.9 for a saddle point of order 2 and in Fig. 3.10 for a saddle point of order 3.

In an analogous way, we can easily detect those lines departing from the saddle point z_0 and such that $\Re(f(z))$ undergoes the steepest decrease. Those lines are termed of *steepest descent* and, on account of Eq. (3.147), they are defined by the condition $\cos(\theta + n\,\varphi) = -1$. Then, lines of steepest descent are such that

$$\begin{gathered} \theta + n\,\varphi = (2m+1)\pi \quad \longmapsto \quad \varphi = \frac{2m+1}{n}\,\pi - \frac{\theta}{n} \ , \\ m = 0, 1, 2, \ \ldots \ , \ n-1 \ . \end{gathered} \tag{3.149}$$

Again, there exist n different possible angles φ, predicted by Eq. (3.149) and, hence, there are n different paths of steepest descent, for $\Re(f(z))$, departing from z_0. These paths can be easily detected in Figs. 3.7 and 3.8 and are explicitly displayed as thick solid lines in Figs. 3.9 and 3.10 for saddle points of order 2 and 3, respectively.

We note that, along the lines of steepest ascent or steepest descent of $\Re(f(z))$ departing from a saddle point z_0, the imaginary part of $f(z)$ remains constant. In fact, Eqs. (3.148) and (3.149) imply that, along lines of steepest ascent or steepest

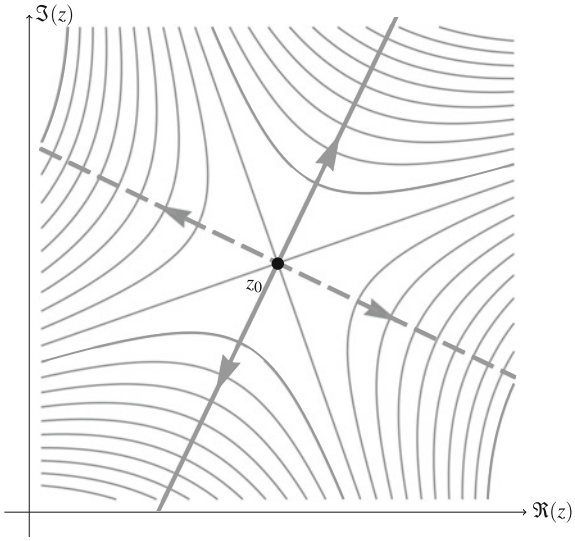

Fig. 3.9 Contour lines of the real part of $f(z)$ around a saddle point z_0 of order 2. The thick solid lines are the paths of steepest descent, while the thick dashed lines are the paths of steepest ascent

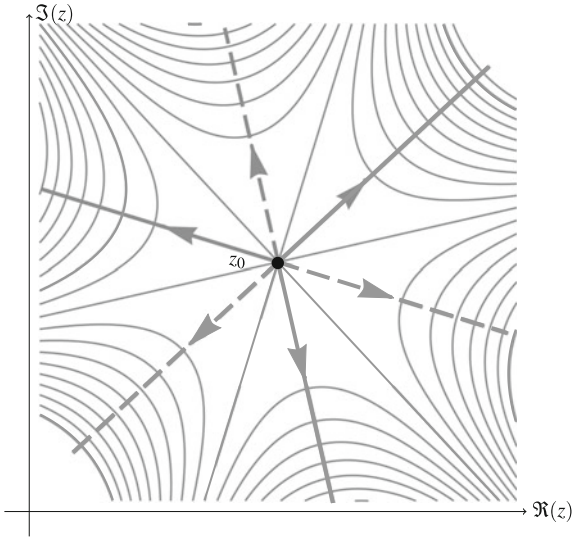

Fig. 3.10 Contour lines of the real part of $f(z)$ around a monkey saddle point, i.e. a saddle point z_0 of order 3. The thick solid lines are paths of steepest descent, while the thick dashed lines are paths of steepest ascent

descent of $\Re(f(z))$, $\theta + n\,\varphi$ is an integer multiple of π, so that $\sin(\theta + n\,\varphi)$ is zero. Thus, Eq. (3.147) implies that $\Im(f(z)) = \Im(f(z_0))$ along lines of steepest ascent or steepest descent of $\Re(f(z))$. In other words, the lines of steepest ascent or steepest descent of $\Re(f(z))$ are contour lines of $\Im(f(z))$.

3.5.3 Asymptotic Behaviour of Wave Packets at Large Times

Let us consider the three-dimensional wave packet given by Eq. (2.98),

$$\psi(\mathbf{x}, t) = \int_{-\infty}^{\infty} b(k, y, z, t)\, \mathrm{e}^{\mathrm{i}\,[kx - \omega(k)\,t]}\, \mathrm{d}\,k\ . \tag{3.150}$$

A particularly interesting case is one where the dependence on time of $b(k, y, z, t)$ is through an exponential function,

$$b(k, y, z, t) = \hat{b}(k, y, z)\, \mathrm{e}^{\eta(k)\,t}\ . \tag{3.151}$$

Then, on account of Eqs. (3.150) and (3.151), the expression of $\psi(\mathbf{x}, t)$, for a fixed position $\mathbf{x} = (x, y, z)$, is given by the time-dependent integral

$$I(t) = \int_{-\infty}^{\infty} \phi(k)\, \mathrm{e}^{\lambda(k)\,t}\, \mathrm{d}\,k\ . \tag{3.152}$$

Here, the complex function $\lambda(k)$ is defined as

$$\lambda(k) = \eta(k) - \mathrm{i}\,\omega(k)\ , \tag{3.153}$$

while

$$\phi(k) = \hat{b}(k, y, z)\, \mathrm{e}^{\mathrm{i}\,kx}\ . \tag{3.154}$$

The dependence of $\phi(k)$ on (x, y, z) is not explicitly declared with this notation as what really matters, in the forthcoming analysis, is just the dependence on time of the integral $I(t)$ or, equivalently, we can consider our reasoning as relative to a fixed position (x, y, z).

We aim to determine an approximate evaluation of $I(t)$ for large times t. This task can be managed by employing Theorem 3.3. In fact, integral $I(t)$ given by Eq. (3.152) can be considered as a path integral along a contour line γ coincident with the real axis in the complex plane and oriented along its positive direction,

$$I(t) = \int_{\gamma} \phi(k)\, \mathrm{e}^{\lambda(k)\,t}\, \mathrm{d}\,k\ . \tag{3.155}$$

Let us first imagine a situation where there exists a unique saddle point of function $\lambda(k)$, namely $k_0 \in \mathbb{C}$, and that $\phi(k)$ is not singular in k_0. We can imagine to deform path γ to γ^*, where γ^* crosses the saddle point k_0. A sketch of γ and γ^* is provided in Fig. 3.11. The question is whether $I(t)$ coincides with

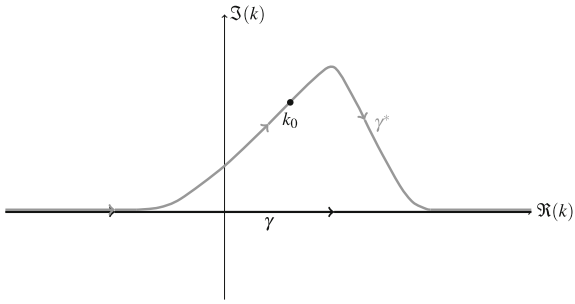

Fig. 3.11 Qualitative sketch of path γ, coincident with the real axis, and γ^* crossing the saddle point k_0 of $\lambda(k)$

$$I^*(t) = \int_{\gamma^*} \phi(k)\, \mathrm{e}^{\lambda(k)\, t}\, \mathrm{d}\, k \ . \tag{3.156}$$

The answer relies on Theorem 3.3. Integrals $I(t)$ and $I^*(t)$ coincide if path γ can be continuously deformed into γ^* within the domain where the integrand $\phi(k)\, \mathrm{e}^{\lambda(k)\, t}$ is holomorphic. In other words, one must check that no singularity of $\phi(k)\, \mathrm{e}^{\lambda(k)\, t}$ exists within the region bounded by $\gamma \cup \gamma^*$. This feature will be hereafter termed *holomorphy requirement*.

An interesting case is when γ^* locally coincides with a steepest descent path for $\Re(\lambda(k))$, crossing k_0. If k_0 is a second-order saddle point, in a small neighbourhood of k_0, we can approximate the integrand $\phi(k)\, \mathrm{e}^{\lambda(k)\, t}$, according to Eq. (3.144), as

$$\phi(k)\, \mathrm{e}^{\lambda(k)\, t} \approx \phi(k_0)\, \mathrm{e}^{\lambda(k_0)\, t}\, \mathrm{e}^{\lambda''(k_0)(k-k_0)^2\, t/2} \ . \tag{3.157}$$

Thus, following Eqs. (3.147) and (3.149) with $n = 2$, we get

$$\phi(k)\, \mathrm{e}^{\lambda(k)\, t} \approx \phi(k_0)\, \mathrm{e}^{\lambda(k_0)\, t}\, \mathrm{e}^{-\,|\lambda''(k_0)|r^2\, t/2} \ . \tag{3.158}$$

A change of r in the small interval $[0, \varepsilon]$, for a positive $\varepsilon \ll 1$, provides a local parametrization of γ^* in a small neighbourhood of k_0.

A key point in the formulation of the *steepest-descent approximation* is the following. The dominant contribution to $I^*(t)$ comes from a small neighbourhood of k_0, where the exponential $|\mathrm{e}^{\lambda(k)\, t}| = \mathrm{e}^{\Re(\lambda(k))\, t}$ is at its largest. In other words, an approximation of $I^*(t)$ is given by

$$I^*(t) = \int_{\gamma^*} \phi(k)\, \mathrm{e}^{\lambda(k)\, t}\, \mathrm{d}\, k \approx 2\, \mathrm{e}^{\mathrm{i}\, \varphi}\, \phi(k_0)\, \mathrm{e}^{\lambda(k_0)\, t} \int_0^{\varepsilon} \mathrm{e}^{-\,|\lambda''(k_0)|r^2\, t/2}\, \mathrm{d}\, r \ , \tag{3.159}$$

where the parametrization $k = k_0 + r\, \mathrm{e}^{\mathrm{i}\, \varphi}$, Eq. (3.144), has been used. We note that factor 2 comes from doubling the contribution of the integral over $r \in [0, \varepsilon]$ to include a piece of steepest ascent path to reach k_0 and one of steepest descent departing from

k_0. When t is very large, the integral of $\mathrm{e}^{-|\lambda''(k_0)|r^2 t/2}$ over $r \in [0, \varepsilon]$ does not differ much from the integral over $r \in [0, \infty]$, as the Gaussian function undergoes a rapid decay to 0 as r increases. Thus, we can write

$$I^*(t) \approx 2\,\mathrm{e}^{\mathrm{i}\,\varphi}\,\phi(k_0)\,\mathrm{e}^{\lambda(k_0)\,t} \int_0^\infty \mathrm{e}^{-|\lambda''(k_0)|r^2\,t/2}\,\mathrm{d}\,r$$
$$= \mathrm{e}^{\mathrm{i}\,\varphi}\,\phi(k_0)\,\mathrm{e}^{\lambda(k_0)\,t}\sqrt{\frac{2\pi}{|\lambda''(k_0)|\,t}}\ . \tag{3.160}$$

From Eq. (3.149), we infer that φ is either $\pi/2 - \theta/2$ or $3\pi/2 - \theta/2$, where θ is the argument of $\lambda''(k_0)$. As a consequence, we obtain

$$I^*(t) \approx \pm\,\mathrm{i}\,\mathrm{e}^{-\mathrm{i}\,\theta/2}\,\phi(k_0)\,\mathrm{e}^{\lambda(k_0)\,t}\sqrt{\frac{2\pi}{|\lambda''(k_0)|\,t}}\ . \tag{3.161}$$

Let us assume the validity of the holomorphy requirement, then Theorem 3.3 ensures that $I(t) = I^*(t)$ and we achieve the steepest-descent approximation of $I(t)$ at large times,

$$I(t) = \int_{-\infty}^{\infty} \phi(k)\,\mathrm{e}^{\lambda(k)\,t}\,\mathrm{d}\,k \approx \pm\,\mathrm{i}\,\mathrm{e}^{-\mathrm{i}\,\theta/2}\,\phi(k_0)\,\mathrm{e}^{\lambda(k_0)\,t}\sqrt{\frac{2\pi}{|\lambda''(k_0)|\,t}}\ . \tag{3.162}$$

The ambiguity in the sign of the approximated integral is a consequence of the a-priori twofold choice in the definition of the steepest descent path that drives k away from k_0 along path γ^*, as suggested by Fig. 3.9. This is not a big problem when one is interested just in the large-time behaviour of $|I(t)|$, given by

$$|I(t)| \approx |\phi(k_0)|\,\mathrm{e}^{\Re(\lambda(k_0))\,t}\sqrt{\frac{2\pi}{|\lambda''(k_0)|\,t}}\ . \tag{3.163}$$

If we now relax the assumption that k_0 is a second-order saddle point of $\lambda(k)$ and assume a $n > 2$ order of the saddle point, Eq. (3.158) is now replaced by

$$\phi(k)\,\mathrm{e}^{\lambda(k)\,t} \approx \phi(k_0)\,\mathrm{e}^{\lambda(k_0)\,t}\,\mathrm{e}^{-|\lambda^{(n)}(k_0)|r^n\,t/n!}\ . \tag{3.164}$$

Equation (3.160) is modified into

$$I^*(t) \approx 2\,\mathrm{e}^{\mathrm{i}\,\varphi}\,\phi(k_0)\,\mathrm{e}^{\lambda(k_0)\,t}\int_0^\infty \mathrm{e}^{-\,|\lambda^{(n)}(k_0)|r^n\,t/n!}\,\mathrm{d}\,r$$

$$= \frac{2}{n}\,\mathrm{e}^{\mathrm{i}\,\varphi}\,\phi(k_0)\,\Gamma\left(\frac{1}{n}\right)\mathrm{e}^{\lambda(k_0)\,t}\left(\frac{n!}{|\lambda^{(n)}(k_0)|\,t}\right)^{1/n}. \tag{3.165}$$

Here, $\Gamma(z)$ is *Euler's gamma function* [2],

$$\Gamma(z) = \int_0^\infty s^{\,z-1}\,\mathrm{e}^{-s}\,\mathrm{d}\,s\ . \tag{3.166}$$

Finally, Eqs. (3.162) and (3.163) are generalised to

$$I(t) = \int_{-\infty}^{\infty}\phi(k)\,\mathrm{e}^{\lambda(k)\,t}\,\mathrm{d}\,k$$

$$\approx \frac{2}{n}\,\mathrm{e}^{\mathrm{i}\,(2m+1)\pi/n}\,\mathrm{e}^{-\mathrm{i}\,\theta/n}\,\phi(k_0)\,\Gamma\left(\frac{1}{n}\right)\mathrm{e}^{\lambda(k_0)\,t}\left(\frac{n!}{|\lambda^{(n)}(k_0)|\,t}\right)^{1/n}, \tag{3.167}$$

where $m = 0, 1, 2, \ \ldots\ , n-1$, and

$$|I(t)| \approx \frac{2}{n}\,|\phi(k_0)|\,\Gamma\left(\frac{1}{n}\right)\mathrm{e}^{\Re(\lambda(k_0))\,t}\left(\frac{n!}{|\lambda^{(n)}(k_0)|\,t}\right)^{1/n}. \tag{3.168}$$

Equation (3.167) shows the effects of the multiplicity of the possible steepest descent paths that depart from k_0, resulting in n possible values of the positive integer m. As m appears just in a phase factor, this multiplicity is ineffective when one deals with $|I(t)|$, as shown by Eq. (3.168).

We assumed the existence of just one saddle point of $\lambda(k)$. What if there are more? With several saddle points, the steepest-descent approximation just keeps that or those leading to the largest $\Re(\lambda(k_0))$, so that one filters the leading contribution to the integral $I(t)$. It is possible that two or more saddle points share the same value of $\Re(\lambda(k_0))$. In that case, their contributions have to be summed up in order to form the asymptotic approximation of the integral $I(t)$.

For a more detailed and exhaustive discussion of the steepest-descent approximation of time-dependent integrals, we refer the reader to textbooks on applied mathematics such as Ablowitz and Fokas [1], Bender and Orszag [5], or the more recent Arfken et al. [4]. All these books include a discussion of several examples where the steepest-descent approximation is employed.

Example 3.7 Let us consider a case where $I(t)$, given by Eq. (3.152), is defined with $\phi(k) = 1$ and

$$\lambda(k) = -4k^2 + 2k + 4\,\mathrm{i}\,k\ , \tag{3.169}$$

namely

$$I(t) = \int_{-\infty}^{\infty} \mathrm{e}^{(-4k^2+2k+4\,\mathrm{i}\,k)\,t}\,\mathrm{d}\,k\ . \tag{3.170}$$

The integral on the right-hand side of Eq. (3.170) can be evaluated analytically, so that we obtain

$$I(t) = \frac{1}{2}\sqrt{\frac{\pi}{t}}\,\mathrm{e}^{-3\,t/4}\,\mathrm{e}^{\mathrm{i}\,t}\ . \tag{3.171}$$

There is an interesting fact about Eqs. (3.170) and (3.171). The integrand in Eq. (3.170) tends to ∞ when $t \to \infty$, for every k such that $0 < k < 1/2$. On the other hand, Eq. (3.171) shows that $I(t)$ tends to 0 when $t \to \infty$. This situation is often reproduced with wave packets: although there are normal modes whose amplitude grows in time, the wave packet as a whole might tend to 0 in the limit $t \to \infty$.

One can apply to Eq. (3.170) the steepest-descent approximation. Since

$$\lambda'(k) = -8k + 2 + 4\,\mathrm{i}\ , \qquad \lambda''(k) = -8\ , \tag{3.172}$$

there is a single saddle point,

$$k_0 = \frac{1+2\,\mathrm{i}}{4}\ , \tag{3.173}$$

of order $n = 2$. We have

$$\lambda(k_0) = -\frac{3}{4} + \mathrm{i}\ . \tag{3.174}$$

Function $\lambda(k)$ satisfies the holomorphy requirement over the whole complex plane. We can thus apply Eq. (3.163) to obtain

$$|I(t)| \approx \frac{1}{2}\sqrt{\frac{\pi}{t}}\,\mathrm{e}^{-3\,t/4}\ . \tag{3.175}$$

In fact, in this case, the steepest-descent approximation yields the exact result for $|I(t)|$, as it can be easily checked by comparing Eqs. (3.171) and (3.175).

Example 3.8 A classical application of the steepest-descent method is given by *Stirling's approximation* of the factorial [2]. We base the evaluation on Euler's gamma function, defined by Eq. (3.166), and on its property that, if n is a natural number, then $n! = \Gamma(n+1)$ [2]. In fact, from Eq. (3.166), we can write

$$n! = \int_0^{\infty} s^n\,\mathrm{e}^{-s}\,\mathrm{d}\,s\ . \tag{3.176}$$

We change the variable of integration to $r = s/n$, so that we obtain

$$n! = n^{n+1} \int_0^\infty \mathrm{e}^{[\ln(r)-r]\,n}\,\mathrm{d}\,r\ . \tag{3.177}$$

We aim to achieve an approximate expression of the integral on the right-hand side of Eq. (3.177) when n is very large. Then, we invoke the steepest-descent approximation. We have

$$\lambda(r) = \ln(r) - r\ . \tag{3.178}$$

There is just one saddle point, $\lambda'(r_0) = 0$, namely $r_0 = 1$. We obtain

$$\lambda(r_0) = -1\ , \qquad \lambda''(r_0) = -1\ . \tag{3.179}$$

The saddle point is placed on the real axis and it is of order $n = 2$. The argument of $\lambda''(r_0)$ is $\theta = \pi$ and the steepest descent path just coincides with the real axis oriented along its positive direction. This is a simple case where $\gamma = \gamma^*$. From Eqs. (3.162) and (3.177), we can finally write

$$n! \approx \sqrt{2\pi}\ n^{n+1/2}\ \mathrm{e}^{-n}\ , \tag{3.180}$$

which is the well-known Stirling's approximation for the factorial of a large natural number n.

References

1. Ablowitz MJ, Fokas AS (2003) Complex variables: introduction and applications. Cambridge University Press, Cambridge
2. Abramowitz M, Stegun I (1968) Handbook of mathematical functions. Dover, New York
3. Apostol TM (1967) Calculus, vol. 2: multi-variable calculus and linear algebra with applications to differential equations and probability. Wiley, New York
4. Arfken GB, Weber HJ, Harris FE (2012) Mathematical methods for physicists: a comprehensive guide. Elsevier, New York
5. Bender CM, Orszag SA (1999) Advanced mathematical methods for scientists and engineers I. Springer, New York
6. Cartan H (1995) Elementary theory of analytic functions of one or several complex variables. Dover, New York
7. Debnath L, Bhatta D (2014) Integral transforms and their applications. CRC Press, New York
8. Priestley HA (2003) Introduction to complex analysis. Oxford University Press, Oxford
9. Schiff JL (1999) The Laplace transform: theory and applications. Springer, New York

Chapter 4
Instability of a Flow System

4.1 Stability and Instability of a Mechanical System

The concepts presented in this section are a simplified version of what is available in many textbooks on dynamical systems and classical mechanics. For a deeper discussion of the topics proposed here, we refer the reader to Hirsch et al. [8] and Arnold [1].

The state of a mechanical system is uniquely determined by a number N of spatial coordinates, $q_1, q_2, \ldots, q_N$, and a number N of velocities associated with these coordinates, $v_1, v_2, \ldots, v_N$. The state of the system is thus a point of a $2N$-dimensional space called *phase space*. The number N is the *number of degrees of freedom* of the system.

For simplicity of notation, the N coordinates will be denoted by the N-dimensional vector $\mathbf{q}$, while the N velocities will be denoted by the N-dimensional vector $\mathbf{v}$. The motion of the mechanical system is described by the system of first-order differential equations,

$$\begin{cases} \dfrac{\mathrm{d}\,\mathbf{q}}{\mathrm{d}\,t} = \mathbf{v}\ , \\ \dfrac{\mathrm{d}\,\mathbf{v}}{\mathrm{d}\,t} = \mathbf{F}(\mathbf{q}, \mathbf{v})\ , \end{cases} \tag{4.1}$$

where the N-dimensional vector $\mathbf{F}$ is built with the components of the force per unit mass acting on the system. For instance, let the studied system consist of N_p pointlike masses, then $N = 3\,N_p$. In this case, if q_i is the jth coordinate (where j varies from 1 to 3) of the ℓth pointlike mass (where ℓ varies from 1 to N_p) with mass m_ℓ, then the component $F_i(\mathbf{q}, \mathbf{v})$ is the jth component of the force acting on the ℓth pointlike mass of the system divided by the mass m_ℓ.

The original version of this chapter was revised: For detailed information please see correction. The correction to this chapter is available at https://doi.org/10.1007/978-3-030-06194-4_11

A. Barletta, *Routes to Absolute Instability in Porous Media*,
https://doi.org/10.1007/978-3-030-06194-4_4

The solution of Eq. (4.1) requires the specification of the *initial state*, or the state $\{\mathbf{q}(0), \mathbf{v}(0)\}$ owned by the system at the initial instant of time, $t = 0$. Geometrically, this solution yields a trajectory in the phase space.

The concept of stability of a solution of Eq. (4.1) is formulated according to *Lyapunov's definition*.[1] A motion of the mechanical system, i.e. a solution $\{\mathbf{q}(t), \mathbf{v}(t)\}$ of the system of Eqs. (4.1), is called *stable* if for any positive real number ε, there is a corresponding positive real number δ_ε such that if the distance between two initial conditions, $\{\mathbf{q}(0), \mathbf{v}(0)\}$ and $\{\mathbf{q}^\star(0), \mathbf{v}^\star(0)\}$, is less than δ_ε, then the two trajectories in the phase space, $\{\mathbf{q}(t), \mathbf{v}(t)\}$ and $\{\mathbf{q}^\star(t), \mathbf{v}^\star(t)\}$, have a distance less than ε for every instant of time $t > 0$. In mathematical form, this definition can be expressed as follows,

$$\forall\, \varepsilon > 0\,, \quad \exists\, \delta_\varepsilon > 0: \qquad \left\| \{\mathbf{q}(0), \mathbf{v}(0)\} - \{\mathbf{q}^\star(0), \mathbf{v}^\star(0)\} \right\| < \delta_\varepsilon \tag{4.2}$$

implies that

$$\left\| \{\mathbf{q}(t), \mathbf{v}(t)\} - \{\mathbf{q}^\star(t)\,, \mathbf{v}^\star(t)\} \right\| < \varepsilon\,, \quad \forall\, t > 0\,. \tag{4.3}$$

The distance $\|\cdot\|$ between any two points in the phase space is the Euclidean distance

$$\left\| \{\mathbf{q}, \mathbf{v}\} - \{\mathbf{q}^\star, \mathbf{v}^\star\} \right\| = \left[\frac{1}{\mathscr{A}} \sum_{i=1}^{N} (q_i - q_i^\star)^2 + \frac{1}{\mathscr{V}^2} \sum_{i=1}^{N} (v_i - v_i^\star)^2 \right]^{1/2}, \tag{4.4}$$

where we introduced two constants, $\mathscr{A}$ and $\mathscr{V}$, with the dimensions of a length and a velocity, respectively. These constants, whose value is set conventionally, are introduced for the sole purpose of defining the distance between any two points of the phase space in a dimensionless way.

In order to give a visual representation of the concept of stability of motion as stated above, we can imagine that around a stable trajectory in phase space, there is a cylinder of radius ε within which all the trajectories that differ from the stable trajectory for a small perturbation of the initial conditions are contained. A graphical representation of this notion is given in Fig. 4.1.

The concept of stability of motion for a mechanical system also applies to those particular motions of the system that correspond to equilibrium states. A solution of the equations of motion (4.1) is called an *equilibrium state* if it takes the form

$$\{\mathbf{q}(t), \mathbf{v}(t)\} = \{\mathbf{q}_0, \mathbf{0}\}\,, \qquad \forall\, t \geq 0\,, \tag{4.5}$$

where $\mathbf{q}_0$ is an N-dimensional constant vector, and $\mathbf{0}$ is the N-dimensional vector with zero components. Thus, an equilibrium state corresponds to a trivial trajectory that degenerates into a point. The equilibrium states admitted by a system of forces $\mathbf{F}(\mathbf{q}, \mathbf{v})$ are of course obtained as solutions of the vector equation

[1] Aleksandr Mikhailovich Lyapunov (1857–1918) was a Russian mathematician. He defended his doctoral thesis, entitled "The general problem of the stability of motion", at the University of Moscow in 1892.

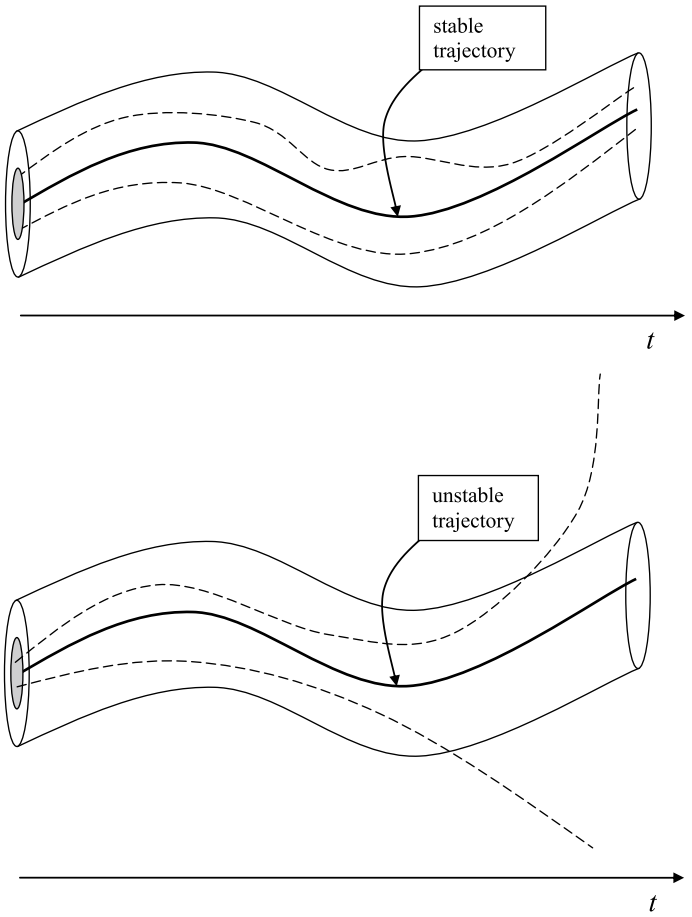

Fig. 4.1 Qualitative sketch of stable and unstable trajectories in phase space according to Lyapunov's definition

$$\mathbf{F}(\mathbf{q}, \mathbf{0}) = \mathbf{0} \,. \tag{4.6}$$

According to the most general definition expressed by Eqs. (4.2) and (4.3), an equilibrium state is deemed stable if

$$\forall\, \varepsilon > 0 \,, \quad \exists\, \delta_\varepsilon > 0 : \qquad \left\| \{\mathbf{q}_0, \mathbf{0}\} - \{\mathbf{q}^\star(0), \mathbf{v}^\star(0)\} \right\| < \delta_\varepsilon \tag{4.7}$$

implies that

$$\left\| \{\mathbf{q}_0, \mathbf{0}\} - \{\mathbf{q}^\star(t) \,, \mathbf{v}^\star(t)\} \right\| < \varepsilon \,, \quad \forall\, t > 0 \,. \tag{4.8}$$

This notion of stability of an equilibrium state is often referred to as stability according to Lyapunov.

A stable equilibrium state, $\{\mathbf{q}_0, \mathbf{0}\}$, of a mechanical system is called *asymptotically stable* if there exists a positive real number $\mathscr{R}$ such that

$$\left\| \{\mathbf{q}_0, \mathbf{0}\} - \{\mathbf{q}^\star(0), \mathbf{v}^\star(0)\} \right\| < \mathscr{R} \tag{4.9}$$

implies that

$$\lim_{t \to \infty} \left\| \{\mathbf{q}_0, \mathbf{0}\} - \{\mathbf{q}^\star(t), \mathbf{v}^\star(t)\} \right\| = 0 \, . \tag{4.10}$$

For an asymptotically stable equilibrium state, any trajectory in phase space that originates from an initial state $\{\mathbf{q}^\star(0), \mathbf{v}^\star(0)\}$, lying in a small neighbourhood of the equilibrium state $\{\mathbf{q}_0, \mathbf{0}\}$, tends to collapse to this state when time tends to infinity.

We note that asymptotic stability is a condition stronger than stability, so that asymptotic stability of an equilibrium state implies stability, but not vice versa.

It should also be noted that the concepts of stability and of asymptotic stability for an equilibrium state have, in general, a local meaning. In other words, these concepts are the result of a criterion, Lyapunov's criterion, which refers only to those motions that originate from the neighbourhood of an equilibrium state, i.e. for initial conditions that lie in a neighbourhood of this state. Lyapunov's criterion does not provide information on those trajectories whose initial condition is very far from the equilibrium state. The local or global nature of the stability of an equilibrium state of a mechanical system relies, ultimately, on the linearity or nonlinearity of the system. A mechanical system is said to be *linear* if the vector function $\mathbf{F}(\mathbf{q}, \mathbf{v})$ is linear, otherwise it is deemed *nonlinear*. Generally speaking, the stability has a local character for nonlinear mechanical systems and has a global character for linear systems. For nonlinear mechanical systems, around an asymptotically stable equilibrium state, there is a region of phase space called *basin of attraction*, such that any state within the basin of attraction evolves along a trajectory that for $t \to \infty$ collapses onto the equilibrium state. On the contrary, any state outside the basin of attraction evolves along a trajectory that cannot enter the basin of attraction, for every instant of time $t > 0$.

4.1.1 A Simple Mechanical System

As an example, consider the simplest case of a mechanical system, namely a system with only one degree of freedom, $N = 1$. For this system, the phase space is two-dimensional, the state is described by the pair $\{q, v\}$, and the equations of motion take the form

$$\begin{cases} \dfrac{\mathrm{d}\, q}{\mathrm{d}\, t} = v \, , \\ \dfrac{\mathrm{d}\, v}{\mathrm{d}\, t} = F(q, v) \, . \end{cases} \tag{4.11}$$

In other terms, we consider a pointlike mass m subject to an external force. We assume that the function $F(q, v)$ is given by

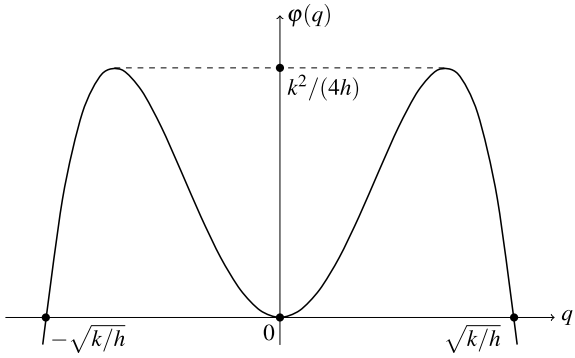

Fig. 4.2 Plot of the potential energy $\varphi(q)$

$$F(q, v) = \frac{1}{m}\left(-k\,q + h\,q^3 - \beta\,v\right) , \tag{4.12}$$

where the constants k, h and β are non-negative. The system is therefore subject to an attractive elastic force, $-k\,q$, a repulsive force, $h\,q^3$, and a dissipative friction force, $-\beta\,v$.

If $k \neq 0$ and $h \neq 0$, we may infer that there are three equilibrium states of the system corresponding to the positions,

$$F(q, 0) = 0 \quad \Rightarrow \quad q = 0\,, \quad q = \pm\sqrt{\frac{k}{h}}\,. \tag{4.13}$$

Conversely, if either $k = 0$ or $h = 0$, there is only one equilibrium state in the position $q = 0$.

We can associate a potential energy to the attractive and repulsive forces, given by

$$\varphi(q) = k\,\frac{q^2}{2} - h\,\frac{q^4}{4}\,. \tag{4.14}$$

The trend of the potential energy $\varphi(q)$ is shown in Fig. 4.2. Therefore, Eq. (4.12) can be rewritten as

$$F(q, v) = -\frac{1}{m}\left[\frac{\mathrm{d}\,\varphi(q)}{\mathrm{d}\,q} + \beta\,v\right] . \tag{4.15}$$

We can also define a total energy defined as the sum of the kinetic energy and the potential energy,

$$E(q, v) = m\,\frac{v^2}{2} + \varphi(q)\,. \tag{4.16}$$

The derivative of E with respect to time reads

$$\frac{\mathrm{d}\,E}{\mathrm{d}\,t} = m\,v\,\frac{\mathrm{d}\,v}{\mathrm{d}\,t} + \frac{\mathrm{d}\,\varphi}{\mathrm{d}\,q}\,\frac{\mathrm{d}\,q}{\mathrm{d}\,t} = -v\left(\frac{\mathrm{d}\,\varphi}{\mathrm{d}\,q} + \beta\,v\right) + \frac{\mathrm{d}\,\varphi}{\mathrm{d}\,q}\,v = -\beta\,v^2\,, \tag{4.17}$$

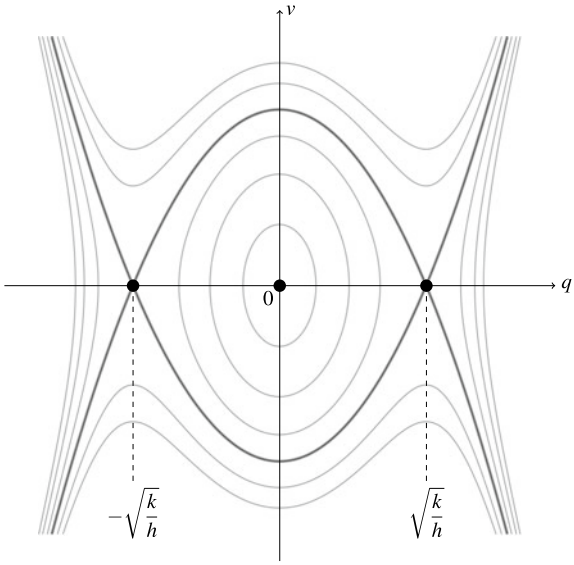

Fig. 4.3 Constant energy curves in the phase space. The thicker line corresponds to $E = \varphi_{\max}$

where Eqs. (4.11) and (4.15) have been employed. In the non-dissipative case, where $\beta = 0$, Eq. (4.17) leads to the conclusion that the total energy remains invariant during the system evolution. In this case, the force per unit mass F acting on the system is associated with the potential energy,

$$F = -\frac{1}{m}\frac{\mathrm{d}\varphi}{\mathrm{d}q} \,. \tag{4.18}$$

Since the force can be expressed in terms of the gradient of the potential energy, then the system is conservative. On the other hand, the energy E is not invariant in the dissipative case, $\beta \neq 0$. The effect of the dissipative force is a decrease in time of the total energy, E, as demonstrated by Eq. (4.17).

Thus, if $\beta = 0$, every trajectory of the system corresponds to a given energy E. Stated differently, in the non-dissipative case, the trajectories in phase phase coincide with the curves at constant energy.

Figure 4.3 displays curves at constant energy. Among them, a special one is the curve corresponding to $E = \varphi_{\max}$, where $\varphi_{\max}$ is the maximum value of the potential energy, Eq. (4.14), given by

$$\varphi_{\max} = \frac{k^2}{4\,h} \,. \tag{4.19}$$

The shape of the trajectories for $\beta = 0$ suggests that, among the three equilibrium states defined by Eq. (4.13), only one is stable: that corresponding to the position $q = 0$. Within this domain, all constant energy curves are closed orbits of smaller and smaller size as E decreases. Lyapunov's criterion is then satisfied by the equilibrium

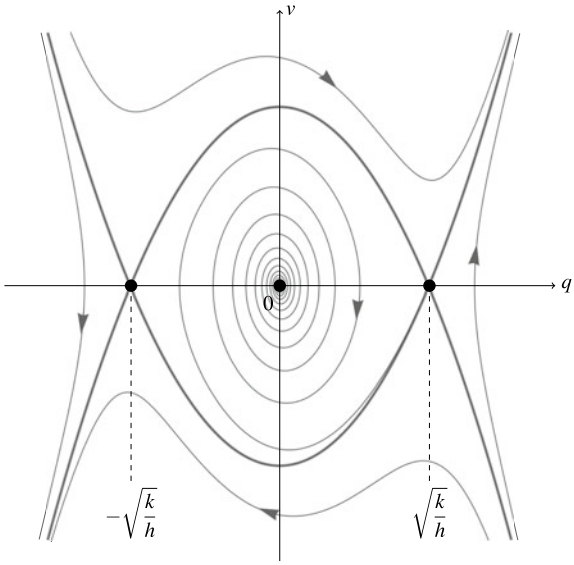

Fig. 4.4 Trajectories in phase space for $\beta > 0$. The thicker line is the constant energy curve for $E = \varphi_{\max}$

state with $q = 0$. On the contrary, all trajectories around the equilibrium states with $q = \pm\sqrt{k/h}$ cannot be confined within a small neighbourhood of these points. This behaviour is the effect of instability.

If $\beta > 0$, nothing changes both with respect to the stability of the state $\{0, 0\}$ and the instability of the states $\{-\sqrt{k/h}, 0\}$ and $\{\sqrt{k/h}, 0\}$ (Fig. 4.4). Nevertheless, there is an important difference: the energy defined by Eq. (4.16) is not conserved along the trajectories in phase space. In other words, the trajectories do not coincide with the closed curves of constant energy. The stable equilibrium state $\{0, 0\}$ is now asymptotically stable. The basin of attraction of such a state of equilibrium is extended to that limited domain around the origin enclosed by the curve $E = \varphi_{\max}$. Within the basin of attraction, the trajectories are not closed orbits, as in the non-dissipative case, $\beta = 0$. On the contrary, they appear as spirals converging to the stable equilibrium state $\{0, 0\}$. This behaviour is typical of asymptotic stability as described by Eq. (4.10).

4.1.2 The Method of Small Perturbations

An alternative analysis of the stability or instability of the equilibrium states of a mechanical system is based on the method of small perturbations. We consider again the simple mechanical system described in Sect. 4.1.1. Its equations of motion are given by Eqs. (4.11) and (4.12), namely

$$\begin{cases} \dfrac{\mathrm{d}\,q}{\mathrm{d}\,t} = v \ , \\ \dfrac{\mathrm{d}\,v}{\mathrm{d}\,t} = \dfrac{1}{m}\left(-k\,q + h\,q^3 - \beta\,v\right) \ . \end{cases} \tag{4.20}$$

If $\{q_0, 0\}$ is any equilibrium state, then it is a solution of Eq. (4.20). Let us *perturb* this equilibrium state by superposing a very small disturbance. Mathematically, this means writing

$$q = q_0 + \varepsilon\,\hat{q} \ , \quad v = 0 + \varepsilon\,\hat{v} = \varepsilon\,\hat{v} \ , \tag{4.21}$$

where ε is a positive and very small number, called *perturbation parameter*. By substituting Eq. (4.21) into the equations of motion, (4.20), we obtain

$$\begin{cases} \varepsilon\,\dfrac{\mathrm{d}\,\hat{q}}{\mathrm{d}\,t} = \varepsilon\,\hat{v} \ , \\ \varepsilon\,\dfrac{\mathrm{d}\,\hat{v}}{\mathrm{d}\,t} = \dfrac{1}{m}\left[-k\,q_0 - k\,\varepsilon\,\hat{q} + h\left(q_0 + \varepsilon\,\hat{q}\right)^3 - \beta\,\varepsilon\,\hat{v}\right] \ . \end{cases} \tag{4.22}$$

Since $\{q_0, 0\}$ is a solution of the equations of motion, we can simplify Eq. (4.22),

$$\begin{cases} \varepsilon\,\dfrac{\mathrm{d}\,\hat{q}}{\mathrm{d}\,t} = \varepsilon\,\hat{v} \ , \\ \varepsilon\,\dfrac{\mathrm{d}\,\hat{v}}{\mathrm{d}\,t} = \dfrac{1}{m}\left[-k\,\varepsilon\,\hat{q} + h\left(\varepsilon^3\,\hat{q}^3 + 3\,\varepsilon^2\,\hat{q}^2\,q_0 + 3\,\varepsilon\,\hat{q}\,q_0^2\right) - \beta\,\varepsilon\,\hat{v}\right] \ . \end{cases} \tag{4.23}$$

The perturbation parameter is small, namely $\varepsilon \ll 1$, so that we can safely neglect terms $O(\varepsilon^2)$ or higher with respect to terms $O(\varepsilon)$. Thus, Eq. (4.23) yields

$$\begin{cases} \varepsilon\,\dfrac{\mathrm{d}\,\hat{q}}{\mathrm{d}\,t} = \varepsilon\,\hat{v} \ , \\ \varepsilon\,\dfrac{\mathrm{d}\,\hat{v}}{\mathrm{d}\,t} = \dfrac{1}{m}\left(-k\,\varepsilon\,\hat{q} + 3\,\varepsilon\,h\,\hat{q}\,q_0^2 - \beta\,\varepsilon\,\hat{v}\right) \ . \end{cases} \tag{4.24}$$

Division by ε now leads to the equations of motion for small perturbations.

$$\begin{cases} \dfrac{\mathrm{d}\,\hat{q}}{\mathrm{d}\,t} = \hat{v} \ , \\ \dfrac{\mathrm{d}\,\hat{v}}{\mathrm{d}\,t} = \dfrac{1}{m}\left(-k\,\hat{q} + 3\,h\,\hat{q}\,q_0^2 - \beta\,\hat{v}\right) \ . \end{cases} \tag{4.25}$$

Equations (4.25) are linear. This is a consequence of having neglected terms of order higher than ε. For this reason, the assumption of small perturbations leads to *linearised equations of motion*.

Equation (4.25) can be collapsed into a single differential equation, namely

$$\frac{\mathrm{d}^2\hat{q}}{\mathrm{d}\,t^2} = \frac{1}{m}\left(-k\,\hat{q} + 3\,h\,\hat{q}\,q_0^2 - \beta\,\frac{\mathrm{d}\,\hat{q}}{\mathrm{d}\,t}\right) . \tag{4.26}$$

For the three equilibrium states $q_0 = 0$ and $q_0 = \pm\sqrt{k/h}$, we get analytical solutions. In particular, for $q_0 = 0$, we obtain

$$\hat{q}(t) = \mathrm{e}^{-\beta t/(2m)}\left[\hat{q}(0)\cosh\left(\frac{\sqrt{\beta^2 - 4\,k\,m}}{2\,m}\,t\right)\right.$$
$$\left.+\frac{2\,m\,\hat{v}(0) + \beta\,\hat{q}(0)}{\sqrt{\beta^2 - 4\,k\,m}}\,\sinh\left(\frac{\sqrt{\beta^2 - 4\,k\,m}}{2\,m}\,t\right)\right] . \tag{4.27}$$

Equation (4.27) shows that the perturbation $\hat{q}(t)$ always decreases in time if $\beta > 0$. If $\beta^2 \geqslant 4\,k\,m$, the perturbation undergoes an exponential decay, where the leading exponential is

$$\exp\left[-\left(\frac{\beta}{2\,m} - \frac{\sqrt{\beta^2 - 4\,k\,m}}{2\,m}\right)t\right] . \tag{4.28}$$

One can easily check that the coefficient of this exponential is always negative, if $k > 0$, or zero, if $k = 0$. In both cases, the perturbation remains $O(\varepsilon)$ for every $t > 0$, thus ensuring stability according to Lyapunov's criterion. If $0 < \beta^2 < 4\,k\,m$, the argument of the hyperbolic cosine and sine becomes imaginary, so that these contributions can be rewritten in terms of trigonometric cosine and sine. As a consequence, in this case, Eq. (4.27) describes a decaying exponential multiplied by a periodic function of time. Again, we have a response of stability for the equilibrium state $q_0 = 0$. Finally, if we consider the non-dissipative case, $\beta = 0$, Eq. (4.27) shows that the solution is purely oscillatory, so that the perturbation remains $O(\varepsilon)$ at any time.

For $q_0 = \pm\sqrt{k/h}$, the analytical solution of Eq. (4.26) is

$$\hat{q}(t) = \mathrm{e}^{-\beta t/(2m)}\left[\hat{q}(0)\cosh\left(\frac{\sqrt{\beta^2 + 8\,k\,m}}{2\,m}\,t\right)\right.$$
$$\left.+\frac{2\,m\,\hat{v}(0) + \beta\,\hat{q}(0)}{\sqrt{\beta^2 + 8\,k\,m}}\,\sinh\left(\frac{\sqrt{\beta^2 + 8\,k\,m}}{2\,m}\,t\right)\right] . \tag{4.29}$$

The solution has an exponential behaviour in time, where the leading exponential is

$$\exp\left[\left(\frac{\sqrt{\beta^2 + 8\,k\,m}}{2\,m} - \frac{\beta}{2\,m}\right)t\right] . \tag{4.30}$$

This exponential grows in time for every $k > 0$. This means that the perturbation will not remain confined in a small neighbourhood of the equilibrium state and, hence,

we have instability in the sense of Lyapunov. Considering $k = 0$ is not significant as $q_0 = \pm\sqrt{k/h}$ would coincide with $q_0 = 0$.

We can conclude that the method of small perturbations entirely confirms the results of the stability analysis obtained by a direct evaluation of the trajectories in phase space undergone by the mechanical system. A limitation in the use of this method arises due to the local character of the information. We can only consider small distances of the initial conditions from the equilibrium state. Moreover, in the case of instability, we can only predict the time evolution of perturbations at the earlier instants of time. When the growth in time makes the perturbation of order larger than ε, then the linearised Eq. (4.26) becomes unreliable. In other words, nonlinearity becomes dominant in governing the time evolution of the system.

4.2 Flow Stability with Burgers Equation

Let us consider the one-dimensional *Burgers equation* with a linear forcing term,

$$\frac{\partial W}{\partial t} + W\,\frac{\partial W}{\partial x} = \frac{\partial^2 W}{\partial x^2} + R\,(W - W_0)\ , \tag{4.31}$$

where $R \in \mathbb{R}$ and $W_0 \in \mathbb{R}$. We mention that Burgers equation is a toy model for the one-dimensional flow of a fluid. In a paper by J. M. Burgers of 1939, entitled "Mathematical examples illustrating relations occurring in the theory of turbulent fluid motion", a slightly different form of Eq. (4.31) was presented as a simplified governing equation of a system developing turbulence [13].

Evidently, $W = W_0$ is a solution of Eq. (4.31). This solution is stationary and, as a consequence, it can be defined as an equilibrium state for Eq. (4.31). We can investigate the stability of this equilibrium state, according to Lyapunov's theory, by perturbing it and checking the evolution in time of the perturbation. This procedure is an extension of what has been found for a discrete mechanical system in Sect. 4.1. Here, we have a continuous flow system, meaning that we have a partial differential governing equation, Eq. (4.31), where the variable evolving in time is distributed in space. In this simple model, space is one-dimensional and, hence, flow is one-dimensional as well occurring along the real x-axis.

Hereafter, $W = W_0$ will be called the *basic solution* of Eq. (4.31). To test its stability, we will carry out an analysis of small perturbations according to the lines discussed in Sect. 4.1.2.

4.2.1 Linear Stability Analysis

A linear stability analysis of the basic solution, $W = W_0$, is performed by superposing a small perturbation to the basic solution, namely

$$W = W_0 + \varepsilon\, w\ , \qquad \varepsilon > 0\ , \tag{4.32}$$

where ε is a perturbation parameter such that $\varepsilon \ll 1$. We now substitute Eq. (4.32) into (4.31),

$$\varepsilon\, \frac{\partial w}{\partial t} + \varepsilon\, W_0\, \frac{\partial w}{\partial x} + \varepsilon^2\, w\, \frac{\partial w}{\partial x} = \varepsilon\, \frac{\partial^2 w}{\partial x^2} + \varepsilon\, R\, w\ . \tag{4.33}$$

Then, neglecting terms $O(\varepsilon^2)$ and dividing by ε, we obtain

$$\frac{\partial w}{\partial t} + W_0\, \frac{\partial w}{\partial x} = \frac{\partial^2 w}{\partial x^2} + R\, w\ . \tag{4.34}$$

We employ the Fourier transform to solve Eq. (4.34), namely

$$\begin{aligned} \tilde{w}(k,t) &= \frac{1}{\sqrt{2\pi}} \int_{-\infty}^{\infty} w(x,t)\, \mathrm{e}^{-\mathrm{i}\,kx}\, \mathrm{d}\,x\ , \\ w(x,t) &= \frac{1}{\sqrt{2\pi}} \int_{-\infty}^{\infty} \tilde{w}(k,t)\, \mathrm{e}^{\mathrm{i}\,kx}\, \mathrm{d}\,k\ . \end{aligned} \tag{4.35}$$

Here, k is the wave number. We can transform Eq. (4.34) by employing the properties of the Fourier transform of partial derivatives, given by Eqs. (2.17) and (2.18). Thus, we obtain

$$\frac{\partial \tilde{w}}{\partial t} = \lambda(k)\, \tilde{w}\ , \tag{4.36}$$

where

$$\lambda(k) = R - k^2 - \mathrm{i}\,k\, W_0\ . \tag{4.37}$$

The solution of Eq. (4.36) is

$$\tilde{w}(k,t) = \tilde{w}(k,0)\ \mathrm{e}^{\lambda(k)\,t}\ . \tag{4.38}$$

If we substitute Eq. (4.38) into the expression of $w(x,t)$ given by Eq. (4.35), we can write the perturbation as

$$w(x,t) = \frac{1}{\sqrt{2\pi}} \int_{-\infty}^{\infty} \tilde{w}(k,0)\ \mathrm{e}^{\mathrm{i}\,kx}\, \mathrm{e}^{\lambda(k)\,t}\, \mathrm{d}\,k\ . \tag{4.39}$$

The solution $w(x,t)$ expressed by Eq. (4.39) depends on the initial condition, $w(x,0)$, through its Fourier transform $\tilde{w}(k,0)$. Moreover, $w(x,t)$ is represented as a wave packet where

$$\omega(k) = -\Im(\lambda(k)) = k\, W_0 \tag{4.40}$$

is the angular frequency, and

$$b(k,t) = \frac{1}{\sqrt{2\pi}}\,\tilde{w}(k,0)\,\mathrm{e}^{\Re(\lambda(k))\,t} \tag{4.41}$$

is the time-dependent amplitude of the normal mode. The single normal mode, with a given wave number k_a, represents the evolution of an initial perturbation having the shape of a plane wave, namely

$$w(x,0) = \frac{1}{\sqrt{2\pi}}\,\mathrm{e}^{\mathrm{i}\,k_a x}\ . \tag{4.42}$$

In fact, on account of Eqs. (2.9) and (2.10), from Eq. (4.42) one obtains a Dirac's delta distribution for $\tilde{w}(k,0)$,

$$\tilde{w}(k,0) = \delta(k-k_a)\ . \tag{4.43}$$

Then, Eq. (4.39) yields

$$w(x,t) = \frac{\mathrm{e}^{\Re(\lambda(k_a))\,t}}{\sqrt{2\pi}}\,\mathrm{e}^{\mathrm{i}[k_a x-\omega(k_a)t]}\ , \tag{4.44}$$

where the angular frequency $\omega(k)$ is given by Eq. (4.40). Equation (4.44) defines a plane wave perturbation propagating with a phase velocity $\omega(k_a)/k_a$, whose amplitude grows unboundedly in time if $\Re(\lambda(k_a)) > 0$, or it is damped in time if $\Re(\lambda(k_a)) < 0$. The former alternative defines an unstable behaviour, while the latter yields a stable character of the perturbation. We can now formally define the concept of *convective instability*.

Definition 4.1 (*Convective Instability*) A single normal mode perturbation with a given wave number k is deemed to be convectively stable if $\Re(\lambda(k)) < 0$. It is said convectively unstable if $\Re(\lambda(k)) > 0$. The marginal condition where $\Re(\lambda(k)) = 0$ is called *neutral stability*.

On account of Eq. (4.37), the condition of convective instability reads

$$R > k^2\ , \tag{4.45}$$

with the curve given by $R = k^2$ defining neutral stability.

A simple sketch resuming the concept of convective instability and the marginal condition of neutral stability is displayed in Fig. 4.5. In this figure, only the domain of positive wave numbers is represented, as the condition of convective instability just involves k^2 and is thus independent of the sign of k.

We note that convective instability, to some wave number k, is possible only when R exceeds a *critical value*, denoted as R_c, which corresponds to the absolute

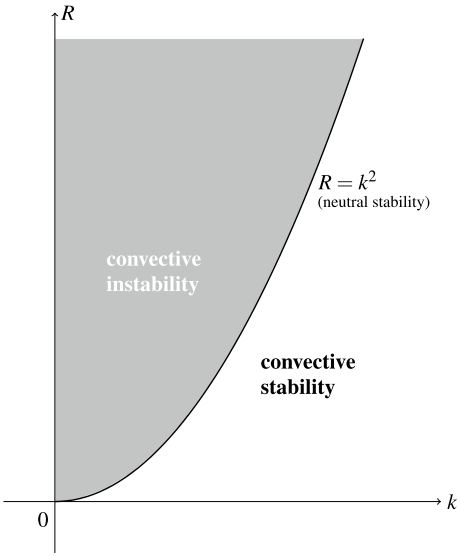

Fig. 4.5 Qualitative sketch of the definition of convective instability as implied by Eq. (4.45)

minimum of R along the neutral stability curve. The corresponding value of k is the critical wave number, k_c. Thus, we have

$$k_c = 0\,, \qquad R_c = 0\,. \tag{4.46}$$

Hereafter, a situation where $R < R_c = 0$ will be termed *subcritical*, while the condition $R > R_c = 0$ will be termed *supercritical*.

The convective instability regards the behaviour of quite special initial perturbations of the basic solution, having the form of plane waves with a given wave number. These perturbations have an intrinsic non-local character as their support is widespread all over the real x-axis. A more general perturbation comes from a superposition of infinite plane waves with all possible wave numbers, as represented by the Fourier integral, Eq. (4.39). These wave packets may describe perturbations with a local support as it could be, for instance, when the initial condition $w(x, 0)$ is a Gaussian signal. In general, as pointed out in Sect. 2.2.1, the initial condition $w(x, 0)$ must be absolutely integrable over the real x-axis. Otherwise, the Fourier integral can only make sense in a space of generalised functions, or distributions. This is the reason why the normal mode initial condition, given by Eq. (4.42), leads to a Fourier transform given by a Dirac's delta. A normal mode is not absolutely integrable and Dirac's delta is not a function in the traditional sense, but a distribution.

Definition 4.2 (*Absolute Instability*) A perturbation $w(x, t)$ is deemed to be absolutely unstable if it is absolutely integrable over the real x-axis and if

$$\lim_{t \to +\infty} |w(x, t)| = +\infty\,, \tag{4.47}$$

for every $x \in \mathbb{R}$.

Deciding whether a perturbation $w(x,t)$ expressed through Eq. (4.39) is absolutely unstable means checking the large-time behaviour of the Fourier integral on the right-hand side of Eq. (4.39). This task can be accomplished by employing the steepest-descent approximation described in Sect. 3.5.3. The first step is to determine the saddle points of $\lambda(k)$. In fact, Eq. (4.37) yields

$$\lambda'(k) = -2\,k - \mathrm{i}\,W_0 \,. \tag{4.48}$$

Equation (4.48) shows that there is just one, purely imaginary, saddle point,

$$k_0 = -\frac{\mathrm{i}\,W_0}{2} \,. \tag{4.49}$$

We must now check that the holomorphy requirement is satisfied by $\tilde{w}(k,t)$ expressed by Eq. (4.38). We know that $\lambda(k)$ is holomorphic for every $k \in \mathbb{C}$. On the other hand, $\tilde{w}(k,0)$ is arbitrary. However, in order to employ the steepest-descent approximation as specified in Sect. 3.5.3, we need the assumption that no singularity of $\tilde{w}(k,0)$ exists in the region of the complex plane bounded by the real k-axis, $\Im(k) = 0$, and the deformed curve γ^* locally crossing k_0 through a path of steepest descent. If this hypothesis regarding the initial state $w(x,0)$ holds, we can approximately evaluate $|w(x,t)|$ for large times, by employing Eq. (3.163), as

$$|w(x,t)| \approx \frac{|\tilde{w}(k_0,0)|}{\sqrt{2\,t}}\,\mathrm{e}^{\Re(\lambda(k_0))\,t} \,. \tag{4.50}$$

As a consequence of Eqs. (4.47) and (4.50), one can conclude that absolute instability is attained when $\Re(\lambda(k_0)) > 0$. On account of Eqs. (4.37) and (4.49), this means

$$R > R_\mathrm{a} = \frac{W_0^2}{4} \,, \tag{4.51}$$

where R_a denotes the threshold for the onset of absolute instability. It is important to emphasize that the condition of absolute instability is independent of the details of the initial perturbation, $w(x,0)$, inasmuch as it is absolutely integrable over the real x-axis and its Fourier transform, $\tilde{w}(k,0)$, allows one to satisfy the holomorphy requirement relative to the steepest-descent method applied to the integral on the right-hand side of Eq. (4.39).

A qualitative sketch of the concepts of convective instability and absolute instability is displayed in Fig. 4.6. This figure highlights that absolute instability is not a modal condition, meaning that its validity does not depend on the behaviour of individual normal modes, but on the asymptotic behaviour of a general class of perturbations. Interestingly enough, the condition of absolute instability turns out to be a parametric condition, given by Eq. (4.51), mostly independent on the detailed characteristics of the initial perturbations superposed to the basic stationary solution through Eq. (4.32).

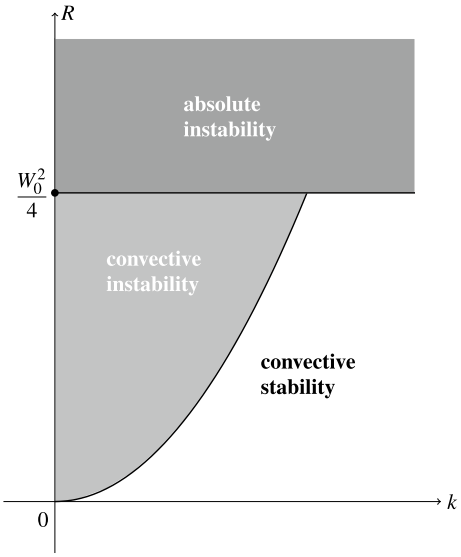

Fig. 4.6 Qualitative sketch of the definitions of convective instability and absolute instability as implied by Eqs. (4.45) and (4.51)

There is a physical picture of how the mathematical condition of absolute instability can be viewed. One can imagine the basic flow W_0 as observed by a *laboratory reference frame* and by a *co-moving reference frame*. An observer in the latter frame travels downstream with speed W_0 and detects normal modes of perturbation growing in time or damped in time. On the other hand, the view of an observer in the laboratory reference frame is different. Such an observer sees the flowing fluid with uniform velocity W_0, detects the perturbations, but will also experience some difficulty in checking the ultimate behaviour of perturbations at large times. In fact, normal modes of perturbation initially growing in time are convected downstream by the basic flow, so that a growing normal mode can be driven away so fast that its time growth is not actually perceived with the instruments employed by this observer. If the basic flow velocity W_0 is sufficiently low (remember that the absolute instability condition can be reformulated as $W_0^2 < 4\,R$), then any actually unbounded growth of each growing normal mode is correctly detected in the laboratory reference frame.

4.2.2 Time Evolution of a Special Perturbation Wave Packet

We can check the results of the steepest-descent approximation by a direct evaluation of $w(x, t)$ for a very special initial wave packet given by a Gaussian distribution,

$$w(x, 0) = \mathrm{e}^{-x^2} \,. \tag{4.52}$$

Its Fourier transform is readily determined, namely

$$\tilde{w}(k,0) = \frac{1}{\sqrt{2}}\, \mathrm{e}^{-\frac{k^2}{4}} \,. \tag{4.53}$$

Then, from Eqs. (4.37) and (4.38), we obtain

$$\tilde{w}(k,t) = \frac{1}{\sqrt{2}}\, \exp\left[-\frac{k^2}{4} + (R - k^2 - \mathrm{i}\, k\, W_0)\, t\right] \,. \tag{4.54}$$

The inverse Fourier transform of $\tilde{w}(k,t)$, given by Eq. (4.54), is evaluated analytically as

$$w(x,t) = \frac{1}{\sqrt{4\,t+1}}\, \exp\left[R\,t - \frac{(x - W_0\,t)^2}{4t+1}\right] \,. \tag{4.55}$$

Plots showing the time evolution of $w(x,t)$, given by Eq. (4.55), are presented in Fig. 4.7 for the choice $W_0 = 1$. Different positions, x, are considered. Each frame

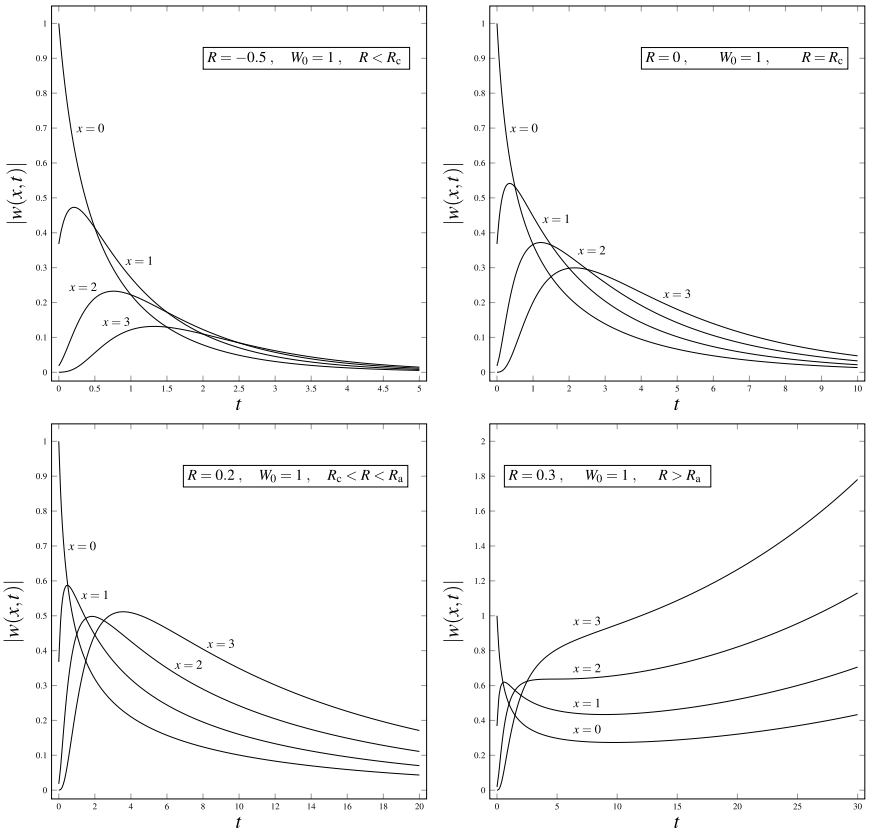

Fig. 4.7 Plots of the time evolution of the Gaussian perturbation for $W_0 = 1$, at different positions, x, and with different values of R such that $R < R_c$, $R = R_c$, $R_c < R < R_a$ and $R > R_a$

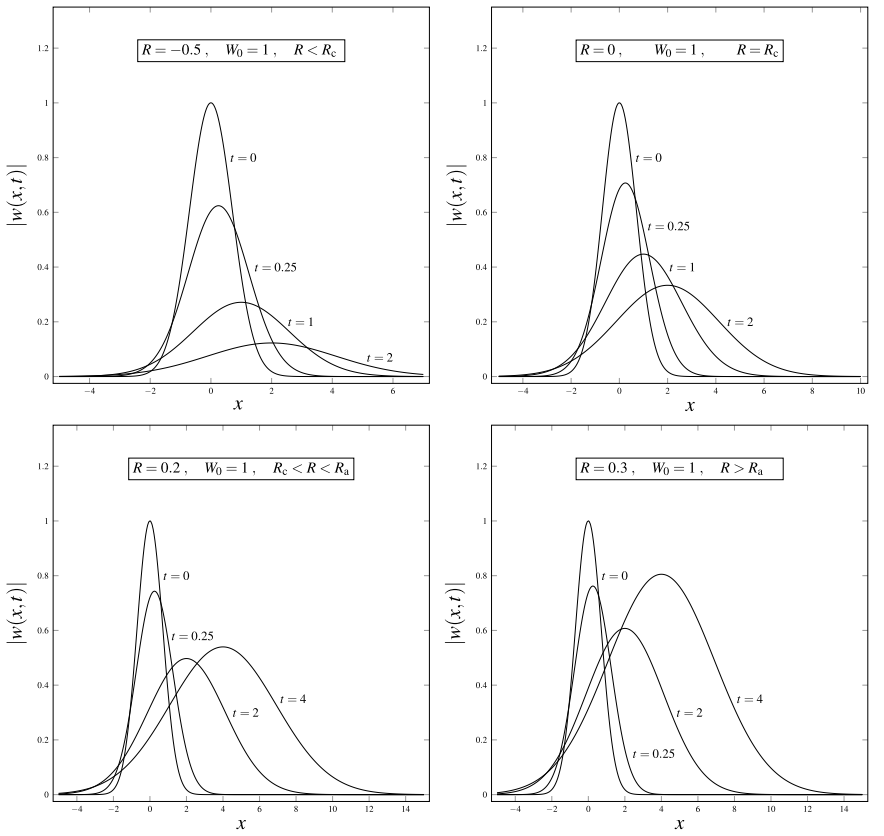

Fig. 4.8 Plots of the spatial distribution of the Gaussian perturbation for $W_0 = 1$, at different times, t, and with different values of R such that $R < R_c$, $R = R_c$, $R_c < R < R_a$ and $R > R_a$

corresponds to a value of R that is either subcritical, critical or supercritical. Among the supercritical cases, $R = 0.2$ or $R = 0.3$, it is clearly displayed the expected difference between the behaviour when $R < R_a$ and that when $R > R_a$. The frame with $R = 0.3$ clearly shows the large-time growing trend of the plots of $|w(x, t)|$ versus t for different positions, x. This behaviour is precisely what one expects on the basis of the asymptotic expression of $|w(x, t)|$ given by Eq. (4.50), and based on the steepest-descent approximation.

The spatial distribution of the Gaussian perturbation at different times is illustrated in Fig. 4.8. The same cases considered in Fig. 4.7 are reported. We see that, when R is subcritical or critical, there is a net decrease in height of the Gaussian maximum, accompanied by a rightward displacement and a spreading, as time increases. This is not the case when R is supercritical, as the maximum decreases at first, reaches a minimum, but eventually it increases unboundedly in time. This behaviour is easily gathered from Eq. (4.55), as the position of the maximum is $x = W_0 t$, and its

height is

$$\max_{x\in\mathbb{R}} |w(x,t)| = \frac{1}{\sqrt{4\,t+1}}\,\mathrm{e}^{R\,t}\ . \tag{4.56}$$

The height decreases monotonically when $R \leqslant 0$, but it behaves non-monotonically when $0 < R < 2$. In fact, it decreases at first, reaches a minimum when

$$t = \frac{2-R}{4\,R}\ , \tag{4.57}$$

and then it increases unboundedly. This explains the behaviour of the frames in Fig. 4.8 corresponding to $R = 0.2$ and $R = 0.3$. What makes the difference between the supercritical behaviour for $R < R_\mathrm{a}$ and $R > R_\mathrm{a}$, so well evident in Fig. 4.7, is the competition between the speed of the rightward displacement and the gradual increase of the maximum height at sufficiently large times. This competition results in a signal at a given x gradually decreasing in time, if $R < R_\mathrm{a}$, and gradually increasing in time, if $R > R_\mathrm{a}$. This is the essence of the transition from convective to absolute instability.

4.3 Stability of Channelised Burgers Flow

The analysis of the instability occurring in Burgers flow can be modelled as three-dimensional if we imagine that the flow along the x direction is directed, in fact, through a channel with a rectangular cross section. In a rectangular channel, where $x \in \mathbb{R}$, $y \in [0, L_1]$ and $z \in [0, L_2]$, the three-dimensional version of Burgers equation (4.31) is given by

$$\frac{\partial \mathbf{W}}{\partial t} + (\mathbf{W}\cdot\boldsymbol{\nabla})\,\mathbf{W} = \nabla^2\mathbf{W} + R\,(\mathbf{W}-\mathbf{W}_0)\ , \tag{4.58}$$

where $\mathbf{W}_0$ is the constant vector $(W_0, 0, 0)$, and $W_0 \in \mathbb{R}$ is the same constant considered in the one-dimensional case envisaged in Sect. 4.2. Evidently, a basic stationary solution of Eq. (4.58) is

$$\mathbf{W} = \mathbf{W}_0\ . \tag{4.59}$$

We imagine the confining walls of the channel positioned at $y = 0$, $y = L_1$, $z = 0$, $z = L_2$ as impermeable surfaces moving along the flow direction with velocity $\mathbf{W}_0$. This assumption is compatible with a uniform velocity in the channel, as implied by Eq. (4.59). Thus, we assume the system of boundary conditions,

$$\begin{aligned} &t > 0\ ;\quad x \in \mathbb{R}\ ;\quad y = 0,\ L_1\ ;\quad z \in [0, L_2]\ :\quad \mathbf{W} = \mathbf{W}_0\ ,\\ &t > 0\ ;\quad x \in \mathbb{R}\ ;\quad y \in [0, L_1]\ ;\quad z = 0,\ L_2\ :\quad \mathbf{W} = \mathbf{W}_0\ . \end{aligned} \tag{4.60}$$

4.3.1 Linear Stability Analysis

The linear stability analysis of the solution, $\mathbf{W} = \mathbf{W}_0$, can be carried out by writing

$$\mathbf{W} = \mathbf{W}_0 + \varepsilon\, \mathbf{w}\,, \qquad \varepsilon > 0\,, \tag{4.61}$$

where ε is a small perturbation parameter, $\varepsilon \ll 1$. By substituting Eq. (4.61) into Eq. (4.58),

$$\varepsilon\, \frac{\partial \mathbf{w}}{\partial t} + \varepsilon\, W_0\, \frac{\partial \mathbf{w}}{\partial x} + \varepsilon^2\, (\mathbf{w} \cdot \boldsymbol{\nabla})\, \mathbf{w} = \varepsilon\, \nabla^2 \mathbf{w} + R\, \varepsilon\, \mathbf{w}\,. \tag{4.62}$$

We neglect terms $O(\varepsilon^2)$ and divide by ε, so that we obtain

$$\frac{\partial \mathbf{w}}{\partial t} + W_0\, \frac{\partial \mathbf{w}}{\partial x} = \nabla^2 \mathbf{w} + R\, \mathbf{w}\,. \tag{4.63}$$

Equation (4.63) governs the evolution of the linear perturbations $\mathbf{w}$ and, as a consequence of Eqs. (4.60) and (4.61), its boundary conditions are

$$\begin{aligned} &t > 0\,; \quad x \in \mathbb{R}\,; \quad y = 0,\ L_1\,; \quad z \in [0, L_2] \ : \qquad \mathbf{w} = 0\,, \\ &t > 0\,; \quad x \in \mathbb{R}\,; \quad y \in [0, L_1]\,; \quad z = 0,\ L_2 \ : \qquad \mathbf{w} = 0\,. \end{aligned} \tag{4.64}$$

Due to the linearity of Eqs. (4.63) and (4.64), solutions can be sought as a series. The method to be employed is the separation of variables, described in Appendix A. Thus, we can write

$$\mathbf{w} = \sum_{n=1}^{\infty} \sum_{m=1}^{\infty} \mathbf{w}_{nm}(x, t)\ \sin(\alpha_n\, y)\ \sin(\beta_m\, z)\,, \tag{4.65}$$

where

$$\alpha_n = \frac{\pi\, n}{L_1}\,, \quad \beta_m = \frac{\pi\, m}{L_2}\,. \tag{4.66}$$

Series solutions described by Eq. (4.66) identically satisfy the boundary conditions, Eq. (4.65), provided that $\mathbf{w}_{nm}(x, t)$ is a solution of

$$\frac{\partial \mathbf{w}_{nm}}{\partial t} + W_0\, \frac{\partial \mathbf{w}_{nm}}{\partial x} = \frac{\partial^2 \mathbf{w}_{nm}}{\partial x^2} + \left(R - \alpha_n^2 - \beta_m^2\right) \mathbf{w}_{nm}\,. \tag{4.67}$$

We note that Eq. (4.34) is entirely equivalent to Eq. (4.67), provided that we replace R with

$$R_{nm} = R - \alpha_n^2 - \beta_m^2\,, \tag{4.68}$$

and $w(x, t)$ with the vector function $\mathbf{w}_{nm}(x, t)$. Thus, $\mathbf{w}_{nm}(x, t)$ can be expressed through the Fourier integral

$$\mathbf{w}_{nm}(x,t) = \frac{1}{\sqrt{2\pi}} \int_{-\infty}^{\infty} \tilde{\mathbf{w}}_{nm}(k,0)\, \mathrm{e}^{\mathrm{i}kx}\, \mathrm{e}^{\lambda(k)t}\, \mathrm{d}k \;, \tag{4.69}$$

where $\lambda(k)$ is now given by

$$\lambda(k) = R_{nm} - k^2 - \mathrm{i}\,k\,W_0 \;, \tag{4.70}$$

and $\tilde{\mathbf{w}}_{nm}(k,0)$ is the Fourier transform of the initial perturbation $\mathbf{w}_{nm}(x,0)$.

We can follow step by step the analysis described in Sect. 4.2.1 to conclude that, on account of Eq. (4.45), convective instability occurs when

$$R_{nm} > k^2 \;. \tag{4.71}$$

This means

$$R > \alpha_n^2 + \beta_m^2 + k^2 \;. \tag{4.72}$$

This condition is satisfied with the minimum value of R occurring when $n = 1, m = 1$ and $k = 0$. In other words, the critical values $(k_\mathrm{c}, R_\mathrm{c})$ for the onset of convective instability are

$$k_\mathrm{c} = 0 \;, \quad R_\mathrm{c} = \frac{\pi^2}{L_1^2} + \frac{\pi^2}{L_2^2} \;. \tag{4.73}$$

On the other hand, on account of Eq. (4.51), absolute instability is detected when

$$R_{nm} > \frac{W_0^2}{4} \;. \tag{4.74}$$

As for the convective instability, the modes that allow the inequality (4.74) to be satisfied with the least value of R are those with $n = 1$ and $m = 1$. Thus, the widest region of absolute instability is defined by

$$R > R_\mathrm{a} = \frac{W_0^2}{4} + \frac{\pi^2}{L_1^2} + \frac{\pi^2}{L_2^2} \;. \tag{4.75}$$

The channelisation of Burgers flow thus yields a stabilisation of the basic solution, Eq. (4.59), by raising the thresholds to convective instability, R_c, and to absolute instability, R_a. The stabilisation is due to the restriction imposed with respect to the allowed modes of perturbation implied by the boundary conditions, Eq. (4.60). In fact, the results described in Sect. 4.2.1 for the one-dimensional study are readily recovered on taking the limit of an infinite channel cross section, namely $L_1 \to \infty$ and $L_2 \to \infty$.

4.4 Stability of a Convective Cahn–Hilliard Process

The convective Cahn–Hilliard equation is a partial differential equation formulated as a model of the phase separation due to spinodal decomposition [6, 7]. In one-dimensional form, it can be written as,

$$\frac{\partial \Psi}{\partial t} = \alpha\, \Psi\, \frac{\partial \Psi}{\partial x} - \frac{\partial^2}{\partial x^2}\left(\Psi - \Psi^3 + \frac{\partial^2 \Psi}{\partial x^2}\right) , \tag{4.76}$$

where α is a real positive constant which represents the driving force parameter. Equation (4.76) can be equivalently expressed as

$$\frac{\partial \Psi}{\partial t} = \alpha\, \Psi\, \frac{\partial \Psi}{\partial x} + 6\, \Psi \left(\frac{\partial \Psi}{\partial x}\right)^2 + \left(3\, \Psi^2 - 1\right) \frac{\partial^2 \Psi}{\partial x^2} - \frac{\partial^4 \Psi}{\partial\, x^4} , \tag{4.77}$$

A possible basic stationary solution of Eq. (4.77) is given by

$$\Psi = \Psi_0 = constant\ . \tag{4.78}$$

4.4.1 Linear Stability Analysis

The linear stability of the basic solution, $\Psi = \Psi_0$, is studied by superposing to Ψ_0 a small perturbation, namely

$$\Psi = \Psi_0 + \varepsilon\, \psi\ , \qquad \varepsilon > 0\ . \tag{4.79}$$

As always, we consider ε as a small perturbation parameter, $\varepsilon \ll 1$. Substitution of Eq. (4.79) into (4.77) yields

$$\begin{aligned} \varepsilon\, \frac{\partial \psi}{\partial t} = {} & \varepsilon\, \alpha\, \Psi_0\, \frac{\partial \psi}{\partial x} + \varepsilon^2\, \alpha\, \psi\, \frac{\partial \psi}{\partial x} + 6\, \varepsilon^2\, \Psi_0 \left(\frac{\partial \psi}{\partial x}\right)^2 + 6\, \varepsilon^3\, \psi \left(\frac{\partial \psi}{\partial x}\right)^2 \\ & + \varepsilon \left(3\, \Psi_0^2 - 1\right) \frac{\partial^2 \psi}{\partial x^2} + 6\, \varepsilon^2\, \Psi_0\, \psi\, \frac{\partial^2 \psi}{\partial x^2} + 3\, \varepsilon^3\, \psi^2\, \frac{\partial^2 \psi}{\partial x^2} - \varepsilon\, \frac{\partial^4 \psi}{\partial\, x^4}\ . \end{aligned} \tag{4.80}$$

According to the hypothesis of small perturbations, we neglect the terms $O(\varepsilon^2)$ and $O(\varepsilon^3)$. Then, we divide Eq. (4.80) by ε, and we obtain the linearised equation

$$\frac{\partial \psi}{\partial t} = \alpha\, \Psi_0\, \frac{\partial \psi}{\partial x} + \left(3\, \Psi_0^2 - 1\right) \frac{\partial^2 \psi}{\partial x^2} - \frac{\partial^4 \psi}{\partial\, x^4}\ . \tag{4.81}$$

Let us apply the Fourier transform to solve Eq. (4.81), namely

$$\tilde{\psi}(k, t) = \frac{1}{\sqrt{2\pi}} \int_{-\infty}^{\infty} \psi(x, t)\, \mathrm{e}^{-\mathrm{i}\, k x}\, \mathrm{d}\, x\ ,$$

$$\psi(x,t) = \frac{1}{\sqrt{2\pi}} \int_{-\infty}^{\infty} \tilde{\psi}(k,t)\, \mathrm{e}^{\mathrm{i}kx}\, \mathrm{d}k \ . \tag{4.82}$$

The transform of Eq. (4.81) is obtained by employing the properties of the Fourier transform of partial derivatives, given by Eqs. (2.17) and (2.18). Then, we write

$$\frac{\partial \tilde{\psi}}{\partial t} = \lambda(k)\, \tilde{\psi} \ , \tag{4.83}$$

where

$$\lambda(k) = \mathrm{i}\,\alpha\, \Psi_0\, k - \left(3\,\Psi_0^2 - 1\right) k^2 - k^4 \ . \tag{4.84}$$

The solution of Eq. (4.83) is

$$\tilde{\psi}(k,t) = \tilde{\psi}(k,0)\ \mathrm{e}^{\lambda(k)\,t} \ . \tag{4.85}$$

On substituting Eq. (4.85) into the expression of $\psi(x,t)$ given by Eq. (4.82), we write the perturbation as

$$\psi(x,t) = \frac{1}{\sqrt{2\pi}} \int_{-\infty}^{\infty} \tilde{\psi}(k,0)\ \mathrm{e}^{\mathrm{i}kx}\, \mathrm{e}^{\lambda(k)\,t}\, \mathrm{d}k \ . \tag{4.86}$$

As implied by Definition 4.1, convective instability occurs when $\Re(\lambda(k)) > 0$. On account of Eq. (4.84), this means

$$|\Psi_0| < \sqrt{\frac{1-k^2}{3}} \ . \tag{4.87}$$

We note that the right-hand side of Eq. (4.87) is a function of k with an upper bound, $1/\sqrt{3}$. Thus, the meaning of Eq. (4.87) is that, whatever is the real value of the constants $\Psi_0 < 1/\sqrt{3}$ and α, there always exists a normal mode with a suitable wave number k that can destabilise the basic solution $\Psi = \Psi_0$. In other words, convective instability to some normal modes is always possible provided that $\Psi_0 < 1/\sqrt{3}$. Furthermore, the value of the constant α does not influence in any way the onset of convective instability.

We now investigate the transition from convective to absolute instability by employing Definition 4.2 and the steepest-descent approximation described in Sect. 3.5.3. We first determine the saddle points of $\Re(\lambda(k))$, namely the solutions of

$$\lambda'(k) = \mathrm{i}\,\alpha\, \Psi_0 - 2\left(3\,\Psi_0^2 - 1\right) k - 4\,k^3 = 0 \ . \tag{4.88}$$

For every assigned pair (α, Ψ_0), there are three saddle points: k_{01}, k_{02} and k_{03}. In general, by fixing the value of Ψ_0, we can trace graphically the value of $\Re(\lambda(k_{0i}))$, with $i = 1, 2, 3$, as a function of α.

A notable case is the limit where the driving force becomes vanishingly small, $\alpha \to 0$. In this limit, the three saddle points are

$$k_{01} = 0\,, \quad k_{02} = \sqrt{\frac{1 - 3\,\Psi_0^2}{2}}\,, \quad k_{03} = -\sqrt{\frac{1 - 3\,\Psi_0^2}{2}}\,. \tag{4.89}$$

The saddle points k_{02} and k_{03} can be either purely imaginary or real depending on whether $|\Psi_0|$ is larger or smaller than $1/\sqrt{3}$. In every case, we obtain from Eq. (4.84)

$$\lambda(k_{01}) = 0\,, \quad \lambda(k_{02}) = \lambda(k_{03}) = \frac{1}{4}\left(3\,\Psi_0^2 - 1\right)^2\,. \tag{4.90}$$

The conclusion drawn from Eq. (4.90) is that the large-time approximation of the wave packet growth rate can never be negative. Thus, according to the steepest-descent approximation of Eq. (4.86), the dominant saddle points for the assessment of the large-time behaviour of $|\psi(x,t)|$ are k_{02} and k_{03}, which are endowed with the largest value of $\Re(\lambda)$. This means that, for every choice of Ψ_0, there is a transition from stability to absolute instability in the limiting case $\alpha \to 0$ when $\Psi_0 = 1/\sqrt{3}$. Stated differently, in the limit $\alpha \to 0$, every constant solution $\Psi = \Psi_0 < 1/\sqrt{3}$ can be destabilised by normal modes with suitable values of k. Moreover, the amplitude of a wave packet perturbation of $\Psi = \Psi_0 < 1/\sqrt{3}$ ultimately grows in time, when t is sufficiently large.

Let us now consider a nonzero driving force parameter, α. A quite simple case is $\Psi_0 = 1/\sqrt{3}$, where we obtain

$$k_{01} = \left(\frac{\alpha}{4\sqrt{3}}\right)^{1/3} \frac{\sqrt{3}+\mathrm{i}}{2}\,, \quad k_{02} = -\left(\frac{\alpha}{4\sqrt{3}}\right)^{1/3} \frac{\sqrt{3}-\mathrm{i}}{2}\,,$$
$$k_{03} = -\mathrm{i}\left(\frac{\alpha}{4\sqrt{3}}\right)^{1/3}\,. \tag{4.91}$$

On account of Eqs. (4.84) and (4.91), we can write

$$\Re(\lambda(k_{01})) = \Re(\lambda(k_{02})) = -\frac{1}{8}\left(\frac{3}{4}\right)^{1/3} \alpha^{4/3}\,,$$
$$\lambda(k_{03}) = \frac{1}{4}\left(\frac{3}{4}\right)^{1/3} \alpha^{4/3}\,. \tag{4.92}$$

What can be concluded from Eq. (4.92), and from the steepest-descent approximation of the right-hand side of Eq. (4.86), is that the saddle points that are pertinent to establish the large-time behaviour of $|\psi(x,t)|$ are k_{01} and k_{02}. They are equipollent in the sense that they yield the same negative growth rate, $\Re(\lambda(k_{01})) = \Re(\lambda(k_{02}))$, as shown by Eq. (4.92). On the other hand, the saddle point k_{03} is to be excluded as the steepest-descent paths departing from this point run along the imaginary k-axis and cannot be employed for the steepest-descent approximation of the perturbation wave

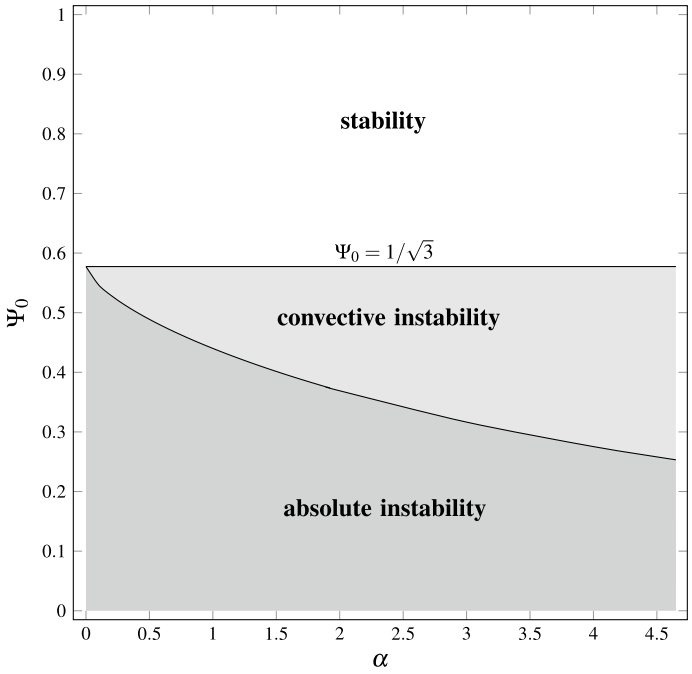

Fig. 4.9 Regions of convective and absolute instabilities for a convective Cahn–Hilliard process

packet. We can state that the solution $\Psi = \Psi_0 = 1/\sqrt{3}$ is linearly stable for every positive value of α. The same conclusion is achieved for every choice of Ψ_0 with $\Psi_0 > 1/\sqrt{3}$. On the other hand, when $0 < \Psi_0 < 1/\sqrt{3}$, the transition to absolute instability takes place only for a sufficiently small α, as illustrated in Fig. 4.9.

We point out that the holomorphy requirement is automatically satisfied, as $\lambda(k)$ is holomorphic throughout the complex k-plane, as it is shown by Eq. (4.84). Obviously, since we are applying the steepest-descent approximation to the wave packet $\psi(x,t)$ expressed by Eq. (4.86), the initial condition must be such that $\tilde{\psi}(k,0)$ is a holomorphic function of k. In fact, as discussed in Sect. 3.5.3, we have to assume the absence of any singularity of $\tilde{\psi}(k,0)$ in the region of the complex plane bounded by the real k-axis, $\Im(k) = 0$, and the deformed curve γ^* locally crossing the pertinent saddle points through a path of steepest descent.

4.5 Some Considerations on Convective and Absolute Instabilities

There is a wide literature regarding the concepts of convective and absolute instabilities. Most of the references regard fluid dynamics and, among them, we mention the books by Charru [15], Manneville [12], Schmid and Henningson [4]. A quite

detailed analysis of absolute instability in flow system can be found in the review papers by Huerre [9] and Huerre and Monkewitz [10].

The origin of the concept of absolute instability is usually dated back to studies in the field of plasma physics as reported by Dysthe [5]. A discussion of the concept of absolute instability compared to convective instability is available in the second edition of the book on fluid mechanics by Landau and Lifshitz [11].[2] It is also worth being mentioned that a slightly different version of the example of one-dimensional Burgers flow, employed in Sect. 4.2 as a test case to introduce convective and absolute instabilities, was previously discussed by Brevdo and Bridges [3], as well as by Barletta and Alves [2].

Several studies available in the literature, and the paper by Brevdo and Bridges [3] is an example, approach the discussion of the transition from convective to absolute instability by employing a representation of the perturbation wave packet in terms of a double Fourier–Laplace transform. This choice yields a mildly complicated version of the mathematical analysis employed for the study of instability, and generally speaking, it is not strictly necessary to achieve a rigorous definition of the concept of absolute instability.

Another aspect of the literature that somehow tends to complicate life for the newcomers of absolute instability is the tendency to mix this topic with that of *spatial normal modes*. Spatial stability analysis aims to establish the growth or decay of a localized perturbation, periodic in time downstream of the basic flow. Hence, things are adjusted as to control the growth in space of a perturbation instead of assessing its growth in time at a given position, as happens with the convective stability analysis. In practice, spatial normal modes differ from the *temporal normal modes*, that is the usual Fourier modes employed throughout this book, as the former type of modes features a complex wave number, k, and a purely imaginary time growth, $\Re(\lambda(k)) = 0$, which is often described as a purely real angular frequency. For instance, the book by Schmid and Henningson [15] presents spatial normal modes as some sort of prerequisite for the rigorous definition of absolute instability. This choice is perfectly correct although the purely mathematical process of saddle-point detection in the complex k-plane is endowed with a physical meaning, i.e. the dynamics of spatial normal modes, that may sound a bit cryptical for a first approach to absolute instability. In fact, the analysis in the complex k-plane is needed as an implementation of the steepest-descent approximation of a wave packet perturbation. As such, no physical meaning for the complex values of k is strictly necessary as a justification of the method. Following the presentation of absolute instability in terms of spatial normal modes, what is purely mathematical, as the holomorphy requirement discussed in Sect. 3.5.3, becomes a physical process of collision between different branches of spatial normal modes, described through the so-called *Briggs' method* [14, 15]. Such a scheme, only apparently different from that presented here, can be extremely suggestive when the concept of absolute instability is familiar to the reader. On the other hand, it may appear to be a little convoluted as a first approach to this matter.

[2] In this book, the terminology *convected* instability is used instead of convective instability.

References

1. Arnold VI (1989) Mathematical methods of classical mechanics. Springer, New York
2. Barletta A, Alves LSDB (2017) Absolute instability: a toy model and an application to the Rayleigh–Bénard problem with horizontal flow in porous media. Int J Heat Mass Transf 104:438–455
3. Brevdo L, Bridges TJ (1996) Absolute and convective instabilities of spatially periodic flows. Philos Trans R Soc Lond A 354:1027–1064
4. Charru F (2011) Hydrodynamic instabilities. Cambridge University Press, Cambridge
5. Dysthe KB (1966) Convective and absolute instability. Nucl Fusion 6:215–222
6. Emmott C, Bray A (1996) Coarsening dynamics of a one-dimensional driven Cahn–Hilliard system. Phys Rev E 54:4568–4575
7. Golovin AA, Nepomnyashchy AA, Davis SH, Zaks MA (2001) Convective Cahn–Hilliard models: from coarsening to roughening. Phys Rev Lett 86:1550–1553
8. Hirsch MW, Smale S, Devaney RL (2004) Differential equations, dynamical systems, and an introduction to chaos. Academic Press, New York
9. Huerre P (2000) Open shear flow instabilities. In: Batchelor GK, Moffatt HK, Worster MG (eds) Perspectives in fluid dynamics. Cambridge University Press, Cambridge, pp 159–229
10. Huerre P, Monkewitz PA (1990) Local and global instabilities in spatially developing flows. Annu Rev Fluid Mech 22:473–537
11. Landau L, Lifshitz E (1987) Fluid Mechanics, 2nd edn. Pergamon Press, Oxford
12. Manneville P (2004) Instabilities, chaos and turbulence. Imperial College Press, London
13. Nieuwstadt FTM, Steketee JA (1995) Selected papers of J. M. Burgers. Springer, Dordrecht
14. Rose DJ, Chung K, Parker RR, Wagner C, Manheimer W, Brown T, Dupree TH, McNary C, Davis J, Briggs R, et al (1967) Plasmas and controlled nuclear fusion. Technical report, Research Laboratory of Electronics (RLE) at the Massachusetts Institute of Technology (MIT), Cambridge
15. Schmid PJ, Henningson DS (2001) Stability and transition in shear flows. Springer, New York

Part II
Flow and Convection in Porous Media

The physics of fluid flow is illustrated through its governing equations. The balance of extensive physical properties of the fluid such as mass, momentum and energy is exploited by introducing the Reynolds' transport theorem. This mathematical tool allows one to attain a general formulation of the local balance equations needed for the description of fluid flow. The local balance equations are formulated for the seepage flow in porous media. The framework based on the governing equations of fluid flow is applied to the analysis of the Rayleigh–Bénard problem in a fluid and in a saturated porous medium. The convective instability is exploited through the analysis of a number of different conditions and assumptions.

Chapter 5
The Equations of Fluid Flow

5.1 The Description of Fluid Flow

The basic idea behind the classical description of the fluid flow is that a fluid is a *continuous medium*. This means that, although a fluid (liquid or gas) has elementary constituents (atoms, ions and molecules), these constituents are so small that the length scale of every phenomenon involved in the macroscopic fluid flow will be much larger than the molecular scale. Hence, it is perfectly legitimate to consider *infinitesimal fluid elements* (see Fig. 5.1). In fact, the mathematical concept of infinitesimal scale is in any case relative to very small spatial domains where the number of elementary constituents is still extremely large (of the order of Avogadro's constant, 6.022×10^{23}).

The fluid is then described as partitioned in an infinite number of infinitesimal fluid elements each one evolving in time along its own trajectory. This description of the fluid flow presumes that we are able to know which is the spatial position $\mathbf{x} = (x, y, z)$ of every infinitesimal fluid element at every instant of time t. In doing this, we are implicitly assuming that the same spatial position $\mathbf{x} = (x, y, z)$ cannot be occupied by two different infinitesimal fluid elements at the same instant of time t (*localisation hypothesis*).

On tracing the trajectory of an infinitesimal fluid element, we can define its instantaneous velocity $\mathbf{v}$ at every instant of time t. If $\mathbf{x}(t) = (x(t), y(t), z(t))$ is the instantaneous position of an infinitesimal fluid element, its *instantaneous velocity* is defined as

$$\mathbf{v}(t) = \frac{\mathrm{d}\,\mathbf{x}(t)}{\mathrm{d}\,t} \,. \tag{5.1}$$

Therefore, we can define the *velocity field*, $\mathbf{u}(x, y, z, t)$, as the instantaneous velocity $\mathbf{v}(t)$ of the infinitesimal fluid element occupying the position $(x, y, z) = (x(t), y(t), z(t))$ at time t (see Fig. 5.2). The concept of velocity field is well-defined inasmuch as the localisation hypothesis holds.

We assume that the number of atoms, ions or molecules contained in an infinitesimal fluid element is large enough to consider it as a closed thermodynamic system.

A. Barletta, *Routes to Absolute Instability in Porous Media*,
https://doi.org/10.1007/978-3-030-06194-4_5

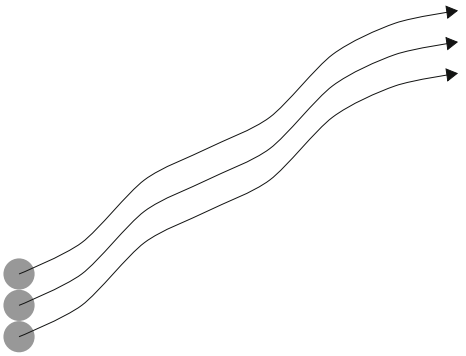

Fig. 5.1 A group of infinitesimal fluid elements evolving along their own trajectories

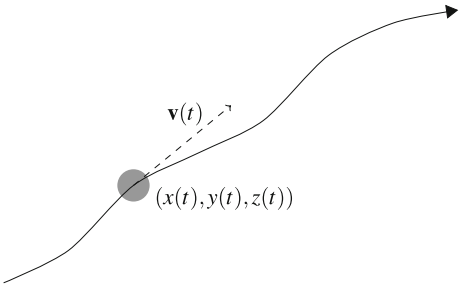

Fig. 5.2 Instantaneous velocity of an infinitesimal fluid element occupying the position $\mathbf{x}(t) = (x(t), y(t), z(t))$ at time t

Then, at every time, we can reasonably think of an "internal" thermodynamic state of the infinitesimal fluid element. The thermodynamic state of the infinitesimal fluid element can be described in a fairly simple way provided that it is a stable equilibrium state. The latter assumption, called *local equilibrium hypothesis*, is a reasonable one if the evolution of this very small thermodynamic system is sufficiently slow for having an instantaneous thermal equilibration of the fluid element. That an infinitesimal time is needed for reaching the thermodynamic equilibrium in a system of infinitesimal size appears as quite conceivable, even if exceptions may arise when the time evolution is so quick that the molecular processes lose coherence. An important characteristic property of the fluid, that will be defined in the last section of this chapter, is the thermal diffusivity α. For a given time scale Δt of the thermodynamic evolution, one can construct a corresponding length scale with $(\alpha\, \Delta t)^{1/2}$. In a gas, the breakdown of the local equilibrium hypothesis can be envisaged when this length scale is of the order of the mean free path of the elementary constituents (atoms, ions and molecules). The mean free path is the average distance travelled by a particle between two collisions and is of variable order of magnitude, ranging from 10^{-7} m for a gas at ambient pressure to several meters for a rarefied gas. In a liquid, the breakdown of the local equilibrium hypothesis is expected when $(\alpha\, \Delta t)^{1/2}$ is of the order of the molecular size (10^{-10} m at its smallest). A consequence of the local equilibrium hypothesis is that the "internal" thermodynamic state of the infinitesimal fluid element is determined by its temperature, T, and density, ρ. All the thermodynamic

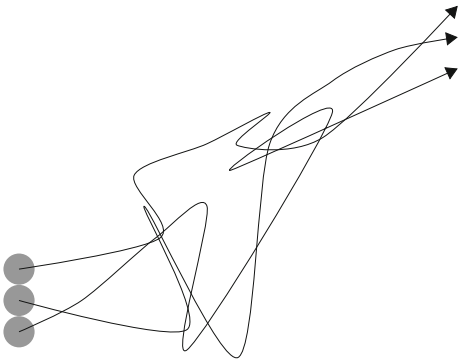

Fig. 5.3 Extremely tangled trajectories of three infinitesimal fluid elements in a turbulent flow

properties of the infinitesimal fluid element, such as the pressure, p, and the internal energy per unit mass, φ, are functions of (ρ, T).

The local equilibrium hypothesis implies that, at a given instant of time t, the infinitesimal fluid element is characterised by a temperature T, a density ρ and a pressure p. Thus, with a procedure perfectly similar to that invoked on defining the velocity field, one can also define the *temperature field*, $T(x, y, z, t)$, as the temperature T of the infinitesimal fluid element occupying the position (x, y, z) at time t. One can define the *density field*, $\rho(x, y, z, t)$, as the density ρ of the infinitesimal fluid element occupying the position (x, y, z) at time t. Finally, one can define the *pressure field*, $p(x, y, z, t)$, as the pressure p of the infinitesimal fluid element occupying the position (x, y, z) at time t. We stress that this procedure makes sense only if there is one and only one infinitesimal fluid element occupying the position (x, y, z) at time t. The localisation hypothesis does not hold for every flow regime, so that there exist fluid flows where the velocity field, the temperature field, the density field, the pressure field cannot be consistently defined. These flows generally take place when the flow rates are very high. When this happens, the flow experiences a transition from laminar to turbulent. For turbulent flows, the localisation hypothesis does not hold any more.

One can imagine the lack of validity of the localisation hypothesis as being a consequence of the extremely tangled geometry of the trajectories in a turbulent flow (see Fig. 5.3). The point is in fact even more complicated. The concept of infinitesimal fluid element and of trajectory of an infinitesimal fluid element loses any conceivability when the flow is turbulent. The physical reason is that molecular diffusion mechanisms arise, leading to an internal mixing at the molecular scale. Therefore, a given amount of fluid occupying an infinitesimal volume at the initial instant of time $t = 0$ may be spread over a finite region, even of very large size, at later times $t > 0$ (see Fig. 5.4).

We can conclude that we have a good paradigm for the description of fluid flows of laminar nature, but we have no consistent paradigm for the description of turbulent fluid flows. This problem prevents the possibility of a theory of turbulence, that is in fact still lacking. What physicists and engineers can say about turbulence has been

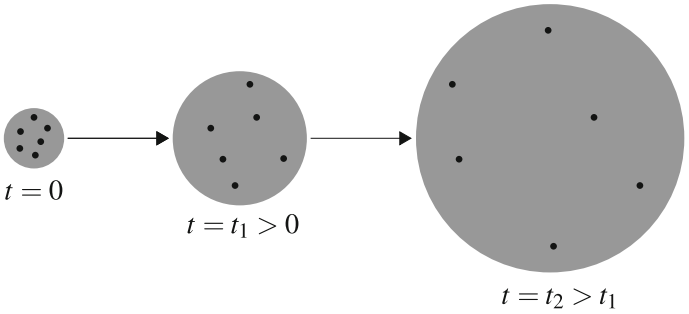

Fig. 5.4 Spreading over larger regions of an initially infinitesimal fluid element

conveyed during the last century into phenomenological models of turbulent flows, that cannot in any case be considered as theories of turbulence.

5.2 Reynolds' Transport Theorem

In order to describe fluid flow in a given region of space $\mathscr{R}$, it is convenient to investigate the displacements undergone, in a given time interval, by a *fluid body*, i.e. a fluid part bounded by an ideal surface impermeable with respect to mass flux. Obviously, this definition implies that a fluid body is a closed thermodynamic system. The concept of fluid body is the basis of the *Lagrangian description* of fluid flow.[1]

Let us consider a fluid body having mass M e let us denote by $\mathscr{R}_t \subset \mathscr{R}$ the region of space occupied by the fluid body at time t. Under fluid flow, the region of space $\mathscr{R}_t$ is continuously displaced driven by the moving fluid. The boundary of $\mathscr{R}_t$ is supposed to be a regular closed surface denoted by $\partial\mathscr{R}_t$. Each point in $\mathscr{R}_t$ is identified by the changing coordinates $(x(t), y(t), z(t))$. The outward unit normal to $\partial\mathscr{R}_t$ is denoted by $\mathbf{n}$ (see Fig. 5.5).

Let us consider any *extensive property*, Ψ, of the fluid body. In thermodynamics, one calls extensive any property of a system whose instantaneous value can be evaluated by summing up the values of the property assumed by all the subsystems of the given system. Mass, volume, energy and entropy are just a few examples of extensive properties. The mass of a system partitioned into two halves is the sum of the masses of the two halves.

To every extensive property Ψ of the fluid body, one can always associate a corresponding *specific property*, ψ, obtained by locally dividing the value of Ψ of any subsystem by its mass. If the subsystem employed to define ψ is an infinitesimal fluid element of mass $\mathrm{d}M = \rho\,\mathrm{d}V$, then one can intend ψ as a local field depending

[1] As opposed to the Lagrangian description, the Eulerian description is based on a fixed volume through which the fluid flows. Thus, the Eulerian description is focussed on an open thermodynamic system.

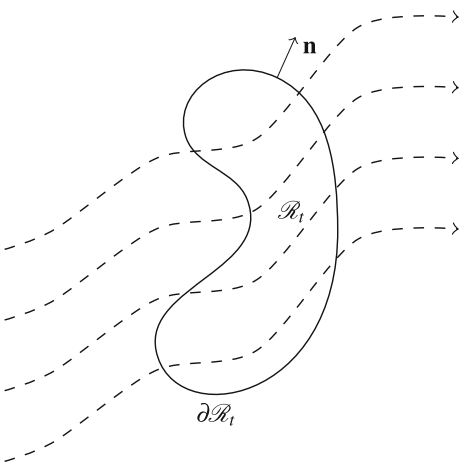

Fig. 5.5 Displacement of the fluid body occupying the moving region $\mathscr{R}_t$

on the local coordinates, as well as on time. Hence, the extensive character of the property Ψ allows one to write

$$\Psi(t) = \iiint_{\mathscr{R}_t} \rho\, \psi \, \mathrm{d}x\, \mathrm{d}y\, \mathrm{d}z \ , \tag{5.2}$$

where the integration measure $\mathrm{d}x\, \mathrm{d}y\, \mathrm{d}z$ describes the infinitesimal moving volume $\mathrm{d}V$. By tracing the trajectory of each infinitesimal fluid element, one has a one–to–one correspondence between the position at time t, $(x(t), y(t), z(t))$, and the corresponding position at initial time, $t = 0$, namely $(x(0), y(0), z(0)) = (X, Y, Z)$. Obviously, if $(x(t), y(t), z(t)) \in \mathscr{R}_t$, one has $(X, Y, Z) \in \mathscr{R}_0$. With this in mind, one can change the measure of integration on the right-hand side of equation (5.2), by introducing a suitable Jacobian, J. In particular, one obtains

$$\Psi(t) = \iiint_{\mathscr{R}_0} \rho\, \psi\, J \, \mathrm{d}X\, \mathrm{d}Y\, \mathrm{d}Z \ . \tag{5.3}$$

The Jacobian J is the determinant of the matrix expressing the change of coordinates [1], from $(x(t), y(t), z(t))$ to (X, Y, Z). Hence, we can express J by employing the Levi-Civita symbol, ε_{ijk}, and Einstein's notation for repeated indices, namely

$$J = \det \begin{pmatrix} \dfrac{\partial x}{\partial X} & \dfrac{\partial x}{\partial Y} & \dfrac{\partial x}{\partial Z} \\ \dfrac{\partial y}{\partial X} & \dfrac{\partial y}{\partial Y} & \dfrac{\partial y}{\partial Z} \\ \dfrac{\partial z}{\partial X} & \dfrac{\partial z}{\partial Y} & \dfrac{\partial z}{\partial Z} \end{pmatrix} = \varepsilon_{ijk} \frac{\partial x_1}{\partial X_i} \frac{\partial x_2}{\partial X_j} \frac{\partial x_3}{\partial X_k} \ . \tag{5.4}$$

In Eq. (5.4), symbols (x_1, x_2, x_3) and (X_1, X_2, X_3) have been used instead of (x, y, z) and (X, Y, Z), respectively, as they are more convenient to implement Einstein's notation for sums over repeated indices. For readers unfamiliar with Levi-Civita symbol, or Kronecker's delta, or Einstein's notation for tensor operations, we refer to Appendix B. In particular, the expression of J in Eq. (5.4) is a consequence of equation (B.22) of Appendix B. We want to evaluate the time derivative of $\Psi(t)$. From Eq. (5.3), we obtain

$$\begin{aligned}\frac{\mathrm{d}\,\Psi}{\mathrm{d}\,t} &= \iiint_{\mathscr{R}_0} \left[\frac{\partial(\rho\,\psi)}{\partial t}\; J + \frac{\partial(\rho\,\psi)}{\partial x_i}\; \frac{\mathrm{d}\,x_i}{\mathrm{d}\,t}\; J + \rho\,\psi\; \frac{\partial J}{\partial t} \right] \mathrm{d}X\,\mathrm{d}Y\,\mathrm{d}Z \\ &= \iiint_{\mathscr{R}_0} \left[\frac{\partial(\rho\,\psi)}{\partial t}\; J + \frac{\partial(\rho\,\psi)}{\partial x_i}\; u_i\; J + \rho\,\psi\; \frac{\partial J}{\partial t} \right] \mathrm{d}X\,\mathrm{d}Y\,\mathrm{d}Z\;, \end{aligned} \tag{5.5}$$

where the definitions of instantaneous velocity over a trajectory, and of velocity field, $\mathbf{u}$ with components u_i, have been employed. We now express the derivative $\partial J/\partial t$, by using again the definition of velocity field,

$$\begin{aligned}\frac{\partial J}{\partial t} &= \varepsilon_{ijk}\, \frac{\partial u_1}{\partial X_i}\, \frac{\partial x_2}{\partial X_j}\, \frac{\partial x_3}{\partial X_k} + \varepsilon_{ijk}\, \frac{\partial x_1}{\partial X_i}\, \frac{\partial u_2}{\partial X_j}\, \frac{\partial x_3}{\partial X_k} + \varepsilon_{ijk}\, \frac{\partial x_1}{\partial X_i}\, \frac{\partial x_2}{\partial X_j}\, \frac{\partial u_3}{\partial X_k} \\ &= \frac{\partial u_1}{\partial x_\ell}\, \varepsilon_{ijk}\, \frac{\partial x_\ell}{\partial X_i}\, \frac{\partial x_2}{\partial X_j}\, \frac{\partial x_3}{\partial X_k} + \frac{\partial u_2}{\partial x_m}\, \varepsilon_{ijk}\, \frac{\partial x_1}{\partial X_i}\, \frac{\partial x_m}{\partial X_j}\, \frac{\partial x_3}{\partial X_k} \\ &\qquad + \frac{\partial u_3}{\partial x_n}\, \varepsilon_{ijk}\, \frac{\partial x_1}{\partial X_i}\, \frac{\partial x_2}{\partial X_j}\, \frac{\partial x_n}{\partial X_k} \\ &= \left(\frac{\partial u_1}{\partial x_1} + \frac{\partial u_2}{\partial x_2} + \frac{\partial u_3}{\partial x_3} \right) \varepsilon_{ijk}\, \frac{\partial x_1}{\partial X_i}\, \frac{\partial x_2}{\partial X_j}\, \frac{\partial x_3}{\partial X_k} = (\boldsymbol{\nabla} \cdot \mathbf{u})\, J\;, \end{aligned} \tag{5.6}$$

where we recognised that ℓ can only be equal to 1, m can only be equal to 2, and n can only be equal to 3. In fact, expressions such as

$$\varepsilon_{ijk}\, \frac{\partial x_\ell}{\partial X_i}\, \frac{\partial x_2}{\partial X_j}\, \frac{\partial x_3}{\partial X_k}\;,$$

yield the determinant of a matrix with two equal rows, which is zero, unless $\ell = 1$. On account of Eq. (5.6), Eq. (5.5) can be rewritten as

$$\begin{aligned}\frac{\mathrm{d}\,\Psi}{\mathrm{d}\,t} &= \iiint_{\mathscr{R}_0} \left[\frac{\partial(\rho\,\psi)}{\partial t} + \mathbf{u} \cdot \boldsymbol{\nabla}(\rho\,\psi) + \rho\,\psi\, \boldsymbol{\nabla} \cdot \mathbf{u} \right] J\, \mathrm{d}X\,\mathrm{d}Y\,\mathrm{d}Z \\ &= \iiint_{\mathscr{R}_0} \left[\frac{\partial(\rho\,\psi)}{\partial t} + \boldsymbol{\nabla} \cdot (\rho\,\psi\,\mathbf{u}) \right] J\, \mathrm{d}X\,\mathrm{d}Y\,\mathrm{d}Z\;, \end{aligned} \tag{5.7}$$

so that one finally has

$$\frac{\mathrm{d}\,\Psi}{\mathrm{d}\,t} = \iiint_{\mathscr{R}_t} \left[\frac{\partial(\rho\,\psi)}{\partial t} + \nabla \cdot (\rho\,\psi\,\mathbf{u}) \right] \mathrm{d}x\,\mathrm{d}y\,\mathrm{d}z\ . \tag{5.8}$$

Equation (5.8) represents the statement of Reynolds' transport theorem.

5.3 Local Mass Balance Equation

In this section, the first and simplest application of Reynolds' transport theorem is presented: the deduction of the local mass balance equation. Let us assume that the extensive property Ψ is the mass M of the fluid element. Since the fluid element is a closed thermodynamic system, M does not change with time. Hence, the left-hand side of equation (5.8) is zero. The specific property ψ is obtained as the ratio between Ψ and the mass, so that one has $\psi = 1$ in this case. As a consequence, Eq. (5.8) allows one to infer that

$$\iiint_{\mathscr{R}_t} \left[\frac{\partial\rho}{\partial t} + \nabla \cdot (\rho\,\mathbf{u}) \right] \mathrm{d}x\,\mathrm{d}y\,\mathrm{d}z = 0\ . \tag{5.9}$$

Since Eq. (5.9) must hold for every possible choice of the fluid body and, thus, for every region of space $\mathscr{R}_t$ included in the domain $\mathscr{R}$ occupied by the fluid, the integrand must be identically zero. In other words, one has

$$\frac{\partial\rho}{\partial t} + \nabla \cdot (\rho\,\mathbf{u}) = 0\ . \tag{5.10}$$

The partial differential equation (5.10) is the *local mass balance equation*, well known also as the *equation of continuity*. One can easily conclude that, if the density field ρ can be considered as time independent and uniform, i.e. for an *incompressible flow*, the equation of continuity is reduced to $\nabla \cdot \mathbf{u} = 0$. Hence, in this case, the velocity field is *solenoidal*.[2]

Equation (5.10) allows one to reformulate Reynolds' transport theorem through the following equation:

$$\begin{aligned}\frac{\mathrm{d}\,\Psi}{\mathrm{d}\,t} &= \iiint_{\mathscr{R}_t} \left[\rho\,\frac{\partial\psi}{\partial t} + \psi\,\frac{\partial\rho}{\partial t} + \rho\,\mathbf{u}\cdot\nabla\psi + \psi\,\nabla\cdot(\rho\,\mathbf{u}) \right] \mathrm{d}x\,\mathrm{d}y\,\mathrm{d}z \\ &= \iiint_{\mathscr{R}_t} \rho \left(\frac{\partial\psi}{\partial t} + \mathbf{u}\cdot\nabla\psi \right) \mathrm{d}X\,\mathrm{d}Y\,\mathrm{d}Z = \iiint_{\mathscr{R}_t} \rho\,\frac{\mathrm{D}\psi}{\mathrm{D}\,t}\,\mathrm{d}x\,\mathrm{d}y\,\mathrm{d}z\ .\end{aligned} \tag{5.11}$$

[2]The term solenoidal comes from electromagnetism as the magnetic induction field in a solenoid is a vector field with zero divergence.

In obtaining Eq. (5.11), use has been made of the mathematical identity

$$\nabla \cdot (\rho\, \psi\, \mathbf{u}) = \rho\, \mathbf{u} \cdot \nabla \psi + \psi\, \nabla \cdot (\rho\, \mathbf{u}) \,, \tag{5.12}$$

and of the definition of *substantial derivative*,

$$\frac{\mathrm{D}\psi}{\mathrm{D}\,t} = \frac{\partial \psi}{\partial t} + \mathbf{u} \cdot \nabla \psi \,. \tag{5.13}$$

Hereafter, for the sake of brevity, the measure $\mathrm{d}x\,\mathrm{d}y\,\mathrm{d}z$ will be simply denoted by $\mathrm{d}V$ so that Eq. (5.11) reads

$$\frac{\mathrm{d}\,\Psi}{\mathrm{d}\,t} = \iiint_{\mathscr{R}_t} \rho\, \frac{\mathrm{D}\psi}{\mathrm{D}\,t}\, \mathrm{d}V \,. \tag{5.14}$$

The alternative formulation of equation (5.10), based on Einstein's notation, is given by

$$\frac{\partial \rho}{\partial t} + \frac{\partial (\rho\, u_j)}{\partial x_j} = 0 \,. \tag{5.15}$$

5.4 Forces Acting on a Fluid Body

The forces acting on the fluid body occupying the moving region $\mathscr{R}_t$ can be classified as *body forces* acting on the infinitesimal fluid elements in the interior of $\mathscr{R}_t$, and as *surface forces* acting on the boundary $\partial\mathscr{R}_t$. When dealing with surface forces, one defines the *traction*, meaning the force per unit area acting on the boundary of the fluid body.

Let b_i denote the ith component of the body force, i.e. of the force per unit volume acting on the fluid element and due to external fields of either gravitational, electric or magnetic origin. Thus, the ith component of the resultant body force acting on the fluid element is

$$F_i^{(\mathrm{b})} = \iiint_{\mathscr{R}_t} b_i\, \mathrm{d}V \,. \tag{5.16}$$

In the following, it will be tacitly assumed that the body force is of gravitational origin, so that $\mathbf{b} = \rho\, \mathbf{g}$, where $\mathbf{g}$ is the gravitational acceleration. However, there can be applications where also contributions due to external electric and magnetic fields are important, as in the study of magnetohydrodynamics (MHD) [5].

In the evaluation of the total force F_i applied to the fluid element, one must consider, in addition to the gravitational body force contribution, also the resultant $F_i^{(\mathrm{s})}$ of the traction acting on the boundary surface of the fluid element, namely

$$F_i^{(\mathrm{s})} = \iint_{\partial \mathscr{R}_t} f_i \, \mathrm{d}S \ , \tag{5.17}$$

where f_i is the ith component of the traction, i.e. the force per unit area, acting on the boundary surface $\partial \mathscr{R}_t$ of the fluid element, and $\mathrm{d}S$ is the measure of the surface integral.

The traction f_i can be expressed through the *mechanical stress tensor* σ as

$$f_i = \sigma_{ij} \, n_j \ , \tag{5.18}$$

where n_j is the jth component of the unit outward normal $\mathbf{n}$ to $\partial \mathscr{R}_t$ (see Fig. 5.5). By employing Gauss' theorem (see Appendix B), Eqs. (5.17) and (5.18) yield an expression of $F_i^{(\mathrm{s})}$ in terms of a volume integral, namely

$$F_i^{(\mathrm{s})} = \iiint_{\mathscr{R}_t} \frac{\partial \sigma_{ij}}{\partial x_j} \, \mathrm{d}V \ , \tag{5.19}$$

so that the resultant force acting on the fluid body is given by

$$F_i = F_i^{(\mathrm{b})} + F_i^{(\mathrm{s})} = \iiint_{\mathscr{R}_t} \left(\rho \, g_i + \frac{\partial \sigma_{ij}}{\partial x_j} \right) \mathrm{d}V \ . \tag{5.20}$$

5.5 Local Momentum Balance Equation

Let the extensive property Ψ be the ith component of momentum. On account of the definition of momentum of a point-like object, one can easily conclude that the corresponding specific property ψ is the ith component of the velocity field, u_i. From elementary mechanics, we know that the time derivative of the ith component of momentum is equal to the ith component of the resultant force, F_i, acting on the mechanical system. Then, Reynolds' transport theorem (5.14) yields

$$\iiint_{\mathscr{R}_t} \rho \, \frac{\mathrm{D}\, u_i}{\mathrm{D}\, t} \, \mathrm{d}V = F_i \ , \tag{5.21}$$

so that, by employing equation (5.20), one obtains

$$\iiint_{\mathscr{R}_t} \left(\rho \, \frac{\mathrm{D}\, u_i}{\mathrm{D}\, t} - \rho \, g_i - \frac{\partial \sigma_{ij}}{\partial x_j} \right) \mathrm{d}V = 0 \ . \tag{5.22}$$

We are in a situation identical to Eq. (5.9). The integral on the left-hand side of equation (5.22) must be zero for every possible choice of the region of space $\mathscr{R}_t$, so that the integrand must be identically zero,

$$\rho \frac{\mathrm{D}\, u_i}{\mathrm{D}\, t} = \rho\, g_i + \frac{\partial \sigma_{ij}}{\partial x_j} \,. \tag{5.23}$$

Equation (5.23) is the *local momentum balance equation*.

5.6 Local Angular Momentum Balance Equation

One of the main properties of the mechanical stress tensor σ is its symmetry, $\sigma_{ij} = \sigma_{ji}$. The symmetry of the mechanical stress tensor is a consequence of the local balance of the angular momentum.

By remembering that the moment of a force is obtained through the vector product between the position vector $\mathbf{x}$ and the force, the resultant moment of the forces acting on the fluid body contained in $\mathscr{R}_t$ can be expressed, on account of equations (5.16) and (5.17), as

$$\mathbf{K} = \iiint_{\mathscr{R}_t} \mathbf{x} \times (\rho\, \mathbf{g})\, \mathrm{d}V + \iint_{\partial \mathscr{R}_t} \mathbf{x} \times \mathbf{f}\, \mathrm{d}S \,. \tag{5.24}$$

Once more, we refer the reader to Appendix B for the properties of the Levi-Civita symbol. By using Eqs. (5.18) and (B.20), we can write the ith component of $\mathbf{K}$ as

$$\begin{aligned} K_i &= \iiint_{\mathscr{R}_t} \rho\, \varepsilon_{ijk}\, x_j\, g_k\, \mathrm{d}V + \iint_{\partial \mathscr{R}_t} \varepsilon_{ijk}\, x_j\, f_k\, \mathrm{d}S \\ &= \iiint_{\mathscr{R}_t} \rho\, \varepsilon_{ijk}\, x_j\, g_k\, \mathrm{d}V + \iint_{\partial \mathscr{R}_t} \varepsilon_{ijk}\, x_j\, \sigma_{k\ell}\, n_\ell\, \mathrm{d}S \,. \end{aligned} \tag{5.25}$$

By employing Gauss' theorem, the surface integral over $\partial \mathscr{R}_t$ can be rewritten as a volume integral, so that Eq. (5.25) reads

$$K_i = \iiint_{\mathscr{R}_t} \varepsilon_{ijk} \left[\rho\, x_j\, g_k + \frac{\partial (x_j\, \sigma_{k\ell})}{\partial x_\ell} \right] \mathrm{d}V \,. \tag{5.26}$$

Let the extensive property Ψ be the ith component of the angular momentum, L_i. Then, from elementary mechanics, the corresponding specific quantity ψ is $\varepsilon_{ijk}\, x_j\, u_k$. As a consequence of Reynolds' transport theorem, Eq. (5.14), one can write

$$\frac{\mathrm{d}\,L_i}{\mathrm{d}\,t} = \iiint\limits_{\mathscr{R}_t} \rho\ \varepsilon_{ijk}\ \frac{\mathrm{D}(x_j\,u_k)}{\mathrm{D}\,t}\ \mathrm{d}V = \iiint\limits_{\mathscr{R}_t} \rho\ \varepsilon_{ijk}\left[x_j\ \frac{\partial u_k}{\partial t} + u_\ell\ \frac{\partial (x_j\,u_k)}{\partial x_\ell}\right]\mathrm{d}V$$

$$= \iiint\limits_{\mathscr{R}_t} \rho\left[\varepsilon_{ijk}\,x_j\ \frac{\partial u_k}{\partial t} + \varepsilon_{ijk}\,u_\ell\,\delta_{j\ell}\,u_k + \varepsilon_{ijk}\,x_j\,u_\ell\ \frac{\partial u_k}{\partial x_\ell}\right]\mathrm{d}V$$

$$= \iiint\limits_{\mathscr{R}_t} \rho\left[\varepsilon_{ijk}\,x_j\ \frac{\partial u_k}{\partial t} + \varepsilon_{ijk}\,u_j\,u_k + \varepsilon_{ijk}\,x_j\,u_\ell\ \frac{\partial u_k}{\partial x_\ell}\right]\mathrm{d}V$$

$$= \iiint\limits_{\mathscr{R}_t} \rho\ \varepsilon_{ijk}\,x_j\ \frac{\mathrm{D}u_k}{\mathrm{D}\,t}\ \mathrm{d}V\ , \tag{5.27}$$

where we recognised that $\partial x_j/\partial x_\ell = \delta_{j\ell}$, and that $\varepsilon_{ijk}\,u_j\,u_k = 0$ as it represents the ith component of the vector product of $\mathbf{u}$ with itself. The mechanical balance of angular momentum prescribes that

$$\frac{\mathrm{d}\,L_i}{\mathrm{d}\,t} = K_i\ . \tag{5.28}$$

Then, we obtain

$$\iiint\limits_{\mathscr{R}_t} \varepsilon_{ijk}\left[\rho\,x_j\ \frac{\mathrm{D}u_k}{\mathrm{D}\,t} - \rho\,x_j\,g_k - \frac{\partial (x_j\,\sigma_{k\ell})}{\partial x_\ell}\right]\mathrm{d}V = 0\ , \tag{5.29}$$

which can be rewritten as

$$\iiint\limits_{\mathscr{R}_t} \varepsilon_{ijk}\left[\rho\,x_j\ \frac{\mathrm{D}u_k}{\mathrm{D}\,t} - \rho\,x_j\,g_k - x_j\ \frac{\partial \sigma_{k\ell}}{\partial x_\ell} - \sigma_{kj}\right]\mathrm{d}V = 0\ . \tag{5.30}$$

By employing the local momentum balance equation (5.23), one can rewrite Eq. (5.30) as

$$\iiint\limits_{\mathscr{R}_t} \varepsilon_{ijk}\,\sigma_{kj}\ \mathrm{d}V = 0\ . \tag{5.31}$$

Following the usual argument, since Eq. (5.31) must hold for every possible choice of the region $\mathscr{R}_t$, the integrand must be zero, so that we can write the local equation

$$\varepsilon_{ijk}\,\sigma_{kj} = 0\ . \tag{5.32}$$

Due to the properties of the Levi-Civita symbol (see Appendix B), Eq. (5.32) with $i = 1, 2, 3$ yields the equalities

$$\sigma_{32} = \sigma_{23} \ , \quad \sigma_{31} = \sigma_{13} \ , \quad \sigma_{12} = \sigma_{21} \ . \tag{5.33}$$

This just means that σ is a symmetric tensor, i.e. that $\sigma_{ij} = \sigma_{ji}$.

5.7 Local Energy Balance Equation

Let us now assume that the extensive property Ψ is the energy E of the fluid element. The energy per unit mass of the fluid, ψ, can be expressed as

$$\psi = \varphi + \frac{\mathbf{u} \cdot \mathbf{u}}{2} \ , \tag{5.34}$$

where φ is the internal energy per unit mass. In other words, we are assuming that ψ is the sum of the internal energy per unit mass and of the kinetic energy per unit mass. On account of equations (5.14) and (5.34), Reynolds' transport theorem yields

$$\frac{\mathrm{d}\, E}{\mathrm{d}\, t} = \iiint\limits_{\mathscr{R}_t} \rho \left(\frac{\mathrm{D}\varphi}{\mathrm{D}t} + \mathbf{u} \cdot \frac{\mathrm{D}\mathbf{u}}{\mathrm{D}t} \right) \mathrm{d}V \ . \tag{5.35}$$

The thermodynamic energy balance can be written as

$$\frac{\mathrm{d}\, E}{\mathrm{d}\, t} = \dot{Q} + \dot{W} \ , \tag{5.36}$$

where $\dot{Q}$ and $\dot{W}$ are, respectively, the thermal power and the mechanical power received by the fluid body. At time t, the thermal power received by the fluid body that occupies the region of space $\mathscr{R}_t$ is the sum of two terms: the thermal power $\dot{Q}_\mathrm{s}$ that crosses the boundary surface $\partial\mathscr{R}_t$ of the body; the thermal power $\dot{Q}_\mathrm{g}$ generated within the fluid element (due to phenomena such as, for instance, the Joule effect in the case of a conducting fluid carrying an electric current). The quantity $\dot{Q}_\mathrm{g}$ can be expressed by introducing the thermal power generated per unit volume within the fluid, q_g, so that one has

$$\dot{Q}_\mathrm{g} = \int\limits_{\mathscr{R}_t} q_\mathrm{g} \, \mathrm{d}V \ . \tag{5.37}$$

The quantity $\dot{Q}_\mathrm{s}$ can be determined by means of the *heat flux density* $\mathbf{q}$,

$$\dot{Q}_\mathrm{s} = - \iint\limits_{\partial\mathscr{R}_t} \mathbf{q} \cdot \mathbf{n} \, \mathrm{d}S \ , \tag{5.38}$$

where $\mathbf{n}$ is the outward normal unit vector to $\partial\mathscr{R}_t$. By invoking Gauss' theorem, one can write

$$\dot{Q}_\mathrm{s} = -\iiint_{\mathscr{R}_t} \nabla\cdot\mathbf{q}\,\mathrm{d}V\ . \tag{5.39}$$

Then, one has

$$\dot{Q} = \dot{Q}_\mathrm{g} + \dot{Q}_\mathrm{s} = \iiint_{\mathscr{R}_t} \left(q_\mathrm{g} - \nabla\cdot\mathbf{q}\right)\,\mathrm{d}V\ . \tag{5.40}$$

The mechanical power $\dot{W}$ received from the fluid body coincides with the work per unit time produced by the gravitational body force and by the traction acting on the boundary $\partial\mathscr{R}_t$ of the fluid body. Inside $\mathscr{R}_t$, one has a work per unit time due to the gravitational field and acting on each infinitesimal volume element, given by $\rho\,\mathbf{g}\cdot\mathbf{u}\,\mathrm{d}V$. Moreover, at every position in $\partial\mathscr{R}_t$, one has an infinitesimal work per unit time $\mathbf{f}\cdot\mathbf{u}\,\mathrm{d}S$, so that

$$\dot{W} = \iiint_{\mathscr{R}_t} \rho\,\mathbf{g}\cdot\mathbf{u}\,\mathrm{d}V + \iint_{\partial\mathscr{R}_t} \mathbf{f}\cdot\mathbf{u}\,\mathrm{d}S = \iiint_{\mathscr{R}_t} \rho\,g_i\,u_i\,\mathrm{d}V + \iint_{\partial\mathscr{R}_t} f_i\,u_i\,\mathrm{d}S\ . \tag{5.41}$$

On account of equation (5.18), and by employing Gauss' theorem, Eq. (5.41) can be rewritten as

$$\begin{aligned}\dot{W} &= \iiint_{\mathscr{R}_t} \rho\,g_i\,u_i\,\mathrm{d}V + \iint_{\partial\mathscr{R}_t} \sigma_{ij}\,u_i\,n_j\,\mathrm{d}S = \iiint_{\mathscr{R}_t} \left[\rho\,g_i\,u_i + \frac{\partial(\sigma_{ij}\,u_i)}{\partial x_j}\right]\mathrm{d}V \\ &= \iiint_{\mathscr{R}_t} \left[\rho\,g_i\,u_i + u_i\,\frac{\partial\sigma_{ij}}{\partial x_j} + \sigma_{ij}\,\frac{\partial u_i}{\partial x_j}\right]\mathrm{d}V\ .\end{aligned} \tag{5.42}$$

On account of equations (5.35), (5.36), (5.40) and (5.42), one obtains

$$\begin{aligned}\iiint_{\mathscr{R}_t} \Bigg[\rho\left(\frac{\mathrm{D}\varphi}{\mathrm{D}t} + u_i\,\frac{\mathrm{D}u_i}{\mathrm{D}t}\right) - q_\mathrm{g} + \frac{\partial q_j}{\partial x_j} - \rho\,g_i\,u_i \\ - u_i\,\frac{\partial\sigma_{ij}}{\partial x_j} - \sigma_{ij}\,\frac{\partial u_i}{\partial x_j}\Bigg]\mathrm{d}V = 0\ .\end{aligned} \tag{5.43}$$

Equation (5.43) can be rewritten as

$$\begin{aligned}\iiint_{\mathscr{R}_t} \Bigg[\rho\,\frac{\mathrm{D}\varphi}{\mathrm{D}t} + \left(\rho\,\frac{\mathrm{D}u_i}{\mathrm{D}t} - \rho\,g_i - \frac{\partial\sigma_{ij}}{\partial x_j}\right)u_i \\ - q_\mathrm{g} + \frac{\partial q_j}{\partial x_j} - \sigma_{ij}\,\frac{\partial u_i}{\partial x_j}\Bigg]\mathrm{d}V = 0\ .\end{aligned} \tag{5.44}$$

Thus, by employing equation (5.23), Eq. (5.44) can be simplified to

$$\iiint_{\mathscr{R}_t} \left[\rho \, \frac{\mathrm{D}\varphi}{\mathrm{D}t} - q_\mathrm{g} + \frac{\partial q_j}{\partial x_j} - \sigma_{ij} \, \frac{\partial u_i}{\partial x_j} \right] \mathrm{d}V = 0 \, . \tag{5.45}$$

Once again, we have reached a situation where an integral over $\mathscr{R}_t$ is zero. Due to the arbitrary choice of the integration domain, we an conclude that the integrand is zero. Thus, we obtain the *local energy balance equation*, namely

$$\rho \, \frac{\mathrm{D}\varphi}{\mathrm{D}t} = -\frac{\partial q_j}{\partial x_j} + q_\mathrm{g} + \sigma_{ij} \, \frac{\partial u_i}{\partial x_j} \, . \tag{5.46}$$

5.8 Viscous Stresses and Heat Flux

With fluids, the mechanical stress tensor is decomposed into an isotropic part and a traceless part,

$$\sigma_{ij} = -p \, \delta_{ij} + \tau_{ij} \, . \tag{5.47}$$

The term *isotropic* literally means independent of direction. In mathematics, a second-rank tensor is termed isotropic when it is the product of a scalar and Kronecker's delta. In fact, Kronecker's delta has the special feature that its components are the same in any Cartesian reference frame arbitrarily rotated around its origin. In Eq. (5.47), p is the pressure field and τ is a second-rank tensor with zero trace, that is $\tau_{ii} = 0$, called *viscous stress tensor*. It models the viscous behaviour of the fluid, which strongly depends on the specific fluid examined. There are several types of fluids that fall into two main categories: *Newtonian* and *non-Newtonian* fluids. Fluids falling in the former category are most of the fluids encountered in Nature, such as water, oil or gases. For Newtonian fluids, τ is usually represented as

$$\tau_{ij} = 2 \, \mu \, \mathscr{D}_{ij} - \frac{2}{3} \, \mu \, (\boldsymbol{\nabla} \cdot \mathbf{u}) \, \delta_{ij} \, , \tag{5.48}$$

where $\mathscr{D}_{ij}$ is the *strain tensor*, defined as

$$\mathscr{D}_{ij} = \frac{1}{2} \left(\frac{\partial u_i}{\partial x_j} + \frac{\partial u_j}{\partial x_i} \right) \, , \tag{5.49}$$

and μ is the *dynamic viscosity*. The latter quantity is, in general, a thermodynamic property of the fluid depending on its local temperature and pressure. One may easily check from Eq. (5.49) that the trace of $\mathscr{D}$ coincides with $\boldsymbol{\nabla} \cdot \mathbf{u}$, so that Eq. (5.48) implies that the trace of τ is in fact zero. Equations (5.48) and (5.49) are consistent with the symmetry property of the mechanical stress tensor σ.

On account of equations (5.47)–(5.49), the term $\partial\sigma_{ij}/\partial x_j$ on the right-hand side of equation (5.23) can be rewritten as

$$\frac{\partial \sigma_{ij}}{\partial x_j} = -\frac{\partial p}{\partial x_i} + \frac{\partial \tau_{ij}}{\partial x_j} = -\frac{\partial p}{\partial x_i} + \frac{\partial}{\partial x_j}\left[\mu\left(\frac{\partial u_i}{\partial x_j} + \frac{\partial u_j}{\partial x_i}\right)\right] - \frac{2}{3}\frac{\partial}{\partial x_i}\left(\mu\,\boldsymbol{\nabla}\cdot\mathbf{u}\right) . \tag{5.50}$$

A specially interesting case is one where μ undergoes negligible changes in space and time, so that it can be considered as a constant,

$$\begin{aligned}\frac{\partial \sigma_{ij}}{\partial x_j} &= -\frac{\partial p}{\partial x_i} + \mu\left(\frac{\partial^2 u_i}{\partial x_j\,\partial x_j} + \frac{\partial^2 u_j}{\partial x_i\,\partial x_j}\right) - \frac{2}{3}\,\mu\,\frac{\partial}{\partial x_i}\left(\boldsymbol{\nabla}\cdot\mathbf{u}\right) \\ &= -\frac{\partial p}{\partial x_i} + \mu\,\nabla^2 u_i + \frac{1}{3}\,\mu\,\frac{\partial}{\partial x_i}\left(\boldsymbol{\nabla}\cdot\mathbf{u}\right) .\end{aligned} \tag{5.51}$$

Another quantity that involves the mechanical stress tensor is the term $\sigma_{ij}\,\partial u_i/\partial x_j$ appearing on the right-hand side of equation (5.46). Again, by invoking Eq. (5.47), one can write

$$\begin{aligned}\sigma_{ij}\,\frac{\partial u_i}{\partial x_j} &= -p\,\boldsymbol{\nabla}\cdot\mathbf{u} + \tau_{ij}\,\frac{\partial u_i}{\partial x_j} \\ = -p\,\boldsymbol{\nabla}\cdot\mathbf{u} + \frac{1}{2}\,\tau_{ij}\left(\frac{\partial u_i}{\partial x_j} + \frac{\partial u_j}{\partial x_i}\right) &= -p\,\boldsymbol{\nabla}\cdot\mathbf{u} + \tau_{ij}\,\mathscr{D}_{ij} ,\end{aligned} \tag{5.52}$$

where the symmetry of the mechanical stress tensor σ, and hence of the viscous stress tensor τ, has been employed. We mention that each term appearing in Eq. (5.52) has a specific name and implied physical meaning,

$$\begin{aligned} -p\,\boldsymbol{\nabla}\cdot\mathbf{u} \quad &\Longrightarrow \quad \textit{pressure work}, \\ \tau_{ij}\,\mathscr{D}_{ij} \quad &\Longrightarrow \quad \textit{viscous dissipation}. \end{aligned} \tag{5.53}$$

Pressure work expresses, within the local energy balance, the contribution due to dilation or compression processes experienced by the fluid. On the other hand, viscous dissipation accounts for the frictional heat generation caused by the fluid viscosity. On account of equations (5.48) and (5.49), when the focus is on Newtonian fluids, the viscous dissipation term can be expressed as

$$\tau_{ij}\,\mathscr{D}_{ij} = 2\,\mu\,\mathscr{D}_{ij}\,\mathscr{D}_{ij} - \frac{2}{3}\,\mu\,(\boldsymbol{\nabla}\cdot\mathbf{u})^2 . \tag{5.54}$$

The double, implicit, sum over i and j means that $\mathscr{D}_{ij}\,\mathscr{D}_{ij}$ is expanded into nine terms. Three of them, namely the diagonal ones, yield $(\boldsymbol{\nabla}\cdot\mathbf{u})^2$. The conclusion is that the right hand side of equation (5.54) cannot in any case be negative. Physically, this means that viscous dissipation is a heat source term contribution to the energy

balance of the fluid, whose cause is the flow itself. We mention that the viscous dissipation term is often written in the form

$$\tau_{ij}\, \mathscr{D}_{ij} = \mu\, \Phi \ , \tag{5.55}$$

where Φ is called the *dissipation function*,

$$\Phi = 2\, \mathscr{D}_{ij}\, \mathscr{D}_{ij} - \frac{2}{3}\ (\nabla \cdot \mathbf{u})^2 \ . \tag{5.56}$$

Equation (5.56) shows that the dissipation function depends only on the velocity field.

An important term of the local energy balance equation (5.46) is that expressing heat diffusion, namely $-\nabla \cdot \mathbf{q}$. This term can be rewritten on account of *Fourier's law*,

$$\mathbf{q} = -\varkappa\, \nabla T \ , \tag{5.57}$$

where $\varkappa$ is the *thermal conductivity* of the fluid. This quantity is a thermodynamic property of the fluid and, in general, it depends on both temperature and pressure.

By taking into account Eqs. (5.50), (5.52), (5.54) and (5.57), one obtains an expression of the local balance equations (5.15), (5.23) and (5.46) for a Newtonian fluid given by

$$\frac{\partial \rho}{\partial t} + \frac{\partial (\rho\, u_j)}{\partial x_j} = 0 \ , \tag{5.58}$$

$$\rho \left(\frac{\partial u_i}{\partial t} + u_j\, \frac{\partial u_i}{\partial x_j} \right) = \rho\, g_i - \frac{\partial p}{\partial x_i} + \frac{\partial}{\partial x_j} \left[\mu \left(\frac{\partial u_i}{\partial x_j} + \frac{\partial u_j}{\partial x_i} \right) \right] - \frac{2}{3}\, \frac{\partial}{\partial x_i} \left(\mu\, \frac{\partial u_j}{\partial x_j} \right) \ , \tag{5.59}$$

$$\rho \left(\frac{\partial \varphi}{\partial t} + u_j\, \frac{\partial \varphi}{\partial x_j} \right) = \frac{\partial}{\partial x_j} \left(\varkappa\, \frac{\partial T}{\partial x_j} \right) + q_{\mathrm{g}} - p\, \frac{\partial u_j}{\partial x_j} + 2\, \mu\, \mathscr{D}_{ij}\, \mathscr{D}_{ij} - \frac{2}{3}\, \mu \left(\frac{\partial u_j}{\partial x_j} \right)^2 \ . \tag{5.60}$$

Equation (5.59) is well known as the *Navier–Stokes equation*.

The information conveyed by Eqs. (5.58)–(5.60) is not enough to determine theoretically the fluid flow. More details are needed such as the interplay between thermodynamic properties, say $\varkappa$ or μ, and the local fluid temperature or pressure. Convection studies often rely on an approximated scheme called the *Oberbeck–Boussinesq approximation*.

5.9 The Oberbeck–Boussinesq Approximation

When convection in fluids takes place, the mass density ρ can be approximated as a reference constant density, ρ_0, except for the gravitational body force term, $\rho\, g_i$ in Eq. (5.59), where the variability of ρ is taken into account. Moreover, both the dynamic viscosity and the thermal conductivity are assumed to be constant. Therefore, the local mass, momentum and energy balance equations can be simplified to

$$\frac{\partial u_j}{\partial x_j} = 0 \,, \tag{5.61}$$

$$\rho_0 \left(\frac{\partial u_i}{\partial t} + u_j \, \frac{\partial u_i}{\partial x_j} \right) = \rho \, g_i - \frac{\partial p}{\partial x_i} + \mu \, \nabla^2 u_i \,, \tag{5.62}$$

$$\rho_0 \left(\frac{\partial \varphi}{\partial t} + u_j \, \frac{\partial \varphi}{\partial x_j} \right) = \varkappa \nabla^2 T + q_\mathrm{g} + 2 \, \mu \, \mathscr{D}_{ij} \, \mathscr{D}_{ij} \,. \tag{5.63}$$

The density ρ, in the term $\rho\, g_i$ is assumed to be a function of temperature only, $\rho(T)$, thus considering the dependence on the pressure as negligible. The linear equation of state

$$\rho(T) = \rho_0 \left[1 - \beta \, (T - T_0) \right] \,, \tag{5.64}$$

is assumed, where β is the *isobaric coefficient of thermal expansion*,

$$\beta = - \frac{1}{\rho} \left(\frac{\partial \rho}{\partial T} \right)_p \,, \tag{5.65}$$

at the reference temperature T_0. The coefficient β is positive. In Eq. (5.64), the dependence on T is considered sufficiently weak as to be approximated linearly in a neighbourhood of the reference value T_0. This means that Eq. (5.64) can be intended as a Taylor series expansion of ρ around T_0,

$$\rho \, (T) = \rho_0 + \left. \frac{\partial \rho}{\partial T} \right|_{T_0} (T - T_0) + O\big((T - T_0)^2 \big) \,. \tag{5.66}$$

From Eq. (5.64), the expression

$$\rho \, g_i - \frac{\partial p}{\partial x_i}$$

in the local momentum balance equation (5.62) can be rewritten as

$$- \rho_0 \, \beta \, (T - T_0) \, g_i - \frac{\partial P}{\partial x_i}$$

where P is called *piezometric head*, and it is defined as

$$P = p - \rho_0 \, g_i \, x_i \ . \tag{5.67}$$

The quantity P is the difference between the pressure p and the hydrostatic pressure $\rho_0 \, g_i \, x_i$. As a consequence, Eqs. (5.61)–(5.63) can be rewritten as

$$\frac{\partial u_j}{\partial x_j} = 0 \ , \tag{5.68}$$

$$\rho_0 \left(\frac{\partial u_i}{\partial t} + u_j \, \frac{\partial u_i}{\partial x_j} \right) = -\rho_0 \, \beta \, (T - T_0) \, g_i - \frac{\partial P}{\partial x_i} + \mu \, \nabla^2 u_i \ , \tag{5.69}$$

$$\rho_0 \left(\frac{\partial \varphi}{\partial t} + u_j \, \frac{\partial \varphi}{\partial x_j} \right) = \varkappa \nabla^2 T + q_{\mathrm{g}} + 2 \, \mu \, \mathscr{D}_{ij} \, \mathscr{D}_{ij} \ . \tag{5.70}$$

The term

$$-\rho_0 \, \beta \, (T - T_0) \, g_i$$

is directed vertically, either in the direction of $\mathbf{g}$ or in the opposite direction, depending on the sign of $T - T_0$. Due to this term in the momentum balance, fluid elements with a temperature higher than T_0 are pushed upwards, while fluid elements with a temperature lower than T_0 are pushed downwards. This term is usually called the *buoyancy force* and represents the common sense effect that the lighter (hotter) fluid floats on top of the heavier (cooler) one. When the buoyancy force is negligible with respect to the pressure force,

$$\rho_0 \, \beta \, |T - T_0| \, g \ll |\nabla P| \, ,$$

where g is the modulus of $\mathbf{g}$, the convection flow process is called *forced convection*. In this flow regime, the buoyancy force term can be neglected in Eq. (5.69), so that both Eqs. (5.68) and (5.69) do not contain any contribution of the temperature field. Therefore, in a forced convection problem, these equations can be solved independently of equation (5.70), i.e. the local energy balance equation.

When the buoyancy force cannot be neglected, the convection flow process is called either *free convection*, or *natural convection*, or *mixed convection*, or *combined forced and free convection*, or *buoyant flow*. In this flow regime, the buoyancy force term cannot be neglected in Eq. (5.69), so that this equation contains the temperature field. Therefore, in a buoyant flow problem, Eqs. (5.68)–(5.70) form a system of partial differential equations, so that they cannot be solved separately. We mention that the terms free convection or natural convection are used when the flow is driven only by the buoyancy force.

Thermodynamics ensures that $\varphi = \varphi(T, \rho)$ for every single-phase or two-phase stable equilibrium states [4, 6]. In the special case of a perfect gas, it is well known that $\varphi = \varphi(T)$, so that [6]

$$\mathrm{d}\varphi = c_{\mathrm{v}} \, \mathrm{d}T \ , \tag{5.71}$$

where c_v is the *specific heat* at constant volume. In the case of either a liquid or a real gas, one must rely on the Oberbeck–Boussinesq approximation by assuming that an approximate equation of state $\rho = \rho(T)$ can be applied. This implies that the pressure of the fluid does not change appreciably. Since $\rho = \rho(T)$ and since the pair (T, ρ) yields a unique stable equilibrium state, then one concludes that all the thermodynamic properties may be considered as functions of T. This conclusion holds for the internal energy per unit mass, so that a relationship,

$$\mathrm{d}\varphi = c\,\mathrm{d}T\ , \tag{5.72}$$

can be established. The thermodynamic coefficient c, in general, does not coincide either with c_v or with the specific heat at constant pressure, c_p. In fact, c is the total derivative of the function $\varphi = \varphi(T, \rho(T))$ with respect to T, and not the partial derivative of $\varphi = \varphi(T, \rho)$ with respect to T, when ρ is kept constant. As is well known, the latter is the correct thermodynamic definition of c_v. The equation of state $\rho = \rho(T)$ is one regarding a set of stable equilibrium states of the fluid with approximately the same pressure. Then, one has

$$c = \left(\frac{\partial \varphi}{\partial T}\right)_p\ . \tag{5.73}$$

Equation (5.73) is not the definition of the specific heat at constant pressure c_p. As is well known, c_p is in fact defined as

$$c_p = \left(\frac{\partial h}{\partial T}\right)_p\ , \tag{5.74}$$

where $h = \varphi + p/\rho$ is the *enthalpy* per unit mass. Then, one can easily write the following relationship:

$$c = c_p - \frac{p\,\beta}{\rho}\ . \tag{5.75}$$

Then, c is smaller than c_p and differs from c_v, except for the limiting case of a perfect gas. Indeed, in the latter case, one can easily show that the equation of state of the perfect gas and Eq. (5.75) ensures that $c = c_v$, so that Eqs. (5.71) and (5.72) are perfectly consistent.

One can question about the extent to which c_p and c_v differ from c in the case of liquids. This topic has been examined by Barletta [3]. For water at atmospheric pressure, as well as for most liquids, the assumption

$$c \approx c_p \tag{5.76}$$

is a definitely reliable one. By using Eq. (5.72), one has

$$\frac{\partial \varphi}{\partial t} = c\,\frac{\partial T}{\partial t}\,, \qquad \frac{\partial \varphi}{\partial x_j} = c\,\frac{\partial T}{\partial x_j}\,, \tag{5.77}$$

so that Eqs. (5.68)–(5.70) can be rewritten as

$$\frac{\partial u_j}{\partial x_j} = 0\,, \tag{5.78}$$

$$\rho_0\left(\frac{\partial u_i}{\partial t} + u_j\,\frac{\partial u_i}{\partial x_j}\right) = -\rho_0\,\beta\,(T - T_0)\,g_i - \frac{\partial P}{\partial x_i} + \mu\,\nabla^2 u_i\,, \tag{5.79}$$

$$\rho_0\,c\left(\frac{\partial T}{\partial t} + u_j\,\frac{\partial T}{\partial x_j}\right) = \varkappa\,\nabla^2 T + q_{\mathrm{g}} + 2\,\mu\,\mathscr{D}_{ij}\,\mathscr{D}_{ij}\,. \tag{5.80}$$

An alternative expression for Eqs. (5.78)–(5.80) is obtained on introducing the *kinematic viscosity*,

$$\nu = \frac{\mu}{\rho_0}\,, \tag{5.81}$$

and the *thermal diffusivity*,

$$\alpha = \frac{\varkappa}{\rho_0\,c}\,. \tag{5.82}$$

Thus, we can write

$$\frac{\partial u_j}{\partial x_j} = 0\,, \tag{5.83}$$

$$\frac{\partial u_i}{\partial t} + u_j\,\frac{\partial u_i}{\partial x_j} = -\beta\,(T - T_0)\,g_i - \frac{1}{\rho_0}\,\frac{\partial P}{\partial x_i} + \nu\,\nabla^2 u_i\,, \tag{5.84}$$

$$\frac{\partial T}{\partial t} + u_j\,\frac{\partial T}{\partial x_j} = \alpha\,\nabla^2 T + \frac{q_{\mathrm{g}}}{\rho_0\,c} + 2\,\frac{\nu}{c}\,\mathscr{D}_{ij}\,\mathscr{D}_{ij}\,. \tag{5.85}$$

Typical boundary conditions prescribed for the velocity field are *impermeability* at the surface of a solid wall, meaning that the normal component of **u** is zero at this boundary. Also, the tangential components of velocity must vanish at the surface of a solid wall, and these conditions are termed *no-slip conditions*.

5.10 Governing Equations of Mass Diffusion

In general, the local mass balance equation of a fluid is given by Eq. (5.58). This equation holds either for a fluid with a single chemical constituent or for a multicomponent fluid. However, if one has a multicomponent fluid made up of N different chemical species, one can imagine the fluid as the superposition of N pure fluids coexisting in the same region of space. This means that, instead of a single velocity

field $\mathbf{u}$, one has to define N velocity fields $\mathbf{u}_n$, where $n = 1, 2, \ldots, N$, one for each constituent. Moreover, one must define a mass density field, C_n, for the nth constituent as

$$C_n = \frac{M_n}{V} \,, \tag{5.86}$$

where M_n is the mass of the nth constituent contained in an elementary volume V.

The overall fluid mass density is made up by the densities C_n of the constituents,

$$\rho = \sum_{n=1}^{N} C_n \,. \tag{5.87}$$

It is a common practice calling *concentrations* the mass densities of the N pure fluids.

The overall velocity field $\mathbf{u}$ of the multicomponent fluid can be defined as a weighted mean value of the velocity fields $\mathbf{u}_n$,

$$\mathbf{u} = \frac{1}{\rho} \sum_{n=1}^{N} C_n \, \mathbf{u}_n \,. \tag{5.88}$$

5.10.1 Transport Theorem for Mass Diffusion

We know that Eq. (5.58) arises from Reynolds' transport theorem relative to the multicomponent fluid. With reference to the nth pure fluid, the transport theorem can be formulated as

$$\frac{\mathrm{d}\,\Psi_n}{\mathrm{d}\,t} = \iiint_{\mathscr{R}_t} \left[\frac{\partial (C_n \, \psi_n)}{\partial t} + \nabla \cdot (C_n \, \psi_n \, \mathbf{u}_n) \right] \mathrm{d}V \,, \quad n = 1, 2, \ldots, N \,, \tag{5.89}$$

where Ψ_n is any extensive property of the nth pure fluid, while ψ_n is the corresponding specific property, i.e. the property obtained from the division of Ψ_n by the mass of the nth constituent. The region $\mathscr{R}_t$ is that occupied by a given multicomponent fluid body at time t. Again, the region $\mathscr{R}_t$ defines a closed thermodynamic system. If $\Psi_n = M_n$ is the mass of the nth chemical species contained in the volume $\mathscr{R}_t$ at time t, then $\psi_n = 1$. Unlike the overall fluid mass M contained in $\mathscr{R}_t$ at time t, the mass M_n is not independent of time since chemical reactions may occur in the fluid system. Then, one may write

$$\frac{\mathrm{d}\,M_n}{\mathrm{d}\,t} = \iiint_{\mathscr{R}_t} \dot{m}_n \, \mathrm{d}V \,, \tag{5.90}$$

where $\dot{m}_n$ is the local mass production rate per unit volume of the nth chemical species. On substituting $\Psi_n = M_n$ and $\psi_n = 1$ in Eq. (5.89), one obtains

$$\iiint_{\mathscr{R}_t} \left[\frac{\partial C_n}{\partial t} + \nabla \cdot (C_n \, \mathbf{u}_n) - \dot{m}_n \right] \mathrm{d}V = 0, \quad n = 1, 2, \ldots, N \, . \tag{5.91}$$

Since the region $\mathscr{R}_t$ has been chosen arbitrarily, the integral conditions can be satisfied only if the integrand vanishes locally at every position in the domain occupied by the fluid, namely if the local mass balance equations,

$$\frac{\partial C_n}{\partial t} + \nabla \cdot (C_n \, \mathbf{u}_n) - \dot{m}_n = 0 \, , \quad n = 1, 2, \ldots, N \, , \tag{5.92}$$

hold. By summing all the N Eqs. (5.92), one obtains

$$\frac{\partial \rho}{\partial t} + \nabla \cdot (\rho \, \mathbf{u}) - \sum_{n=1}^{N} \dot{m}_n = 0 \, , \tag{5.93}$$

where Eqs. (5.87) and (5.88) have been invoked. A comparison between Eqs. (5.93) and (5.58) allows us to infer that

$$\sum_{n=1}^{N} \dot{m}_n = 0 \, . \tag{5.94}$$

Equation (5.94) implies that the chemical reactions possibly occurring in the fluid system do not yield either a source or a sink for the overall fluid mass, i.e. the overall fluid mass is locally conserved.

5.10.2 Concentrations and Mass Fluxes

Mass diffusion occurs within the fluid when, locally, the overall fluid velocity $\mathbf{u}$ differs from the velocity $\mathbf{u}_n$ of the nth constituent. Then, if the mass diffusion takes place, one may define a *mass flux* for each constituent,

$$\mathbf{J}_n = C_n \, (\mathbf{u}_n - \mathbf{u}) \, , \quad n = 1, 2, \ldots, N \, . \tag{5.95}$$

As a consequence, Eq. (5.92) yields

$$\frac{\partial C_n}{\partial t} + \nabla \cdot (C_n \, \mathbf{u}) + \nabla \cdot \mathbf{J}_n - \dot{m}_n = 0 \, , \quad n = 1, 2, \ldots, N \, , \tag{5.96}$$

that can be rewritten as

$$\frac{\partial C_n}{\partial t} + \mathbf{u} \cdot \nabla C_n + C_n \, \nabla \cdot \mathbf{u} + \nabla \cdot \mathbf{J}_n - \dot{m}_n = 0 \, , \quad n = 1, 2, \ldots, N \, . \tag{5.97}$$

5.10.3 The Oberbeck–Boussinesq Approximation

The Oberbeck–Boussinesq approximation is based on the assumption that the overall fluid density ρ may be treated as a constant in the local mass, momentum and energy balance equations of the fluid, except for the gravitational body force in the momentum balance. This exception allows one to model the density changes through the effects of the buoyancy force. When mass diffusion takes place, the overall fluid density ρ is considered not only as a function of the temperature T, but also of $N-1$ concentrations, $C_1, C_2, \ldots, C_{N-1}$, treated as independent variables. The latter conclusion may be inferred from Eq. (5.87). The fluid density ρ may be either considered as a function of $C_1, C_2, \ldots, C_N$ assumed as independent, or as a function of the independent variables $T, C_1, C_2, \ldots, C_{N-1}$. In fact, each concentration C_n is a function of T.

With small density changes occurring within the fluid, one can express ρ as a linear function of the independent variables $T, C_1, C_2, \ldots, C_{N-1}$,

$$\rho = \rho_0 \left[1 - \beta \left(T - T_0 \right) - \sum_{n=1}^{N-1} \beta_{C,n} \left(C_n - C_{n,0} \right) \right] , \tag{5.98}$$

where T_0 is the reference temperature, $C_{n,0}$ is the reference concentration of the nth component, ρ_0 is the overall fluid density evaluated in the reference state, while

$$\beta = -\frac{1}{\rho} \frac{\partial \rho}{\partial T} , \qquad \beta_{C,n} = -\frac{1}{\rho} \frac{\partial \rho}{\partial C_n} , \qquad n = 1, 2, \ldots, N-1 , \tag{5.99}$$

are the isobaric coefficient of thermal expansion and the *concentration expansion coefficients*, respectively. While β is positive, the coefficients $\beta_{C,n}$ can be either positive or negative. In Eq. (5.99), these coefficients are evaluated at the reference conditions $T = T_0$ and $C_n = C_{n,0}$.

On the basis of equation (5.98), one can express the approximated momentum balance. Therefore, the set of local balance equations to be solved in the Oberbeck–Boussinesq approximation are

$$\nabla \cdot \mathbf{u} = 0 , \tag{5.100}$$

$$\frac{\partial \mathbf{u}}{\partial t} + (\mathbf{u} \cdot \nabla) \mathbf{u} = -\frac{1}{\rho_0} \nabla P - \beta \left(T - T_0 \right) \mathbf{g} - \sum_{n=1}^{N-1} \beta_{C,n} \left(C_n - C_{n,0} \right) \mathbf{g} + \nu \nabla^2 \mathbf{u} , \tag{5.101}$$

$$\frac{\partial T}{\partial t} + (\mathbf{u} \cdot \nabla) T = \alpha \nabla^2 T + \frac{q_g}{\rho_0 c} + \frac{\nu}{c} \Phi , \tag{5.102}$$

$$\frac{\partial C_n}{\partial t} + (\mathbf{u} \cdot \nabla) C_n = -\nabla \cdot \mathbf{J}_n + \dot{m}_n , \qquad n = 1, 2, \ldots, N-1 . \tag{5.103}$$

We note that instead of the N equations (5.103), we have written just $N-1$ equations. The reason is that the overall fluid mass balance equation (5.100) and the N mass balance equations for the constituents of the multicomponent fluid are not independent, as a consequence of the constraint equation (5.87).

The local momentum balance equation (5.101) displays two kinds of buoyancy force: a *thermal buoyancy* induced by a possibly non-uniform temperature field,

$$-\beta\,(T-T_0)\,\mathbf{g}\,,$$

and a *mass diffusion buoyancy* induced by possibly non-uniform concentrations of the chemical components,

$$-\sum_{n=1}^{N-1}\beta_{C,n}\left(C_n-C_{n,0}\right)\mathbf{g}\,.$$

5.10.4 A Two-Component Mixture and Fick's Law

Here, we refer for simplicity to a two-component fluid ($N=2$). Since $N=2$, we have two concentrations C_1 and C_2, but just one of them is an independent variable as a consequence of equation (5.87). We denote this concentration as C and the corresponding mass flux as $\mathbf{J}$.

Thus, from Eqs. (5.100)–(5.103), we have four local balance equations that we can write, for convenience, according to Einstein's notation

$$\frac{\partial u_j}{\partial x_j}=0\,, \tag{5.104}$$

$$\frac{\partial u_i}{\partial t}+u_j\,\frac{\partial u_i}{\partial x_j}=-\beta\,(T-T_0)\,g_i - \beta_C\,(C-C_0)\,g_i-\frac{1}{\rho_0}\,\frac{\partial P}{\partial x_i}+\nu\,\nabla^2 u_i\,, \tag{5.105}$$

$$\frac{\partial T}{\partial t}+u_j\,\frac{\partial T}{\partial x_j}=\alpha\,\nabla^2 T+\frac{q_{\mathrm{g}}}{\rho_0\,c}+2\,\frac{\nu}{c}\,\mathscr{D}_{ij}\,\mathscr{D}_{ij}\,, \tag{5.106}$$

$$\frac{\partial C}{\partial t}+u_j\,\frac{\partial C}{\partial x_j}=-\frac{\partial J_j}{\partial x_j}+\dot{m}\,. \tag{5.107}$$

We note that the set of four local balance equations (5.104)–(5.107) can be solved to determine the four unknown fields u_i, p, T and C. However, we have a further unknown: the mass flux J_i. Hence, the differential problem is under-determined (there are more unknowns than equations).

In 1855, a German physiologist and physicist, Adolf Eugen Fick, obtained a phenomenological law establishing a relationship between J_i and C. This law is now

well known as *Fick's law* and can be formulated as [2]

$$J_i = -\alpha_{\mathrm{m}} \frac{\partial C}{\partial x_i} , \tag{5.108}$$

where the positive quantity α_{m} is the *mass diffusivity*. The mass diffusivity is a thermodynamic property of the two-component mixture and, coherently with the Oberbeck–Boussinesq approximation, it is considered as a constant. Then Eq. (5.107) can be rewritten as

$$\frac{\partial C}{\partial t} + u_j \frac{\partial C}{\partial x_j} = \alpha_{\mathrm{m}} \nabla^2 C + \dot{m} . \tag{5.109}$$

In this form, the local mass balance equation for the component with concentration C exploits the strong mathematical analogy between the heat diffusion, described by Eq. (5.106), and mass diffusion, described by Eq. (5.109).

Here, we have three fluid properties, α, α_{m} and ν having the same units, and thus defining two characteristic dimensionless ratios, the *Prandtl number* and the *Schmidt number*,

$$Pr = \frac{\nu}{\alpha} , \quad Sc = \frac{\nu}{\alpha_{\mathrm{m}}} . \tag{5.110}$$

5.11 Local Entropy Balance Equation

The entropy $\mathscr{S}$ of the fluid body contained in the region of space $\mathscr{R}_t$ is an extensive property. If we denote with s the specific entropy, then Reynolds' transport theorem, Eq. (5.14), yields

$$\frac{\mathrm{d}\,\mathscr{S}}{\mathrm{d}\,t} = \iiint_{\mathscr{R}_t} \rho \frac{\mathrm{D}s}{\mathrm{D}\,t} \,\mathrm{d}V . \tag{5.111}$$

We rely on *Gibbs' equation* for an expression of $\mathrm{d}s$ [6],

$$\mathrm{d}s = \frac{1}{T} \,\mathrm{d}\varphi - \frac{p}{\rho^2 T} \,\mathrm{d}\rho . \tag{5.112}$$

From Eq. (5.112), one obtains an expression for the substantial derivative of s,

$$\frac{\mathrm{D}s}{\mathrm{D}\,t} = \frac{1}{T} \frac{\mathrm{D}\varphi}{\mathrm{D}\,t} - \frac{p}{\rho^2 T} \frac{\mathrm{D}\rho}{\mathrm{D}\,t} = \frac{1}{T} \frac{\mathrm{D}\varphi}{\mathrm{D}\,t} + \frac{p}{\rho T} \boldsymbol{\nabla} \cdot \mathbf{u} , \tag{5.113}$$

where Eqs. (5.10) and (5.13) have been employed. Substitution of Eq. (5.113) into Eq. (5.111) yields

$$\frac{\mathrm{d}\mathscr{S}}{\mathrm{d}t} = \iiint\limits_{\mathscr{R}_t} \left(\frac{\rho}{T} \frac{\mathrm{D}\varphi}{\mathrm{D}t} + \frac{p}{T} \nabla \cdot \mathbf{u} \right) \mathrm{d}V \,. \tag{5.114}$$

The second law of thermodynamics leads to an entropy balance equation where the infinitesimal change of entropy in a process is the sum of an entropy flux and an entropy production due to irreversibility [6]. Thus, we can write

$$\frac{\mathrm{d}\mathscr{S}}{\mathrm{d}t} = - \iint\limits_{\partial\mathscr{R}_t} \frac{\mathbf{q} \cdot \mathbf{n}}{T} \, \mathrm{d}S + \dot{\mathscr{S}}_{\mathrm{irr}} \,, \tag{5.115}$$

where $\dot{\mathscr{S}}_{\mathrm{irr}}$ is the *entropy production rate*. As the entropy is an extensive property, the entropy production rate can be expressed through a volume integral,

$$\dot{\mathscr{S}}_{\mathrm{irr}} = \iiint\limits_{\mathscr{R}_t} \sigma_{\mathrm{irr}} \, \mathrm{d}V \,. \tag{5.116}$$

Here, σ_{irr} represents the entropy production rate per unit volume. Its local value cannot be negative, due to the second law of thermodynamics,

$$\sigma_{\mathrm{irr}} \geqslant 0 \,, \tag{5.117}$$

where the equal sign implies reversibility. We also mention that the minus sign in front of the surface integral on the right-hand side of equation (5.115) is motivated by the need to express the incoming entropy flux across the boundary, whereas $\mathbf{n}$ is the outward normal to $\partial\mathscr{R}_t$.

By employing Gauss' theorem and Eq. (5.116), Eqs. (5.114) and (5.115) yield

$$\iiint\limits_{\mathscr{R}_t} \left(\frac{\rho}{T} \frac{\mathrm{D}\varphi}{\mathrm{D}t} + \frac{p}{T} \nabla \cdot \mathbf{u} - \frac{1}{T^2} \, \mathbf{q} \cdot \nabla T + \frac{1}{T} \nabla \cdot \mathbf{q} - \sigma_{\mathrm{irr}} \right) \mathrm{d}V = 0 \,. \tag{5.118}$$

We now invoke the local energy balance equation (5.46) and Eq. (5.52), so that we obtain

$$\iiint\limits_{\mathscr{R}_t} \left(\frac{q_{\mathrm{g}}}{T} + \frac{1}{T} \, \tau_{ij} \, \mathscr{D}_{ij} - \frac{1}{T^2} \, q_j \, \frac{\partial T}{\partial x_j} - \sigma_{\mathrm{irr}} \right) \mathrm{d}V = 0 \,. \tag{5.119}$$

As usual, Eq. (5.119) can be satisfied with an arbitrary domain of integration $\mathscr{R}_t$ if the integrand is zero, namely if

$$\sigma_{\mathrm{irr}} = \frac{q_{\mathrm{g}}}{T} + \frac{1}{T} \, \tau_{ij} \, \mathscr{D}_{ij} - \frac{1}{T^2} \, q_j \, \frac{\partial T}{\partial x_j} \,. \tag{5.120}$$

Equation (5.120) is the *local entropy balance equation*. Due to Eq. (5.117), the local entropy balance is effectively an inequality,

$$\frac{q_{\mathrm{g}}}{T} + \frac{1}{T}\,\tau_{ij}\,\mathscr{D}_{ij} - \frac{1}{T^2}\,q_j\,\frac{\partial T}{\partial x_j} \geqslant 0\,. \tag{5.121}$$

If one deals with a Newtonian fluid and if Fourier's law (5.57) is employed, the contributions of viscous dissipation, $\tau_{ij}\,\mathscr{D}_{ij}/T$, and of heat diffusion, $-(q_j\,\partial T/\partial x_j)/T^2$, are both non-negative. In this situation, the inequality (5.121) becomes an effective restriction only if one has to model heat sinks ($q_{\mathrm{g}} < 0$). This situation may occur, for instance, in the case of endothermic chemical reactions.

References

1. Apostol TM (1967) Calculus. vol. 2: multi-variable calculus and linear algebra with applications to differential equations and probability. Wiley, New York
2. Baehr H, Park N, Stephan K (2011) Heat and mass transfer, 3rd edn. Springer, Berlin
3. Barletta A (2009) Local energy balance, specific heats and the Oberbeck-Boussinesq approximation. Int J Heat Mass Transf 52:5266–5270
4. Callen HB (1985) Thermodynamics and an introduction to thermostatistics. Wiley, New York
5. Davidson PA (2001) An introduction to magnetohydrodynamics. Cambridge University Press, Cambridge
6. Gyftopoulos EP, Beretta GP (2005) Thermodynamics: foundations and applications. Dover, New York

Chapter 6
Fluid Flow in Porous Media

6.1 The Basic Features of Flow in Porous Media

There are several excellent books regarding the dynamics of flow and convection in a fluid-saturated porous medium. We mention Bear [3], Kaviany [6], Nield and Bejan [17], Straughan [11] as examples of reference texts on these topics. This chapter is just an outline of the main mathematical models employed in the stability analysis of convection in porous media, with no ambition of being a complete or exhaustive presentation of the state of the art.

The oldest, the simplest and the most widely employed model of fluid flow in porous media is named after Darcy,[1] a French scientist with a strong professional interest in hydraulics. During his life, he was a civil engineer in the city of Dijon in France. He projected and built a pressurised water distribution system in Dijon. A few years before his death, he conducted the experiments that allowed him to formulate what today is well known as *Darcy's law*. His publication *The Public Fountains of the City of Dijon* contains an appendix written in 1856 entitled *Determination of the Laws of Water Flow Through Sand* where his law is formulated.

Fluid flow in porous media is of paramount importance both for geophysical applications such as filtration of water, hydrocarbons and gases in the soil and for engineering. For instance, one may point out the interest of porous media with reference to hydrology of aquifers, underground repositories used for sequestering nuclear waste, heat pipes, underground spreading of chemical waste, drainage and irrigation in agriculture, thermal insulation engineering, enhanced recovery of petroleum reservoirs, grain storage, water flow in geothermal reservoirs.

Before formulating Darcy's law, let us review the main features of the macroscopic description of fluid flow in porous media.

A porous medium is a solid material with void inner structures saturated by a fluid, liquid or gas. One can think to sand, pebbles, bread or to a metallic foam. One

[1] Henry Philibert Gaspard Darcy (1803–1858).

A. Barletta, *Routes to Absolute Instability in Porous Media*,
https://doi.org/10.1007/978-3-030-06194-4_6

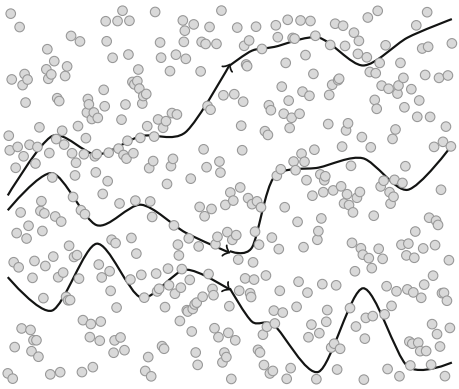

Fig. 6.1 Irregular trajectories of fluid elements moving inside a random cloud of solid particles

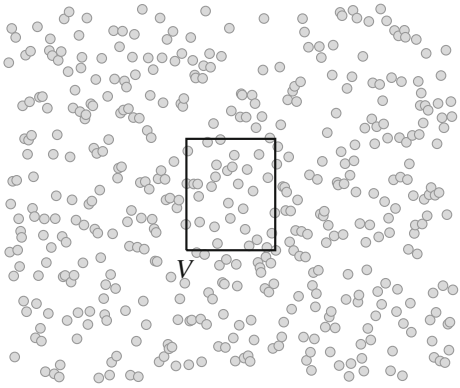

Fig. 6.2 Representative elementary volume V

can imagine that the void spaces within the solid are entirely filled by the moving fluid (see Fig. 6.1).

A basic quantity for the description of a porous medium is the ratio between the volume occupied by the fluid (voids) and the total volume including voids and solid. Referring to Fig. 6.2, one can consider a representative elementary volume V, often abbreviated as REV, small on a macroscopic scale even if large on the scale of the single grain, pebble or microchannel that may be present inside the porous medium. If V_f is the void part of V, we call *porosity*, φ, the ratio

$$\varphi = \frac{V_\mathrm{f}}{V} \,. \tag{6.1}$$

The porosity is a dimensionless quantity strictly smaller than unity.

The study of convection in porous media is based on the assumption that a fluid-saturated porous medium can be described as a continuum. This means that, in the representative volume V of the system, the number of pores is very high. Therefore, one can define a local fluid velocity field as an average value of the local fluid

velocity $\mathbf{u}^*$. There are two possible average values of $\mathbf{u}^*$ usually introduced: the *intrinsic velocity*, namely

$$\mathbf{U} = \frac{1}{V_f} \iiint_{V_f} \mathbf{u}^* \, \mathrm{d}V \ , \tag{6.2}$$

and the *seepage velocity* (also known as *Darcy's velocity*), namely

$$\mathbf{u} = \frac{1}{V} \iiint_{V} \mathbf{u}^* \, \mathrm{d}V \ . \tag{6.3}$$

The intrinsic velocity is defined as an average performed in the void part V_f of the representative volume V. Since $\mathbf{u}^* = 0$ in the part of V not included in V_f, the two integrals on the right-hand sides of Eqs. (6.2) and (6.3) are equal. Then, one can establish a very simple relationship between $\mathbf{U}$ and $\mathbf{u}$, namely

$$\mathbf{u} = \varphi \, \mathbf{U} \ . \tag{6.4}$$

This equation is well known as *Dupuit–Forchheimer relationship*.

The local value of the seepage velocity $\mathbf{u}$ depends on the shape and the size of the pores as well as on the causes that determine the fluid motion. The relationship between the local value of $\mathbf{u}$ and the forces acting on the fluid can be deduced by an appropriate local average over the representative elementary volume of the Navier–Stokes momentum balance, Eq. (5.59). However, due to the complexity of the system, in most cases this relationship is postulated through a constitutive equation validated experimentally.

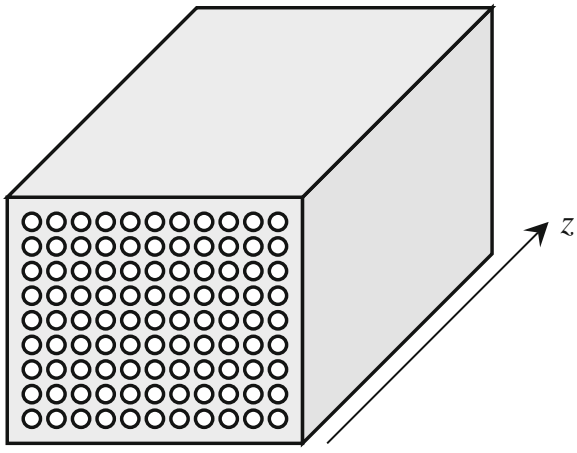

Fig. 6.3 Engineered porous medium described in Example 6.1

6.2 Local Momentum Balance in a Porous Medium

The simplest constitutive equation expressing the local seepage velocity of the fluid is *Darcy's law*, namely

$$\frac{\mu}{K}\,\mathbf{u} = -\,\nabla p + \mathbf{b}\,, \tag{6.5}$$

where K is a property of the system called *permeability*, μ is the dynamic viscosity of the fluid, p is the fluid pressure, and $\mathbf{b}$ is the external body force per unit volume applied to the fluid (in the simplest case, the gravitational body force $\rho\,\mathbf{g}$).

The rationale behind the assumption given by Eq. (6.5) relies on the observation that a porous medium can be thought of as a network of microscopic ducts where the fluid flows. In the absence of external body forces, the pressure gradient along a duct is proportional to the average fluid velocity in the duct itself, if the flow is laminar. On the other hand, if the flow is highly turbulent (hydraulic regime), the pressure gradient along a duct is proportional to the square of the average fluid velocity in the duct itself. Darcy's law refers to the case of laminar flow in the porous medium, so that the permeability K is considered as a property of the medium depending on the number of pores per unit area present in a cross-section transverse to the fluid flow, on the shape of the pores and on their size.

Example 6.1 Let us consider an engineered porous medium such that the pores form an ordered array of parallel infinitely long circular ducts each with a diameter d (Fig. 6.3). Let z be the axis parallel to the ducts, and let the number of ducts per unit area in a transverse section of the medium be N. Then, by comparison with the relationship between the average velocity u_m^* and pressure drop Δp in this kind of ducts, it is easily verified that

$$K = \frac{N\pi\, d^4}{128}\,.$$

In fact, it is well known that the average velocity u_{m}^* of fully developed laminar flow in a circular duct, namely *Hagen–Poiseuille flow*, is given by

$$u_{\mathrm{m}}^* = -\frac{d^2}{32\,\mu}\,\frac{\mathrm{d}p}{\mathrm{d}z}\,.$$

One may notice that $u_{\mathrm{m}}^* = U$; i.e. u_{m}^* coincides with the intrinsic velocity U. Moreover, the porosity is given by $\varphi = N\,\pi\,d^2/4$. Then, on account of Dupuit–Forchheimer relationship, the Darcy velocity u is given by

$$u = \frac{N\pi\, d^2}{4}\,u_{\mathrm{m}}^* = -\frac{N\pi\, d^4}{128\,\mu}\,\frac{\mathrm{d}p}{\mathrm{d}z}\,.$$

As a consequence of Eq. (6.5), one obtains the expression for K.

A variant version of Darcy's law is formulated by including an extra inertial term proportional to $\partial \mathbf{u}/\partial t$,

$$\rho\, C_{\mathrm{a}}\, \frac{\partial \mathbf{u}}{\partial t} + \frac{\mu}{K}\, \mathbf{u} = -\nabla p + \mathbf{b}\,, \tag{6.6}$$

where C_{a} is called *acceleration coefficient*. With a further generalisation, the dimensionless scalar coefficient C_{a} is replaced by a tensor coefficient, by taking into account the non-isotropic character of the inertial effect [11].

If the hypothesis of laminar fully developed flow in each pore cannot be applied, then proportionality between acting forces and the resulting fluid velocity must be relaxed in favour of a gradual transition towards a hydraulic regime where acting forces are proportional to the square of the fluid velocity in each pore. An extended form of Eq. (6.5) has been proposed which accounts for this effect, i.e. *Darcy–Forchheimer's model*,

$$\frac{\mu}{K}\left(1 + \frac{F\,\rho\,\sqrt{K}}{\mu}\,|\mathbf{u}|\right)\mathbf{u} = -\nabla p + \mathbf{b}\,. \tag{6.7}$$

In Eq. (6.7), $|\mathbf{u}|$ is the modulus of $\mathbf{u}$, ρ is the fluid mass density, and F is a property of the porous medium called the *form-drag coefficient*. It is easily verified that F is a dimensionless property of the porous medium.

Obviously, Darcy–Forchheimer's model includes Darcy's law as a special case, i.e. in the limit $F \to 0$. On the other hand, whenever $F\,\rho\,|\mathbf{u}|\sqrt{K}/\mu \gg 1$, transition to an hydraulic regime for the fluid flow inside the pores occurs. A widely accepted criterion to establish when Darcy's law must be abandoned in favour of Darcy–Forchheimer's model is formulated with the permeability-based Reynolds number,

$$Re_{\mathrm{K}} = \frac{\rho\,|\mathbf{u}|\,\sqrt{K}}{\mu}\,. \tag{6.8}$$

Darcy's law gradually loses its validity when $Re_K \sim 1/F$ or greater. From Eq. (6.8), a clever way to apply this criterion is taking $|\mathbf{u}|$ as the maximum value over the flow domain.

A common feature of Darcy's law and of Forchheimer's extension of this law is that they refer to a tightly packed solid with a fluid flowing in very small pores. Indeed, this is a circumstance very far from a free-flowing fluid. One can complete either Eq. (6.5) or (6.7) with just one velocity boundary condition on each boundary surface. This boundary condition can be, for instance, *impermeability* ($\mathbf{u}\cdot\mathbf{n} = 0$, where $\mathbf{n}$ is the unit vector normal to the surface). However, one cannot allow also a no-slip condition on the same surface, as the problem would be over-specified. This is due to the low differential order of Darcy's and Darcy–Forchheimer's models of local momentum balance in a fluid-saturated porous medium.

The impossibility to prescribe no-slip conditions at the boundary walls creates a sharp distinction between the Navier–Stokes fluid model and the models of fluid-saturated porous media based either on Darcy's law or on Forchheimer's extension of this law. In some cases, a continuous transition from the momentum balance equation of a clear fluid (Navier–Stokes equation) to Darcy's law is considered as realistic. Along this direction, it has been proposed the so-called *Brinkman's model* for fluid flow in a porous medium. This model allows one to prescribe no-slip wall conditions as for a Navier–Stokes clear fluid. According to Brinkman's model, Eq. (6.5) must be replaced by

$$\frac{\mu}{K}\,\mathbf{u} - \mu_{\text{eff}}\,\nabla^2\mathbf{u} = -\,\boldsymbol{\nabla} p + \mathbf{b}\;, \tag{6.9}$$

where the quantity μ_{eff} is called *effective viscosity*: it depends on the fluid viscosity μ and on the porosity of the medium where the fluid flows. A commonly employed correlation for the effective viscosity is *Einstein's formula* for dilute suspensions, namely

$$\mu_{\text{eff}} = \mu\,[1 + 2.5\,(1-\varphi)]\;. \tag{6.10}$$

If the porosity is equal to 1, one has a clear fluid and Eq. (6.10) implies that $\mu_{\text{eff}} = \mu$. If $\varphi = 1$, Eq. (6.10) reduces to the Navier–Stokes equation without the inertial contribution (negligible acceleration), provided that the limit of infinite permeability is also taken ($K \to \infty$). On the other hand, in the limit of a very small permeability ($K \to 0$), the first term on the left-hand side of Eq. (6.10), $\mu\mathbf{u}/K$, becomes much larger than the second term, $\mu_{\text{eff}}\,\nabla^2\mathbf{u}$. Therefore, in the limit $K \to 0$, Brinkman's model reduces to Darcy's law, Eq. (6.5). It must be pointed out that the limit $K \to 0$ yields a singular behaviour next to the impermeable boundaries where the no-slip conditions cannot be applied anymore.

6.3 Local Mass and Energy Balance Equations

By employing a local volume averaging procedure, the mass and energy balance equations of a fluid-saturated porous medium can be expressed as

$$\varphi\,\frac{\partial \rho}{\partial t} + \boldsymbol{\nabla}\cdot(\rho\,\mathbf{u}) = 0\;, \tag{6.11}$$

and

$$\rho\,c\left(\sigma\,\frac{\partial T}{\partial t} + \mathbf{u}\cdot\boldsymbol{\nabla} T\right) = \varkappa_{\text{eff}}\,\nabla^2 T + q_{\text{g}} + \mu\,\Phi\;. \tag{6.12}$$

In Eq. (6.12), the thermal conductivities of the solid and of the fluid are considered as constant, σ is the *heat capacity ratio* defined as

$$\sigma = \frac{\varphi\,\rho\,c + (1-\varphi)\,\rho_{\mathrm{s}}\,c_{v_{\mathrm{s}}}}{\rho\,c}\ , \tag{6.13}$$

while $\varkappa_{\mathrm{eff}}$ is the *effective thermal conductivity* of the fluid-saturated porous medium defined as

$$\varkappa_{\mathrm{eff}} = \varphi\,\varkappa + (1-\varphi)\,\varkappa_{\mathrm{s}}\ . \tag{6.14}$$

In Eqs. (6.13) and (6.14), the properties ρ, c and $\varkappa$ refer to the fluid, while ρ_{s}, $c_{v_{\mathrm{s}}}$ and $\varkappa_{\mathrm{s}}$ refer to the solid matrix.

The term q_{g} in Eq. (6.12) is the power generated per unit volume in the fluid-saturated porous medium by, for instance, Joule heating or chemical reactions. The last term on the right-hand side of Eq. (6.12), $\mu\,\Phi$, is the power per unit volume generated by viscous dissipation.

Consistently with Eq. (6.11), if the seepage flow involves mass diffusion in the fluid, the concentration C of the diffusing species satisfies the partial differential equation

$$\varphi\,\frac{\partial C}{\partial t} + \mathbf{u}\cdot\boldsymbol{\nabla} C = \alpha_{\mathrm{m,eff}}\,\nabla^2 C + \varphi\,\dot{m}\ , \tag{6.15}$$

where $\alpha_{\mathrm{m,eff}} = \varphi\,\alpha_{\mathrm{m}}$ is the effective mass diffusivity of the fluid saturating the porous medium. Equation (6.15) is the porous medium version of Eq. (5.109), and it is relative to a binary mixture.

6.3.1 Local Thermal Non-equilibrium

In the *local thermal non-equilibrium model* (LTNE), the heat transfer across the fluid-saturated porous medium is described with two distinct temperature fields. Thus, one defines two different local temperatures, one for the solid and one for the fluid. There is an inter-phase heat transfer rate, modelled through a constant coefficient h multiplying the local temperature difference between the phases. Thus, two energy balance equations have to be written for the two phases [8, 11, 15],

$$(1-\varphi)\ \rho_{\mathrm{s}}\,c_{v_{\mathrm{s}}}\,\frac{\partial T_{\mathrm{s}}}{\partial t} = (1-\varphi)\,\varkappa_{\mathrm{s}}\,\nabla^2 T_{\mathrm{s}} + (1-\varphi)\,q_{g_{\mathrm{s}}} + h\,(T_{\mathrm{f}} - T_{\mathrm{s}})\ , \tag{6.16}$$

$$\varphi\,\rho\,c\,\frac{\partial T_{\mathrm{f}}}{\partial t} + \rho\,c\,\mathbf{u}\cdot\boldsymbol{\nabla} T_{\mathrm{f}} = \varphi\,\varkappa\,\nabla^2 T_{\mathrm{f}} + \mu\,\Phi + \varphi\,q_{g_{\mathrm{f}}} + h\,(T_{\mathrm{s}} - T_{\mathrm{f}})\ . \tag{6.17}$$

The inter-phase heat transfer coefficient h in Eqs. (6.16) and (6.17) describes the thermal energy exchange between the solid and the fluid phase. In Eqs. (6.16) and (6.17), two independent heat sources are envisaged in the solid and in the fluid, $q_{g_{\mathrm{s}}}$ and $q_{g_{\mathrm{f}}}$.

The lack of local thermal equilibrium between the solid and fluid phases is exploited by locally and instantaneously distinct values of the temperature. Such

situation actually arises when very fast transient processes occur. It is definitely favoured also under stationary conditions when there are markedly different values of the fluid and solid thermal conductivities, as well as for sufficiently low values of the inter-phase heat transfer coefficient h. The latter condition tends to favour an independent behaviour of the two temperature fields.

The two-temperature model based on Eqs. (6.16) and (6.17) actually leads to the local energy balance with local inter-phase equilibrium, Eq. (6.12), when the coefficient h tends to infinity. This feature is easily verified if one writes the sum of Eqs. (6.16) and (6.17), together with Eq. (6.16),

$$\begin{aligned}(1-\varphi)\ \rho_{\mathrm{s}}\, c_{\mathrm{v_s}} \frac{\partial T_{\mathrm{s}}}{\partial t} + \varphi\, \rho\, c\ \frac{\partial T_{\mathrm{f}}}{\partial t} + \rho\, c\, \mathbf{u}\cdot\boldsymbol{\nabla} T_{\mathrm{f}} \\ = (1-\varphi)\, \varkappa_{\mathrm{s}}\, \nabla^2 T_{\mathrm{s}} + \varphi\, \varkappa\, \nabla^2 T_{\mathrm{f}} + \mu\, \Phi + (1-\varphi)\, q_{\mathrm{g_s}} + \varphi\, q_{\mathrm{g_f}}\ ,\end{aligned} \tag{6.18}$$

$$(1-\varphi)\ \rho_{\mathrm{s}}\, c_{\mathrm{v_s}} \frac{\partial T_{\mathrm{s}}}{\partial t} = (1-\varphi)\, \varkappa_{\mathrm{s}}\, \nabla^2 T_{\mathrm{s}} + (1-\varphi)\, q_{\mathrm{g_s}} + h\,(T_{\mathrm{f}} - T_{\mathrm{s}})\ . \tag{6.19}$$

If one takes the limit $h \to \infty$ in Eq. (6.19), one just retains the leading contribution, namely the last term on the right-hand side. Thus, Eq. (6.19) yields in this limit the local thermal equilibrium condition, $T_{\mathrm{f}} = T_{\mathrm{s}}$. By substituting this limiting condition in Eq. (6.18), one is led to Eq. (6.12), completed by the definitions given by Eqs. (6.13) and (6.14). The power generated per unit volume is to be intended as

$$q_{\mathrm{g}} = (1-\varphi)\, q_{\mathrm{g_s}} + \varphi\, q_{\mathrm{g_f}}\ . \tag{6.20}$$

The use of the two-temperature model for the local energy balance poses a problem regarding the correct formulation of the boundary conditions to be prescribed for T_{f} and T_{s}. The condition of a prescribed boundary temperature has in fact a natural formulation where a local thermal equilibrium is assumed at the boundary,

$$T_{\mathrm{f}} = T_{\mathrm{s}} = T_{\mathrm{w}}(\mathbf{x}, t)\ , \tag{6.21}$$

where $T_{\mathrm{w}}(\mathbf{x}, t)$ is a known function expressing the wall temperature distribution which, in general, depends both on the position $\mathbf{x}$ and on time t.

Things are definitely more complicated when a condition of prescribed wall heat flux is to be allowed at the boundary. In this case, the solid and fluid phases are potentially independent absorbers of the incoming heat flux at the boundary. There are several studies of this problem, and a survey can be found, for instance, in Alazmi and Vafai [2]. The simplest model to be adopted when a wall heat flux distribution $q_{\mathrm{w}}(\mathbf{x}, t)$ is prescribed can be formulated as

$$T_{\mathrm{f}} = T_{\mathrm{s}}\ , \qquad -(1-\varphi)\, \varkappa_{\mathrm{s}}\, \frac{\partial T_{\mathrm{s}}}{\partial n} - \varphi\, \varkappa\, \frac{\partial T_{\mathrm{f}}}{\partial n} = q_{\mathrm{w}}(\mathbf{x}, t)\ , \tag{6.22}$$

where $\partial/\partial n$ denotes the normal derivative to the boundary. The model expressed by Eq. (6.22) makes sense when the bounding wall has a very high thermal conductivity so that a local equilibration of the otherwise different temperatures of the two phases, T_f and T_s, is a sensible assumption.

6.3.2 *Viscous Dissipation*

We pointed out that, either in Eqs. (6.12) or (6.17), the term $\mu\,\Phi$ yields the power per unit volume generated by viscous dissipation. The expression of $\mu\,\Phi$ depends on the model for momentum balance employed. As pointed out in Nield [10], the term $\mu\,\Phi$ can be evaluated according to the general rule,

$$\mu\,\Phi = \mathbf{f}_\mathrm{d}\cdot\mathbf{u}\,, \tag{6.23}$$

where

$$\mathbf{f}_d = -\nabla p + \mathbf{b}\,, \tag{6.24}$$

is the drag force. The drag force has an expression which depends on the model adopted for the momentum transfer,

$$\text{Darcy's law} \longrightarrow \qquad \mathbf{f}_d = \frac{\mu}{K}\,\mathbf{u}\,; \tag{6.25}$$

$$\text{Darcy–Forchheimer's model} \longrightarrow \quad \mathbf{f}_d = \frac{\mu}{K}\left(1 + \frac{F\,\rho\,\sqrt{K}}{\mu}\,|\mathbf{u}|\right)\mathbf{u}\,; \tag{6.26}$$

$$\text{Brinkman's model} \longrightarrow \qquad \mathbf{f}_d = \frac{\mu}{K}\,\mathbf{u} - \mu_\mathrm{eff}\,\nabla^2\mathbf{u}\,. \tag{6.27}$$

Nield's rule expressed by Eq. (6.23) is still the object of some controversies especially with reference to its application in the case of Brinkman's model. Let us refer for simplicity to an incompressible flow, $\nabla\cdot\mathbf{u} = 0$. One would expect that, in the limiting case of an infinite permeability $K \to \infty$, the expression of $\mu\,\Phi$ implied by Eqs. (6.23) and (6.27) is consistent with the expression of the dissipation function for a Navier–Stokes fluid, Eq. (5.56), namely

$$\Phi = 2\,\mathscr{D}_{ij}\,\mathscr{D}_{ij}, \qquad \mathscr{D}_{ij} = \frac{1}{2}\left(\frac{\partial u_i}{\partial x_j} + \frac{\partial u_j}{\partial x_i}\right)\,. \tag{6.28}$$

On the contrary, in the limit $K \to \infty$ and $\varphi \to 1$, Eqs. (6.23) and (6.27) yield

$$\Phi = -\,\mathbf{u}\cdot\nabla^2\mathbf{u}\,, \tag{6.29}$$

since $\mu_{\text{eff}} = \mu$ in the limiting case of a fluid clear of solid material, as implied by Eq. (6.10). The difference between the expressions of Φ given in Eqs. (6.28) and (6.29) is apparent as Eq. (6.28) yields an expression containing only first-order derivatives of the velocity components, while the right-hand side of Eq. (6.29) contains second-order derivatives of the velocity components. Moreover, while Φ given by Eq. (6.28) can only be positive or zero, there could be flows such that the right-hand side of Eq. (6.29) is negative.

Al-Hadhrami et al. [1] proposed a different expression of Φ in the case of Brinkman's model, namely

$$\Phi = \frac{1}{K}\,\mathbf{u}\cdot\mathbf{u} + 2\,\frac{\mu_{\text{eff}}}{\mu}\,\mathscr{D}_{ij}\,\mathscr{D}_{ij}\ . \tag{6.30}$$

The advantage of the expression of Φ as given by Eq. (6.30) is that Φ cannot be negative, and the two limiting cases of Darcy's law ($K \to 0$) and Navier–Stokes fluid ($K \to \infty$, $\varphi \to 1$) are correctly recovered. However, the scientific debate on this subject is still open. An interesting contribution on this topic comes from the paper by Breugem and Rees [4].

6.4 The Buoyancy Force

The Oberbeck–Boussinesq approximation can be invoked for the seepage flow in porous media, along the same lines defined in Sect. 5.9. Again, the basic idea is assuming a variable density only in the gravitational body force $\mathbf{b} = \rho\,\mathbf{g}$. Then, a Taylor series expansion of the fluid density as a function of T, around the reference temperature T_0, truncated to first order is written, as in Eq. (5.66), and this leads to the definition of a piezometric head, as in Eq. (5.67), and a buoyancy force proportional to $T - T_0$.

If one invokes the validity of Darcy's law, the set of local balance equations according to the Oberbeck–Boussinesq approximation is given by

$$\frac{\partial u_j}{\partial x_j} = 0\ , \tag{6.31}$$

$$\frac{\mu}{K}\,u_i = -\rho_0\,\beta\,(T - T_0)\,g_i - \frac{\partial P}{\partial x_i}\ , \tag{6.32}$$

$$\rho_0\,c\left(\sigma\,\frac{\partial T}{\partial t} + u_j\,\frac{\partial T}{\partial x_j}\right) = \varkappa_{\text{eff}}\,\nabla^2 T + q_{\text{g}} + \frac{\mu}{K}\,u_j\,u_j\ . \tag{6.33}$$

In the domain of validity of Darcy–Forchheimer's model, Eqs. (6.31)–(6.33) are to be replaced by

$$\frac{\partial u_j}{\partial x_j} = 0 \,, \tag{6.34}$$

$$\frac{\mu}{K}\left(1 + \frac{F\,\rho\,\sqrt{K}}{\mu}\,|\mathbf{u}|\right) u_i = -\rho_0\,\beta\,(T - T_0)\,g_i - \frac{\partial P}{\partial x_i} \,, \tag{6.35}$$

$$\rho_0\,c\left(\sigma\,\frac{\partial T}{\partial t} + u_j\,\frac{\partial T}{\partial x_j}\right) = \varkappa_{\text{eff}}\,\nabla^2 T + q_{\text{g}} + \frac{\mu}{K}\left(1 + \frac{F\,\rho\,\sqrt{K}}{\mu}\,|\mathbf{u}|\right) u_j\,u_j \,. \tag{6.36}$$

Another formulation of the Oberbeck–Boussinesq approximation based on Brinkman's model can be written in a similar manner. In this case, the only conjectural element is the form of the viscous dissipation contribution in the local energy balance equation, as discussed in Sect. 6.3.2.

6.5 Non-Newtonian Flow in Porous Media

The seepage flow of non-Newtonian fluids in porous media has been the object of a widespread interest over the past decades. Many situations in the real world involve departure from the Newtonian fluid behaviour. This may happen with the flow of polymeric fluids, and of heavy oils or liquid hydrocarbons. The non-Newtonian character of the fluid yields modified formulations of the local momentum balance equation with respect to Darcy's law. Different formulations occur for different classes of non-Newtonian fluids [13, 16].

The simplest case is that of power-law fluids, where the relationship between the viscous stress tensor and the strain tensor is nonlinear. In the simple case where the velocity field is solenoidal, Eq. (5.48) is replaced by

$$\tau_{ij} = 2\,\hat{\mu}\;(\mathscr{D}_{k\ell}\,\mathscr{D}_{k\ell})^{(n-1)/2}\;\mathscr{D}_{ij} \,, \tag{6.37}$$

where $\hat{\mu}$ is the *consistency factor*, while n is the *power-law index*. For the seepage flow of a power-law fluid in a porous medium, Darcy's law is to be extended according to a formulation originally proposed by Christopher and Middleman [5],

$$\frac{\hat{\mu}^*}{K}\,|\mathbf{u}|^{n-1}\mathbf{u} = -\nabla p + \mathbf{b} \,, \tag{6.38}$$

where $\hat{\mu}^*$ is the *effective consistency factor*. Obviously, both Eqs. (6.37) and (6.38) yield their Newtonian counterparts when $n = 1$. In particular, Eq. (6.38) coincides with Eq. (6.5) when $n = 1$, provided that the effective consistency factor is identified with the dynamic viscosity of the Newtonian fluid.

A more complicated type of non-Newtonian fluids is that described by the *Bingham model*. Fluids within this class display a behaviour which is intermediate between a solid and a Newtonian fluid. In other words, a tangential stress imposed on the boundary of the fluid determines a corresponding nonzero strain only if the tangential stress exceeds a threshold value. When this threshold is exceeded, the excess tangential stress applied to the boundary is proportional to the strain as for Newtonian fluids. Several biological fluids behave in this manner. A thorough analysis of Bingham flow in porous media has been presented by Rees [14] and by Nash and Rees [9]. In particular, the simplest mathematical formulation of the extended Darcy's law for Bingham fluids was expressed by Pascal [12],

$$\begin{cases} \mathbf{u} = 0 \ , & |\mathbf{f}_\mathrm{d}| < \xi \ , \\ \dfrac{\mu}{K}\left(1 + \dfrac{K\,\xi}{\mu\,|\mathbf{u}|}\right)\mathbf{u} = \mathbf{f}_\mathrm{d} \ , & |\mathbf{f}_\mathrm{d}| > \xi \ . \end{cases} \tag{6.39}$$

Here, $\mathbf{f}_\mathrm{d}$ is the drag force, defined by Eq. (6.24), namely $\mathbf{f}_\mathrm{d} = -\boldsymbol{\nabla} p + \mathbf{b}$. The positive parameter ξ is the *yield pressure gradient* distinguishing the stagnant regime, $\mathbf{u} = 0$, from flow, $\mathbf{u} \neq 0$. Darcy's law for a Newtonian fluid is easily recovered from Eq. (6.39) in the limit $\xi \to 0$.

Several studies on convection in porous media involve *viscoelastic fluids*. These fluids display a nature that includes both the viscous damping, typical of Newtonian fluids, and the elastic response typical of solids. When the flow of these non-Newtonian fluids happens in porous media, the extension of Darcy's law is based on the so-called *Oldroyd-B model*, as mentioned by Khuzhayorov et al. [7],

$$\frac{\mu}{K}\left(1 + \tau_2 \frac{\partial}{\partial t}\right)\mathbf{u} = \left(1 + \tau_1 \frac{\partial}{\partial t}\right)\mathbf{f}_\mathrm{d} \ . \tag{6.40}$$

Again, the drag force $\mathbf{f}_\mathrm{d}$ is given by Eq. (6.24), while τ_1 and τ_2 are the *relaxation time* and the *retardation time*, respectively. The formulation based on Eq. (6.40) is consistent only if $\tau_1 \geq \tau_2$. The special case $\tau_1 = \tau_2$ yields the Newtonian behaviour, while the limit $\tau_2 \to 0$ corresponds to the so-called *Maxwell model* for linear viscoelasticity. Equation (6.40) shows that, in the case of stationary fluid flow in porous media, there is no difference between the behaviour of a Newtonian fluid and that of a linear viscoelastic fluid, as the time derivatives in Eq. (6.40) are ineffective.

References

1. Al-Hadhrami AK, Elliott L, Ingham DB (2003) A new model for viscous dissipation in porous media across a range of permeability values. Transp Porous Media 53:117–122
2. Alazmi B, Vafai K (2002) Constant wall heat flux boundary conditions in porous media under local thermal non-equilibrium conditions. Int J Heat Mass Transf 45:3071–3087
3. Bear J (1988) Dynamics of fluids in porous media. Dover, New York

4. Breugem WP, Rees DAS (2006) A derivation of the volume-averaged Boussinesq equations for flow in porous media with viscous dissipation. Transp Porous Media 63:1–12
5. Christopher RH, Middleman S (1965) Power-law flow through a packed tube. Ind Eng Chem Fundam 4:422–426
6. Kaviany M (2001) Principles of heat transfer in porous media, 2nd edn. Springer, New York
7. Khuzhayorov B, Auriault JL, Royer P (2000) Derivation of macroscopic filtration law for transient linear viscoelastic fluid flow in porous media. Int J Eng Sci 38:487–504
8. Kuznetsov AV (1998) Thermal nonequilibrium forced convection in porous media. In: Ingham DB, Pop I (eds) Transport phenomena in porous media. Pergamon Press, Oxford, pp 103–129
9. Nash S, Rees DAS (2017) The effect of microstructure on models for the flow of a Bingham fluid in porous media: one-dimensional flows. Transp Porous Media 116:1073–1092
10. Nield DA (2007) The modeling of viscous dissipation in a saturated porous medium. J Heat Transf 129:1459–1463
11. Nield DA, Bejan A (2017) Convection in porous media, 5th edn. Springer, New York
12. Pascal H (1983) Rheological behaviour effect of non-Newtonian fluids on steady and unsteady flow through a porous medium. Int J Numer Anal Methods Geomech 7:289–303
13. Pearson JRA, Tardy PMJ (2002) Models for flow of non-Newtonian and complex fluids through porous media. J Non-Newtonian Fluid Mech 102:447–473
14. Rees DAS (2015) Convection of a Bingham fluid in a porous medium. In: Vafai K (ed) Handbook of porous media, 3rd edn. CRC Press, Boca Raton, pp 559–595
15. Rees DAS, Pop I (2005) Local thermal non-equilibrium in porous medium convection. In: Ingham DB, Pop I (eds) Transport phenomena in porous media III. Pergamon Press, Oxford, pp 147–173
16. Shenoy AV (1994) Non-Newtonian fluid heat transfer in porous media. Adv Heat Transf 24:102–191
17. Straughan B (2008) Stability and wave motion in porous media. Springer, New York

Chapter 7
Rayleigh–Bénard Convection

7.1 Heating a Fluid Layer from Below

The investigation of the fluid dynamics thermally induced by a vertical temperature gradient imposed on a fluid layer initiated with the experiments carried out by Bénard [1] at the beginning of the twentieth century. Such investigation was the subject of Henri Claude Bénard's doctoral thesis defended at Sorbonne University, in Paris. These experiments documented the formation of flow cells in a shallow fluid layer where the temperature on the lower wall is higher than on the upper free surface, provided that the prescribed temperature difference is higher than a threshold value. Bénard's experiments were carried out with the prescribed higher temperature within a range between 50 °C and 100 °C, by employing liquids such as wax and whale oil (spermaceti), which melt in this temperature range and do not display significant surface evaporation. For the readers interested in the scientific biography of Bénard, we recommend the review written by Wesfreid and published in Chapter 1 of the book edited by Mutabazi et al. [8].

Pearson [11] gave theoretical support to the idea that the thermal buoyancy force was not responsible of the phenomenon observed in Bénard's experiments. In Pearson's paper, his conclusion is: "we see that the buoyancy mechanism has no chance of causing convection cells, while the surface tension mechanism is almost certain to do so, and that observations support this". On the other hand, the theoretical scheme adopted for many years to explain Bénard's observations is that the thermal expansion of fluid elements close to the lower hot wall determines a vertical buoyancy force compensated by the viscous resistance. When these competing forces reach an equilibrium and, eventually, the buoyancy force prevails over the viscous resistance, the convection cellular flow is established [10]. The dimensionless parameter comparing the extent of the buoyancy force to that of the viscous resistance is nowadays well known as the *Rayleigh number*,

$$Ra = \frac{g\,\beta\,(T_1 - T_2)\,L^3}{\nu\,\alpha}\,. \tag{7.1}$$

A. Barletta, *Routes to Absolute Instability in Porous Media*,
https://doi.org/10.1007/978-3-030-06194-4_7

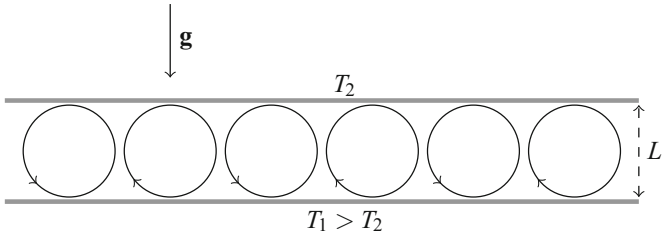

Fig. 7.1 A train of counter-rotating cells in a fluid layer bounded by two isothermal planes

As shown in Fig. 7.1, $T_1 > T_2$ is the temperature of the lower heated wall, while T_2 is the temperature of the upper free boundary, g is the modulus of the gravitational acceleration **g**, and L is the thickness of the fluid layer. Actually, it is the Rayleigh number that displays a threshold, called the *critical value*, Ra_c, which defines the condition for the onset of the buoyancy-induced cells, namely $Ra > Ra_c$. Despite the correctness of Pearson's conclusions [11] about Bénard's experiments, there are several other experimental circumstances where the onset of the flow cells is in fact caused by the thermal buoyancy force and, hence, by the condition $Ra > Ra_c$. This happens, for instance, in the classical experiment reported by Schmidt and Milverton [15], as well as in many natural situations quite common in oceanography, meteorology, or geophysics [10]. Figure 7.1 shows that the flow pattern is a train of counter-rotating cells.

In the following, we will not investigate the role played by the surface tension, highlighted by Pearson [11], and focus our attention on the thermal buoyancy force as the cause of cells. This approach stems from the pioneering paper by Lord Rayleigh [13], and it has been developed by several authors, over an entire century, in a really huge literature. Extensive surveys on this topic can be found in many books. Just a few examples are Chandrasekhar [2], Koschmieder [6], Getling [4], Drazin and Reid [3].

7.2 The Rayleigh–Bénard Problem

The onset of buoyancy-induced cells is a classical problem of free convection in a horizontal fluid layer heated from below, viz. the well-known *Rayleigh–Bénard problem*. More precisely, in its simplified formulation, one assumes an infinitely wide horizontal fluid layer bounded by two isothermal planes. The lower boundary plane is kept isothermal at temperature T_1, while the upper boundary plane is kept isothermal at temperature $T_2 < T_1$. As is well known, buoyancy-induced cells appear when the Rayleigh number exceeds the critical value Ra_c. The critical value depends on the boundary conditions assumed at the isothermal boundaries. There are three main cases, classically devised in the literature:

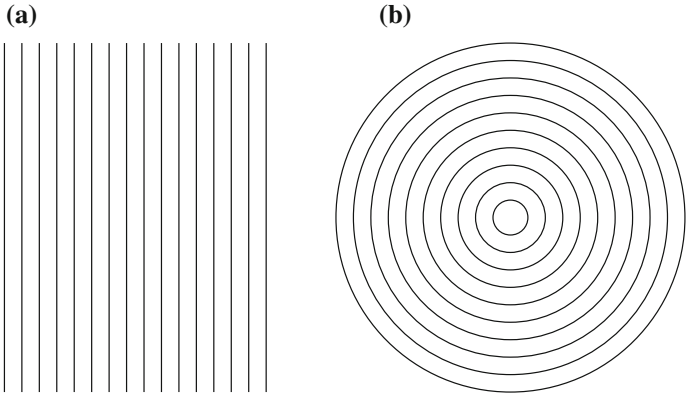

Fig. 7.2 Simple planforms of the convection cells: **a** straight rolls; **b** toroidal rolls

- Both boundaries are rigid and impermeable walls, so that impermeability and no-slip boundary conditions are prescribed on the velocity field. In this case, $Ra_c \approx 1707.76$.
- The lower boundary is a rigid and impermeable wall, while the upper boundary is a stress-free surface. With stress-free surface, we mean that the boundary conditions for the velocity are impermeability and vanishing tangential components of the viscous stress tensor, τ_{ij}. In this case, $Ra_c \approx 1100.65$.
- Both boundaries are stress-free surfaces. In this case, $Ra_c = 27\,\pi^4/4 \approx 657.511$.

The third case is the only one admitting a fully analytical solution, and it was originally regarded in the paper by Lord Rayleigh [13]. We mention that the stress-free boundary conditions embody a simplified physical model of the interface between a viscous liquid and a low-viscosity gas.

We have established that the boundary conditions prescribed at the horizontal boundary planes of the fluid layer influence the critical value of the Rayleigh number for the onset of the instability. The vertical sidewalls bounding laterally the shallow layer play an important role in shaping the planform of the buoyancy-induced cells. The planform is in fact the shape of the cells as detected on a plane cutting horizontally the fluid layer. The planform of the buoyancy-induced cells depends on several features of the system including the shape of the lateral confining walls, even when the fluid layer is extremely shallow. Two sample cases are illustrated in Fig. 7.2, namely that of the straight rolls, and that of the toroidal rolls. The latter planform is favoured when the sidewall is a vertical cylindrical surface with circular cross section.

The onset of buoyancy-induced cells in a fluid initially at rest may be viewed as a manifestation of the convective instability of the rest state, where the fluid velocity $\mathbf{u}$ is zero everywhere. In this sense, in the study of the Rayleigh–Bénard problem, we employ a linear stability analysis, so that the critical condition $Ra = Ra_c$ represents the threshold for the rest state to become convectively unstable.

At this stage, the reader may have noticed the twofold meaning of the terms "convection", "convective" and "convectively" in the present discussion. These terms naturally address a special type of heat transfer occurring in the fluid, i.e. the convection, and the specific type of instability arising in the fluid, i.e. the convective instability. As it should be clear from our definition given in Chap. 4, the convective instability may well emerge in flow systems where no convection heat transfer is present or may take place. There is no reasonable way to overcome this terminological conflict without introducing artificial terms different from those commonly employed in the literature. The author is confident that the context where the term is used makes its meaning unambiguous in every case.

If we consider a fluid layer, initially at rest, subject to an externally imposed temperature difference (heating from below), the rest state becomes unstable giving rise to buoyancy-induced cells when the Rayleigh number becomes sufficiently high.

In order to regard the Rayleigh–Bénard problem as a stability analysis, we need to develop the governing equations for the perturbations superposed onto a basic stationary state of the fluid.

7.3 Stability and Instability of Fluid Systems

As extensively discussed in Chap. 4, the basic idea behind Lyapunov's concept of instability is that we must consider an initial state of a system and a trajectory originating from this initial state. Then, we slightly perturb the initial state and examine the perturbed trajectory. If the small perturbation results, for a sufficiently large time, in a definitely different trajectory, then we have an unstable behaviour. Otherwise, we have stability. Instability is a consequence of an extremely strong dependence of the time evolution on the initial conditions.

If we apply Lyapunov's idea to the governing equations of a fluid, we must think of a trajectory as the time evolution of a given flow and we must think of an equilibrium state as a stationary flow. On checking the stability of a stationary flow, we must slightly perturb the velocity, pressure and temperature fields and see if the perturbation drives the system far away from its original stationary flow. If this happens, then we have an unstable flow. Otherwise, we have a stable flow.

A fluid flow can be unstable even in the absence of a thermal coupling, i.e. if the flow is isothermal or if the buoyancy force is negligible. In this case, the origin of the instability is in the governing mass and momentum balance equations and, in particular, in the nonlinear inertial term,

$$u_j \frac{\partial u_i}{\partial x_j} ,$$

of the local momentum balance equation (5.84),

$$\frac{\partial u_i}{\partial t} + u_j \frac{\partial u_i}{\partial x_j} = -\frac{1}{\rho_0} \frac{\partial P}{\partial x_i} + \nu \nabla^2 u_i \ .$$

In the absence of this nonlinear term, every stationary flow without a thermal coupling would be stable. The instability of an isothermal, or forced convection, flow is called *hydrodynamic instability*. Since, in this case, the temperature field does not appear either in the local mass balance equation or in the local momentum balance equation, the analysis of the hydrodynamic instability does not involve the solution of the local energy balance equation.

Another kind of instability is that driven by the thermal coupling of the velocity field through the buoyancy force. This kind of instability is called *thermal instability*. The thermal instability depends not only on the nonlinearity of the local momentum balance, but it is also driven by the nonlinear convective term,

$$u_j \frac{\partial T}{\partial x_j} \ ,$$

as well as by the nonlinear viscous dissipation term, $2\,\nu\,\mathscr{D}_{ij}\,\mathscr{D}_{ij}/c$, of the local energy balance equation (5.85),

$$\frac{\partial T}{\partial t} + u_j \frac{\partial T}{\partial x_j} = \alpha \nabla^2 T + \frac{q_g}{\rho_0\, c} + \frac{2\,\nu}{c}\, \mathscr{D}_{ij}\, \mathscr{D}_{ij} \ .$$

In order to illustrate the method for testing the stability or instability of a basic fluid flow, we refer to a Newtonian fluid and we consider the governing local balance equations (5.83)–(5.85), within the Oberbeck–Boussinesq approximation,

$$\frac{\partial u_j}{\partial x_j} = 0 \ , \tag{7.2}$$

$$\frac{\partial u_i}{\partial t} + u_j \frac{\partial u_i}{\partial x_j} = -\beta\,(T - T_0)\, g_i - \frac{1}{\rho_0} \frac{\partial P}{\partial x_i} + \nu \nabla^2 u_i \ , \tag{7.3}$$

$$\frac{\partial T}{\partial t} + u_j \frac{\partial T}{\partial x_j} = \alpha \nabla^2 T + \frac{q_g}{\rho_0\, c} + \frac{2\,\nu}{c}\, \mathscr{D}_{ij}\, \mathscr{D}_{ij} \ , \tag{7.4}$$

where the thermal power generated per unit volume, $q_g(\mathbf{x}, t)$, is considered as a known function, independent of the fields $(\mathbf{u}, P, T)$. If we want to test the stability of a *basic solution*, $(\mathbf{u}_b, P_b, T_b)$, of Eqs. (7.2)–(7.4), we proceed as follows. We perturb the basic solution, i.e., we express the fields $(\mathbf{u}, P, T)$ as

$$u_i = u_{bi} + \varepsilon\, U_i \ , \qquad P = P_b + \varepsilon\, \Pi \ , \qquad T = T_b + \varepsilon\, \Theta \ , \tag{7.5}$$

where ε is the perturbation parameter. The terms $\varepsilon\, U_i$, $\varepsilon\, \Pi$ and $\varepsilon\, \Theta$ express the perturbation of the basic solution. We remember that the basic solution $(\mathbf{u}_b, P_b, T_b)$ satisfies

Eqs. (7.2)–(7.4), and, on substituting Eq. (7.5) into Eqs. (7.2)–(7.4), we obtain

$$\varepsilon \, \frac{\partial U_j}{\partial x_j} = 0 \, , \tag{7.6}$$

$$\varepsilon \, \frac{\partial U_i}{\partial t} + \varepsilon \, U_j \, \frac{\partial u_{\mathrm{b}i}}{\partial x_j} + \varepsilon \, u_{\mathrm{b}j} \, \frac{\partial U_i}{\partial x_j} + \varepsilon^2 \, U_j \, \frac{\partial U_i}{\partial x_j}$$

$$= -\varepsilon \, \beta \, \Theta \, g_i - \frac{\varepsilon}{\rho_0} \, \frac{\partial \Pi}{\partial x_i} + \varepsilon \, \nu \, \nabla^2 U_i \, , \tag{7.7}$$

$$\varepsilon \, \frac{\partial \Theta}{\partial t} + \varepsilon \, u_{\mathrm{b}j} \, \frac{\partial \Theta}{\partial x_j} + \varepsilon \, U_j \, \frac{\partial T_{\mathrm{b}}}{\partial x_j} + \varepsilon^2 \, U_j \, \frac{\partial \Theta}{\partial x_j}$$

$$= \varepsilon \, \alpha \, \nabla^2 \Theta + \frac{4 \, \varepsilon \, \nu}{c} \, \mathscr{D}_{\mathrm{b}ij} \, \mathfrak{D}_{ij} + \frac{2 \, \varepsilon^2 \nu}{c} \, \mathfrak{D}_{ij} \, \mathfrak{D}_{ij} \, , \tag{7.8}$$

where

$$\mathscr{D}_{\mathrm{b}ij} = \frac{1}{2} \left(\frac{\partial u_{\mathrm{b}i}}{\partial x_j} + \frac{\partial u_{\mathrm{b}j}}{\partial x_i} \right) \, , \qquad \mathfrak{D}_{ij} = \frac{1}{2} \left(\frac{\partial U_i}{\partial x_j} + \frac{\partial U_j}{\partial x_i} \right) \, . \tag{7.9}$$

We mention that the non-homogeneous term, q_{g}, in Eqs. (7.2)–(7.4) does not appear any more in the perturbation Eqs. (7.6)–(7.8), since $(u_{\mathrm{b}i}, P_{\mathrm{b}}, T_{\mathrm{b}})$ is a solution of Eqs. (7.2)–(7.4).

Equations (7.6)–(7.8) express the governing equations for the perturbation fields (U_i, Π, Θ). We note that these equations contain a coupling to the basic solution $(u_{\mathrm{b}i}, P_{\mathrm{b}}, T_{\mathrm{b}})$ only as a consequence of the nonlinear terms

$$u_j \, \frac{\partial u_i}{\partial x_j} \, , \qquad u_j \, \frac{\partial T}{\partial x_j} \, , \qquad \frac{2 \, \nu}{c} \, \mathscr{D}_{ij} \, \mathscr{D}_{ij} \, ,$$

that appear in Eqs. (7.3) and (7.4). Without these nonlinear terms, the perturbations would be uncoupled to the basic solution, so that the perturbation of the basic solution would be independent of the basic solution. This circumstance would result in a stability of the basic solution whatever it may be. Thus, we have established a link between the instability and the nonlinearity of the governing equations.

At this point, we have two alternatives: we may assume that the perturbations are small, or we may investigate perturbations of arbitrarily large amplitude. In the first case, we perform a linear stability analysis. In the second case, we investigate the nonlinear stability of the flow. The first option is the simplest one, and we will restrict all the forthcoming discussion to this case. Assuming small perturbations means assuming $\varepsilon \ll 1$, so that we can neglect the terms $O\left(\varepsilon^2\right)$ with respect to the terms $O(\varepsilon)$ in Eqs. (7.6)–(7.8). Therefore, we can simplify ε from Eqs. (7.6)–(7.8) and rewrite them as

$$\frac{\partial U_j}{\partial x_j} = 0 \,, \tag{7.10}$$

$$\frac{\partial U_i}{\partial t} + U_j \, \frac{\partial u_{\mathrm{b}i}}{\partial x_j} + u_{\mathrm{b}j} \, \frac{\partial U_i}{\partial x_j} = -\beta \, \Theta \, g_i - \frac{1}{\rho_0} \, \frac{\partial \Pi}{\partial x_i} + \nu \, \nabla^2 U_i \,, \tag{7.11}$$

$$\frac{\partial \Theta}{\partial t} + u_{\mathrm{b}j} \, \frac{\partial \Theta}{\partial x_j} + U_j \, \frac{\partial T_{\mathrm{b}}}{\partial x_j} = \alpha \, \nabla^2 \Theta + \frac{4 \, \nu}{c} \, \mathscr{D}_{\mathrm{b}ij} \, \mathfrak{D}_{ij} \,. \tag{7.12}$$

One may solve Eqs. (7.10)–(7.12) and check what the time evolution of the perturbation is like: if it leads to an increasingly large departure from the basic solution, or if it leads to an asymptotic recovery of the basic solution. In the first case, we have a response of instability for the basic flow, while in the second case, we have an outcome of stability.

7.4 Formulation of the Rayleigh–Bénard Problem

In Sect. 7.2, we have seen that a crucial point in modelling the Rayleigh–Bénard system is the definition of the velocity boundary conditions. As illustrated in Fig. 7.3, the z-axis is taken as vertical, while the x and y axes are horizontal. For the sake of mathematical simplicity, we will initially model the boundaries $z = 0$ and $z = L$ as impermeable and stress-free. In doing this, we follow the approach chosen by Lord Rayleigh [13] in his pioneering paper. The determination of the onset conditions for the development of convection cells can be approached by a linear stability analysis, based on Eqs. (7.10)–(7.12).

7.4.1 Governing Equations

The critical condition for the onset of convection cells in the fluid layer is obtained starting from the basic state where the fluid is at rest,

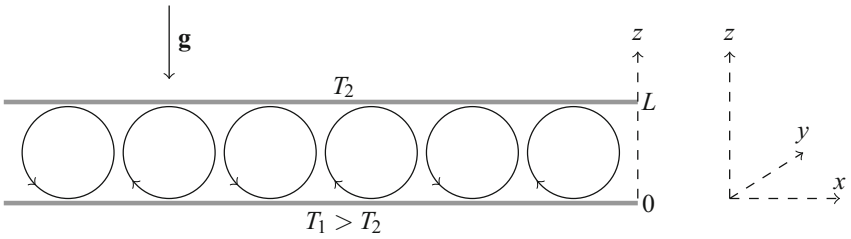

Fig. 7.3 Rayleigh–Bénard system: choice of the coordinate axes

$$u_{bi} = 0 \,, \qquad T_b = T_1 - (T_1 - T_2)\,\frac{z}{L} \,. \tag{7.13}$$

In fact, one may easily verify that Eq. (7.13) is a solution of the local mass, momentum and energy balance equations (7.2)–(7.4) under the assumption that no volumetric heat source is present in the fluid, namely $q_g = 0$. We also mention that Eq. (7.13) is compatible with the conditions of stress-free and impermeable boundaries, as the velocity is zero everywhere. Also the thermal boundary conditions of isothermal surfaces at $z = 0$ and $z = L$, with temperatures T_1 and T_2, are satisfied. Thus, Eqs. (7.10)–(7.12) yield

$$\frac{\partial U_j}{\partial x_j} = 0 \,,$$

$$\frac{\partial U_i}{\partial t} = -\beta\,\Theta\,g_i - \frac{1}{\rho_0}\,\frac{\partial \Pi}{\partial x_i} + \nu\,\nabla^2 U_i \,,$$

$$\frac{\partial \Theta}{\partial t} - W\,\frac{T_1 - T_2}{L} = \alpha\,\nabla^2\Theta \,, \tag{7.14}$$

where we denoted as (U, V, W) the (x, y, z) components of the velocity perturbation U_i. The boundary conditions for the velocity and temperature fields model the constraints of uniform temperature, impermeability and vanishing tangential viscous stresses at $z = 0,\ L$. Here, we define the viscous stress tensor associated with the velocity perturbation,

$$\mathscr{T}_{ij} = \mu\left(\frac{\partial U_i}{\partial x_j} + \frac{\partial U_j}{\partial x_i}\right) \,. \tag{7.15}$$

Thus, the boundary conditions can be written either as

$$z = 0,\ L \ : \qquad W = 0 = \Theta \,, \quad \mathscr{T}_{zx} = 0 = \mathscr{T}_{zy} \,, \tag{7.16}$$

or, equivalently, as

$$z = 0,\ L \ : \qquad W = 0 = \Theta \,, \quad \frac{\partial W}{\partial x} + \frac{\partial U}{\partial z} = 0 = \frac{\partial W}{\partial y} + \frac{\partial V}{\partial z} \,. \tag{7.17}$$

Since $W = 0$ at $z = 0,\ L$, we can rewrite Eq. (7.17) as

$$z = 0,\ L \ : \qquad W = 0 = \Theta \,, \quad \frac{\partial U}{\partial z} = 0 = \frac{\partial V}{\partial z} \,. \tag{7.18}$$

The perturbation equations can be further simplified by allowing an appropriate scaling of the quantities, so that the study is carried out with a dimensionless formulation,

$$\frac{U_i}{\alpha/L} \to U_i \,, \qquad \frac{\Theta}{T_1 - T_2} \to \Theta \,, \qquad \frac{\Pi}{\rho_0 \nu \alpha / L^2} \to \Pi \,,$$

$$\frac{x_i}{L} \to x_i \ , \qquad \frac{t}{L^2/\alpha} \to t \ . \tag{7.19}$$

Thus, Eqs. (7.14) and (7.18) can be rewritten in a dimensionless form as

$$\frac{\partial U_j}{\partial x_j} = 0 \ , \tag{7.20}$$

$$\frac{1}{Pr}\frac{\partial U_i}{\partial t} = Ra\,\Theta\,\delta_{i3} - \frac{\partial \Pi}{\partial x_i} + \nabla^2 U_i \ , \tag{7.21}$$

$$\frac{\partial \Theta}{\partial t} - W = \nabla^2 \Theta \ , \tag{7.22}$$

$$z = 0,\ 1 \ : \qquad W = 0 = \Theta \ , \quad \frac{\partial U}{\partial z} = 0 = \frac{\partial V}{\partial z} \ , \tag{7.23}$$

where δ_{i3} is the $(i, 3)$ component of Kronecker's delta, namely the ith component of the unit vector $\mathbf{e}_z = (0, 0, 1)$, while the dimensionless parameters Pr and Ra are the *Prandtl number* and the Rayleigh number defined as

$$Pr = \frac{\nu}{\alpha} \ , \qquad Ra = \frac{g\beta(T_1 - T_2)L^3}{\nu\alpha} \ . \tag{7.24}$$

The term $-\,\partial\Pi/\partial x_i$ can be encompassed by taking the curl of the momentum balance equation so that one obtains:

$$\left(\frac{1}{Pr}\frac{\partial}{\partial t} - \nabla^2\right)\left(\frac{\partial W}{\partial x} - \frac{\partial U}{\partial z}\right) = Ra\,\frac{\partial \Theta}{\partial x} \ , \tag{7.25}$$

$$\left(\frac{1}{Pr}\frac{\partial}{\partial t} - \nabla^2\right)\left(\frac{\partial W}{\partial y} - \frac{\partial V}{\partial z}\right) = Ra\,\frac{\partial \Theta}{\partial y} \ . \tag{7.26}$$

We derive Eq. (7.25) with respect to x, and Eq. (7.26) with respect to y. Then, we sum the two resulting equations, so that we obtain

$$\left(\frac{1}{Pr}\frac{\partial}{\partial t} - \nabla^2\right)\left[\nabla^2 W - \frac{\partial}{\partial z}\left(\frac{\partial U_j}{\partial x_j}\right)\right] = Ra\,\nabla_2^2 \Theta \ , \tag{7.27}$$

where ∇_2^2 is the two-dimensional Laplace operator, defined as

$$\nabla_2^2 \Theta = \frac{\partial^2 \Theta}{\partial x^2} + \frac{\partial^2 \Theta}{\partial y^2} \ . \tag{7.28}$$

By taking into account the local mass balance equation, $\partial U_j/\partial x_j = 0$, we can extract a set of two partial differential equations in the unknowns (W, Θ), which describe the linear stability problem,

$$\left(\frac{1}{Pr}\,\frac{\partial}{\partial t} - \nabla^2\right)\nabla^2 W = Ra\,\nabla_2^2\Theta\ ,$$

$$\frac{\partial\Theta}{\partial t} - W = \nabla^2\Theta\ ,$$

$$z = 0,\ 1\ :\qquad W = 0 = \Theta\ ,\quad \frac{\partial^2 W}{\partial z^2} = 0\ , \tag{7.29}$$

The boundary conditions $\partial^2 W/\partial z^2 = 0$, at $z = 0, 1$, are retrieved by deriving the stress-free conditions at $z = 0, 1$, given by Eq. (7.23),

$$\frac{\partial U}{\partial z} = 0\ ,\qquad \frac{\partial V}{\partial z} = 0\ ,$$

with respect to x and y, respectively, by summing them so that one obtains

$$\frac{\partial}{\partial z}\left(\frac{\partial U_j}{\partial x_j}\right) - \frac{\partial^2 W}{\partial z^2} = 0\ ,$$

and finally by employing the local mass balance equation, $\partial U_j/\partial x_j = 0$.

7.4.2 Normal Mode Analysis

Equations (7.29) can be solved by employing the Fourier transform method. We will follow a procedure similar to that described, for instance, in Sect. 4.2. The significant difference is that we now employ two-dimensional Fourier transforms, defined by Eqs. (2.91) and (2.92)

$$\tilde{W}(k_x, k_y, z, t) = \frac{1}{2\pi}\int_{-\infty}^{\infty}\int_{-\infty}^{\infty} W(x, y, z, t)\,\mathrm{e}^{-\mathrm{i}(k_x x + k_y y)}\,\mathrm{d}\,x\,\mathrm{d}\,y\ ,$$

$$W(x, y, z, t) = \frac{1}{2\pi}\int_{-\infty}^{\infty}\int_{-\infty}^{\infty} \tilde{W}(k_x, k_y, z, t)\,\mathrm{e}^{\mathrm{i}(k_x x + k_y y)}\,\mathrm{d}\,k_x\,\mathrm{d}\,k_y\ ,$$

$$\tilde{\Theta}(k_x, k_y, z, t) = \frac{1}{2\pi} \int_{-\infty}^{\infty} \int_{-\infty}^{\infty} \Theta(x, y, z, t)\, \mathrm{e}^{-\mathrm{i}(k_x x + k_y y)}\, \mathrm{d}\, x\, \mathrm{d}\, y \ ,$$

$$\Theta(x, y, z, t) = \frac{1}{2\pi} \int_{-\infty}^{\infty} \int_{-\infty}^{\infty} \tilde{\Theta}(k_x, k_y, z, t)\, \mathrm{e}^{\mathrm{i}(k_x x + k_y y)}\, \mathrm{d}\, k_x\, \mathrm{d}\, k_y \ . \tag{7.30}$$

In other words, we are seeking solutions expressed through a superposition of Fourier modes, or normal modes, propagating in the (x, y) plane along the direction of the wave vector (k_x, k_y). We are dealing with two-dimensional and, hence, double Fourier transforms. This means that the property of partial derivatives expressed by Eq. (2.18) applies to the derivatives both with respect to x and those with respect to y. This means that the Fourier transforms of $\nabla^2 W$, $\nabla^2 \Theta$ and $\nabla_2^2 \Theta$ are given, respectively, by

$$\left(\frac{\partial^2}{\partial z^2} - k^2\right) \tilde{W} \ , \qquad \left(\frac{\partial^2}{\partial z^2} - k^2\right) \tilde{\Theta} \ , \qquad -k^2\, \tilde{\Theta} \ ,$$

where $k = (k_x^2 + k_y^2)^{1/2}$ is the wave number.

The use of the Fourier transform method, for the solution of Eq. (7.29), implies that $\tilde{W}$ and $\tilde{\Theta}$ are the new unknowns to be determined. This task can be accomplished by using the separation of variables, described in Appendix A, namely by separating the dependence on z and on t. Thus, we can express $\tilde{W}$ and $\tilde{\Theta}$ as linear combinations of separated solutions written as

$$\tilde{W} = f(z)\, \mathrm{e}^{\lambda t} \ , \qquad \tilde{\Theta} = h(z)\, \mathrm{e}^{\lambda t} \ , \tag{7.31}$$

where $\lambda = \eta - \mathrm{i}\, \omega \in \mathbb{C}$ is a complex parameter, $\omega \in \mathbb{R}$ is the angular frequency, and $\eta \in \mathbb{R}$ is the growth rate. As usual, for a given k, $\eta > 0$ means convective instability, $\eta < 0$ means stability, while $\eta = 0$ indicates the threshold condition of neutral, or marginal, stability.

By evaluating the two-dimensional Fourier transform of Eq. (7.29), and by employing Eq. (7.31), the stability problem is formulated as

$$\left(\frac{1}{Pr}\, \lambda - \frac{\mathrm{d}^2}{\mathrm{d}\, z^2} + k^2\right) \left(\frac{\mathrm{d}^2}{\mathrm{d}\, z^2} - k^2\right) f + Ra\, k^2\, h = 0 \ , \tag{7.32}$$

$$\left(\lambda - \frac{\mathrm{d}^2}{\mathrm{d}\, z^2} + k^2\right) h - f = 0 \ , \tag{7.33}$$

$$z = 0, 1 : \qquad f = 0 \ , \quad \frac{\mathrm{d}^2 f}{\mathrm{d}\, z^2} = 0 \ , \quad h = 0 \ . \tag{7.34}$$

We can combine the two Eqs. (7.32) and (7.33) into a single (sixth-order) ordinary differential equation in the sole unknown function h,

$$\left(\frac{1}{Pr}\,\lambda - \frac{\mathrm{d}^2}{\mathrm{d}\,z^2} + k^2\right)\left(\frac{\mathrm{d}^2}{\mathrm{d}\,z^2} - k^2\right)\left(\lambda - \frac{\mathrm{d}^2}{\mathrm{d}\,z^2} + k^2\right) h + Ra\,k^2\,h = 0\,, \quad (7.35)$$

with the boundary conditions

$$z = 0, 1: \qquad h = 0\,, \quad \frac{\mathrm{d}^2 h}{\mathrm{d}\,z^2} = 0\,, \quad \frac{\mathrm{d}^4 h}{\mathrm{d}\,z^4} = 0\,. \quad (7.36)$$

We mention that the boundary conditions $\mathrm{d}^2h/\mathrm{d}z^2 = 0$ are obtained from Eq. (7.33) by taking the limits $z \to 0$ and $z \to 1$ and by using Eq. (7.34). Likewise, the boundary conditions $\mathrm{d}^4h/\mathrm{d}z^4 = 0$ are obtained from Eq. (7.33) derived twice with respect to z.

A solution of the differential problem, expressed by Eqs. (7.35) and (7.36), is easily found, namely

$$h(z) = \sin(n\,\pi\,z)\,, \quad n = 1, 2, 3, \ldots\,, \quad (7.37)$$

provided that

$$\left(\frac{1}{Pr}\,\lambda + n^2\,\pi^2 + k^2\right)\left(n^2\,\pi^2 + k^2\right)\left(\lambda + n^2\,\pi^2 + k^2\right) - Ra\,k^2 = 0\,, \quad (7.38)$$

The additional algebraic equation (7.38) is the so-called *dispersion relation* of stability. Since $\lambda = \eta - \mathrm{i}\,\omega$, the imaginary part of the dispersion relation vanishes if and only if

$$\omega\left(n^2\pi^2 + k^2\right)\left[2\,\eta + (Pr + 1)\left(n^2\pi^2 + k^2\right)\right] = 0\,. \quad (7.39)$$

For convectively unstable or neutrally stable modes, i.e. for $\eta \geq 0$, this equation can be satisfied only if $\omega = 0$, meaning that only zero-frequency normal modes are allowed. This result is well known in the literature as the *principle of exchange of stabilities* [12]. As it has been pointed out by Pellew and Southwell [12], the physical meaning of this principle is that "while oscillatory motions are not excluded by this investigation, they are permitted only in circumstances making for stability, i.e. in which they decay". In fact, also stable modes cannot be oscillatory as it will be shown in Sect. 7.5.1.

7.4.3 Neutral Stability

Since $\omega = 0$ when $\eta \geq 0$, for convectively unstable or neutrally stable states, the real part of the dispersion relation (7.38) vanishes if

$$Ra = \frac{\left(n^2\pi^2 + k^2\right)\left(\eta + n^2\pi^2 + k^2\right)\left(Pr^{-1}\eta + n^2\pi^2 + k^2\right)}{k^2} \,. \tag{7.40}$$

Convective instability means that there exists a positive integer, $n = 1, 2, 3, \ldots$), such that the growth rate is positive, namely $\eta > 0$. On gradually increasing Ra starting from zero, one encounters instability first with $n = 1$, so that one has

$$Ra = \frac{\left(\pi^2 + k^2\right)^3}{k^2} \,, \quad \text{(neutral stability)},$$

$$Ra > \frac{\left(\pi^2 + k^2\right)^3}{k^2} \,, \quad \text{(convective instability)},$$

and thus, necessarily,

$$Ra < \frac{\left(\pi^2 + k^2\right)^3}{k^2} \,,$$

implies stability. Figure 7.4 displays the neutral stability curve, namely the plot of function

$$Ra(k) = \frac{\left(\pi^2 + k^2\right)^3}{k^2} \,. \tag{7.41}$$

Its minimum defines the onset of convection cells,

$$k_\mathrm{c} = \frac{\pi}{\sqrt{2}} \approx 2.22144 \,, \qquad Ra_\mathrm{c} = \frac{27\pi^4}{4} \approx 657.511 \,. \tag{7.42}$$

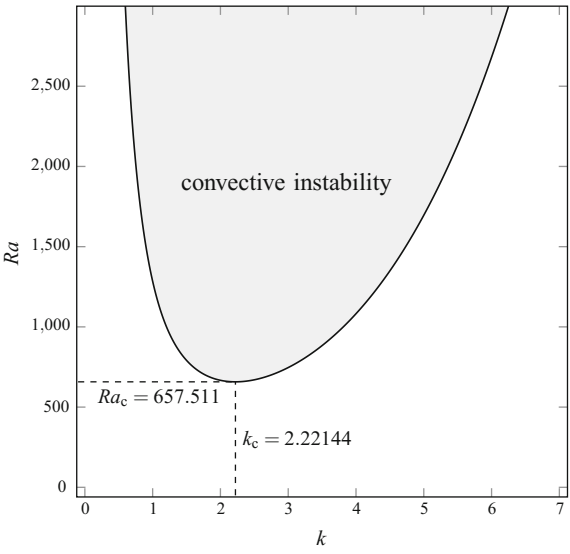

Fig. 7.4 Neutral stability curve for the Rayleigh–Bénard problem with stress-free and impermeable boundary conditions at $z = 0, 1$

7.5 Rayleigh–Bénard Problem with Other Types of Boundary Conditions

In cases where the boundary surfaces $z = 0, 1$ are not both stress-free, the convective stability analysis partly changes. For instance, when both surfaces $z = 0, 1$ are rigid impermeable walls, no-slip boundary conditions for the velocity have to be imposed at $z = 0, 1$. Thus, Eq. (7.29) changes to the form

$$\left(\frac{1}{Pr}\,\frac{\partial}{\partial t} - \nabla^2\right)\nabla^2 W = Ra\,\nabla_2^2\Theta\ ,$$

$$\frac{\partial\Theta}{\partial t} - W = \nabla^2\Theta\ ,$$

$$z = 0,\ 1\ :\qquad W = 0 = \Theta\ ,\quad \frac{\partial W}{\partial z} = 0\ . \tag{7.43}$$

In the intermediate case, where $z = 0$ is subject to no-slip conditions and $z = 1$ is stress-free, we have

$$\left(\frac{1}{Pr}\,\frac{\partial}{\partial t} - \nabla^2\right)\nabla^2 W = Ra\,\nabla_2^2\Theta\ ,$$

$$\frac{\partial\Theta}{\partial t} - W = \nabla^2\Theta\ ,$$

$$z = 0\ :\qquad W = 0 = \Theta\ ,\quad \frac{\partial W}{\partial z} = 0\ ,$$

$$z = 1\ :\qquad W = 0 = \Theta\ ,\quad \frac{\partial^2 W}{\partial z^2} = 0\ . \tag{7.44}$$

In other terms, the partial differential equations for the perturbations are unaffected by changed boundary conditions, the only change being the boundary conditions for W and Θ. The reason is simple. The governing partial differential equations for the perturbations just depend on the basic solution that satisfies both stress-free boundary conditions and no-slip boundary conditions at $z = 0, 1$. In all these cases, the basic solution is given by Eq. (7.13). Equations (7.43) and (7.44) show that, when a boundary surface turns from stress-free to no-slip, one of the boundary conditions turns from $\partial^2 W/\partial z^2 = 0$ to $\partial W/\partial z = 0$. The reason is that the condition of vanishing second derivative $\partial^2 W/\partial z^2$ is a consequence of the vanishing tangential components of the viscous stress tensor. If a boundary, say $z = 1$, has impermeability and no-slip conditions, then one may write

$$z = 1\ :\qquad U = 0\ ,\quad V = 0\ ,\quad W = 0\ .$$

By employing such conditions, as well as the local mass balance equation (7.20) in the limit $z \to 1$, one readily reaches the conclusion

$$z = 1 \; : \qquad W = 0 \; , \quad \frac{\partial W}{\partial z} = 0 \; .$$

The method described in Sect. 7.4.2 can still be applied, together with the separation of variables expressed by Eq. (7.31). Hence, if no-slip boundary conditions for the velocity are imposed at both $z = 0$ and $z = 1$, Eqs. (7.32)–(7.34) are replaced by

$$\left(\frac{1}{Pr} \lambda - \frac{\mathrm{d}^2}{\mathrm{d}\, z^2} + k^2 \right) \left(\frac{\mathrm{d}^2}{\mathrm{d}\, z^2} - k^2 \right) f + Ra\, k^2\, h = 0 \; , \tag{7.45}$$

$$\left(\lambda - \frac{\mathrm{d}^2}{\mathrm{d}\, z^2} + k^2 \right) h - f = 0 \; , \tag{7.46}$$

$$z = 0, 1 \; : \qquad f = 0 \; , \quad \frac{\mathrm{d}\, f}{\mathrm{d}\, z} = 0 \; , \quad h = 0 \; . \tag{7.47}$$

In the case of mixed no-slip and stress-free boundary conditions at $z = 0$ and $z = 1$, respectively, one has

$$\begin{aligned} z = 0 \; : \qquad & f = 0 \; , \quad \frac{\mathrm{d}\, f}{\mathrm{d}\, z} = 0 \; , \quad h = 0 \; , \\ z = 1 \; : \qquad & f = 0 \; , \quad \frac{\mathrm{d}^2 f}{\mathrm{d}\, z^2} = 0 \; , \quad h = 0 \; , \end{aligned} \tag{7.48}$$

instead of Eq. (7.47).

One may well say that, although possible, an analytical solution for either the differential problems, given by Eqs. (7.45)–(7.47) and by Eqs. (7.45), (7.46) and (7.48), is not the most convenient approach. An easier, reliable and accurate procedure to get the solution of either these differential problems is the use of a numerical solver for differential eigenvalue problems. We refer the reader to Chap. 10 for a discussion of the numerical method, and for the implementation of the code needed to develop this numerical solver. Figures 7.5 and 7.6 display, respectively, the neutral stability curves for the Rayleigh–Bénard problem with rigid and impermeable boundaries, i.e. for the conditions given by Eq. (7.47), and for the mixed case where the lower boundary is rigid while the upper boundary is stress-free, i.e. for the conditions given by Eq. (7.48). The shape of these neutral stability curves is not much different from that of the curve displayed in Fig. 7.4. We will see that this shape is surprisingly common for the diverse variants of the Rayleigh–Bénard problem. The most important difference between Figs. 7.4, 7.5 and 7.6 is in the position of the minimum, namely in the values of k_c and Ra_c. With the boundary conditions expressed by Eq. (7.47), we obtain

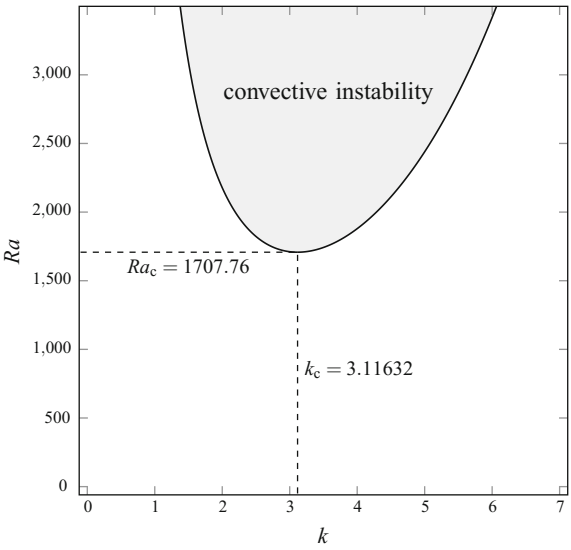

Fig. 7.5 Neutral stability curve for the Rayleigh–Bénard problem with rigid and impermeable boundary conditions at $z = 0, 1$

$$k_c = 3.11632 \,, \qquad Ra_c = 1707.76 \,, \tag{7.49}$$

while in the mixed case given by Eq. (7.48), we obtain

$$k_c = 2.68232 \,, \qquad Ra_c = 1100.65 \,. \tag{7.50}$$

These results allow one to conclude that the presence of stress-free boundaries tends to favour the onset of convective instability. In fact, the case where both the impermeable boundaries are rigid is the one where the instability requires the highest Rayleigh number. The mixed case is intermediate, while the case with two stress-free boundaries is that where the instability emerges at the lowest Rayleigh number. One can rephrase this conclusion by saying that the no-slip condition is a stabilising mechanism for the thermal instability.

7.5.1 The Principle of Exchange of Stabilities

By employing integration by parts over $z \in [0, 1]$, we can write

$$\int_0^1 \bar{f}\, \frac{\mathrm{d}^4 f}{\mathrm{d}\, z^4}\, \mathrm{d}z = -\int_0^1 \frac{\mathrm{d}\, \bar{f}}{\mathrm{d}\, z}\, \frac{\mathrm{d}^3 f}{\mathrm{d}\, z^3}\, \mathrm{d}z = \int_0^1 \left| \frac{\mathrm{d}^2 f}{\mathrm{d}\, z^2} \right|^2 \mathrm{d}z \,, \tag{7.51}$$

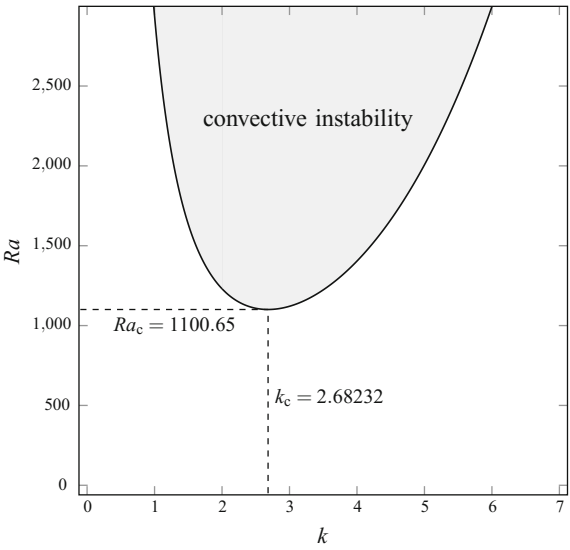

Fig. 7.6 Neutral stability curve for the Rayleigh–Bénard problem with rigid and impermeable boundary conditions at $z = 0$, and with stress-free and impermeable boundary conditions at $z = 1$

$$\int_0^1 \bar{f}\,\frac{\mathrm{d}^2 f}{\mathrm{d}\,z^2}\,\mathrm{d}z = -\int_0^1 \left|\frac{\mathrm{d}\,f}{\mathrm{d}\,z}\right|^2 \mathrm{d}z\,, \tag{7.52}$$

$$\int_0^1 h\,\frac{\mathrm{d}^2 \bar{h}}{\mathrm{d}\,z^2}\,\mathrm{d}z = -\int_0^1 \left|\frac{\mathrm{d}\,h}{\mathrm{d}\,z}\right|^2 \mathrm{d}z\,, \tag{7.53}$$

where the primes denote derivatives with respect to z, the overline denotes complex conjugation, and either the boundary conditions given by Eq. (7.47) or those expressed by Eq. (7.48) are employed.

We stress that the chain of integrations by parts in Eqs. (7.51)–(7.53) holds both with the set of boundary conditions (7.47) and with the set of boundary conditions (7.48). We finally mention that Eqs. (7.51)–(7.53) are valid also in the case where both boundaries are rigid and stress-free, described by Eq. (7.34).

Let us consider Eqs. (7.45) and (7.46). We multiply Eq. (7.45) by $\bar{f}$ and integrate over $z \in [0, 1]$. Then, by employing Eqs. (7.52) and (7.53), we obtain

$$\int_0^1 \left|\frac{\mathrm{d}^2 f}{\mathrm{d}\,z^2}\right|^2 \mathrm{d}z + \left(2\,k^2 + \frac{\lambda}{Pr}\right)\int_0^1 \left|\frac{\mathrm{d}\,f}{\mathrm{d}\,z}\right|^2 \mathrm{d}z + \left(k^2 + \frac{\lambda}{Pr}\right)k^2 \int_0^1 |f|^2\,\mathrm{d}z$$

$$- \; Ra\,k^2 \int_0^1 \bar{f}\,h\,\mathrm{d}z = 0\,. \tag{7.54}$$

Let us write the complex conjugate of Eq. (7.46),

$$\left(\bar{\lambda} - \frac{\mathrm{d}^2}{\mathrm{d}\,z^2} + k^2\right)\bar{h} - \bar{f} = 0\,. \tag{7.55}$$

We multiply Eq. (7.55) by h and integrate over $z \in [0, 1]$. By using Eqs. (7.52) and (7.53), we obtain

$$\int_0^1 \left|\frac{\mathrm{d}\,h}{\mathrm{d}\,z}\right|^2 \mathrm{d}z + \left(\bar{\lambda} + k^2\right)\int_0^1 |h|^2\,\mathrm{d}z - \int_0^1 \bar{f}\,h\,\mathrm{d}z = 0\,. \tag{7.56}$$

We can combine Eqs. (7.54) and (7.56) to obtain

$$\int_0^1 \left|\frac{\mathrm{d}^2 f}{\mathrm{d}\,z^2}\right|^2 \mathrm{d}z + \left(2\,k^2 + \frac{\lambda}{Pr}\right)\int_0^1 \left|\frac{\mathrm{d}\,f}{\mathrm{d}\,z}\right|^2 \mathrm{d}z + \left(k^2 + \frac{\lambda}{Pr}\right)k^2 \int_0^1 |f|^2\,\mathrm{d}z$$

$$- \; Ra\,k^2\left[\int_0^1 \left|\frac{\mathrm{d}\,h}{\mathrm{d}\,z}\right|^2 \mathrm{d}z + \left(\bar{\lambda} + k^2\right)\int_0^1 |h|^2\,\mathrm{d}z\right] = 0\,. \tag{7.57}$$

We recall that $\lambda = \eta - \mathrm{i}\,\omega$. Thus, the imaginary part of Eq. (7.57) is given by

$$\omega\left(\frac{1}{Pr}\int_0^1 \left|\frac{\mathrm{d}\,f}{\mathrm{d}\,z}\right|^2 \mathrm{d}z + \frac{k^2}{Pr}\int_0^1 |f|^2\,\mathrm{d}z + Ra\,k^2\int_0^1 |h|^2\,\mathrm{d}z\right) = 0\,. \tag{7.58}$$

The expression in round brackets on the left-hand side of Eq. (7.58) is positive, unless the perturbation is identically zero, i.e. $f = 0 = h$. Therefore, we can conclude that

$$\omega = 0\,. \tag{7.59}$$

so that the principle of exchange of stabilities holds. If we consider the real part of Eq. (7.57), we obtain

$$\int_0^1 \left|\frac{\mathrm{d}^2 f}{\mathrm{d}\,z^2}\right|^2 \mathrm{d}z + 2\,k^2\int_0^1 \left|\frac{\mathrm{d}\,f}{\mathrm{d}\,z}\right|^2 \mathrm{d}z + k^4\int_0^1 |f|^2\,\mathrm{d}z$$

$$- \; Ra\,k^2\left[\int_0^1 \left|\frac{\mathrm{d}\,h}{\mathrm{d}\,z}\right|^2 \mathrm{d}z + k^2\int_0^1 |h|^2\,\mathrm{d}z\right]$$

$$+\ \eta\left(\frac{1}{Pr}\int_0^1\left|\frac{\mathrm{d}\,f}{\mathrm{d}\,z}\right|^2\mathrm{d}z+\frac{k^2}{Pr}\int_0^1|f|^2\,\mathrm{d}z-Ra\,k^2\int_0^1|h|^2\,\mathrm{d}z\right)=0\,. \qquad (7.60)$$

Equation (7.60) leads to some interesting conclusions. At neutral stability, $\eta = 0$, we infer that Ra is positive for every k and Pr. Moreover, either the neutral stability curve $Ra(k)$ displays a singularity when $k \to 0$ or $\mathrm{d}^2 f/\mathrm{d}z^2$ is identically vanishing in this limit. Indeed, a singular behaviour of the neutral stability curve is implied by Eq. (7.41), for the case where both boundaries are rigid and stress-free.

Another feature which can be inferred from Eq. (7.60) is that, in the limit $Ra \to 0$, the growth rate η cannot be positive. An obvious feature on physical grounds as $Ra \to 0$ is achieved when the temperature difference between the bounding surfaces tends to zero. Under such conditions, the buoyancy force cannot activate and sustain any natural convection flow.

An important aspect of the principle of exchange of stability formulated by the integral method just described is that Eq. (7.59) holds independently of η being negative, zero or positive. This is a slight, but interesting, feature with respect to what we were able to infer from Eq. (7.39) for the case where both boundaries are rigid and stress-free.

7.6 The Horton–Rogers–Lapwood Problem

A stability analysis of the rest state not referring to a clear fluid layer, but to a fluid-saturated porous medium was performed by Horton and Rogers Jr [5], and by Lapwood [7]. The Horton–Rogers–Lapwood (HRL) problem is the porous medium analogue of the Rayleigh–Bénard problem for a clear fluid. The analysis of the HRL problem was originally performed by assuming the validity of Darcy's law and by employing linearised governing equations. During the years, several extensions of the HRL problem have been studied including treatment of Darcy–Forchheimer's model, of Brinkman's model and adopting a weakly nonlinear stability analysis. For a review of these results, one can refer to Rees [14] and Tyvand [16].

7.6.1 Formulation of the Problem

By analogy with the Rayleigh–Bénard problem, let us consider a horizontal fluid-saturated porous layer having thickness L, bounded by two impermeable planes. The lower boundary plane is maintained at temperature T_1, while the upper boundary plane has a uniform temperature $T_2 < T_1$.

For the mathematical formulation of the problem, we rely on the framework discussed in Sect. 6.4. By assuming the validity of Darcy's law, of the Oberbeck–Boussinesq approximation, the governing equations of the saturated porous medium,

without any volumetric heat source, $q_g = 0$, can be written as

$$\frac{\partial u_j}{\partial x_j} = 0 \,,$$

$$\frac{\nu}{K}\, u_i = -\beta\,(T - T_0)\, g_i - \frac{1}{\rho_0}\,\frac{\partial P}{\partial x_i} \,,$$

$$\sigma\,\frac{\partial T}{\partial t} + u_j\,\frac{\partial T}{\partial x_j} = \alpha\,\nabla^2 T + \frac{\nu}{K\,c}\,u_j u_j \,, \tag{7.61}$$

where $\alpha = \varkappa_{\text{eff}}/(\rho_0\, c)$ and $\nu = \mu/\rho_0$. If we want to test the stability of a basic solution, (u_{bi}, P_b, T_b), we proceed as follows. We perturb the basic solution, i.e., we express the fields (u_i, P, T) as

$$u_i = u_{bi} + \varepsilon\, U_i, \qquad P = P_b + \varepsilon\, \Pi, \qquad T = T_b + \varepsilon\, \Theta,$$

where ε is a positive dimensionless quantity, the perturbation parameter. The terms $\varepsilon\, U_i$, $\varepsilon\, \Pi$ and $\varepsilon\, \Theta$ express the perturbation of the basic solution.

Thus, we obtain the perturbation equations,

$$\varepsilon\,\frac{\partial U_j}{\partial x_j} = 0 \,,$$

$$\frac{\varepsilon\,\nu}{K}\, U_i = -\varepsilon\,\beta\,\Theta\, g_i - \frac{\varepsilon}{\rho_0}\,\frac{\partial \Pi}{\partial x_i} \,,$$

$$\varepsilon\,\sigma\,\frac{\partial \Theta}{\partial t} + \varepsilon\, u_{bj}\,\frac{\partial \Theta}{\partial x_j} + \varepsilon\, U_j\,\frac{\partial T_b}{\partial x_j} + \varepsilon^2\, U_j\,\frac{\partial \Theta}{\partial x_j} = \varepsilon\,\alpha\,\nabla^2\Theta$$

$$+\ \frac{2\,\varepsilon\,\nu}{K\,c}\, u_{bj}\, U_j + \frac{\varepsilon^2 \nu}{K\,c}\, U_j\, U_j \,. \tag{7.62}$$

The perturbation equations (7.62) express the dynamics of the perturbation fields (U_i, Π, Θ). We note that these equations contain a coupling with the basic solution (u_{bi}, P_b, T_b) only as an effect of the nonlinear terms

$$u_j\,\frac{\partial T}{\partial x_j} \,, \qquad \frac{\nu}{K\,c}\, u_j u_j \,.$$

As in the case of a clear fluid, we have two alternatives: we may assume that the perturbations are small, or we may investigate perturbations of arbitrarily large amplitude. In the first case, we perform a linear stability analysis. In the second case, we carry out a nonlinear stability analysis.

The first option is the simplest one, and we will restrict all the forthcoming discussion to this case. Assuming small perturbations means requiring $\varepsilon \ll 1$, so that we can neglect the terms $O(\varepsilon^2)$ with respect to the terms $O(\varepsilon)$ in the perturbation equations.

Therefore, we can simplify ε from the perturbation equations (7.62) and rewrite them as

$$\frac{\partial U_j}{\partial x_j} = 0 \,,$$

$$\frac{\nu}{K}\, U_i = -\beta\, \Theta\, g_i - \frac{1}{\rho_0}\, \frac{\partial \Pi}{\partial x_i} \,,$$

$$\sigma\, \frac{\partial \Theta}{\partial t} + u_{\mathrm{b}j}\, \frac{\partial \Theta}{\partial x_j} + U_j\, \frac{\partial T_{\mathrm{b}}}{\partial x_j} = \alpha\, \nabla^2 \Theta + \frac{2\,\nu}{K\,c}\, u_{\mathrm{b}j}\, U_j \,. \tag{7.63}$$

One may solve these equations and check what the time evolution of the perturbation is like: if it leads to an increasingly large departure from the basic solution, or if it leads to an asymptotic recovery of the basic solution. In the first case, we have a response of instability for the basic flow, while in the second case, we have an outcome of stability. The critical condition for the onset of convection in the layer is obtained by a linear stability analysis carried out starting from the basic state,

$$u_{\mathrm{b}i} = 0 \,, \qquad T_{\mathrm{b}} = T_1 - (T_1 - T_2)\, \frac{z}{L} \,. \tag{7.64}$$

The nature of the basic state leads to a dramatic simplification of the linearised perturbation equations. In fact, Eq. (7.63) simplify to

$$\frac{\partial U_j}{\partial x_j} = 0 \,,$$

$$\frac{\nu}{K}\, U_i = -\beta\, \Theta\, g_i - \frac{1}{\rho_0}\, \frac{\partial \Pi}{\partial x_i} \,,$$

$$\sigma\, \frac{\partial \Theta}{\partial t} - W\, \frac{T_1 - T_2}{L} = \alpha\, \nabla^2 \Theta \,. \tag{7.65}$$

The perturbation equations can be further simplified by allowing an appropriate scaling of the physical quantities, in order to carry out the study through a dimensionless formulation. Hence, we define the dimensionless quantities by means of the scalings,

$$\frac{U_i}{\alpha/L} \to U_i \,, \quad \frac{\Theta}{T_1 - T_2} \to \Theta \,,$$

$$\frac{\Pi}{\rho_0 \nu \alpha / K} \to \Pi \,, \quad \frac{x_i}{L} \to x_i \,, \quad \frac{t}{\sigma\, L^2/\alpha} \to t \,, \tag{7.66}$$

so that the dimensionless perturbation equations can be written as

$$\frac{\partial U_j}{\partial x_j} = 0 \,,$$

$$U_i = R\,\Theta\,\delta_{i3} - \frac{\partial \Pi}{\partial x_i} \,,$$

$$\frac{\partial \Theta}{\partial t} - W = \nabla^2 \Theta \,, \tag{7.67}$$

with the boundary conditions,

$$z = 0, 1: \qquad W = 0 = \Theta \,. \tag{7.68}$$

In particular, the conditions $W = 0$ express the impermeability of the boundaries. The parameter R defines the *Darcy–Rayleigh number*,

$$R = \frac{g\beta(T_1 - T_2)KL}{\nu\alpha} \,. \tag{7.69}$$

A comparison with Eq. (7.24) reveals that the Darcy–Rayleigh number differs from the Rayleigh number of a clear fluid mainly due to the factor $K\,L$ instead of L^3.

The term $-\partial\Pi/\partial x_i$ can be encompassed by taking the curl of the momentum balance equation, which yields

$$\frac{\partial W}{\partial x} - \frac{\partial U}{\partial z} = R\,\frac{\partial \Theta}{\partial x} \,, \tag{7.70}$$

$$\frac{\partial W}{\partial y} - \frac{\partial V}{\partial z} = R\,\frac{\partial \Theta}{\partial y} \,. \tag{7.71}$$

We derive Eq. (7.70) with respect to x and Eq. (7.71) with respect to y. Then, we sum the two resulting equations, so that we obtain

$$\nabla^2 W = R\,\nabla_2^2 \Theta + \frac{\partial}{\partial z}\left(\frac{\partial U_j}{\partial x_j}\right) \,. \tag{7.72}$$

By taking into account the local mass balance equation, $\partial U_j/\partial x_j = 0$, we can extract a set of two partial differential equations in the unknowns (W, Θ), describing the stability problem,

$$\nabla^2 W = R\,\nabla_2^2 \Theta \,,$$

$$\frac{\partial \Theta}{\partial t} - W = \nabla^2 \Theta \,, \tag{7.73}$$

with the boundary conditions

$$z = 0, 1: \qquad W = 0 = \Theta \,. \tag{7.74}$$

7.6.2 Normal Modes

As in the Rayleigh–Bénard problem, the governing equations for the perturbations can be solved by employing the Fourier transform method. With the definitions formulated in Eqs. (7.30) and (7.31), we can express the Fourier transformed stability problem in the form

$$\left(\frac{\mathrm{d}^2}{\mathrm{d}\,z^2} - k^2\right) f + R\,k^2\,h = 0 \,,$$

$$\left(\lambda - \frac{\mathrm{d}^2}{\mathrm{d}\,z^2} + k^2\right) h - f = 0 \,, \tag{7.75}$$

with the boundary conditions

$$z = 0, 1: \qquad f = 0 = h \,. \tag{7.76}$$

We can combine the two equations into a single (fourth-order) ordinary differential equation,

$$\left(\frac{\mathrm{d}^2}{\mathrm{d}\,z^2} - k^2\right)\left(\lambda - \frac{\mathrm{d}^2}{\mathrm{d}\,z^2} + k^2\right) h + R\,k^2\,h = 0 \,,$$

$$z = 0, 1: \qquad h = 0 \,, \quad \frac{\mathrm{d}^2 h}{\mathrm{d}\,z^2} = 0 \,. \tag{7.77}$$

A solution of this differential problem is easily found, namely

$$h(z) = \sin(n\,\pi\,z), \quad n = 1, 2, 3, \ \ldots \,, \tag{7.78}$$

provided that

$$(n^2\pi^2 + k^2)\left(\lambda + n^2\pi^2 + k^2\right) - R\,k^2 = 0 \,. \tag{7.79}$$

This additional algebraic equation is the dispersion relation of stability. We recall that the complex parameter λ can be expressed in terms of its real part η and its imaginary part $-\,\omega$, that is $\lambda = \eta - \mathrm{i}\,\omega$. Thus, the imaginary part of the right-hand side of Eq. (7.79) vanishes if and only if

$$\omega\left(n^2\pi^2 + k^2\right) = 0 \,. \tag{7.80}$$

This equation can be satisfied if and only if $\omega = 0$, meaning that only normal modes with zero frequency are allowed (principle of exchange of stabilities).

7.6.3 Neutral Stability

Since $\omega = 0$, the real part of the dispersion relation given by Eq. (7.79) yields

$$R = \frac{(n^2\pi^2 + k^2)\left(\eta + n^2\pi^2 + k^2\right)}{k^2} \,. \tag{7.81}$$

Stability means that, for all $n = 1, 2, 3, \ldots$), one has a negative growth rate, $\eta < 0$. In other words, one may conclude that

$$R < \frac{\left(\pi^2 + k^2\right)^2}{k^2} \,,$$

implies stability, while

$$R = \frac{\left(\pi^2 + k^2\right)^2}{k^2} \,,$$

yields neutral stability, and

$$R > \frac{\left(\pi^2 + k^2\right)^2}{k^2} \,,$$

defines convective instability. The neutral stability curve, namely the plot of function

$$R(k) = \frac{\left(\pi^2 + k^2\right)^2}{k^2} \tag{7.82}$$

is displayed in Fig. 7.7. The minimum of this curve yields the conditions for the onset of convection cells in the porous layer,

$$k_c = \pi \approx 3.14159 \,, \qquad R_c = 4\,\pi^2 \approx 39.4784 \,. \tag{7.83}$$

It has been shown that the critical value of the Rayleigh number for the onset of convective cells in Rayleigh–Bénard convection is given by either Eq. (7.42), or Eq. (7.49), or Eq. (7.50), depending on the prescribed velocity boundary conditions. If one compares these results with Eq. (7.83), the first-glance conclusion is that it is easier to have convective instabilities in a Darcy porous medium than in a clear fluid. However, this is false as the Rayleigh number Ra is proportional to L^3, while the Darcy–Rayleigh number R is proportional to KL. Since the permeability K is usually very small [9], it is much more common having a clear fluid layer with $Ra \sim 10^3$ than a fluid-saturated porous layer with $R \sim 10$.

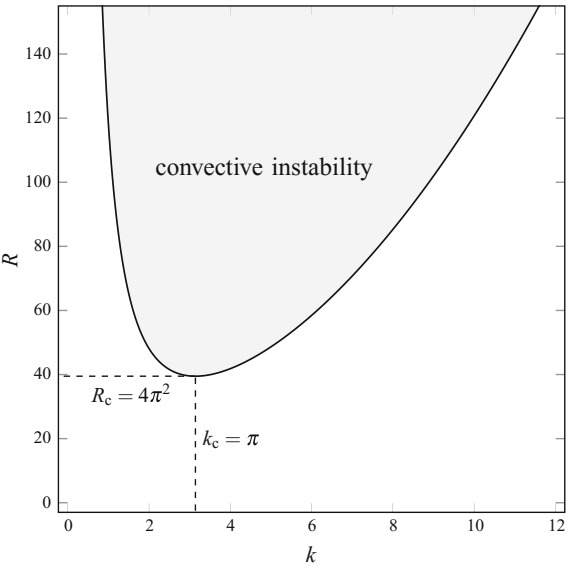

Fig. 7.7 Neutral stability curve for the Horton–Rogers–Lapwood problem with impermeable and isothermal boundary conditions at $z = 0, 1$

7.6.4 Form-Drag Effect

If one assumes Darcy–Forchheimer's model for local momentum balance, instead of Darcy's model, the set of governing equations is changed to

$$\frac{\partial u_j}{\partial x_j} = 0 \,,$$

$$\frac{\nu}{K}\left(1 + \frac{F\sqrt{K}}{\nu}\sqrt{u_\ell u_\ell}\right) u_i = -\beta\,(T - T_0)\,g_i - \frac{1}{\rho_0}\,\frac{\partial P}{\partial x_i} \,,$$

$$\sigma\,\frac{\partial T}{\partial t} + u_j\,\frac{\partial T}{\partial x_j} = \alpha\,\nabla^2 T + \frac{\nu}{K\,c}\left(1 + \frac{F\sqrt{K}}{\nu}\sqrt{u_\ell u_\ell}\right) u_j u_j \,. \tag{7.84}$$

The terms proportional to the form-drag coefficient F do not affect the linearised perturbation equations when the basic state is a rest state, namely when $u_{\mathrm{b}i} = 0$. In fact, the terms proportional to F yield contributions of order ε^2 or ε^3 when the rest state is perturbed. In this case, both the basic solution

$$u_{\mathrm{b}i} = 0 \,, \qquad T_{\mathrm{b}} = T_1 - (T_1 - T_2)\,\frac{z}{L} \,. \tag{7.85}$$

and the linearised perturbation equations

$$\frac{\partial U_j}{\partial x_j} = 0 \,,$$

$$\frac{\nu}{K}\, U_i = -\beta\, \Theta\, g_i - \frac{1}{\rho_0}\, \frac{\partial \Pi}{\partial x_i} \,,$$

$$\sigma\, \frac{\partial \Theta}{\partial t} - W\, \frac{T_1 - T_2}{L} = \alpha\, \nabla^2 \Theta \,. \tag{7.86}$$

are exactly the same as those obtained by employing Darcy's law. Thus, the condition for the onset of convection cells is not affected by the form-drag effect.

7.6.5 Brinkman's Model

Changing the local momentum balance equation from Darcy's model to Brinkman's model and, thus, allowing for a Laplacian term contribution, as well as for no-slip conditions at the boundaries, sensibly affects the linear stability analysis.

A new parameter appears in the dimensionless perturbation equations, the *Darcy number*, namely

$$Da = \frac{\mu_{\text{eff}}\, K}{\mu\, L^2} \,, \tag{7.87}$$

where μ_{eff} is the effective viscosity. When $Da \to 0$, the results obtained by employing Darcy's law are recovered. On the other hand, we recover the results obtained for a Navier–Stokes fluid when $Da \to \infty$. Darcy's limit is $Da \to 0$ since the Darcy's law behaviour happens when the permeability is much smaller than the macroscopic scale of the porous medium, namely $K \ll L^2$. By the same reasoning, we can state that the clear fluid limit is approached when the porous medium has an extremely large permeability, so that $K \gg L^2$. In describing the transition from Darcy's flow to clear fluid flow, the Darcy number Da plays a key role. In general, the critical values $(k_{\text{c}}, R_{\text{c}})$ depend on Da.

In the case of Brinkman's model, the local mass, momentum and energy balance equations admit the same basic solution as with the other models, namely

$$u_{\text{b}i} = 0 \,, \qquad T_{\text{b}} = T_1 - (T_1 - T_2)\, \frac{z}{L} \,. \tag{7.88}$$

Therefore, the linearised local balance equations for the perturbation fields can be written as

$$\frac{\partial U_j}{\partial x_j} = 0 \,,$$

$$\frac{\nu}{K}\, U_i - \nu_{\text{eff}}\, \nabla^2 U_i = -\beta\, \Theta\, g_i - \frac{1}{\rho_0}\, \frac{\partial \Pi}{\partial x_i} \,,$$

$$\sigma \frac{\partial \Theta}{\partial t} - W \frac{T_1 - T_2}{L} = \alpha \nabla^2 \Theta \ , \tag{7.89}$$

where $\nu_{\text{eff}} = \mu_{\text{eff}}/\rho_0$. It is worth noting that the local energy balance equation for the perturbations given by the third Eq. (7.89), as expected, does not contain any contribution from the viscous dissipation effect, as such term is of higher order in the perturbation parameter ε and, hence, it is neglected in the linear approximation. This feature arises despite the uncertain form of the viscous dissipation function, either if it is given by Eq. (6.29) or by Eq. (6.30).

We introduce the same scaling defined by Eq. (7.66) in order to rewrite Eqs. (7.89) in a dimensionless form,

$$\frac{\partial U_j}{\partial x_j} = 0 \ ,$$

$$U_i - Da \nabla^2 U_i = R \Theta \delta_{i3} - \frac{\partial \Pi}{\partial x_i} \ ,$$

$$\frac{\partial \Theta}{\partial t} - W = \nabla^2 \Theta \ . \tag{7.90}$$

By evaluating the curl of the momentum balance equation, we obtain

$$\left(1 - Da \nabla^2\right) \left(\frac{\partial W}{\partial x} - \frac{\partial U}{\partial z} \right) = R \frac{\partial \Theta}{\partial x} \ , \tag{7.91}$$

$$\left(1 - Da \nabla^2\right) \left(\frac{\partial W}{\partial y} - \frac{\partial V}{\partial z} \right) = R \frac{\partial \Theta}{\partial y} \ . \tag{7.92}$$

We now derive Eq. (7.91) with respect to x, and Eq. (7.92) with respect to y. Then, we sum the two resulting equations, so that we obtain

$$\left(1 - Da \nabla^2\right) \left[\nabla^2 W - \frac{\partial}{\partial z} \left(\frac{\partial U_j}{\partial x_j} \right) \right] = R \nabla_2^2 \Theta \ , \tag{7.93}$$

and, by employing the local mass balance equation, $\partial U_j / \partial x_j = 0$, we can write

$$\left(1 - Da \nabla^2\right) \nabla^2 W = R \nabla_2^2 \Theta \ . \tag{7.94}$$

As for the Rayleigh–Bénard problem, the boundary conditions can be expressed so that both boundary walls are isothermal, impermeable and stress-free, namely

$$z = 0, 1 : \qquad W = 0 = \Theta \ , \quad \frac{\partial^2 W}{\partial z^2} = 0 \ . \tag{7.95}$$

Thus, the stability problem is formulated in terms of the scalar fields W and Θ.

$$\left(1 - Da\,\nabla^2\right)\nabla^2 W = R\,\nabla_2^2 \Theta \;,$$

$$\frac{\partial \Theta}{\partial t} - W = \nabla^2 \Theta \;,$$

$$z = 0, 1: \qquad W = 0 = \Theta \;, \quad \frac{\partial^2 W}{\partial z^2} = 0 \;. \tag{7.96}$$

The Fourier transform is employed to determine the solution of Eqs. (7.96). Accordingly, we use the definitions given by Eqs. (7.30) and (7.31), so that Eqs. (7.96) yield

$$\left(1 - Da\,\frac{\mathrm{d}^2}{\mathrm{d}\,z^2} + Da\,k^2\right)\left(\frac{\mathrm{d}^2}{\mathrm{d}\,z^2} - k^2\right) f + R\,k^2\,h = 0 \;,$$

$$\left(\lambda - \frac{\mathrm{d}^2}{\mathrm{d}\,z^2} + k^2\right) h - f = 0 \;,$$

$$z = 0, 1: \qquad f = 0 \;, \quad \frac{\mathrm{d}^2 f}{\mathrm{d}\,z^2} = 0 \;, \quad h = 0 \;. \tag{7.97}$$

The solution of Eqs. (7.97) can be sought in the form

$$h(z) = \sin(n\,\pi\,z) \;, \quad n = 1, 2, 3, \ldots \;, \tag{7.98}$$

provided that the dispersion relation,

$$\left(1 + Da\,n^2\,\pi^2 + Da\,k^2\right)\left(n^2\,\pi^2 + k^2\right)\left(\lambda + n^2\,\pi^2 + k^2\right) - R\,k^2 = 0 \;, \tag{7.99}$$

holds. Since $\lambda = \eta - \mathrm{i}\,\omega$, the imaginary part of Eq. (7.99) yields

$$\omega\left(1 + Da\,n^2\,\pi^2 + Da\,k^2\right)\left(n^2\,\pi^2 + k^2\right) = 0 \;. \tag{7.100}$$

This means that the principle of exchange of stabilities is valid or, equivalently, that only non-travelling normal modes are allowed, i.e. those with $\omega = 0$. The real part of Eq. (7.99) yields

$$R = \frac{\left(1 + Da\,n^2\,\pi^2 + Da\,k^2\right)\left(n^2\,\pi^2 + k^2\right)\left(\eta + n^2\,\pi^2 + k^2\right)}{k^2} \;. \tag{7.101}$$

Instability is activated first by the $n = 1$ normal modes. Then, neutral stability happens with

$$R = \frac{\left(1 + Da\,\pi^2 + Da\,k^2\right)\left(\pi^2 + k^2\right)^2}{k^2} \;, \tag{7.102}$$

convective instability ($\eta > 0$) occurs with

$$R > \frac{\left(1 + Da\,\pi^2 + Da\,k^2\right)\left(\pi^2 + k^2\right)^2}{k^2}\,, \tag{7.103}$$

and stability is confined in the parametric region where

$$R < \frac{\left(1 + Da\,\pi^2 + Da\,k^2\right)\left(\pi^2 + k^2\right)^2}{k^2}\,. \tag{7.104}$$

The neutral stability condition, Eq. (7.102), suggests that the neutrally stable value of R for a given k increases with Da. The limit $Da \to 0$ yields a perfect agreement between Eqs. (7.102) and (7.82). In fact, in the limit $Da \to 0$, Brinkman's law reduces to Darcy's law. In order to recover the case of a clear fluid, whose neutral stability condition is expressed through Eq. (7.41), we must take the limit $Da \to \infty$. This limit can be taken consistently by employing the Rayleigh number,

$$Ra = \frac{R}{Da} = \frac{g\beta(T_1 - T_2)L^3}{\nu_{\text{eff}}\,\alpha}\,, \tag{7.105}$$

instead of the Darcy–Rayleigh number. Here, Eqs. (7.69) and (7.87) have been employed. We note that there is a slight difference between the definitions of Ra given by Eqs. (7.1) and (7.105). The difference is in the denominator of Eq. (7.105) where ν_{eff} appears instead of the fluid kinematic viscosity ν. Such a discrepancy has no effect when the limit of a clear fluid is approached, i.e. the limit where the porosity tends to one, $\varphi \to 1$. In this limit, ν_{eff} and ν tend to coincide. This circumstance is evident by employing the definition $\nu_{\text{eff}} = \mu_{\text{eff}}/\rho_0$ and Eq. (6.10). The neutral stability condition given by Eq. (7.102) can be reformulated in terms of Ra as

$$Ra = \left(\frac{1}{Da} + \pi^2 + k^2\right)\frac{\left(\pi^2 + k^2\right)^2}{k^2}\,. \tag{7.106}$$

Evidently, Eq. (7.106) agrees with Eq. (7.41) when $Da \to \infty$. Plots of the neutral stability curves are displayed in Figs. 7.8 and 7.9, in the (k, R) plane or in the (k, Ra) plane, for different values of Da.

We have already mentioned that the critical values of k, R and Ra depend on the Darcy number. The evaluation of the minimum for the neutral stability functions $R(k)$ and $Ra(k)$ yields

$$k_{\text{c}} = \frac{1}{2}\sqrt{\frac{\sqrt{\left(Da\,\pi^2 + 1\right)\left(9\,Da\,\pi^2 + 1\right)} - Da\,\pi^2 - 1}{Da}}\,,$$

$$R_{\text{c}} = \frac{27\,Da^2\,\pi^4 + 18\,Da\,\pi^2 - 1}{8\,Da} + \frac{\left(9\,Da\,\pi^2 + 1\right)^{3/2}}{8\,Da}\sqrt{Da\,\pi^2 + 1}\,,$$

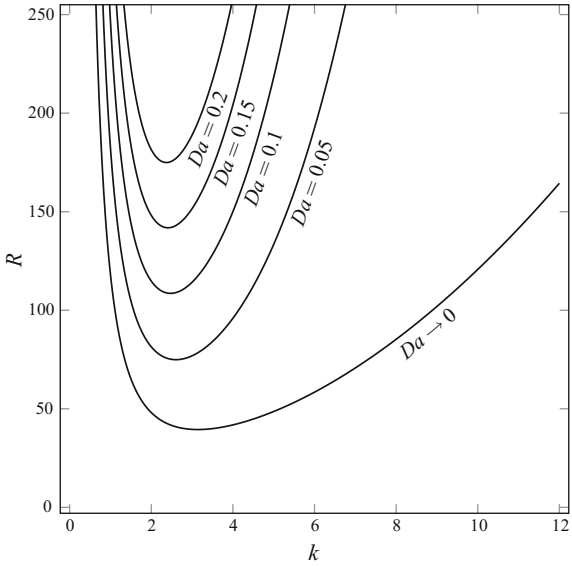

Fig. 7.8 Neutral stability curves $R(k)$ for the Rayleigh–Bénard problem in a porous layer, according to Brinkman's model, with impermeable and stress-free boundary conditions at $z = 0, 1$

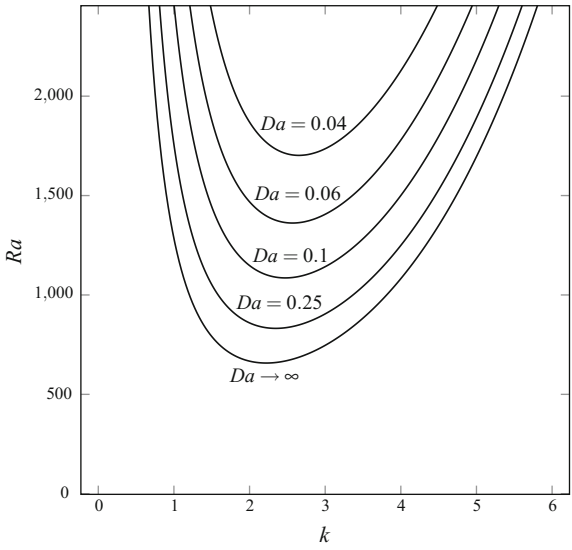

Fig. 7.9 Neutral stability curves $Ra(k)$ for the Rayleigh–Bénard problem in a porous layer, according to Brinkman's model, with impermeable and stress-free boundary conditions at $z = 0, 1$

$$Ra_c = \frac{R_c}{Da} \,. \tag{7.107}$$

By taking the limit $Da \to 0$ of k_c and R_c, one obtains the results given by Eq. (7.83). On the other hand, the limit $Da \to \infty$ of k_c and Ra_c yields the results given by Eq. (7.42). The plots reported in Figs. 7.8 and 7.9 suggest that the use of R is suitable to describe cases close to Darcy's regime, where Da is very small. The Rayleigh

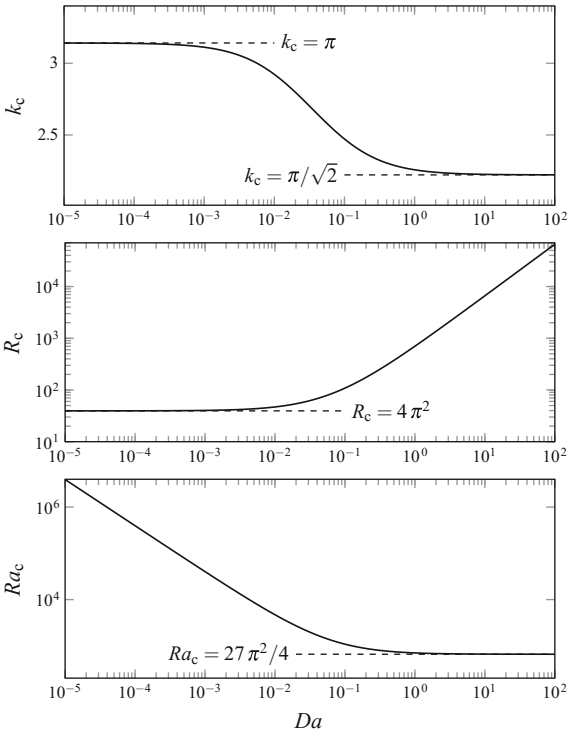

Fig. 7.10 Plots of k_c, R_c and Ra_c for the Rayleigh–Bénard problem in a porous layer, according to Brinkman's model, with impermeable and stress-free boundary conditions at $z = 0, 1$

number, Ra, is the suitable parameter when the flow takes place in a highly permeable medium, that is in a regime of large Darcy number, under conditions fairly close to those of a clear fluid. The behaviour of the critical values k_c, R_c and Ra_c versus Da is displayed in Fig. 7.10. These plots suggest that the critical values of k and Ra for a clear fluid are in fact almost attained when $Da \sim 1$. The Darcy's law regime, on the other hand, requires values of Da smaller than 10^{-3}.

7.7 A Porous Layer with Uniform Heat Flux Boundaries

Interesting variants of the Horton–Rogers–Lapwood problem come out when the thermal boundary conditions switch from isothermal to uniform heat flux. The mechanism of heating from below can be thermal contact, at the lower boundary, with an external thermal reservoir at a given temperature higher than that prescribed at the upper boundary. Alternatively, one can think to a given heat supply at the lower boundary provided through, say, an electric resistance. In this case, the boundary condition becomes one of uniform heat flux. Hence, we can devise a situation where, at $z = 0$, we have a uniform incoming heat flux q_0 and, at $z = L$, we have a uniform temperature T_0. In this case, we prescribe

$$z = 0 : \qquad -\varkappa_{\text{eff}} \frac{\partial T}{\partial z} = q_0 \, ,$$

$$z = L : \qquad T = T_2 \, . \tag{7.108}$$

For the sake of simplicity, we rely on Darcy's law. The basic state of the Horton–Rogers–Lapwood problem is slightly modified,

$$u_{\text{b}i} = 0 \, , \qquad T_{\text{b}} = T_2 + \frac{q_0 \, (L - z)}{\varkappa_{\text{eff}}} \, . \tag{7.109}$$

The differential equations for the perturbations of the basic state are still given by Eq. (7.65), provided that one defines

$$T_1 = T_2 + \frac{q_0 \, L}{\varkappa_{\text{eff}}} \, . \tag{7.110}$$

The dimensionless scaling of the governing equations can be carried out by employing Eq. (7.66), then Eqs. (7.67) are still valid, while Eq. (7.68) is replaced by

$$z = 0 : \qquad W = 0 = \frac{\partial \Theta}{\partial z} \, ,$$

$$z = 1 : \qquad W = 0 = \Theta \, . \tag{7.111}$$

We employ the Fourier transform method for the solution of Eqs. (7.67) and (7.111). Hence, we use Eqs. (7.30) and (7.31) to obtain

$$\left(\frac{\mathrm{d}^2}{\mathrm{d}\, z^2} - k^2 \right) f + R \, k^2 \, h = 0 \, ,$$

$$\left(\lambda - \frac{\mathrm{d}^2}{\mathrm{d}\, z^2} + k^2 \right) h - f = 0 \, ,$$

$$z = 0 : \qquad f = 0 = \frac{\mathrm{d}\, h}{\mathrm{d}\, z} \, ,$$

$$z = 1 : \qquad f = 0 = h \, . \tag{7.112}$$

The difference with respect to the corresponding formulation of the Horton–Rogers–Lapwood problem, Eqs. (7.75) and (7.76), is just in the boundary condition at $z = 0$. This change makes a significant difference with respect to the complexity of the mathematical solution.

7.7.1 The Principle of Exchange of Stabilities

The boundary conditions in Eq. (7.112) allow one to write the following formulas of integration by parts:

$$\int_0^1 \bar{f}\,\frac{\mathrm{d}^2 f}{\mathrm{d}\,z^2}\,\mathrm{d}z = -\int_0^1 \left|\frac{\mathrm{d}\,f}{\mathrm{d}\,z}\right|^2 \mathrm{d}z\,, \qquad \int_0^1 \frac{\mathrm{d}^2\bar{h}}{\mathrm{d}\,z^2}\,h\,\mathrm{d}z = -\int_0^1 \left|\frac{\mathrm{d}\,h}{\mathrm{d}\,z}\right|^2 \mathrm{d}z\,. \tag{7.113}$$

On multiplying by $\bar{f}$ the first Eq. (7.112), and multiplying by h the complex conjugate of the second Eq. (7.112), we obtain

$$\int_0^1 \left|\frac{\mathrm{d}\,f}{\mathrm{d}\,z}\right|^2 \mathrm{d}z + k^2 \int_0^1 |f|^2\,\mathrm{d}z$$

$$- R\,k^2 \left[\int_0^1 \left|\frac{\mathrm{d}\,h}{\mathrm{d}\,z}\right|^2 \mathrm{d}z + \left(\bar{\lambda} + k^2\right) \int_0^1 |h|^2\,\mathrm{d}z\right] = 0\,. \tag{7.114}$$

We recall that $\lambda = \eta - \mathrm{i}\,\omega$, so that the imaginary part of Eq. (7.114) reads

$$\omega\,R\,k^2 \int_0^1 |h|^2\,\mathrm{d}z = 0\,. \tag{7.115}$$

The integral on the left-hand side of Eq. (7.115) is positive, unless the perturbation is identically zero, i.e. $h = 0$. If h is identically zero, then Eq. (7.114) implies that also f is identically zero. Hence, we conclude that Eq. (7.115) can be satisfied by perturbations not identically zero, if $\omega = 0$. This means that the principle of exchange of stabilities holds, i.e., only Fourier modes with a zero phase velocity, $\omega/k = 0$, are allowed.

7.7.2 Solution of the Instability Eigenvalue Problem

The first and the second Eq. (7.112) can be rewritten as a single fourth-order equation in h. In the following, we will find the solution relative to the condition of neutral stability, so that we set $\lambda = \eta = 0$. Then, we can formulate a differential problem equivalent to Eq. (7.112), namely

$$\left(\frac{\mathrm{d}^2}{\mathrm{d}\,z^2} - k^2\right)^2 h - R\,k^2\,h = 0\,,$$

$$z = 0: \qquad \frac{\mathrm{d}\, h}{\mathrm{d}\, z} = 0\,, \quad \frac{\mathrm{d}^2 h}{\mathrm{d}\, z^2} = k^2\, h\,,$$

$$z = 1: \qquad h = 0\,, \quad \frac{\mathrm{d}^2 h}{\mathrm{d}\, z^2} = 0\,. \tag{7.116}$$

The characteristic equation associated with the differential equation (7.116) is given by

$$\left(s^2 - k^2\right)^2 - R\, k^2 = 0\,. \tag{7.117}$$

Its solutions are $s = \pm\, \chi_1$ and $s = \pm\, \mathrm{i}\, \chi_2$ where

$$\chi_1 = \sqrt{k\left(\sqrt{R} + k\right)}\,, \qquad \chi_2 = \sqrt{k\left(\sqrt{R} - k\right)}\,. \tag{7.118}$$

Hence, $h(z)$ can be written as

$$h(z) = C_1\, \mathrm{e}^{\chi_1 z} + C_2\, \mathrm{e}^{-\chi_1 z} + C_3\, \mathrm{e}^{\mathrm{i}\, \chi_2 z} + C_2\, \mathrm{e}^{-\mathrm{i}\, \chi_2 z}\,. \tag{7.119}$$

The coefficients C_1, C_2, C_3 and C_4 have to be chosen so that the four boundary conditions given by Eq. (7.116) are satisfied. This means that we can write the algebraic equation

$$\begin{pmatrix} \chi_1 & -\chi_1 & \mathrm{i}\, \chi_2 & -\mathrm{i}\, \chi_2 \\ 1 & 1 & -1 & -1 \\ \mathrm{e}^{\chi_1} & \mathrm{e}^{-\chi_1} & \mathrm{e}^{\mathrm{i}\, \chi_2} & \mathrm{e}^{-\mathrm{i}\, \chi_2} \\ \chi_1^2\, \mathrm{e}^{\chi_1} & \chi_1^2\, \mathrm{e}^{-\chi_1} & -\chi_2^2\, \mathrm{e}^{\mathrm{i}\, \chi_2} & -\chi_2^2\, \mathrm{e}^{-\mathrm{i}\, \chi_2} \end{pmatrix} \begin{pmatrix} C_1 \\ C_2 \\ C_3 \\ C_4 \end{pmatrix} = 0\,. \tag{7.120}$$

Equation (7.120) admits only the trivial solution, where all coefficients C_1, C_2, C_3 and C_4 are zero, unless the determinant of the 4×4 matrix is zero. The coefficients cannot be identically zero, because this would imply a vanishing perturbation of the basic state. Then, the condition of zero determinant must hold, namely

$$\chi_2\, \sinh \chi_1\, \cos \chi_2 + \chi_1\, \cosh \chi_1\, \sin \chi_2 = 0\,. \tag{7.121}$$

Equation (7.121), together with Eq. (7.118), yields the dispersion relation at neutral stability in an implicit form where R cannot be explicitly expressed as a function of k. Although analytical, the expression of the dispersion relation given by Eq. (7.121) must be handled with care. In fact, Eq. (7.121) is just a condition of zero determinant and, as such, it may contain spurious solutions. An evident one is $\chi_2 = 0$ or, equivalently, $k = \sqrt{R}$. This solution must be excluded as writing Eq. (7.119) implies that the four solutions $\mathrm{e}^{\pm \chi_1 z}$, $\mathrm{e}^{\pm \mathrm{i}\, \chi_2 z}$ are assumed to be independent. This is untrue if $\chi_2 = 0$. In fact, one may easily check that Eq. (7.116) does not admit any nonzero solution h whenever $k = \sqrt{R}$.

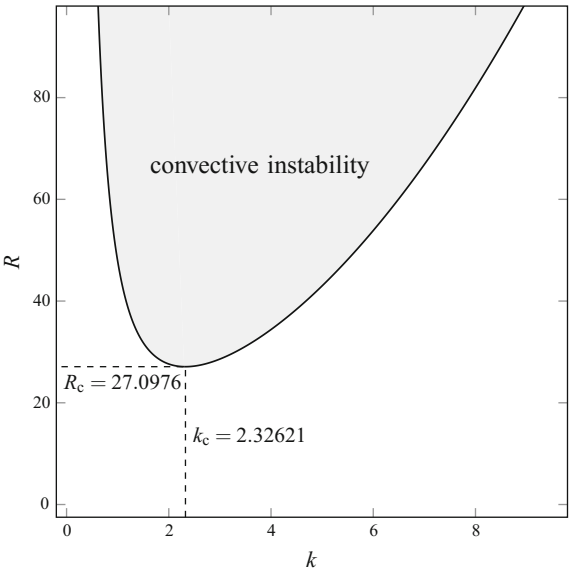

Fig. 7.11 Neutral stability curve for the Horton–Rogers–Lapwood problem with impermeable boundaries, uniform heat flux at $z = 0$ and uniform temperature at $z = 1$

An alternative to using the implicit dispersion relation (7.121) is adopting the numerical method described in Chap. 10 for the solution of Eq. (7.112) with $\lambda = 0$. Either way, one can gather the numerical data needed to draw the neutral stability curve in the (k, R) plane. A plot of the neutral stability curve and of the convective instability region is displayed in Fig. 7.11. This figure shows that the point of minimum R along the curve, namely the critical condition, is identified by

$$k_c = 2.32621 \,, \qquad R_c = 27.0976 \,. \tag{7.122}$$

This result was first pointed out in the paper by Lapwood [7].

7.7.3 *Porous Layer with Uniform Heat Flux at Both Boundaries*

The boundary condition of uniform heat flux can be prescribed both at the lower boundary and at the upper boundary. A situation can be imagined where all the heat supplied to the lower boundary is removed from the upper boundary, so that a steady condition can be allowed. Under such conditions, Eq. (7.108) is replaced by

$$z = 0, \; L: \qquad -\varkappa_{\text{eff}} \frac{\partial T}{\partial z} = q_0 \,. \tag{7.123}$$

The basic state considered in Eq. (7.109) satisfies Eq. (7.123). The only important remark is that the constant temperature T_2 is now undefined or, stated differently, its value can be fixed arbitrarily. The reason is that, in a rest state, the temperature field is determined as a solution of the local energy balance equation which contains only derivatives of T. If the temperature boundary conditions are those given by Eq. (7.123), then one can conclude that T can be determined only up to an arbitrary additive constant.

The change needed in the eigenvalue problem expressed by Eq. (7.112) is just in the boundary conditions. Hence, we can write

$$\left(\frac{\mathrm{d}^2}{\mathrm{d}\,z^2} - k^2\right) f + R\,k^2\,h = 0\,,$$

$$\left(\lambda - \frac{\mathrm{d}^2}{\mathrm{d}\,z^2} + k^2\right) h - f = 0\,,$$

$$z = 0, 1: \qquad f = 0 = \frac{\mathrm{d}\,h}{\mathrm{d}\,z}\,. \tag{7.124}$$

One can easily check that the principle of exchange of stabilities holds. In fact, the integration by parts formulas reported in Eq. (7.113) are still valid, as a consequence of the boundary conditions specified in Eq. (7.124). Then, the same discussion and conclusions reached in Sect. 7.7.1 can be drawn.

The solution of Eq. (7.124) for the neutrally stable modes, with $\lambda = 0$, can be found analytically through the same procedure described in Sect. 7.7.2. Equation (7.116) now reads

$$\left(\frac{\mathrm{d}^2}{\mathrm{d}\,z^2} - k^2\right)^2 h - R\,k^2\,h = 0\,,$$

$$z = 0, 1: \qquad \frac{\mathrm{d}\,h}{\mathrm{d}\,z} = 0\,, \quad \frac{\mathrm{d}^2 h}{\mathrm{d}\,z^2} = k^2\,h\,. \tag{7.125}$$

No change is needed in Eqs. (7.118) and (7.119), as they rely only on the ordinary differential equation. On the other hand, Eq. (7.120) is replaced by

$$\begin{pmatrix} \chi_1 & -\chi_1 & \mathrm{i}\,\chi_2 & -\mathrm{i}\,\chi_2 \\ 1 & 1 & -1 & -1 \\ \chi_1\,\mathrm{e}^{\chi_1} & -\chi_1\,\mathrm{e}^{-\chi_1} & \mathrm{i}\,\chi_2\,\mathrm{e}^{\mathrm{i}\,\chi_2} & -\mathrm{i}\,\chi_2\,\mathrm{e}^{-\mathrm{i}\,\chi_2} \\ \mathrm{e}^{\chi_1} & \mathrm{e}^{-\chi_1} & -\mathrm{e}^{\mathrm{i}\,\chi_2} & -\mathrm{e}^{-\mathrm{i}\,\chi_2} \end{pmatrix} \begin{pmatrix} C_1 \\ C_2 \\ C_3 \\ C_4 \end{pmatrix} = 0\,. \tag{7.126}$$

The condition of zero determinant for the 4×4 matrix yields the dispersion relation,

$$k^2\,\sinh\chi_1\,\sin\chi_2 + \chi_1\,\chi_2\,(\cosh\chi_1\,\cos\chi_2 - 1) = 0\,. \tag{7.127}$$

Through a numerical algorithm for root finding, Eqs. (7.118) and (7.127) can be employed to gather the numerical data needed to draw the neutral stability curve, viz. the lower bound to the convective instability region in the (k, R) plane. Again, the alternative is carrying out a fully numerical solution of the system of ordinary differential stability problem through the shooting method, along the lines discussed in Chap. 10.

The shape of the neutral stability curve is quite dissimilar to that illustrated in Fig. 7.11, relative to the hybrid case where the lower boundary is subject to a uniform heat flux and the upper boundary is kept isothermal. The dissimilarity can be easily revealed by looking for an asymptotic solution in the limit $k \to 0$. By relying on the inverse proportionality between wave number and wavelength, we can define this limit as one of large wavelengths. We express $h(z)$ and R as power series with respect to the small parameter k^2,

$$h(z) = \sum_{n=0}^{\infty} h_n(z)\, k^{2n} \;, \qquad R = \sum_{n=0}^{\infty} R_n\, k^{2n} \;. \tag{7.128}$$

This is perfectly legitimate as the wave number appears in Eq. (7.125) only through its square, k^2. By substituting Eq. (7.128) into (7.125) and collecting like powers of k^2, we obtain the zeroth-order boundary value problem, namely

$$\frac{\mathrm{d}^4 h_0}{\mathrm{d}\, z^4} = 0 \;,$$

$$z = 0, 1: \qquad \frac{\mathrm{d}\, h_0}{\mathrm{d}\, z} = 0 \;, \quad \frac{\mathrm{d}^2 h_0}{\mathrm{d}\, z^2} = 0 \;. \tag{7.129}$$

The solution of Eq. (7.129) is

$$h_0(z) = A \;, \tag{7.130}$$

where A is an arbitrary constant. To first order in k^2, we obtain the boundary value problem

$$\frac{\mathrm{d}^4 h_1}{\mathrm{d}\, z^4} - R_0\, A = 0 \;,$$

$$z = 0, 1: \qquad \frac{\mathrm{d}\, h_1}{\mathrm{d}\, z} = 0 \;, \quad \frac{\mathrm{d}^2 h_1}{\mathrm{d}\, z^2} = A \;. \tag{7.131}$$

Provided that

$$A\,(R_0 - 12) = 0 \;, \tag{7.132}$$

Equation (7.131) yields the solution

$$h_1(z) = B + \frac{A}{2}\, z^2 - A\, z^3 + \frac{A}{2}\, z^4 \;, \tag{7.133}$$

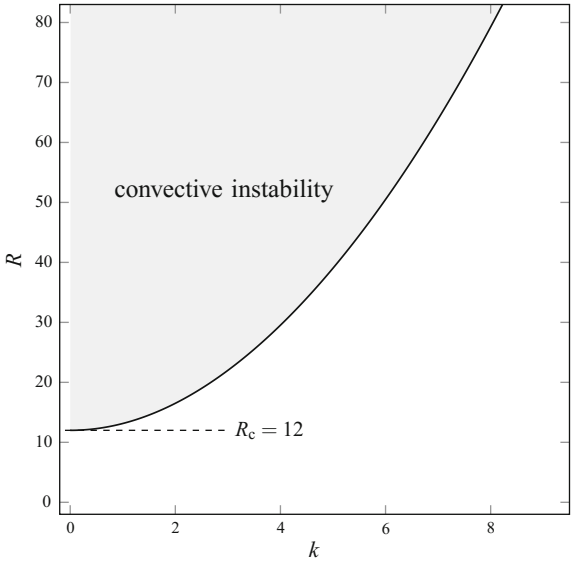

Fig. 7.12 Neutral stability curve for the Horton–Rogers–Lapwood problem with impermeable boundaries having uniform heat flux at $z = 0, 1$

where B is another arbitrary constant. If we assume $A \neq 0$, whatever is its value, we obtain

$$R_0 = 12 \, . \tag{7.134}$$

Equation (7.134), together with Eq. (7.128), leads to the conclusion that the neutral stability function $R(k)$ is not singular when $k \to 0$, as it happens in the cases illustrated in Figs. 7.7 and 7.11. On the other hand, it approaches the constant value 12 when $k \to 0$. Starting from this limiting value, the neutral stability function $R(k)$ is monotonic increasing, as shown in Fig. 7.12. This means that the critical values of k and R for the onset of convective instability are

$$k_c = 0 \, , \qquad R_c = 12 \, . \tag{7.135}$$

We have found that, on replacing the isothermal condition at the lower boundary with a uniform heat flux condition, the critical value of R decreases from $4\,\pi^2 \approx 39.4784$ to 27.0976. If also the upper boundary is subject to a uniform heat flux, then R_c further decreases to 12. Hence, we conclude that boundaries at uniform heat flux yield a destabilisation of the basic state with respect to isothermal boundaries.

7.8 A Note on the Shape of Convection Cells

A visualisation of the convection cells can be easily obtained when a single normal mode with a given wave vector (k_x, k_y) is considered,

$$W = \frac{1}{2\,\pi}\,\tilde{W}\,\mathrm{e}^{\mathrm{i}(k_x\,x+k_y\,y)}\;,\qquad \Theta = \frac{1}{2\,\pi}\,\tilde{\Theta}\,\mathrm{e}^{\mathrm{i}(k_x\,x+k_y\,y)}\;, \tag{7.136}$$

where Eq. (7.30) is taken into account. We have already pointed out, in Sect. 7.2, that manifold shapes of convection cells may arise at the onset of convective instability. The simplest geometry of the convection cells is straight rolls, whose planforms are illustrated in frame (a) of Fig. 7.2. Without any loss of generality, we can choose such straight rolls as having axes perpendicular to the (x, z) plane. The mathematical representation of this case is a wave vector directed along the x-axis, i.e. a situation where $k_x = k$ and $k_y = 0$. In this case, we have no dependence on y, so that the local mass balance equation, that is the condition of zero divergence for the velocity field U_i, can be written as

$$\frac{\partial U}{\partial x} + \frac{\partial W}{\partial z} = 0\;. \tag{7.137}$$

This equation is identically satisfied by defining a *streamfunction*, $\Psi(x, z, t)$, such that

$$U = \frac{\partial \Psi}{\partial z}\;,\qquad W = -\frac{\partial \Psi}{\partial x}\;. \tag{7.138}$$

Obviously, Ψ is defined only up to an arbitrary additive function of t. This function of time can be fixed in a convenient way. For instance, on the basis of Eq. (7.136) and of the assumptions $k_x = k$ and $k_y = 0$, one can define it so that

$$\Psi = \frac{1}{2\,\pi}\,\tilde{\Psi}\,\mathrm{e}^{\mathrm{i}\,k\,x}\;. \tag{7.139}$$

The isolines of Ψ are called the *streamlines*. The streamlines provide a natural description of the two-dimensional velocity field $(U, 0, W)$, as the tangent to the streamlines is the field $(U, 0, W)$ itself. This result is an immediate consequence of the definition given by Eq. (7.138). On account of Eqs. (7.136) and (7.139), we can find a simple equation linking the fields W and Ψ, or $\tilde{W}$ and $\tilde{\Psi}$, namely

$$W = -\mathrm{i}\,k\,\Psi\;,\qquad \tilde{W} = -\mathrm{i}\,k\,\tilde{\Psi}\;. \tag{7.140}$$

As a consequence of Eq. (7.140), we infer that the streamlines are, in fact, coincident with the isolines of W. In order to get a graphical representation of the streamlines, we must remember that the physically significant field is not W, which is complex-valued, but its real part.

In the Rayleigh–Bénard problem, and in all its variants considered in this chapter included the Horton–Rogers–Lapwood problem with either isothermal or isoflux boundary conditions, the principle of exchange of stabilities holds. In particular, this means that the fields $\tilde{W}$ and $\tilde{\Theta}$ are real-valued. Then, we can write

$$\Re(W) = \frac{1}{2\,\pi}\,\tilde{W}\,\cos(k\,x)\;,\qquad \Re(\Psi) = -\frac{1}{2\,\pi\,k}\,\tilde{W}\,\sin(k\,x)\;. \tag{7.141}$$

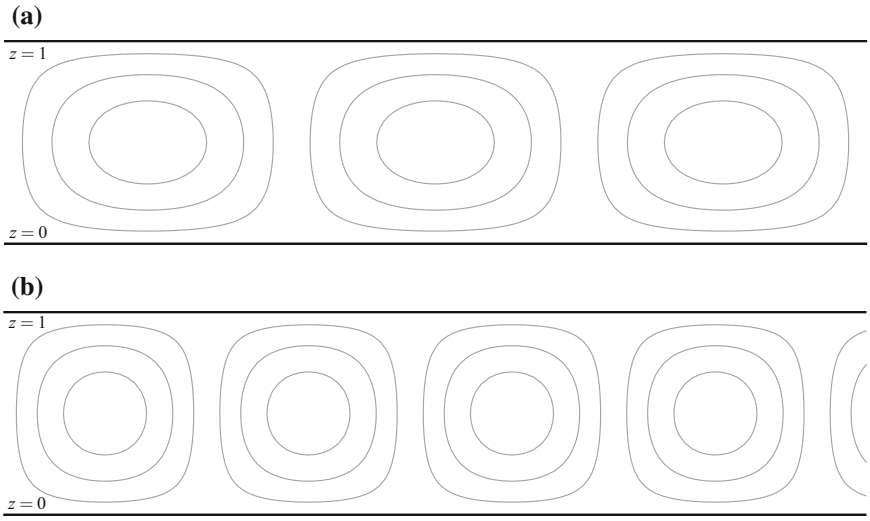

Fig. 7.13 Streamlines of the normal mode perturbation at the onset of convective instability for: **a** the Rayleigh–Bénard problem with stress-free and isothermal boundaries; **b** the Horton–Rogers–Lapwood problem with impermeable and isothermal boundaries

If we consider the Rayleigh–Bénard problem for a fluid layer bounded by stress-free and isothermal planes, or the Horton–Rogers–Lapwood problem for a saturated porous medium bounded by impermeable and isothermal planes, the expression of $\tilde{W}$ is such that

$$\tilde{W} = C \, \sin(n \, \pi \, z) \, \mathrm{e}^{\eta t} \, , \tag{7.142}$$

where C is a constant. Equation (7.142) can be deduced from Eqs. (7.31), (7.33) and (7.37).

A sensible case where one may wish to draw the streamlines of the perturbation normal mode is at the critical conditions for the onset of instability, namely $\eta = 0$, $n = 1$ and $k = k_\mathrm{c}$. With these conditions, Eqs. (7.141) and (7.142) yield

$$\Re(\Psi) = -\frac{C}{2 \, \pi \, k_\mathrm{c}} \, \sin(\pi \, z) \, \sin(k_\mathrm{c} \, x) \, . \tag{7.143}$$

We found that $k_\mathrm{c} = \pi/\sqrt{2}$ for the Rayleigh–Bénard problem and $k_\mathrm{c} = \pi$ for the Horton–Rogers–Lapwood problem, as reported in Eqs. (7.42) and (7.83), respectively. Thus, the streamlines can be easily represented in the (x, z) plane by employing equation (7.143) as the isolines $\Re(\Psi) = constant$.

Figure 7.13 shows the streamlines at the onset of convective instability, relative to a perturbation normal mode, with $k = k_\mathrm{c}$ for either the Rayleigh–Bénard problem or the Horton–Rogers–Lapwood problem. On comparing frames (a) and (b) of Fig. 7.13, one may note the more stretched horizontal width of the Rayleigh–Bénard cells. The

Horton–Rogers–Lapwood cells have a characteristic square shape, due to the critical value $k_c = \pi$ implying the same periodicity of $\Re(\Psi)$ along the x and z directions.

If we move from those cases amenable to a fully analytical solution, then the function $f(z)$ adopted to express $\tilde{W}$ is not given by a simple sine function, but it is determined numerically. This does not change much in what we have said about plotting the streamlines of the normal mode perturbation at critical conditions, except that Eq. (7.143) is in fact replaced by

$$\Re(\Psi) = -\frac{1}{2\,\pi\,k_c}\; f(z)\; \sin(k_c\,x)\;. \tag{7.144}$$

Ultimately, the aspect ratio of the cells is determined uniquely by the value of k_c in each single case.

References

1. Bénard HC (1901) Les tourbillons cellulaires dans une nappe liquide - Méthodes optiques d'observation et d'enregistrement. Journal de Physique Théorique et Appliquée 10:254–266
2. Chandrasekhar S (1981) Hydrodynamic and hydromagnetic stability. Dover, New York
3. Drazin PG, Reid WH (2004) Hydrodynamic stability, 2nd edn. Cambridge University Press, Cambridge
4. Getling AV (1998) Rayleigh–Bénard convection: structures and dynamics. World Scientific, Singapore
5. Horton CW, Rogers FT Jr (1945) Convection currents in a porous medium. J Appl Phys 16:367–370
6. Koschmieder EL (1993) Bénard cells and Taylor vortices. Cambridge University Press, Cambridge
7. Lapwood ER (1948) Convection of a fluid in a porous medium. Math. Proc. Camb. Philos. Soc. 44:508–521
8. Mutabazi I, Wesfreid JE, Guyon E (2006) Dynamics of spatio-temporal cellular structures: Henri Bénard centenary review. Springer, New York
9. Nield DA, Bejan A (2017) Convection in porous media, 5th edn. Springer, New York
10. Normand C, Pomeau Y, Velarde MG (1977) Convective instability: a physicist's approach. Rev Mod Phys 49:581–624
11. Pearson JRA (1958) On convection cells induced by surface tension. J Fluid Mech 4:489–500
12. Pellew A, Southwell RV (1940) On maintained convective motion in a fluid heated from below. Proc R Soc Lond A Math Phys Eng Sci 176:312–343
13. Rayleigh L (1916) On convection currents in a horizontal layer of fluid, when the higher temperature is on the under side. Lond Edinb Dublin Philos Mag J Sci 32:529–546
14. Rees DAS (2000) The stability of Darcy–Bénard convection. In: Vafai K (ed) Handbook of porous media, vol 1. Marcel Dekker, New York, pp 521–588
15. Schmidt RJ, Milverton SW (1935) On the instability of a fluid when heated from below. Proc R Soc Lond Ser A Math Phys Sci 152(877):586–594
16. Tyvand PA (2002) Onset of Rayleigh–Bénard convection in porous bodies. In: Ingham DB, Pop I (eds) Transport Phenomena in porous media II, Pergamon Press, London, pp 82–112

Part III
From Convective to Absolute Instability in Porous Media

The transition from convective to absolute instability in porous media is illustrated through some examples spanning from two-dimensional to three-dimensional cases. The existence of a horizontal flow is the cause of the transition. When the basic flow is switched off, then the onset of convective instability implies the simultaneous onset of absolute instability. Typically, there exists a growing parametric gap between convective and absolute instability, expressed through the Darcy-Rayleigh number, as the basic flow rate increases. Numerical solutions are needed in some cases. A numerical method, that can be employed for the study of both convective and absolute instability, is illustrated in the final chapter.

Chapter 8
Transition to Absolute Instability in Porous Media: Analytical Solutions

8.1 Absolute Instability in Porous Media

Most of the literature regarding the instability of flow in a porous medium is relative to the convective instability. The transition to absolute instability has been studied by some authors, but the literature on this specific subtopic is quite limited. One of the earlier papers on this subject is by Dufour and Néel [9].

The transition to absolute instability in the *Prats problem* is examined within an analytical and numerical study of the instability patterns of mixed convection in a horizontal porous channel. The Prats problem is a widely used denomination for the variant of the Horton–Rogers–Lapwood problem where the only changed feature is the presence of a forced horizontal flow. In fact, the original paper by Prats [12] develops the analysis of the onset of convective instability in a horizontal porous channel bounded by parallel impermeable and isothermal walls, with heating from below, and a uniform horizontal flow. Another study by Joulin and Ouarzazi [11] proposes a more complicated situation where the instability is not only driven by the heat transfer, which is induced by heating from below, but also by a simultaneous mass diffusion caused by the Soret effect. The latter physical effect consists in the existence of a solute mass flux contribution induced by the temperature gradient. Under these conditions, Joulin and Ouarzazi [11] present a thorough analysis of the transition from convective to absolute instability.

Delache et al. [7] further developed the investigation carried out by Dufour and Néel [9] on including also the form-drag term contribution in the momentum balance, i.e., by considering Darcy–Forchheimer's model instead of Darcy's law. These authors also suggest some interesting comparison with experimental results.

The analysis of the transition to absolute instability has been investigated also for non-Newtonian flows in porous media. This is the case of the studies presented by Hirata and Ouarzazi [10] and by Alves and Barletta [1]. The former study is relative to a viscoelastic fluid described through the Oldroyd-B model, while the latter deals with a power-law fluid.

A. Barletta, *Routes to Absolute Instability in Porous Media*,
https://doi.org/10.1007/978-3-030-06194-4_8

A wide research work has been carried out by Brevdo [6], Brevdo and Ruderman [4, 5], Diaz and Brevdo [8]. This work regarded cases where a vertical forced flow through a horizontal porous layer is accompanied by a prescribed horizontal temperature gradient. The authors concluded that the onset of convective instability coincides with the onset of absolute instability whenever the horizontal temperature gradient is zero. In fact, the effect of the horizontal temperature gradient is a secondary horizontal basic flow, which can induce the parametric delay in the onset of absolute instability with respect to convective instability.

The analysis of absolute instability in the Prats problem has been recently reconsidered by Barletta and Alves [2] and by Barletta and Celli [3]. In these papers, the effect of a finite Darcy–Prandtl number and that of an open upper boundary were considered, respectively. We mention that the Darcy–Prandtl number is a dimensionless parameter arising when convection problems in porous media are formulated starting from the local momentum balance given by Eq. (6.6), instead of the usual Darcy's law expressed by Eq. (6.5). When the Darcy–Prandtl number tends to infinity, the convection flow becomes compatible with the local momentum balance expressed by Eq. (6.5) [2].

8.2 Prats Problem

What is now well known as the Prats problem, after Prats [12], is the stability analysis of the uniform horizontal flow in a porous channel bounded by a pair of horizontal parallel planes, both impermeable and isothermal. A sketch of the horizontal porous layer is given in Fig. 8.1. We assume that the flow system is two-dimensional by considering all fields as independent of the spanwise y-coordinate. We also assume that the effect of viscous dissipation is negligible. When taken into account, this effect may alter significantly the stability analysis of the Prats problem.

The two-dimensional velocity field (u, w), lying in the (x, z) plane, the temperature field T, the coordinates (x, z) and time t, can be written in a dimensionless form by adopting the following transformations

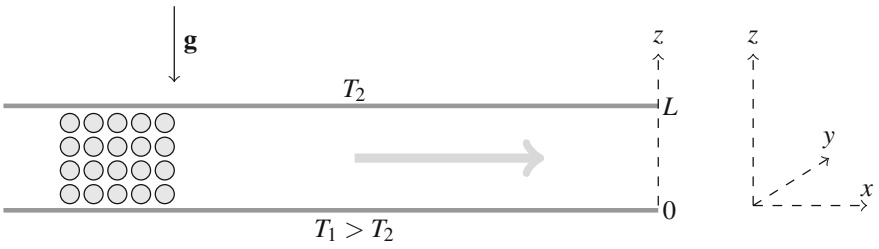

Fig. 8.1 A sketch of the horizontal porous channel, of the (x, y, z) coordinate frame and of the boundary conditions

$$(u, w)\,\frac{L}{\alpha} \to (u, w)\ , \qquad \frac{T - T_2}{T_1 - T_2} \to T\ ,$$
$$(x, z)\,\frac{1}{L} \to (x, z)\ , \qquad \frac{t}{L^2/\alpha} \to t\ . \tag{8.1}$$

Here, L is the height of the channel, as illustrated in Fig. 8.1, while α is the average thermal diffusivity of the porous medium.

Following the Oberbeck–Boussinesq approximation and Darcy's law, the local balance equations of mass, momentum and energy are written as

$$\frac{\partial u}{\partial x} + \frac{\partial w}{\partial z} = 0\ ,$$

$$\frac{\partial u}{\partial z} - \frac{\partial w}{\partial x} = -\,R\,\frac{\partial T}{\partial x}\ ,$$

$$\sigma\,\frac{\partial T}{\partial t} + u\,\frac{\partial T}{\partial x} + w\,\frac{\partial T}{\partial z} = \frac{\partial^2 T}{\partial x^2} + \frac{\partial^2 T}{\partial z^2}\ , \tag{8.2}$$

where σ is the ratio between the average volumetric heat capacity of the saturated porous medium and the volumetric heat capacity of the fluid. In Eq. (8.2), the local momentum balance has been formulated by evaluating the y component of the curl for Darcy's law. The Darcy–Rayleigh number R is defined as

$$R = \frac{g\beta(T_1 - T_2)KL}{\nu\alpha}\ , \tag{8.3}$$

where β is the thermal expansion coefficient of the fluid, and g is the modulus of the gravitational acceleration $\mathbf{g}$.

We prescribed the boundary conditions at $z = 0, 1$ as

$$z = 0\ :\quad w = 0\ ,\quad T = 1\ ,$$
$$z = 1\ :\quad w = 0\ ,\quad T = 0\ . \tag{8.4}$$

We introduce a streamfunction ψ, defined as

$$u = \frac{\partial \psi}{\partial z}\ , \qquad w = -\,\frac{\partial \psi}{\partial x}\ . \tag{8.5}$$

Thus, we satisfy the first equation (8.2), while the second and third differential equations (8.2) can be rewritten as

$$\frac{\partial^2 \psi}{\partial x^2} + \frac{\partial^2 \psi}{\partial z^2} + R\,\frac{\partial T}{\partial x} = 0\ ,$$

$$\sigma\,\frac{\partial T}{\partial t} + \frac{\partial \psi}{\partial z}\,\frac{\partial T}{\partial x} - \frac{\partial \psi}{\partial x}\,\frac{\partial T}{\partial z} = \frac{\partial^2 T}{\partial x^2} + \frac{\partial^2 T}{\partial z^2}\ . \tag{8.6}$$

The boundary conditions (8.4) are now expressed as

$$\begin{aligned} z = 0 \ : \quad & \frac{\partial \psi}{\partial x} = 0 \ , \quad T = 1 \ , \\ z = 1 \ : \quad & \frac{\partial \psi}{\partial x} = 0 \ , \quad T = 0 \ . \end{aligned} \tag{8.7}$$

8.2.1 The Basic Solution

There exists a stationary solution, $(\psi_\mathrm{b}, T_\mathrm{b})$, of Eqs. (8.6) and (8.7) describing a uniform velocity in the x-direction, and a pure conduction regime across the porous channel,

$$\psi_\mathrm{b} = Pe \ z \ , \qquad T_\mathrm{b} = 1 - z \ , \tag{8.8}$$

where

$$Pe = \frac{U_0 \, L}{\alpha} \tag{8.9}$$

is the *Péclet number* associated with the basic horizontal and uniform flow with constant velocity U_0 in the porous channel. One may easily check, from Eq. (8.5), that $\psi_\mathrm{b} = Pe \ z$ yields

$$u_\mathrm{b} = Pe \ , \qquad w_\mathrm{b} = 0 \ . \tag{8.10}$$

Without any loss of generality, we focus on the situation $Pe \geqslant 0$, as negative Péclet numbers do not identify physically different flow conditions.

8.2.2 Stability Analysis

Perturbations of the basic solution are defined as,

$$\psi = \psi_\mathrm{b} + \varepsilon \, \Psi \ , \qquad T = T_\mathrm{b} + \varepsilon \, \Theta \ , \tag{8.11}$$

where $|\varepsilon| \ll 1$. Let us substitute Eq. (8.11) into Eqs. (8.6) and (8.7), by taking into account Eq. (8.8) and by neglecting terms $O(\varepsilon^2)$. Thus, one obtains

$$\frac{\partial^2 \Psi}{\partial x^2} + \frac{\partial^2 \Psi}{\partial z^2} + R \, \frac{\partial \Theta}{\partial x} = 0 \ ,$$

$$\sigma \, \frac{\partial \Theta}{\partial t} + Pe \, \frac{\partial \Theta}{\partial x} + \frac{\partial \Psi}{\partial x} = \frac{\partial^2 \Theta}{\partial x^2} + \frac{\partial^2 \Theta}{\partial z^2} \ ,$$

$$z = 0, 1: \qquad \frac{\partial \Psi}{\partial x} = 0 \,, \quad \Theta = 0 \,. \tag{8.12}$$

We now express (Ψ, Θ) through their Fourier transforms,

$$\tilde{\Psi}(k, z, t) = \frac{1}{\sqrt{2\pi}} \int_{-\infty}^{\infty} e^{-\mathrm{i}\, k\, x}\, \Psi(x, z, t)\, \mathrm{d}\, x,$$

$$\Psi(x, z, t) = \frac{1}{\sqrt{2\pi}} \int_{-\infty}^{\infty} e^{\mathrm{i}\, k\, x}\, \tilde{\Psi}(k, z, t)\, \mathrm{d}\, k,$$

$$\tilde{\Theta}(k, z, t) = \frac{1}{\sqrt{2\pi}} \int_{-\infty}^{\infty} e^{-\mathrm{i}\, k\, x}\, \Theta(x, z, t)\, \mathrm{d}\, x \,,$$

$$\Theta(x, z, t) = \frac{1}{\sqrt{2\pi}} \int_{-\infty}^{\infty} e^{\mathrm{i}\, k\, x}\, \tilde{\Theta}(k, z, t)\, \mathrm{d}\, k \,, \tag{8.13}$$

and we also write

$$\tilde{\Psi} = f(z)\, \mathrm{e}^{\lambda(k)\, t} \,, \qquad \tilde{\Theta} = -\,\mathrm{i}\, k\, h(z)\, \mathrm{e}^{\lambda(k)\, t} \,. \tag{8.14}$$

Then, by employing Eqs. (8.13) and (8.14), we can apply the Fourier transform to Eq. (8.12) and obtain

$$\left(\frac{\mathrm{d}^2}{\mathrm{d}\, z^2} - k^2 \right) f + R\, k^2\, h = 0 \,,$$

$$\left[\frac{\mathrm{d}^2}{\mathrm{d}\, z^2} - k^2 - \sigma\, \lambda(k) - \mathrm{i}\, k\, Pe \right] h + f = 0 \,,$$

$$z = 0, 1 \ : \qquad f = 0 \,, \quad h = 0 \,. \tag{8.15}$$

The solution of the differential eigenvalue problem (8.15) is easily obtained by defining the parameter

$$\gamma(k) = \sigma\, \lambda(k) + \mathrm{i}\, k\, Pe \,, \tag{8.16}$$

so that Eq. (8.15) reads

$$\left(\frac{\mathrm{d}^2}{\mathrm{d}\, z^2} - k^2 \right) f + R\, k^2\, h = 0 \,,$$

$$\left[\frac{\mathrm{d}^2}{\mathrm{d}z^2} - k^2 - \gamma(k)\right] h + f = 0 \,,$$

$$z = 0, 1 \;: \qquad f = 0 \,, \quad h = 0 \,. \tag{8.17}$$

We can easily reckon that the eigenvalue problem (8.17) coincides with that formulated for the Horton–Rogers–Lapwood problem, expressed by Eqs. (7.75) and (7.76). The only difference is that, in Eq. (8.17), γ appears instead of λ. The obvious consequence is that the analytical dispersion relation written for Eq. (8.17) is easily retrieved from Eq. (7.79), namely

$$(n^2\pi^2 + k^2)\left[\gamma(k) + n^2\pi^2 + k^2\right] - Rk^2 = 0 \,, \quad n = 1, 2, 3, \ldots \,. \tag{8.18}$$

One can solve Eq. (8.18) for $\gamma(k)$ and obtain

$$\gamma(k) = \frac{Rk^2 - (n^2\pi^2 + k^2)^2}{n^2\pi^2 + k^2} \,, \quad n = 1, 2, 3, \ldots \,. \tag{8.19}$$

8.2.3 *Convective Instability*

Equation (8.19) is the starting point for both the study of convective instability and that of absolute instability. As for the convective instability, we have to take $k \in \mathbb{R}$ and separate the real and the imaginary parts of Eq. (8.19). We must remember that $\lambda = \eta - \mathrm{i}\,\omega$, where η is the growth rate of the normal mode and ω is the angular frequency. Then, on account of Eqs. (8.16) and (8.19), we can write

$$\eta = \frac{Rk^2 - (n^2\pi^2 + k^2)^2}{\sigma\left(n^2\pi^2 + k^2\right)} \,, \quad \omega = \frac{k\,Pe}{\sigma} \,, \quad n = 1, 2, 3, \ldots \,. \tag{8.20}$$

The first conclusion which can be drawn from Eq. (8.20) regards the angular frequency. The meaning of the equation $\omega = k\,Pe/\sigma$ is that the dimensionless phase velocity of the normal mode with wave number k is a constant, $\omega/k = Pe/\sigma$. The physical implications of this finding are that the normal modes travel along the x-direction with a dimensionless phase velocity different from the dimensionless velocity of the basic flow, Pe. The former can be greater, equal or smaller than the latter depending on the heat capacity ratio, σ, being smaller, equal or greater than 1, respectively. This conclusion can be correctly established only with length, time and velocity scales defined consistently, as we did in Eq. (8.1). The consistency means, in particular, that the velocity scale is the ratio of the length scale and the timescale. Such consistent choice of the scales in defining the dimensionless quantities is an unnecessary complication when handling the Horton–Rogers–Lapwood problem, or its variants explored in Chap. 7. In fact, in those cases, the principle of exchange of stabilities ensures that the phase velocity of the disturbances involved in the onset

of convective instability is zero. Incidentally, the principle of exchange of stabilities is implied by the equation $\omega/k = Pe/\sigma$, as one may easily recognise that the Horton–Rogers–Lapwood problem is nothing but the limiting case of the Prats problem when $Pe \to 0$.

The second conclusion drawn from Eq. (8.20) regards the threshold for the onset of convective instability. Indeed, convective instability arises when the growth rate η becomes positive, i.e. when

$$R > \frac{(\pi^2 + k^2)^2}{k^2} \,, \tag{8.21}$$

while the neutral stability condition is

$$R = \frac{(\pi^2 + k^2)^2}{k^2} \,. \tag{8.22}$$

Both Eqs. (8.21) and (8.22) have been obtained by considering the modes with $n = 1$ as these modes yield the lowest threshold values of R for attaining positive growth rates, $\eta > 0$. The neutral stability function $R(k)$ defined by Eq. (8.22) just coincides with that obtained for the Horton–Rogers–Lapwood problem and given by Eq. (7.82). Obviously, the critical values of k and R are still given by Eq. (7.83).

We remark that the neutral stability condition (8.22) is not influenced by the Péclet number, Pe. The only effect of the horizontal flow regards the travelling nature of the normal modes. The phase velocity tends to zero in the limit $Pe \to 0$, when the Prats problem coincides with the Horton–Rogers–Lapwood problem. Thus, in this limit, one recovers the principle of exchange of stabilities.

8.2.4 *Absolute Instability*

In the analysis of absolute instability, one has to test the asymptotic behaviour of the wave packets,

$$\Psi(x, z, t) = \frac{1}{\sqrt{2\pi}} \int_{-\infty}^{\infty} \mathrm{e}^{\lambda(k)\, t + \mathrm{i}\, k\, x} f(z)\, \mathrm{d}\, k \,,$$

$$\Theta(x, z, t) = -\frac{\mathrm{i}}{\sqrt{2\pi}} \int_{-\infty}^{\infty} k\, \mathrm{e}^{\lambda(k)\, t + \mathrm{i}\, k\, x} h(z)\, \mathrm{d}\, k \,, \tag{8.23}$$

when $t \to \infty$. Equation (8.23) is obtained by substituting Eq. (8.14) into Eq. (8.13). We point out that $f(z)$ and $h(z)$, being determined by solving Eq. (8.15), do depend on k in general. Detecting the asymptotic behaviour at large time of the wave packets given by Eq. (8.23) means adopting the steepest-descent approximation. This approximation is illustrated in Sect. 3.5.3. Simple applications of this

method to the analysis of absolute instability have been discussed in Chap. 4. In fact, absolute instability means that

$$\lim_{t\to+\infty} |\Psi(x,z,t)| = \infty \,, \qquad \lim_{t\to+\infty} |\Theta(x,z,t)| = \infty \,, \tag{8.24}$$

for every $x \in \mathbb{R}$, with $0 < z < 1$. We mention that the wave packets given by Eq. (8.23) implicitly depend on $n = 1, 2, 3, \ldots$. Then, one should define general wave packet perturbations by summing up Fourier integrals with different n. This aspect can be safely left implicit provided that one tests compliance of the limiting conditions (8.24) for, at least, one value of n.

The method based on the steepest-descent approximation is very powerful as it reveals that the fulfilment of the limiting conditions (8.24) just depends on the properties of the dispersion relation (8.19). In fact, from Eq. (8.16), Eq. (8.19) can be rewritten as

$$\sigma\,\lambda(k) = \frac{R\,k^2 - (n^2\pi^2 + k^2)^2}{n^2\pi^2 + k^2} - \mathrm{i}\,k\,Pe \,, \quad n = 1, 2, 3, \ldots \,. \tag{8.25}$$

As illustrated in Sect. 4.2.1, the first step is determining the saddle points of $\lambda(k)$. In other words, we have to determine the roots of equation

$$\lambda'(k) = 0 \,, \tag{8.26}$$

in the complex plane, $k \in \mathbb{C}$. Equations (8.25) and (8.26) yield

$$\frac{2\,k\,R\,n^2\pi^2}{(n^2\pi^2 + k^2)^2} = 2\,k + \mathrm{i}\,Pe \,. \tag{8.27}$$

The solution of Eq. (8.27) is particularly simple in the limiting case of no horizontal flow, $Pe = 0$, namely for the Horton–Rogers–Lapwood problem. In this special case, Eq. (8.27) yields four saddle points, given by

$$k_0^2 = -\,n^2\pi^2 \pm R^{1/2}\,n\,\pi \,. \tag{8.28}$$

With the minus sign in Eq. (8.28), we obtain two purely imaginary saddle points,

$$k_0 = \mathrm{i}\,\sqrt{n^2\pi^2 + R^{1/2}\,n\,\pi} \,, \qquad k_0 = -\,\mathrm{i}\,\sqrt{n^2\pi^2 + R^{1/2}\,n\,\pi} \,. \tag{8.29}$$

Equation (8.25) implies that $\lambda(k)$ has two singularities given by the imaginary simple poles

$$k = \mathrm{i}\,n\,\pi \,, \qquad k = -\mathrm{i}\,n\,\pi \,. \tag{8.30}$$

Then, we conclude that it is impossible to deform continuously the real line $\Im(k) = 0$, without sweeping the two singularities given by Eq. (8.30), so that it becomes locally

a line of steepest descent through the saddle points given by Eq. (8.29). In other words, the two saddle points expressed by Eq. (8.29) are not involved in the steepest-descent approximation of the wave packets defined by Eq. (8.23). Then, we must exclude these saddle points in evaluating the threshold value of R for absolute instability. We are left with the two saddle points given by

$$k_0^2 = -n^2\pi^2 + R^{1/2}\, n\,\pi \ . \tag{8.31}$$

When Eq. (8.31) is substituted into Eq. (8.25) with $Pe = 0$, one has

$$\sigma\ \lambda(k_0) = R^{1/2}\ \left(R^{1/2} - 2\,n\,\pi\right) \ . \tag{8.32}$$

Equation (8.32) reveals that $\lambda(k_0)$ is real and that it is positive when

$$R > 4\,n^2\pi^2 \ . \tag{8.33}$$

This inequality establishes the condition for the onset of absolute instability. In fact, the threshold value $R = R_\mathrm{a}$ for absolute instability is obtained from Eq. (8.33) by considering the most unstable case, namely $n = 1$. Thus, we can write

$$R_\mathrm{a} = 4\,\pi^2 \ . \tag{8.34}$$

By comparing Eqs. (7.83) and (8.34), one can conclude that the threshold value of R for the onset of absolute instability, R_a, coincides with the critical value, R_c. In other words, when instability arises with $Pe = 0$, it is both convective and absolute. This conclusion is what one should expect on purely physical grounds. In fact, we pointed out in Sect. 4.2.1 that absolute instability differs from convective instability inasmuch as there exists a flow which drives the perturbation modes downstream. Such flow can be so intense as to conceal the actual time growth of some normal modes included in a perturbation wave packet by convecting away such modes. When the basic flow is switched off, that is when $Pe = 0$, convective instability implies absolute instability, so that the two thresholds R_c and R_a coincide.

By employing the threshold value of R given by Eq. (8.34), we can evaluate the pertinent saddle points through Eq. (8.31). We obtain

$$k_0 = \pm\,\pi \ . \tag{8.35}$$

On account of Eq. (7.83), this means that the two saddle points lie on the real axis and that $k_0 = \pm\, k_\mathrm{c}$.

Another sensible comment regards the role played by parameter σ. We said that σ does not influence the parametric threshold for convective stability, expressed by Eq. (8.22). We can also infer that the threshold for absolute instability is not influenced by the value of σ, as well. From Eq. (8.34), this is quite evident in the case $Pe = 0$. When $Pe > 0$, just the same conclusion is expected as the saddle points k_0 are evaluated by solving Eq. (8.27) which does not contain σ. Moreover, the condition

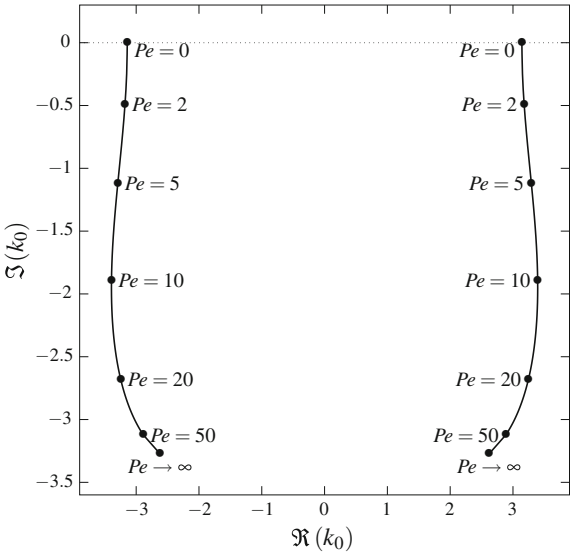

Fig. 8.2 Prats problem: migration of the pertinent saddle points, with increasing values of Pe, for the threshold to absolute instability

of absolute instability is determined by the inequality $\Re(\lambda(k_0)) > 0$, or equivalently $\sigma\,\Re(\lambda(k_0)) > 0$, by employing Eq. (8.25). The right-hand side of Eq. (8.25) does not contain σ. Thus, we conclude that the value of σ only affects the phase velocity of the normal mode perturbations driving the instability.

When $Pe > 0$, detecting the saddle points by employing Eqs. (8.25) and (8.27) implies the solution of a system of two algebraic equations, that is $\lambda'(k_0) = 0$ and $\Re(\lambda(k_0)) = 0$. This means that we find multiple complex roots of Eq. (8.27) for every value of $Pe > 0$. Each saddle point k_0 is associated with a uniquely determined real value of R. By analogy with what we found for the case $Pe = 0$, we expect that just two of these roots represent the pertinent saddle points for establishing the value of R_a. The value of R_a is to be obtained from Eq. (8.25) through the condition $\Re(\lambda(k_0)) = 0$, which yields the threshold for absolute instability.

The practical strategy is starting from $Pe = 0$ and gradually increasing Pe. We assume $n = 1$, consistently with what we did for the case $Pe = 0$. Step by step, one tracks the migration of the saddle points k_0 starting from those found with $Pe = 0$, and given by Eq. (8.35). With each of these saddle points, one evaluates the associated value of R as the root of $\Re(\lambda(k_0)) = 0$. The position of the saddle points which are relevant for the onset of absolute instability is illustrated in Fig. 8.2. Such points are tracked for increasing values of $Pe > 0$. For each value of Pe, there are two twin points differing only by the sign of the real part of k_0. They originate from the pair defined by Eq. (8.35), with $Pe = 0$, and they have drifted to negative values of $\Im(k_0)$, when $Pe > 0$.

There are multiple saddle points k_0 for every assignment of (n, Pe, R). One then associates a value of R to every fixed pair (n, Pe), by imposing the third algebraic equation $\Re(\lambda(k_0)) = 0$. Such procedure can be practically illustrated by considering the case where $n = 1$ and $Pe = 10$. We obtain

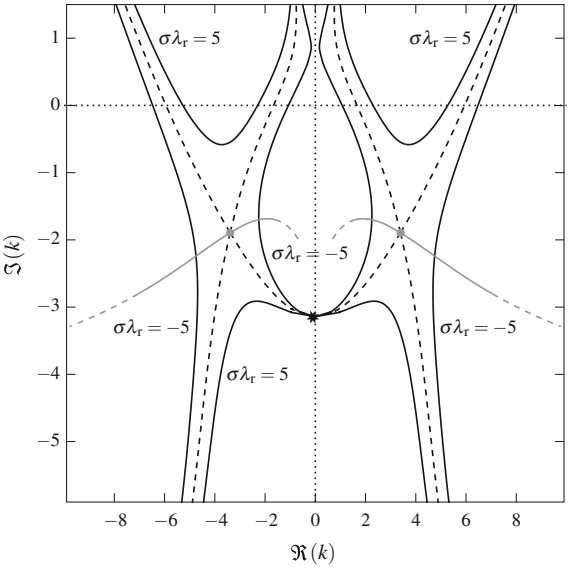

Fig. 8.3 Prats problem: map of the isolines of $\Re(\lambda) = \lambda_r$ (black solid lines) for $Pe = 10$ and $R = R_a = 57.8036$. The dashed black lines are for $\lambda_r = 0$. The grey dots are the saddle points, while the grey lines are the lines of steepest descent. The black asterisk denotes the singularity $k = -i\pi$

$$k_0 = \pm 3.39297 - i\,1.89300\,, \qquad R = 57.8036\,,$$

$$k_0 = \pm 1.84692 + i\,3.39151\,, \qquad R = -36.0935\,,$$

$$k_0 = i\,1.51492\,, \qquad R = 25\,,$$

$$k_0 = -i\,6.51492\,, \qquad R = 25\,. \tag{8.36}$$

We have to exclude the saddle points $k_0 = \pm 1.84692 + i\,3.39151$ as they would yield a negative value of R for the onset of absolute instability, -36.0935, which is unphysical given that we must get $R_a \geqslant R_c$. Just the same argument leads us to the exclusion of the purely imaginary saddle points $k_0 = i\,1.51492$ and $k_0 = -i\,6.51492$. This means that, with $Pe = 10$, the pertinent saddle points for the onset of absolute instability are $k_0 = \pm 3.39297 - i\,1.89300$ and that the threshold for the onset of absolute instability is $R_a = 57.8036$. All this reasoning is to be completed by checking whether the holomorphy requirement is satisfied with $Pe = 10$, $R_a = 57.8036$ and the pair of saddle points $k_0 = \pm 3.39297 - i\,1.89300$.

Figure 8.3 displays a map of the isolines of $\Re(\lambda) = \lambda_r$ in the complex k plane relative to the case $Pe = 10$ and $R = R_a = 57.8036$. The lines of steepest descent crossing the twin saddle points $k_0 = \pm 3.39297 - i\,1.89300$ are displayed in grey. It is evident from Fig. 8.3 that one can continuously deform the path γ given by the real axis, $\Im(k) = 0$, into a path γ^* which crosses both the twin saddle points, $k_0 = \pm 3.39297 - i\,1.89300$. Such deformation can be exploited so that γ^* locally coincides with a line of steepest descent and no singularity of $\lambda(k)$ is enclosed within the region bounded by $\gamma \cup \gamma^*$, as described in Sect. 3.5.3. Then, the premises

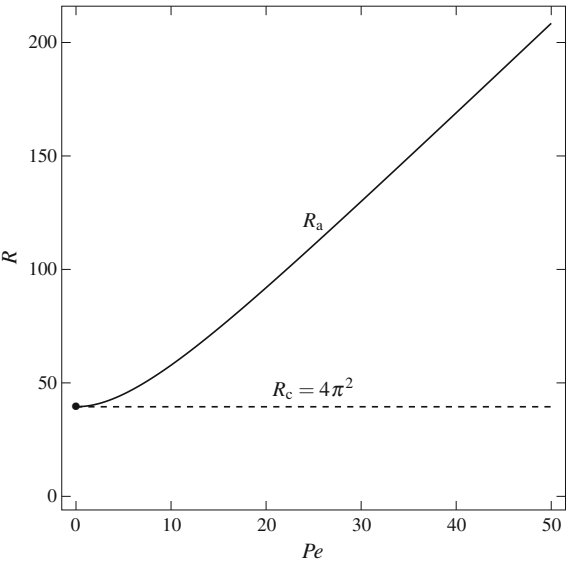

Fig. 8.4 Prats problem: plot of R_a versus Pe as obtained by solving Eq. (8.27) with $\Re(\lambda(k)) = 0$. The values of R_a are compared with $R_c = 4\pi^2$, which is independent of Pe

for applying the steepest-descent approximation, denoted under the shorthand of holomorphy requirement, are all satisfied.

One may wonder whether taking $n > 1$ can affect the conclusion just drawn for $Pe = 10$. If one sets $n = 2$, Eq. (8.36) is to be replaced with

$$\begin{aligned} k_0 &= \pm 6.58511 - \mathrm{i}\, 2.24028 \,, \qquad R = 180.111 \,, \\ k_0 &= \pm 3.02861 + \mathrm{i}\, 6.72099 \,, \qquad R = -69.4442 \,, \\ k_0 &= \mathrm{i}\, 4.26228 \,, \qquad R = 25 \,, \\ k_0 &= -\mathrm{i}\, 9.26228 \,, \qquad R = 25 \,. \end{aligned} \tag{8.37}$$

Again, the values $R = -69.4442$ and $R = 25$ are to be excluded as possible candidates for R_a as they are smaller than R_c. Then, one is left with $R = 180.111$ that, in any case, does not provide a lower threshold to absolute instability than that obtained by considering $n = 1$.

This lengthy description refers to the evaluation of R_a for a very special case, that is, $Pe = 10$. It should be ideally repeated for every value of Pe. In practice, such a check of the holomorphy requirement can only be carried out for a finite number of values of Pe. What one concludes is that the evaluation of R_a can be practically achieved, for a given Pe, by tracking the continuous change of the twin saddle points given by Eq. (8.35) for $Pe = 0$. The resulting evaluation of R_a versus Pe is illustrated in Fig. 8.4. This figure shows that, starting with $R_a = R_c = 4\pi^2$ for $Pe = 0$, a gap exists between the thresholds of convective and absolute instabilities as Pe increases above zero. This gap grows larger and larger with Pe.

A feature highlighted by Fig. 8.4 is the linear behaviour in the trend of R_a versus Pe when Pe becomes very large. The characteristics of this asymptotic regime can be detected by setting

$$R = \xi \, Pe \, , \tag{8.38}$$

where ξ is a constant to be determined. We substitute Eq. (8.38) into Eq. (8.27), and we let $Pe \to \infty$. What we obtain is

$$\frac{2 \, k \, \xi \, n^2 \pi^2}{(n^2 \pi^2 + k^2)^2} = \mathrm{i} \, , \tag{8.39}$$

while the dispersion relation (8.25) can be approximated as

$$\frac{\sigma \, \lambda(k)}{Pe} = \frac{\xi \, k^2}{n^2 \pi^2 + k^2} - \mathrm{i} \, k \, , \quad n = 1, 2, 3, \ldots \, . \tag{8.40}$$

The saddle points k_0 and the corresponding values of ξ are obtained by solving the system made with equations (8.39) and $\Re(\sigma \, \lambda(k)/Pe) = 0$, as expressed by employing Eq. (8.40). The result is

$$\begin{aligned} k_0 &= \pm \frac{\pi \, n}{4} \sqrt{7 + \sqrt{17}} - \frac{\mathrm{i} \, \pi \, n}{4} \sqrt{5 + 3\sqrt{17}} \, , \quad \xi = \frac{\pi \, n}{8} \sqrt{51 \sqrt{17} - 107} \, , \\ k_0 &= \pm \frac{\pi \, n}{4} \sqrt{7 + \sqrt{17}} + \frac{\mathrm{i} \, \pi \, n}{4} \sqrt{5 + 3\sqrt{17}} \, , \quad \xi = -\frac{\pi \, n}{8} \sqrt{51 \sqrt{17} - 107} \, . \end{aligned} \tag{8.41}$$

Obviously, the saddle points leading to a negative ξ are to be rejected as $R_a = \xi \, Pe$, with $Pe > 0$, cannot be negative. Thus, the pair of twin saddle points leading to the threshold of absolute instability in the limit $Pe \to \infty$ is

$$k_0 = \pm \frac{\pi \, n}{4} \sqrt{7 + \sqrt{17}} - \frac{\mathrm{i} \, \pi \, n}{4} \sqrt{5 + 3\sqrt{17}} \approx (\pm 2.61941 - \mathrm{i} \, 3.27327) \, n \, . \tag{8.42}$$

For $n = 1$, the pair of saddle points given by Eq. (8.42) are displayed in Fig. 8.2. One may easily reckon that the location of the saddle points pertinent for evaluating the threshold to absolute instability tends to attain rapidly its asymptotic settlement, defined by Eq. (8.42) with $n = 1$, when Pe becomes larger than 50.

The attainment of the asymptotic regime is in fact illustrated in Fig. 8.5, where the trend of R_a/Pe versus Pe is displayed. This figure shows the asymptote,

$$\frac{R_a}{Pe} = \frac{\pi}{8} \sqrt{51 \sqrt{17} - 107} \approx 3.99084 \, , \tag{8.43}$$

as a dotted line. One may evaluate that R_a/Pe matches its asymptotic value within less than 5 % when $Pe > 45.5$.

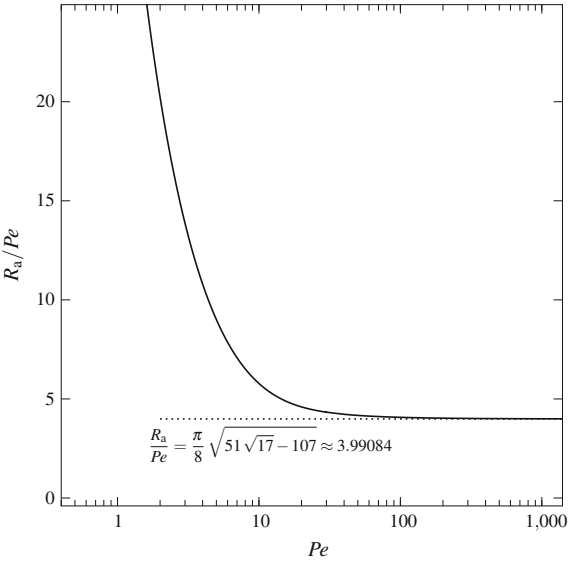

Fig. 8.5 Prats problem: plot of R_a/Pe versus Pe as compared with the asymptotic behaviour for large values of Pe (dotted line) given by Eq. (8.43)

Table 8.1 reports the threshold data defining the transition to absolute instability. The whole range of positive Péclet numbers is spanned, thus showing the extrema of very small Pe, where R_a approaches $R_c = 4\pi^2$, and that of very large Pe, where R_a/Pe approaches its asymptotic value given by Eq. (8.43).

Regarding the possible saddle points obtained by solving Eq. (8.27), for a given (Pe, n), a comment is desirable regarding those expressed analytically as

$$k_0 = -\frac{i}{4}\left(Pe \pm \sqrt{16\,n^2\pi^2 + Pe^2}\right) . \tag{8.44}$$

These saddle points yield simultaneously $\Re(\lambda(k_0)) = 0$ and $\Im(\lambda(k_0)) = 0$, with

$$R = \frac{Pe^2}{4} . \tag{8.45}$$

This family of solutions of the dispersion relation (8.27) has been encountered either in Eq. (8.36) or in Eq. (8.37) relative to the sample case $Pe = 10$ with $n = 1$ and $n = 2$, respectively. In that example, we excluded these saddle points as they were subcritical with $R = Pe^2/4 = 25 < R_c$. However, this is not always the case. In fact, for $n = 1$, these solutions regard the supercritical domain for $Pe > 4\pi \approx 12.5664$ and, provided that Pe is less than approximately 18.6583, they are associated with values of $R = Pe^2/4$ smaller than the values of R_a evaluated so far and reported either in Fig. 8.4 or in Table 8.1. Does it mean that we should amend our conclusions about the threshold to absolute instability for the range $4\pi < Pe < 18.6583$? The answer is negative. If these saddle points were to contribute to the evaluation of R_a, then k_0 should coincide with $k_c = \pi$ when $Pe = 4\pi$ and $R_a = R_c$, but this is

Table 8.1 Prats problem: pertinent saddle points and threshold values of R_a for the onset of absolute instability

Pe	k_0	R_a	R_a/Pe
0	± 3.14159	39.4784	∞
1	$\pm 3.15128 - \mathrm{i}\,0.24846$	39.7269	39.7269
5	$\pm 3.29255 - \mathrm{i}\,1.12014$	45.0277	9.00553
7	$\pm 3.35371 - \mathrm{i}\,1.46714$	49.5519	7.07884
10	$\pm 3.39297 - \mathrm{i}\,1.89300$	57.8036	5.78036
15	$\pm 3.34682 - \mathrm{i}\,2.38924$	74.0236	4.93491
20	$\pm 3.24476 - \mathrm{i}\,2.68308$	91.9528	4.59764
25	$\pm 3.14596 - \mathrm{i}\,2.85317$	110.732	4.42926
30	$\pm 3.06606 - \mathrm{i}\,2.95566$	129.947	4.33158
35	$\pm 3.00401 - \mathrm{i}\,3.02135$	149.404	4.26868
40	$\pm 2.95570 - \mathrm{i}\,3.06602$	169.003	4.22506
45	$\pm 2.91750 - \mathrm{i}\,3.09797$	188.692	4.19315
50	$\pm 2.88675 - \mathrm{i}\,3.12176$	208.441	4.16882
60	$\pm 2.84058 - \mathrm{i}\,3.15458$	248.054	4.13424
70	$\pm 2.80776 - \mathrm{i}\,3.17599$	287.761	4.11087
80	$\pm 2.78332 - \mathrm{i}\,3.19097$	327.522	4.09403
90	$\pm 2.76444 - \mathrm{i}\,3.20201$	367.319	4.08133
100	$\pm 2.74943 - \mathrm{i}\,3.21048$	407.140	4.07140
1000	$\pm 2.63194 - \mathrm{i}\,3.26797$	3998.25	3.99825
∞	$\pm 2.61941 - \mathrm{i}\,3.27327$	∞	3.99084

obviously not the case. Another reason is the following. For every Pe within the range $4\pi < Pe < 18.6583$ and for $n = 1$, the two saddle points given by Eq. (8.44) and corresponding to $Ra = Pe^2/4$ are purely imaginary. One lies between the two singularities $k = \pm \mathrm{i}\,\pi$, while the other one lies below $k = -\mathrm{i}\,\pi$. Trying to draw a deformed path, which is locally of steepest descent and which crosses both these saddle points is not possible without trapping the singularity $k = -\mathrm{i}\,\pi$ within the region of space between the deformed path and the real k-axis. This feature precludes the application of the holomorphy requirement. Thus, we infer that the branches of saddle points defined by Eq. (8.44) are not genuine branches of absolute instability, so that they can be disregarded.

8.3 Prats Problem with Form-Drag Effect

We now explore how our analysis of convective and absolute instabilities in the Prats problem changes by assuming Darcy–Forchheimer's law, instead of Darcy's law, to model the local momentum balance. Again, we carry out a two-dimensional study by assuming that all fields are independent of the spanwise y-coordinate. As in Sect. 8.2, we neglect the effect of viscous dissipation for the sake of simplicity.

The two-dimensional velocity field (u, w), lying in the (x, z) plane, the temperature field T, the coordinates (x, z) and time t, can be written in a dimensionless form by adopting the transformation (8.1).

Following Eq. (7.84), within the Oberbeck–Boussinesq approximation and according to Darcy–Forchheimer's law, the local balance equations of mass, momentum and energy are given by

$$\frac{\partial u}{\partial x} + \frac{\partial w}{\partial z} = 0 \,,$$

$$\frac{\partial(\Xi\, u)}{\partial z} - \frac{\partial(\Xi\, w)}{\partial x} = -\, R\, \frac{\partial T}{\partial x} \,,$$

$$\sigma\, \frac{\partial T}{\partial t} + u\, \frac{\partial T}{\partial x} + w\, \frac{\partial T}{\partial z} = \frac{\partial^2 T}{\partial x^2} + \frac{\partial^2 T}{\partial z^2} \,. \tag{8.46}$$

In Eq. (8.46), the local momentum balance has been formulated by evaluating the curl of the local momentum balance. Function Ξ is defined as

$$\Xi = 1 + G\, \sqrt{u^2 + w^2} \,, \tag{8.47}$$

while the dimensionless parameters R and G are given by

$$R = \frac{g\beta(T_1 - T_2)KL}{\nu\alpha} \,, \qquad G = \frac{F\alpha\sqrt{K}}{\nu L} \,, \tag{8.48}$$

where F is the form-drag coefficient. The governing equations (8.46) are completed by the boundary conditions,

$$\begin{aligned} z = 0 \;:&\quad w = 0 \,, \quad T = 1 \,, \\ z = 1 \;:&\quad w = 0 \,, \quad T = 0 \,. \end{aligned} \tag{8.49}$$

By analogy with Eq. (8.6), we write a streamfunction–temperature formulation of the governing equations and boundary conditions

$$\frac{\partial}{\partial x}\left(\Xi\, \frac{\partial \psi}{\partial x}\right) + \frac{\partial}{\partial z}\left(\Xi\, \frac{\partial \psi}{\partial z}\right) + R\, \frac{\partial T}{\partial x} = 0 \,,$$

$$\sigma\, \frac{\partial T}{\partial t} + \frac{\partial \psi}{\partial z}\, \frac{\partial T}{\partial x} - \frac{\partial \psi}{\partial x}\, \frac{\partial T}{\partial z} = \frac{\partial^2 T}{\partial x^2} + \frac{\partial^2 T}{\partial z^2} \,,$$

$$\begin{aligned} z = 0 \;:&\quad \frac{\partial \psi}{\partial x} = 0 \,, \quad T = 1 \,, \\ z = 1 \;:&\quad \frac{\partial \psi}{\partial x} = 0 \,, \quad T = 0 \,. \end{aligned} \tag{8.50}$$

The same stationary solution, (ψ_b, T_b), expressed by Eqs. (8.8) and (8.9) satisfies also Eq. (8.50). We already pointed out that this solution describes a uniform flow, in the x-direction, with a dimensionless rate expressed by the Péclet number Pe and with a linear temperature distribution along the vertical z-direction. We implicitly consider $Pe \geqslant 0$, as a sign change of Pe does not correspond to physically different situations.

8.3.1 Stability Analysis

We assume perturbations of the basic solution given by,

$$\psi = \psi_b + \varepsilon\, \Psi = Pe\, z + \varepsilon\, \Psi\ , \qquad T = T_b + \varepsilon\, \Theta = 1 - z + \varepsilon\, \Theta\ , \tag{8.51}$$

where $|\varepsilon| \ll 1$. On substituting Eq. (8.51) into Eq. (8.50) and neglecting terms $O(\varepsilon^2)$, one obtains

$$\begin{gathered}
(1 + G\ Pe)\, \frac{\partial^2 \Psi}{\partial x^2} + (1 + 2\, G\ Pe)\, \frac{\partial^2 \Psi}{\partial z^2} + R\, \frac{\partial \Theta}{\partial x} = 0\ , \\
\sigma\ \frac{\partial \Theta}{\partial t} + Pe\ \frac{\partial \Theta}{\partial x} + \frac{\partial \Psi}{\partial x} = \frac{\partial^2 \Theta}{\partial x^2} + \frac{\partial^2 \Theta}{\partial z^2}\ , \\
z = 0, 1\ : \qquad \frac{\partial \Psi}{\partial x} = 0\ , \quad \Theta = 0\ .
\end{gathered} \tag{8.52}$$

Following the usual procedure, established with Eq. (8.13), we write (Ψ, Θ) in terms of their Fourier transforms, $\left(\tilde{\Psi}, \tilde{\Theta}\right)$, given by

$$\tilde{\Psi} = f(z)\, \mathrm{e}^{\lambda(k)\, t}\ , \qquad \tilde{\Theta} = -\,\mathrm{i}\, k\, h(z)\, \mathrm{e}^{\lambda(k)\, t}\ . \tag{8.53}$$

Then, by employing Eqs. (8.13) and (8.53), we employ the Fourier transformation for Eq. (8.52) to write

$$\begin{gathered}
\left[(1 + 2\, G\ Pe)\, \frac{\mathrm{d}^2}{\mathrm{d}\, z^2} - (1 + G\ Pe)\, k^2\right] f + R\, k^2\, h = 0\ , \\
\left[\frac{\mathrm{d}^2}{\mathrm{d}\, z^2} - k^2 - \sigma\, \lambda(k) - \mathrm{i}\, k\, Pe\right] h + f = 0\ , \\
z = 0, 1\ : \qquad f = 0\ , \quad h = 0\ .
\end{gathered} \tag{8.54}$$

The eigenvalue problem (8.54) is solved by combining the two ordinary differential equations into a single one,

$$\left[(1+2\,G\,Pe)\,\frac{\mathrm{d}^2}{\mathrm{d}\,z^2}-(1+G\,Pe)\,k^2\right]\left[\frac{\mathrm{d}^2}{\mathrm{d}\,z^2}-k^2-\gamma(k)\right]h-R\,k^2\,h=0\;, \tag{8.55}$$

where $\gamma(k)$ is defined in the same manner as in the analysis of the Prats problem carried out in terms of Darcy's law, namely

$$\gamma(k)=\sigma\,\lambda(k)+\mathrm{i}\,k\,Pe\;. \tag{8.56}$$

The eigenfunction $h(z)$ can be expressed as

$$h(z)=\sin(n\,\pi\,z)\;,\quad n=1,2,3,\;\ldots\;, \tag{8.57}$$

so that the boundary conditions (8.54) are satisfied, while substitution of Eq. (8.57) into Eq. (8.55) yields the dispersion relation

$$\left[(1+2\,G\,Pe)\,n^2\,\pi^2+(1+G\,Pe)\,k^2\right]\left[n^2\,\pi^2+k^2+\gamma(k)\right]-R\,k^2=0\;. \tag{8.58}$$

Equation (8.58) can be solved for $\gamma(k)$ to obtain

$$\gamma(k)=\frac{R\,k^2-\left[(1+2\,G\,Pe)\,n^2\,\pi^2+(1+G\,Pe)\,k^2\right]\left(n^2\,\pi^2+k^2\right)}{(1+2\,G\,Pe)\,n^2\,\pi^2+(1+G\,Pe)\,k^2}\;, \tag{8.59}$$

with $n=1,2,3,\;\ldots$.

8.3.2 *Convective Instability*

The analysis of the convective instability for the Prats problem with form-drag effect has been carried out by Rees [13].

By recalling that $\lambda=\eta-\mathrm{i}\,\omega$ and by taking into account Eq. (8.56), the imaginary part of the dispersion relation (8.58) yields

$$(\sigma\,\omega-k\,Pe)\left[(1+2\,G\,Pe)\,n^2\,\pi^2+(1+G\,Pe)\,k^2\right]=0\;. \tag{8.60}$$

Thus, we obtain just the same expression of ω as given by Eq. (8.20) for the case where the validity of Darcy's law is invoked,

$$\omega=\frac{k\,Pe}{\sigma}\;. \tag{8.61}$$

As a consequence, we reach the same conclusion discussed for the case of Darcy's flow. The phase velocity of the normal mode with wave number k is a constant, $\omega/k = Pe/\sigma$. On the other hand, the expression of the growth rate η is inferred from Eq. (8.59),

$$\eta = \frac{R\,k^2 - \left[(1 + 2\,G\,Pe)\,n^2\,\pi^2 + (1 + G\,Pe)\,k^2\right]\left(n^2\,\pi^2 + k^2\right)}{\sigma\left[(1 + 2\,G\,Pe)\,n^2\,\pi^2 + (1 + G\,Pe)\,k^2\right]}\,, \tag{8.62}$$

and it depends explicitly on the form-drag parameter G.

Convective instability arises when the growth rate η becomes positive. Equation (8.62) implies that this is the case when

$$R > \frac{\left(\pi^2 + k^2\right)^2}{k^2} + G\,Pe\,\frac{\left(2\,\pi^2 + k^2\right)\left(\pi^2 + k^2\right)}{k^2}\,, \tag{8.63}$$

while the neutral stability condition is written as

$$R = \frac{\left(\pi^2 + k^2\right)^2}{k^2} + G\,Pe\,\frac{\left(2\,\pi^2 + k^2\right)\left(\pi^2 + k^2\right)}{k^2}\,. \tag{8.64}$$

Equations (8.63) and (8.64) are relative to modes with $n = 1$. In fact, these modes yield the least threshold for attaining positive growth rates, $\eta > 0$. In the limit $G \to 0$, that is switching off the form-drag effect, we recover the neutral stability function $R(k)$ determined for the Prats problem modelled by Darcy's law, given by Eq. (8.22). The effect of the form-drag coefficient is a stabilisation of the basic state. In fact, for a given k, the neutral stability value of R, defined by the right-hand side of Eq. (8.64), is an increasing function of the form-drag parameter G. The larger is G, the larger is the value of R needed for the onset of convective instability. The critical values of k and R are given by

$$k_c = \pi\left(\frac{1 + 2\,G\,Pe}{1 + G\,Pe}\right)^{1/4}\,, \quad R_c = \pi^2\left(\sqrt{1 + 2\,G\,Pe} + \sqrt{1 + G\,Pe}\right)^2\,. \tag{8.65}$$

As expected, in the Darcy's law limiting case, $G \to 0$, the critical values of k and R coincide with those expressed by Eq. (7.83).

Unlike the case where Darcy's law hold, when $G > 0$ the neutral stability condition (8.64) is influenced by the Péclet number, Pe, through the product $G\,Pe$. On the other hand, when the basic horizontal flow has a zero rate, $Pe \to 0$, the convective stability analysis of the Prats problem is not influenced by the form-drag effect. In this limit, the neutral stability condition and the critical values (k_c, R_c) coincide with those found for the Horton–Rogers–Lapwood problem, as we pointed out in Sect. 7.6.4.

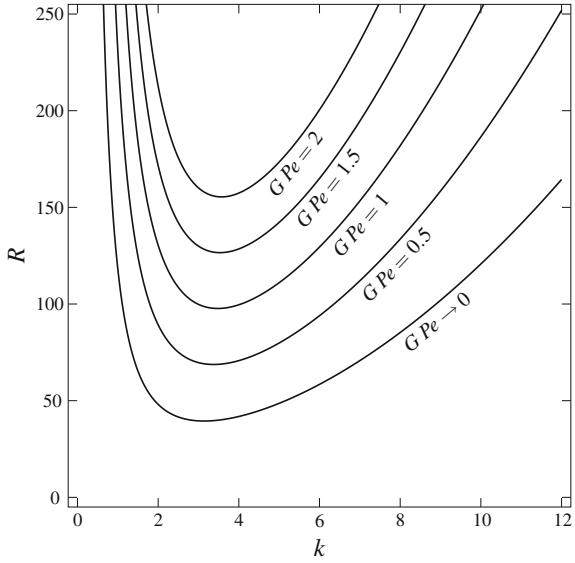

Fig. 8.6 Prats problem with form-drag effect: neutral stability curves in the (k, R) plane for different values of $G\,Pe$

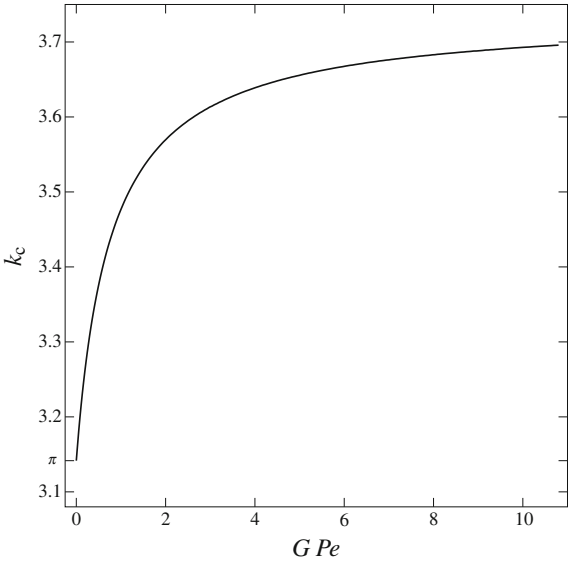

Fig. 8.7 Prats problem with form-drag effect: plot of k_c versus $G\,Pe$

A graphical representation of the neutral stability condition as described by Eq. (8.64) is provided in Fig. 8.6. The stabilising effect of the increasing parameter $G\,Pe$ is clearly illustrated in this figure.

Plots of k_c and R_c versus $G\,Pe$ are reported in Figs. 8.7 and 8.8. These figures clearly indicate that both the critical value of k and that of R, given by Eq. (8.65), increase with the intensification of the form-drag effect.

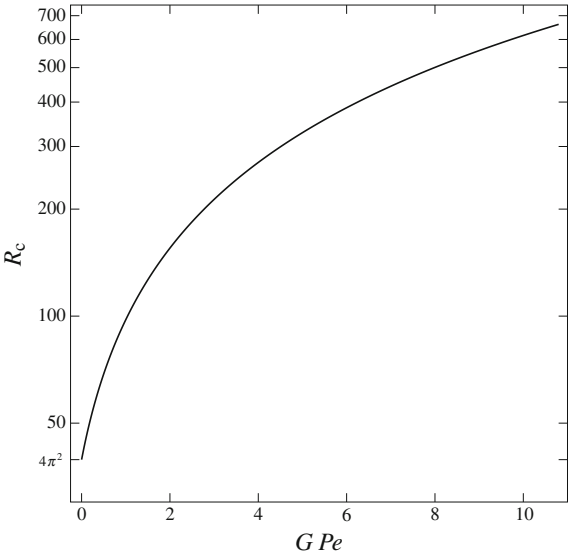

Fig. 8.8 Prats problem with form-drag effect: plot of R_c versus $G\,Pe$

8.3.3 Absolute Instability

The detection of the parametric transition to absolute instability involves the study of the asymptotic behaviour at large times for wave packet disturbances governed by Eq. (8.52). Such wave packets are still given by Eq. (8.23), with $\lambda(k)$ now given by Eqs. (8.56) and (8.59), namely

$$\sigma\,\lambda(k) = \frac{R\,k^2 - \left[(1+2\,G\,Pe)\,n^2\,\pi^2 + (1+G\,Pe)\,k^2\right]\left(n^2\,\pi^2 + k^2\right)}{(1+2\,G\,Pe)\,n^2\,\pi^2 + (1+G\,Pe)\,k^2} - \mathrm{i}\,k\,Pe\ , \tag{8.66}$$

with $n = 1, 2, 3, \ldots$. We follow the usual procedure, so that our first step is determining the saddle points of $\lambda(k)$. This means finding the roots of equation

$$\lambda'(k) = 0\ , \tag{8.67}$$

in the complex plane, $k \in \mathbb{C}$. On account of Eq. (8.66), Eq. (8.67) yields

$$\frac{2\,k\,R\,(1+2\,G\,Pe)\,n^2\pi^2}{\left[(1+2\,G\,Pe)\,n^2\pi^2 + (1+G\,Pe)\,k^2\right]^2} = 2\,k + \mathrm{i}\,Pe\ . \tag{8.68}$$

The solution of Eq. (8.68) to yield the saddle points and the evaluation of the associated values of R by setting $\Re(\lambda(k)) = 0$ goes much in the same manner as described in Sect. 8.2.4 relative to the case of Darcy's flow regime. When the form-drag effect is important, the position of the saddle point depends not only on Pe but also

on G. Unlike in the case of convective instability, where the neutral stability condition depends just on the product $G\,Pe$, here the two parameters G and Pe act independently, as made evident by Eqs. (8.67) and (8.68). What we concluded in Sect. 8.2.4 for the case $Pe = 0$ still holds for every $G > 0$. In fact, the form-drag contribution to the momentum balance is ineffective when $Pe = 0$. This means that Eq. (8.34) holds for every value of G if $Pe = 0$.

The evaluation of the saddle points depends significantly on G. Thus, with $n = 1$, $Pe = 10$ and $G = 0.05$, Eq. (8.36) is now replaced by

$$\begin{gathered} k_0 = \pm\, 3.78103 - \mathrm{i}\, 2.02087\ , \qquad R = 99.7984\ , \\ k_0 = \pm\, 2.13913 + \mathrm{i}\, 3.93823\ , \qquad R = -67.5161\ , \\ k_0 = \mathrm{i}\, 1.57971\ , \qquad R = 53.9911\ , \\ k_0 = -\,\mathrm{i}\, 6.82254\ , \qquad R = 33.9434\ . \end{gathered} \tag{8.69}$$

The determination of the saddle points identifying the transition to absolute instability is straightforward. We exclude those leading to a negative R, and those with R smaller than R_c. With $Pe = 10$ and $G = 0.05$, Eq. (8.65) yields $R_c = 68.7329$. Thus, we conclude that the saddle points which are relevant for the onset of absolute instability are $k_0 = \pm\, 3.78103 - \mathrm{i}\, 2.02087$ and that $R_a = 99.7984$.

Tracking the threshold conditions for absolute instability, with a given G, means recording the evolution of the saddle points as Pe increases above zero. We start from the pair given by Eq. (8.35), and we approach asymptotically the regime defined by the limit $Pe \to \infty$. We can study this asymptotic regime by recognising that the correct scaling of R at large Pe is not given by Eq. (8.38), but we have

$$R = \zeta\, G\, Pe^2\ , \tag{8.70}$$

instead.

Then, we keep the parameters ζ and G finite while $Pe \to \infty$, so that Eqs. (8.39) and (8.40) are now rewritten as

$$\frac{4\,k\,\zeta\,n^2\pi^2}{(2\,n^2\pi^2 + k^2)^2} = \mathrm{i}\ , \tag{8.71}$$

and

$$\frac{\sigma\,\lambda(k)}{Pe} = \frac{\zeta\,k^2}{2\,n^2\pi^2 + k^2} - \mathrm{i}\,k\ , \quad n = 1, 2, 3, \ \ldots\ . \tag{8.72}$$

One identifies the saddle points

$$k_0 = \pm \frac{\pi\, n}{2} \sqrt{\frac{7+\sqrt{17}}{2}} - \frac{\mathrm{i}\,\pi\, n}{2} \sqrt{\frac{5+3\sqrt{17}}{2}} \approx (\pm\, 3.70440 - \mathrm{i}\, 4.62910)\, n\ , \tag{8.73}$$

as associated with the positive value

$$\zeta = \frac{\pi\, n}{4} \sqrt{\frac{51\sqrt{17}-107}{2}} \approx 5.64390\, n\ . \tag{8.74}$$

Thus, we identify the threshold to absolute instability in the limiting case $Pe \to \infty$ by setting $n = 1$, namely

$$\frac{R_\mathrm{a}}{G\, Pe^2} = \frac{\pi}{4} \sqrt{\frac{51\sqrt{17}-107}{2}} \approx 5.64390\ . \tag{8.75}$$

The migration of the saddle points, as Pe increases above zero, starting from those found for $Pe = 0$, is illustrated in Fig. 8.9. The top left frame, relative to $G = 0$, is congruent with Fig. 8.2. A comparison with the top right frame of Fig. 8.9, relative to $G = 0.01$, highlights the discontinuity in the large Pe behaviour when G switches from 0 to an arbitrarily small, but positive, value. This is a consequence of the different behaviours defined by Eqs. (8.43) and (8.75). If $G = 0$, $R_\mathrm{a} \sim Pe$ when Pe is extremely large, while $R_\mathrm{a} \sim Pe^2$ when $G > 0$ and $Pe \gg 1$. In fact, the plots reported for $G = 0$ and $G = 0.01$ compare well for $Pe < 5$, while an increasing discrepancy is detected for higher values of Pe. The evolution of these plots as G becomes larger and larger is displayed in the other frames of Fig. 8.9, relative to $G = 0.02,\ 0.05,\ 0.1,\ 0.2$. What is common to all the frames with $G > 0$ is the position of the saddle points for $Pe = 0$ and $Pe \to \infty$.

Figure 8.10 shows the thresholds to convective instability, $R = R_\mathrm{c}$, and to absolute instability, $R = R_\mathrm{a}$, versus Pe. Different frames are relative to different values of G. We note that the gap between the values of R_a and R_c increases rapidly with Pe, starting from 0 when $Pe = 0$ and tending to infinity when $Pe \to \infty$. The frame for $G = 0$ is congruent with the plots provided in Fig. 8.4. As we already pointed out, this is the only case where R_c is independent of Pe. When $G > 0$, R_c increases with Pe approaching an asymptotic regime where

$$\frac{R_\mathrm{c}}{G\, Pe} = \pi^2 \left(1+\sqrt{2}\right)^2 \approx 57.5243\ , \tag{8.76}$$

when $Pe \gg 1$. Equation (8.76) is a consequence of Eq. (8.65). A comparison between Eqs. (8.75) and (8.76) reveals that R_a grows more rapidly than R_c for large values of Pe, so that

$$\frac{R_\mathrm{a}}{R_\mathrm{c}} = \frac{\left(3\sqrt{2}-4\right)\sqrt{51\sqrt{17}-107}}{8\,\pi}\, Pe \approx 0.0981134\, Pe\ . \tag{8.77}$$

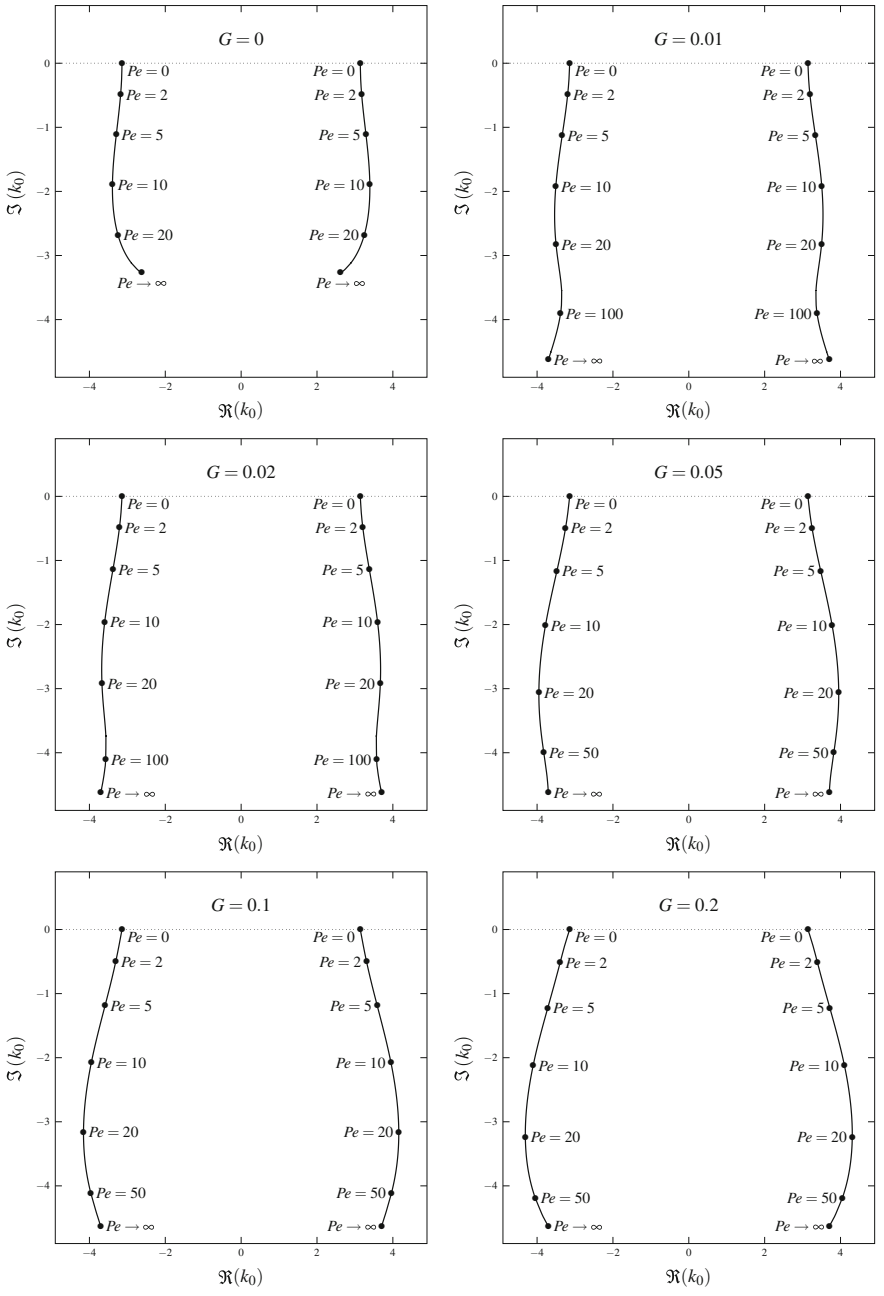

Fig. 8.9 Prats problem with form-drag effect: migration of the pertinent saddle points, with increasing values of Pe and fixed values of G, for the threshold to absolute instability

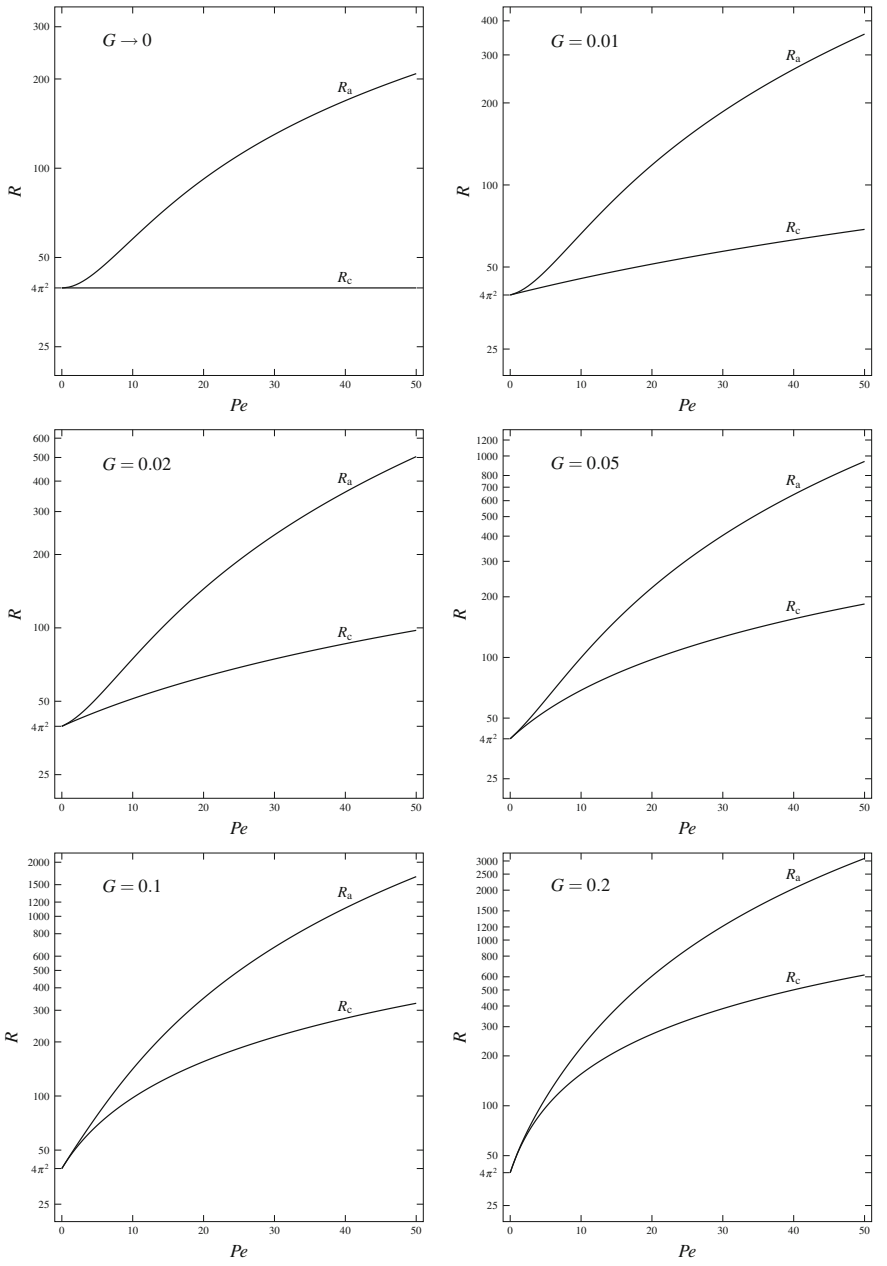

Fig. 8.10 Prats problem with form-drag effect: thresholds R_c and R_a to convective and absolute instabilities versus Pe, with increasing values of G

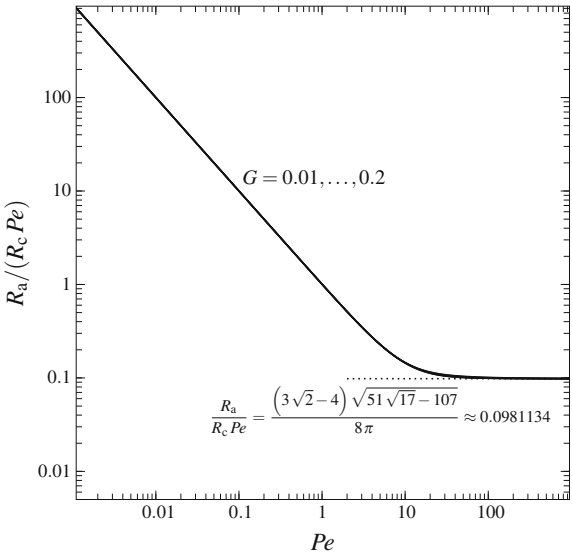

Fig. 8.11 Prats problem with form-drag effect: plots of $R_a/(R_c\,Pe)$ versus Pe within the range $0.01 \leqslant G \leqslant 0.2$

Equation (8.77) is to be intended as an asymptotic formula. Evidently, it does not make any good sense if Pe is smaller than approximately 10.19, as it would predict $R_a < R_c$, which is absurd. Interestingly enough, Eq. (8.77) reveals that the asymptotic behaviour of the ratio R_a/R_c is independent of $G > 0$.

Interestingly enough, on account of Eqs. (7.83) and (8.43), relative to the case $G = 0$, Eq. (8.77) does not hold true in the Darcy's flow limit, as we have

$$\frac{R_a}{R_c} = \frac{\sqrt{51\sqrt{17}-107}}{32\,\pi}\,Pe \approx 0.101089\,Pe\ . \tag{8.78}$$

In practice, the discrepancy between Eq. (8.78), for $G = 0$, and Eq. (8.77), for any $G > 0$, is not very strong, but it is symptomatic of the difference in the asymptotic behaviour detected in these cases when $Pe \gg 1$.

Figure 8.11 displays the trend of $R_a/(R_c\,Pe)$ versus Pe for different values of G within the range $0.01 \leqslant G \leqslant 0.2$. The dependence on G is barely visible, and it is concentrated in a narrow region between $Pe = 10$ and $Pe = 100$. This is an interesting, to some extent expected, behaviour. In fact, when $Pe \ll 1$, one has the asymptotic formula $R_a/(R_c\,Pe) = 1/Pe$, which is independent of G exactly as it happens with Eq. (8.77) for the limiting case $Pe \gg 1$. That a slight dependence on G is indeed present is better illustrated in Fig. 8.12, where the same data reported in Fig. 8.11 are zoomed in the range $10 \leqslant Pe \leqslant 100$.

A check that the holomorphy requirement is satisfied in the limiting case $Pe \to \infty$ is illustrated in Fig. 8.13. This figure displays the behaviour of $\Re(\lambda)$ as a function of the real and imaginary parts of k. Much in the same manner as Fig. 8.3, we reckon that Fig. 8.13 suggests the possibility of a regular deformation of the path $\Im(k) = 0$

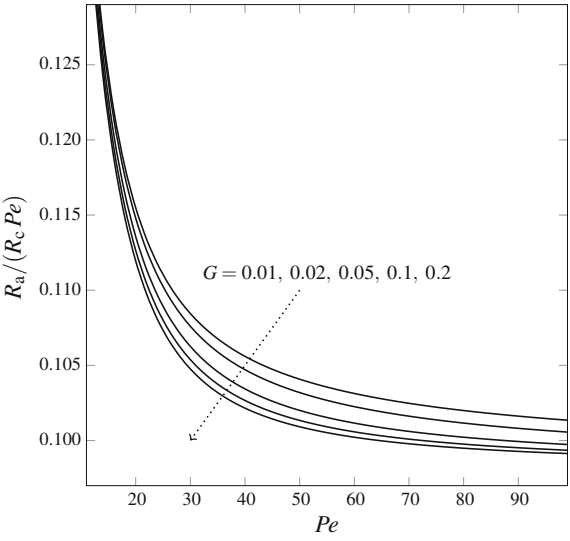

Fig. 8.12 Prats problem with form-drag effect: plots of $R_a/(R_c\,Pe)$ versus Pe within the range $0.01 \leqslant G \leqslant 0.2$

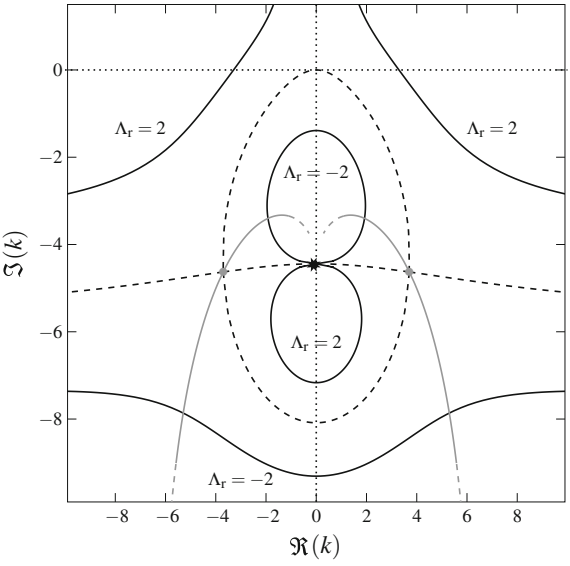

Fig. 8.13 Prats problem with form-drag effect: map of the isolines of $\sigma\,\Re(\lambda)/Pe = \Lambda_r$ (black solid lines) for the limiting case $Pe \to \infty$ with $\zeta = R_a/(G\,Pe^2) = 5.64390$. The dashed black lines are for $\Lambda_r = 0$. The grey dots are the saddle points, while the grey lines are the lines of steepest descent. The black asterisk denotes the singularity of $\lambda(k)$ at $k = -\mathrm{i}\,\pi\,\sqrt{2}$

so that the saddle points k_0, given by Eq. (8.73), are locally crossed along lines of steepest descent. By the adjective "regular", we mean that no singularity of $\Re(\lambda)$ is swept in the deformation, so that the region in the complex plane between $\Im(k) = 0$ and the deformed path does not include any singularity. We need to move along paths of steepest descent only in a neighbourhood of each saddle point. In fact, the Gaussian approximation of the integrand, in the wave packet representation (8.23), is rapidly damped as we depart from the saddle point. We recall that, as illustrated

in Sect. 3.5.3, the Gaussian approximation (3.159) of a time-dependent integral is the core of the steepest-descent method for capturing the large-time behaviour of the integral. In Fig. 8.13, just one singularity is displayed, namely $k = -\mathrm{i}\,\pi\,\sqrt{2}$, as one expects by inspecting equation (8.72) with $n = 1$.

8.4 Moving to Three Dimensions

In the formulation of the Prats problem, discussed in Sect. 8.2, we adopted a two-dimensional scheme disregarding the dependence of all physical fields on the spanwise coordinate y. Such a scheme is legitimate as far as the porous channel has a very small width H in the y-direction, namely $H/L \ll 1$. Assuming non-infinitesimal values of H/L means relaxing the assumption of two-dimensional flow. In this case, the velocity, pressure and temperature fields are to be considered as functions of (x, y, z, t). We rely on Darcy's law, for the sake of simplicity, namely on Eq. (7.61), where we consider the effect of viscous dissipation as negligible.

One may envisage a lateral confinement along the spanwise y-direction with adiabatic and impermeable sidewalls. Hence, a streamfunction formulation is out of the question, as it is feasible only for two-dimensional flows, while a pressure formulation is possible. Starting from Eq. (7.61), where we neglect the viscous dissipation term $\nu\, u_j\, u_j/(K\, c)$, we evaluate the divergence of the local momentum balance equation and we employ the local mass balance equation. Thus, in a dimensionless formulation, we write

$$\frac{\partial^2 P}{\partial x^2} + \frac{\partial^2 P}{\partial y^2} + \frac{\partial^2 P}{\partial z^2} - R\,\frac{\partial T}{\partial z} = 0\,,$$

$$\sigma\,\frac{\partial T}{\partial t} - \frac{\partial P}{\partial x}\,\frac{\partial T}{\partial x} - \frac{\partial P}{\partial y}\,\frac{\partial T}{\partial y} - \left[\frac{\partial P}{\partial z} - R\,(T - r)\right]\frac{\partial T}{\partial z} = \frac{\partial^2 T}{\partial x^2} + \frac{\partial^2 T}{\partial y^2} + \frac{\partial^2 T}{\partial z^2}\,. \tag{8.79}$$

where $r = (T_0 - T_2)/(T_1 - T_2)$ is a parameter depending on the choice of the reference temperature, T_0, for the Oberbeck–Boussinesq approximation.

In Eq. (8.79), a scaling consistent with Eq. (8.1) has been implicitly adopted and we allowed for the definition of the dimensionless quantity P, namely

$$\frac{K}{\mu\,\alpha}\,P \to P\,. \tag{8.80}$$

The basic solution with a uniform velocity profile, given by Eqs. (8.8)–(8.10), still holds. It can be reformulated as

$$\frac{\partial P_\mathrm{b}}{\partial x} = -Pe\ , \quad \frac{\partial P_\mathrm{b}}{\partial y} = 0\ , \quad \frac{\partial P_\mathrm{b}}{\partial z} = R\,(1 - z - r)\ , \quad T_\mathrm{b} = 1 - z\ . \tag{8.81}$$

We note that Eq. (8.81) reflects the adiabatic and impermeable nature of the sidewalls, as one must satisfy the boundary conditions $\partial T/\partial y = 0$ and $\partial P/\partial y = 0$. Hereafter, we will assume the sidewalls to be placed at the dimensionless positions $y = 0, \tau$, where

$$\tau = \frac{H}{L}\ . \tag{8.82}$$

The small perturbations of the basic state (8.81) are defined as

$$P = P_\mathrm{b} + \varepsilon\,\Pi\ , \qquad T = T_\mathrm{b} + \varepsilon\,\Theta\ . \tag{8.83}$$

On substituting Eq. (8.83) into Eq. (8.79) and neglecting the terms $O(\varepsilon^2)$ leads to the governing equations for the three-dimensional perturbations,

$$\begin{gathered}\frac{\partial^2 \Pi}{\partial x^2} + \frac{\partial^2 \Pi}{\partial y^2} + \frac{\partial^2 \Pi}{\partial z^2} - R\,\frac{\partial \Theta}{\partial z} = 0\ , \\ \sigma\ \frac{\partial \Theta}{\partial t} + Pe\,\frac{\partial \Theta}{\partial x} + \frac{\partial \Pi}{\partial z} - R\,\Theta = \frac{\partial^2 \Theta}{\partial x^2} + \frac{\partial^2 \Theta}{\partial y^2} + \frac{\partial^2 \Theta}{\partial z^2}\ .\end{gathered} \tag{8.84}$$

Instead of Eq. (8.12), the boundary conditions are now written as

$$\begin{aligned} y = 0, \tau: &\qquad \frac{\partial \Pi}{\partial y} = 0\ , \quad \frac{\partial \Theta}{\partial y} = 0\ , \\ z = 0, 1: &\qquad \frac{\partial \Pi}{\partial z} = 0\ , \quad \Theta = 0\ . \end{aligned} \tag{8.85}$$

We note that Eqs. (8.84) and (8.85) do not depend on the reference temperature parameter $r = (T_0 - T_2)/(T_1 - T_2)$. This means that the stability analysis is not influenced by the choice of T_0 and, hence, by the value of r. This is an important fact regarding instability in a horizontal channel. We anticipate that the conclusion becomes quite the opposite if we consider flow in a vertical porous channel, as it will become clear in Sect. 9.2.

The perturbations (Π, Θ) are now written as wave packets by employing the Fourier transform,

$$\tilde{\Pi}(k, y, z, t) = \frac{1}{\sqrt{2\pi}} \int_{-\infty}^{\infty} e^{-\mathrm{i}\,k\,x}\,\Pi(x, y, z, t)\ \mathrm{d}\,x\ ,$$

$$\Pi(x,y,z,t) = \frac{1}{\sqrt{2\pi}} \int_{-\infty}^{\infty} e^{\mathrm{i}\,k\,x}\,\tilde{\Pi}(k,y,z,t)\,\mathrm{d}\,k\ ,$$

$$\tilde{\Theta}(k,y,z,t) = \frac{1}{\sqrt{2\pi}} \int_{-\infty}^{\infty} e^{-\mathrm{i}\,k\,x}\,\Theta(x,y,z,t)\,\mathrm{d}\,x\ ,$$

$$\Theta(x,y,z,t) = \frac{1}{\sqrt{2\pi}} \int_{-\infty}^{\infty} e^{\mathrm{i}\,k\,x}\,\tilde{\Theta}(k,y,z,t)\,\mathrm{d}\,k\ . \tag{8.86}$$

We can now separate the dependence on y and z, by writing

$$\tilde{\Pi}(k,y,z,t) = \sum_{\ell=0}^{\infty}\sum_{n=1}^{\infty} \tilde{\Pi}_{\ell,n}(t)\,\cos\left(\frac{\ell\,\pi\,y}{\tau}\right)\cos(n\,\pi\,z)\ ,$$

$$\tilde{\Theta}(k,y,z,t) = \sum_{\ell=0}^{\infty}\sum_{n=1}^{\infty} \tilde{\Theta}_{\ell,n}(t)\,\cos\left(\frac{\ell\,\pi\,y}{\tau}\right)\sin(n\,\pi\,z)\ . \tag{8.87}$$

We easily reckon that Eq. (8.87), when substituted in Eq. (8.86), allows one to infer that the boundary conditions at $y = 0, \tau$ and $z = 0, 1$ declared in Eq. (8.85) are identically satisfied.

The three-dimensional formulation expressed by Eq. (8.87) includes the two-dimensional modes discussed in Sect. 8.2. Such modes are, in fact, those corresponding to $\ell = 0$ as this selection suppresses any dependence on y.

By applying the Fourier transform to Eq. (8.84), one obtains

$$\left(n^2\,\pi^2 + \frac{\ell^2\,\pi^2}{\tau^2} + k^2\right)\tilde{\Pi}_{\ell,n} + n\,\pi\,R\,\tilde{\Theta}_{\ell,n} = 0\ ,$$

$$\left(n^2\,\pi^2 + \frac{\ell^2\,\pi^2}{\tau^2} + k^2\right)\tilde{\Theta}_{\ell,n} + \sigma\,\frac{\mathrm{d}\,\tilde{\Theta}_{\ell,n}}{\mathrm{d}\,t} + \mathrm{i}\,k\,Pe\,\tilde{\Theta}_{\ell,n} - n\,\pi\,\tilde{\Pi}_{\ell,n} - R\,\tilde{\Theta}_{\ell,n} = 0\ , \tag{8.88}$$

where Eq. (8.87) has been taken into account.

Equations (8.88) can be solved by writing

$$\tilde{\Pi}_{\ell,n}(t) = \tilde{\Pi}_{\ell,n}(0)\,\mathrm{e}^{\lambda(k)\,t}\ ,\quad \tilde{\Theta}_{\ell,n}(t) = -\frac{n^2\,\pi^2 + \dfrac{\ell^2\,\pi^2}{\tau^2} + k^2}{n\,\pi\,R}\,\tilde{\Pi}_{\ell,n}(0)\,\mathrm{e}^{\lambda(k)\,t}\ , \tag{8.89}$$

with the dispersion relation now given by

$$\sigma\,\lambda(k) = \frac{R\left(\dfrac{\ell^2\,\pi^2}{\tau^2} + k^2\right) - \left(n^2\pi^2 + \dfrac{\ell^2\,\pi^2}{\tau^2} + k^2\right)^2}{n^2\pi^2 + \dfrac{\ell^2\,\pi^2}{\tau^2} + k^2} - \mathrm{i}\,k\,Pe\ ,$$

$$n = 1, 2, 3, \ \ldots\ , \quad \ell = 0, 1, 2, \ \ldots\ . \tag{8.90}$$

8.4.1 Convective Instability

Following the usual procedure, in the analysis of convective instability, we must remember that $\lambda = \eta - \mathrm{i}\,\omega$, where η is the growth rate of the normal mode and ω is its angular frequency. Thus, by considering the real part and the imaginary part of the dispersion relation (8.90), we obtain

$$\eta = \frac{R\,\kappa^2 - (n^2\pi^2 + \kappa^2)^2}{\sigma\left(n^2\pi^2 + \kappa^2\right)}\ , \quad \omega = \frac{k\,Pe}{\sigma}\ , \quad n = 1, 2, 3, \ \ldots\ , \tag{8.91}$$

where

$$\kappa^2 = \frac{\ell^2\,\pi^2}{\tau^2} + k^2\ , \quad \ell = 0, 1, 2, \ \ldots\ . \tag{8.92}$$

A comparison between Eq. (8.91) and its two-dimensional counterpart (8.20) immediately suggests that the neutral stability condition has formally the same expression as for the two-dimensional case. More precisely, it is given by Eq. (8.22) with parameter κ instead of the wave number k,

$$R = \frac{(\pi^2 + \kappa^2)^2}{\kappa^2}\ . \tag{8.93}$$

This means that the onset of convective instability is still triggered by the $n = 1$ modes. Hence, the minimum of the neutral stability curve is now expressed as

$$\kappa_\mathrm{c} = \pi\ , \qquad R_\mathrm{c} = 4\,\pi^2\ , \tag{8.94}$$

which replaces Eq. (7.83). There is just one difference: κ appears instead of k. This means that, in general, there is not only a two-dimensional mode ($\ell = 0$) as a possible source of convective instability. Obviously, for such mode, one recovers the result found with the two-dimensional analysis, namely $k_\mathrm{c} = \pi$, consistently with Eq. (7.83). However, with three-dimensional modes ($\ell \neq 0$), one has

$$k_\mathrm{c} = \pi\sqrt{1 - \frac{\ell^2}{\tau^2}}\ . \tag{8.95}$$

Evidently, a mode with $\ell = 1$ can be involved only if $\tau \geqslant 1$, a mode with $\ell = 2$ can be involved only if $\tau \geqslant 2$, and so on. This simple observation is coherent with our statement that a two-dimensional analysis is a reliable model when $\tau = H/L$ is small enough. In particular, the two-dimensional nature of the critical mode, with $\kappa_c = k_c = \pi$, arises when $\tau < 1$ as we can only have $\ell = 0$ in this case, meaning y independent modes. When $1 \leqslant \tau < 2$, we have two modes satisfying the criticality condition expressed by Eq. (8.95), namely

$$\ell = 0 \,, \quad k_c = \pi \,,$$

$$\ell = 1 \,, \quad k_c = \pi \sqrt{1 - \frac{1}{\tau^2}} \,. \tag{8.96}$$

When $2 \leqslant \tau < 3$, we have three modes, namely

$$\ell = 0 \,, \quad k_c = \pi \,,$$

$$\ell = 1 \,, \quad k_c = \pi \sqrt{1 - \frac{1}{\tau^2}} \,,$$

$$\ell = 2 \,, \quad k_c = \pi \sqrt{1 - \frac{4}{\tau^2}} \,. \tag{8.97}$$

When $3 \leqslant \tau < 4$, we have four modes, and so forth.

The plurality of possible modes triggering the onset of convective instability widens as τ increases. The simplest case being that with $\tau < 1$ where only the two-dimensional mode with $k_c = \pi$ is involved.

The completely different types of two-dimensional modes potentially driving convective instability are those with $k = 0$ and $\ell \neq 0$. Such modes were not included in the analysis conveyed in Sect. 8.2.3 as they display a dependence on the pair of coordinates (y, z). Furthermore, the modes envisaged in Sect. 8.2.3 do not lead to any instability when $k \to 0$, as testified by the singularity at $k = 0$ in the right-hand side of Eq. (8.22). Equations (8.92) and (8.93) depict a different situation, with the neutral stability value of R being a function of τ for every $\ell \neq 0$ and $k = 0$. In particular, there exists a range of the aspect ratio τ where the modes with $\ell = 1$ are those leading to the lowest neutral stability value of R. There exists a neighbouring range of τ where the modes with $\ell = 2$ prevail, and so forth. The transition from the ℓth mode to the $(\ell + 1)$th mode in the neutral stability condition with an increasing aspect ratio τ is illustrated in Fig. 8.14. This figure shows that, as τ increases, larger and larger values are involved in the onset of convective instability. From Eqs. (8.92) and (8.93), one may infer that the transition value of τ from the range where the ℓth mode triggers the onset of convective instability to the range where the $(\ell + 1)$th mode prevails is

$$\tau = \sqrt{\ell \, (\ell + 1)} \,. \tag{8.98}$$

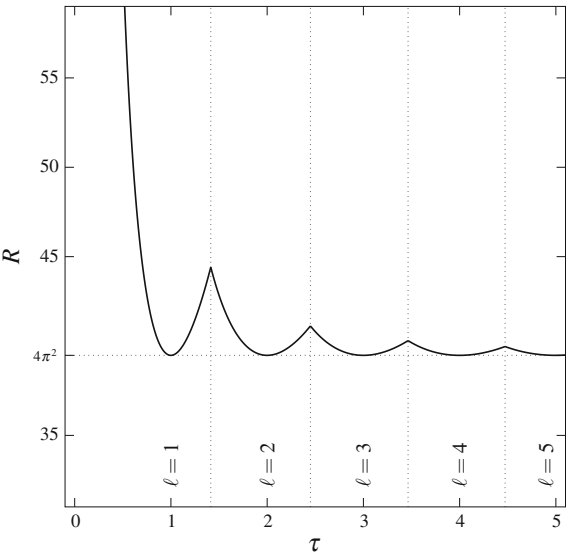

Fig. 8.14 Three-dimensional analysis of the Prats problem: the neutral stability condition for the $k = 0$ modes in the (τ, R) plane (solid line). The vertical dotted lines mark the transition between different ℓ modes. The horizontal dotted line denotes the critical value of R

We note that, on account of Eqs. (8.92) and (8.93), the critical condition $R = R_c = 4\,\pi^2$ occurs with $k = 0$ modes for any $\tau = \ell$, where $\ell = 1, 2, 3, \ldots$. Hence, the neutral stability curve displayed in Fig. 8.14 displays a sequence of minima for $\tau = 1, 2, 3, \ldots$. This conclusion reflects the geometry of the preferred convection cells for the onset of convective instability, i.e., the square geometry. This aspect was pointed out in Sect. 7.8 and illustrated in Fig. 7.13, with reference to the Horton–Rogers–Lapwood problem with impermeable and isothermal boundaries.

8.4.2 Absolute Instability

The analysis of the absolute instability is to be based on the dispersion relation (8.90) and on the derivative of $\lambda(k)$. As usual, $\lambda'(k)$ is to be set equal to zero in order to determine the saddle points, whereas the condition $\Re(\lambda(k)) = 0$ serves to establish the associated value of R. Thus, starting from Eq. (8.90), the condition $\lambda'(k) = 0$ reads

$$\frac{2\,k\,R\,n^2\pi^2}{\left(n^2\pi^2 + \dfrac{\ell^2\,\pi^2}{\tau^2} + k^2\right)^2} = 2\,k + \mathrm{i}\,Pe\ . \tag{8.99}$$

Equations (8.90) and (8.99), differently from Eqs. (8.25) and (8.27), display a dependence on the ratio ℓ/τ. Any value of such ratio is effectively a real positive number that may correspond to different ℓ modes and to different aspect ratios τ. Relatively to the absolute instability analysis, it is quite evident that the $\ell = 0$ modes are to

be considered equivalent to $\ell \neq 0$ modes having an infinite aspect ratio τ. In other words, for $\tau \to \infty$ and for each Péclet number, Pe, the absolute instability threshold, R_a, coincides with that evaluated for the two-dimensional case reported in Sect. 8.2.4.

The two-dimensional case is represented by $\ell/\tau = 0$. Then, we have to test the behaviour of the saddle points k_0 and to the corresponding values of R when ℓ/τ increases above 0. We consider the Péclet number $Pe = 10$ and $n = 1$, so that the saddle points for the two-dimensional case $\ell/\tau = 0$ are expressed by Eq. (8.36). If we take $\ell/\tau = 0.01$, we obtain

$$\begin{aligned} k_0 &= \pm\, 3.39291 - \mathrm{i}\, 1.89310\,, \qquad R = 57.8045\,, \\ k_0 &= \pm\, 1.84689 + \mathrm{i}\, 3.39165\,, \qquad R = -36.0948\,, \\ k_0 &= \mathrm{i}\, 1.51479\,, \qquad R = 25.0108\,, \\ k_0 &= -\mathrm{i}\, 6.51499\,, \qquad R = 25.0006\,, \\ k_0 &= \mathrm{i}\, 0.000500177\,, \qquad R = 98690.8\,. \end{aligned} \tag{8.100}$$

From Eqs. (8.36) and (8.100), we conclude that there is a little difference in the saddle points for $\ell/\tau = 0$ and those for $\ell/\tau = 0.01$. There is indeed a new one, purely imaginary and close to the origin of the k plane, where R is extremely large, $R = 98690.8$. We expect that such saddle point is moved to the origin, with $R \to \infty$, when $\ell/\tau \to 0$. This is the reason why the two-dimensional analysis did not reveal any such point. The other saddle points reported in Eq. (8.100) can be easily put in correspondence with those listed in Eq. (8.36). The numerical values are slightly altered with respect to the two-dimensional case. The interesting fact is that there is no good candidate for the threshold value R_a that can be gathered from Eq. (8.100) to replace that obtained with the two-dimensional analysis, namely $R_a = 57.8036$. In fact, the change from $\ell/\tau = 0$ to $\ell/\tau = 0.01$ does not provide any saddle point whose corresponding R is both larger than $R_c = 4\,\pi^2$ and smaller than the two-dimensional threshold value for absolute instability, $R_a = 57.8036$. Just the same happens if we further increase to $\ell/\tau = 0.1$. We get

$$\begin{aligned} k_0 &= \pm\, 3.38719 - \mathrm{i}\, 1.90297\,, \qquad R = 57.9011\,, \\ k_0 &= \pm\, 1.84401 + \mathrm{i}\, 3.40539\,, \qquad R = -36.2194\,, \\ k_0 &= \mathrm{i}\, 1.50091\,, \qquad R = 26.1248\,, \\ k_0 &= -\mathrm{i}\, 6.52134\,, \qquad R = 25.0581\,, \\ k_0 &= \mathrm{i}\, 0.0518395\,, \qquad R = 980.612\,. \end{aligned} \tag{8.101}$$

The outcome from Eqs. (8.100) and (8.101) is that there is no good candidate that emerges from the three-dimensional analysis for the replacement of our threshold for absolute instability, $R_a = 57.8036$. One can check the saddle points for larger values of ℓ/τ. With $\ell/\tau = 1$, we find

$$\begin{aligned} k_0 &= \pm 3.06328 - \mathrm{i}\, 2.81016 \,, \qquad R = 68.5544 \,, \\ k_0 &= \pm 1.65805 + \mathrm{i}\, 4.59899 \,, \qquad R = -47.3176 \,, \\ k_0 &= -\mathrm{i}\, 7.16371 \,, \qquad R = 30.5193 \,. \end{aligned} \tag{8.102}$$

With $\ell/\tau = 10$, we obtain

$$\begin{aligned} k_0 &= \pm 0.821325 + \mathrm{i}\, 31.5818 \,, \qquad R = -315.833 \,, \\ k_0 &= -\mathrm{i}\, 32.3801 \,, \qquad R = 228.491 \,, \\ k_0 &= -\mathrm{i}\, 30.4151 \,, \qquad R = 435.856 \,, \\ k_0 &= -\mathrm{i}\, 5.05459 \,, \qquad R = 1032.32 \,. \end{aligned} \tag{8.103}$$

Finally, with $\ell/\tau = 100$ we have

$$\begin{aligned} k_0 &= \pm 0.278039 + \mathrm{i}\, 314.175 \,, \qquad R = -3141.75 \,, \\ k_0 &= -\mathrm{i}\, 314.442 \,, \qquad R = 2811.27 \,, \\ k_0 &= -\mathrm{i}\, 313.876 \,, \qquad R = 3511.08 \,, \\ k_0 &= -\mathrm{i}\, 5.00050 \,, \qquad R = 98740.8 \,. \end{aligned} \tag{8.104}$$

The conclusion drawn from Eqs. (8.100)–(8.104) is that, no matter how much we increase the value of ℓ/τ above zero, the three-dimensional analysis does not alter the findings of the two-dimensional analysis. The correct threshold to absolute instability for $Pe = 10$ is detected by setting $\ell/\tau = 0$, namely $R_a = 57.8036$.

The same type of analysis can be carried out with different values of the Péclet number, Pe. Table 8.2 is relative to $Pe = 5$, while Table 8.3 reports the saddle points for $Pe = 20$.

Both these tables allow one to reach the same conclusion declared for $Pe = 10$. On inspecting the behaviour of the saddle points by increasing the value of ℓ/τ above zero, one does not detect any case where the value of R corresponding to a given saddle point is both larger or equal to R_c and smaller than the value of R_a estimated with the two-dimensional analysis ($\ell/\tau = 0$). This means that, whatever is the value of Pe and τ, the three-dimensional analysis does not provide any change with respect to the findings of the two-dimensional analysis, succinctly reported in Table 8.1. In

Table 8.2 Three-dimensional analysis of the Prats problem: saddle points of $\lambda(k)$ and corresponding values of R for $Pe = 5$, $n = 1$ and different values of ℓ/τ

ℓ/τ	k_0	R
0	$\pm\,3.29255 - \mathrm{i}\,1.12014$	45.0277
	$\pm\,1.51430 + \mathrm{i}\,3.36050$	−17.3610
	$\mathrm{i}\,2.13114$	6.25
	$-\mathrm{i}\,4.63114$	6.25
0.01	$\pm\,3.29245 - \mathrm{i}\,1.12022$	45.0281
	$\pm\,1.51428 + \mathrm{i}\,3.36064$	−17.3617
	$\mathrm{i}\,2.13122$	6.25136
	$-\mathrm{i}\,4.63126$	6.25029
	$\mathrm{i}\,0.000250041$	98709.5
0.1	$\pm\,3.28256 - \mathrm{i}\,1.12803$	45.0689
	$\pm\,1.51173 + \mathrm{i}\,3.37459$	−17.4274
	$\mathrm{i}\,2.13932$	6.38733
	$-\mathrm{i}\,4.64281$	6.27873
	$\mathrm{i}\,0.0254128$	1000.38
1	$\pm\,2.60121 - \mathrm{i}\,1.96765$	50.8973
	$\pm\,1.34343 + \mathrm{i}\,4.57619$	−23.1883
	$-\mathrm{i}\,5.67901$	8.87912
10	$\pm\,0.601695 + \mathrm{i}\,31.5779$	−157.892
	$-\mathrm{i}\,32.0817$	98.1192
	$-\mathrm{i}\,30.7344$	253.875
	$-\mathrm{i}\,2.52575$	1013.18
100	$\pm\,0.197378 + \mathrm{i}\,314.175$	−1570.88
	$-\mathrm{i}\,314.359$	1341.65
	$-\mathrm{i}\,313.960$	1839.27
	$-\mathrm{i}\,2.50025$	98722.0

other words, the value of R_a for a given Pe is independent of the aspect ratio τ. This conclusion is in no way the result of a formal mathematical proof, but rather the outcome of an inductive reasoning based on numerical data.

8.4.3 On the Different Meanings of Three Dimensionality

The three-dimensional nature of the instability has been modelled by assuming a pair of plane-parallel sidewalls bounding laterally the horizontal flow. The whole analysis has been based on the assumption that the sidewalls are adiabatic and impermeable.

There are two levels of arbitrariness in our model of three dimensionality. One is the existence and the plane-parallel geometry of the lateral boundaries. The other is the type of boundary conditions assumed at the sidewalls.

Table 8.3 Three-dimensional analysis of the Prats problem: saddle points of $\lambda(k)$ and corresponding values of R for $Pe = 20$, $n = 1$ and different values of ℓ/τ

ℓ/τ	k_0	R
0	$\pm\,3.24476 - \mathrm{i}\,2.68308$	91.9528
	$\pm\,2.13593 + \mathrm{i}\,3.38608$	−74.7989
	$\mathrm{i}\,0.905049$	100
	$-\mathrm{i}\,10.9050$	100
0.01	$\pm\,3.24472 - \mathrm{i}\,2.68320$	91.9548
	$\pm\,2.13590 + \mathrm{i}\,3.38622$	−74.8013
	$\mathrm{i}\,0.904350$	100.121
	$-\mathrm{i}\,10.9051$	100.001
	$\mathrm{i}\,0.00100112$	98615.7
0.1	$\pm\,3.24132 - \mathrm{i}\,2.69522$	92.1583
	$\pm\,2.13278 + \mathrm{i}\,3.39985$	−75.0395
	$\mathrm{i}\,0.822457$	115.111
	$-\mathrm{i}\,10.9069$	100.083
	$\mathrm{i}\,0.113910$	891.598
1	$\pm\,3.10130 - \mathrm{i}\,3.76867$	112.140
	$\pm\,1.93786 + \mathrm{i}\,4.59367$	−96.5459
	$-\mathrm{i}\,11.1053$	108.208
10	$\pm\,1.08953 + \mathrm{i}\,31.5869$	−631.828
	$-\mathrm{i}\,32.8959$	513.232
	$-\mathrm{i}\,29.8254$	775.094
	$-\mathrm{i}\,10.1388$	1109.05
100	$\pm\,0.390162 + \mathrm{i}\,314.175$	−6283.50
	$-\mathrm{i}\,314.562$	5812.17
	$-\mathrm{i}\,313.756$	6793.05
	$-\mathrm{i}\,10.0010$	98815.8

The absence of lateral boundaries can be intended as a limiting case of the analysis carried out so far, with $\tau \to \infty$. There is a spanwise wave number given by $k_s = \ell\,\pi/\tau$ that displays a discrete spectrum for every finite τ. However, in the limiting case, the spectrum becomes continuous as the distance between two neighbouring wave numbers, π/τ, tends to zero when $\tau \to \infty$. Therefore, the normal modes defined by Eqs. (8.86) and (8.87) yield a situation where such modes propagate along a direction described by a wave vector with components (k, k_s) lying in the horizontal (x, y) plane. Thus, the lateral boundaries, when moved to infinity, are ineffective for the convective and absolute stability analysis.

The role of the boundary conditions prescribed at the lateral boundaries, when τ is finite, is another matter. In fact, these boundary conditions are quite important in defining the y-dependent eigenfunctions to be used in Eq. (8.87) instead of the cosine, as well as their corresponding eigenvalues to be employed instead of $k_s = \ell\,\pi/\tau$. To a far deeper extent, the boundary conditions prescribed at the sidewalls

are of paramount importance in assessing the type of stationary flow solution to be considered as the basic state. Not necessarily any possible model of sidewalls can be compatible with the uniform flow endowed with a purely vertical temperature gradient, as described by Eq. (8.81). The nature of the basic state may be deeply influenced by the temperature and pressure constraints prescribed on the lateral boundaries. The sidewalls assumed in the stability analysis carried out in Sects. 8.4.1 and 8.4.2 are a natural expression of the heating-from-below scenario, where the onset of convection cells is a consequence of the vertical temperature gradient induced by the thermal forcing at the lower boundary wall.

References

1. Alves LSB, Barletta A (2015) Convective to absolute instability transition in the Prats flow of a power-law fluid. Int J Thermal Sci 94:270–282
2. Barletta A, Alves LSB (2017) Absolute instability: a toy model and an application to the Rayleigh-Bénard problem with horizontal flow in porous media. Int J Heat Mass Transf 104:438–455
3. Barletta A, Celli M (2017) Convective to absolute instability transition in a horizontal porous channel with open upper boundary. Fluids 2:1–33
4. Brevdo L (2009) Three-dimensional absolute and convective instabilities at the onset of convection in a porous medium with inclined temperature gradient and vertical throughflow. J Fluid Mech 641:475–487
5. Brevdo L, Ruderman MS (2009) On the convection in a porous medium with inclined temperature gradient and vertical throughflow. Part I. Normal modes. Transp Porous Media 80:137–151
6. Brevdo L, Ruderman MS (2009) On the convection in a porous medium with inclined temperature gradient and vertical throughflow. Part II. Absolute and convective instabilities, and spatially amplifying waves. Transp Porous Media 80:153–172
7. Delache A, Ouarzazi MN, Combarnous M (2007) Spatio-temporal stability analysis of mixed convection flows in porous media heated from below: comparison with experiments. Int. J. Heat Mass Transf 50:1485–1499
8. Diaz E, Brevdo L (2011) Absolute/convective instability dichotomy at the onset of convection in a porous layer with either horizontal or vertical solutal and inclined thermal gradients, and horizontal throughflow. J Fluid Mech 681:567–596
9. Dufour F, Néel MC (1998) Numerical study of instability in a horizontal porous channel with bottom heating and forced horizontal flow. Phys Fluids 10:2198–2207
10. Hirata SC, Ouarzazi MN (2010) Three-dimensional absolute and convective instabilities in mixed convection of a viscoelastic fluid through a porous medium. Phys Lett A 374:2661–2666
11. Joulin A, Ouarzazi MN (2000) Convection mixte d'un mélange binaire en milieu poreux. Comptes Rendus de l'Académie des Sciences – Series IIB – Mechanics-Physics-Astronomy 328:311–316
12. Prats M (1966) The effect of horizontal fluid flow on thermally induced convection currents in porous mediums. J Geophys Res 71:4835–4838
13. Rees DAS (1997) The effect of inertia on the onset of mixed convection in a porous layer heated from below. Int Commun Heat Mass Transf 24:277–283

Chapter 9
Transition to Absolute Instability in Porous Media: Numerical Solutions

9.1 A Variant Prats Problem with Uniform Heat Flux

Let us consider a horizontal porous channel having a rectangular cross section with height L. We adopt a two-dimensional description where the coordinates are chosen so that x is the longitudinal horizontal axis and z is the transverse vertical axis. We are assuming heating from below with a uniform heat flux, q_0, at $z = 0$, while the upper boundary, $z = L$, is kept isothermal with temperature T_2. We point out that this setup is just the same considered in Sect. 7.7 as a possible variant of the Horton–Rogers–Lapwood problem. By analogy with the Prats problem [4], the presence of a horizontal flow along the x-direction is taken into account.

9.1.1 Dimensionless Formulation

The velocity field, $\mathbf{u} = (u, w)$, and the temperature field, T, as well as the coordinates, (x, z), and time, t, can be written in a dimensionless form by adopting the transformation

$$(u, w)\,\frac{L}{\alpha} \to (u, w)\ , \qquad (T - T_2)\,\frac{\varkappa_{\text{eff}}}{q_0 L} \to T\ ,$$

$$(x, z)\,\frac{1}{L} \to (x, z)\ , \qquad \frac{t}{L^2/\alpha} \to t\ , \tag{9.1}$$

where α is the average thermal diffusivity and $\varkappa_{\text{eff}}$ is the average thermal conductivity of the porous medium. Through this scaling, the Oberbeck–Boussinesq approximation of the governing local balance equations is still given by Eq. (8.2), where the Darcy–Rayleigh number is now defined as

A. Barletta, *Routes to Absolute Instability in Porous Media*,
https://doi.org/10.1007/978-3-030-06194-4_9

$$R = \frac{g\,\beta\,q_0\,K\,L^2}{\nu\,\alpha\,\varkappa_{\rm eff}}\ , \tag{9.2}$$

while the boundary conditions are expressed as

$$\begin{aligned} z = 0\ :\quad & w = 0\ , \quad \frac{\partial T}{\partial z} = -1\ , \\ z = 1\ :\quad & w = 0\ , \quad T = 0\ . \end{aligned} \tag{9.3}$$

By analogy with what we did for the analysis of the Prats problem carried out in Chap. 8, we introduce a streamfunction ψ, defined as

$$u = \frac{\partial \psi}{\partial z}\ , \qquad w = -\,\frac{\partial \psi}{\partial x}\ , \tag{9.4}$$

so that the governing local balance equations are now formulated as

$$\begin{aligned} & \frac{\partial^2 \psi}{\partial x^2} + \frac{\partial^2 \psi}{\partial z^2} + R\,\frac{\partial T}{\partial x} = 0\ , \\ & \sigma\,\frac{\partial T}{\partial t} + \frac{\partial \psi}{\partial z}\,\frac{\partial T}{\partial x} - \frac{\partial \psi}{\partial x}\,\frac{\partial T}{\partial z} = \frac{\partial^2 T}{\partial x^2} + \frac{\partial^2 T}{\partial z^2}\ . \end{aligned} \tag{9.5}$$

With this formulation, we can express the boundary conditions (9.3) as

$$\begin{aligned} z = 0\ :\quad & \frac{\partial \psi}{\partial x} = 0\ , \quad \frac{\partial T}{\partial z} = -1\ , \\ z = 1\ :\quad & \frac{\partial \psi}{\partial x} = 0\ , \quad T = 0\ . \end{aligned} \tag{9.6}$$

The stationary solution, $(\psi_{\rm b}, T_{\rm b})$, of the governing equations (9.5) and boundary conditions (9.6) is still expressed by Eq. (8.8). It describes a uniform velocity in the x-direction, with a vertical temperature gradient,

$$\psi_{\rm b} = Pe\ z\ , \qquad T_{\rm b} = 1 - z\ . \tag{9.7}$$

Here, Pe is the *Péclet number* relative to the basic horizontal and uniform flow in the porous channel, defined by Eq. (8.9).

The next step is, as usual, assuming small amplitude perturbations of the basic stationary flow,

$$\psi = \psi_{\rm b} + \varepsilon\,\Psi\ , \qquad T = T_{\rm b} + \varepsilon\,\Theta\ , \tag{9.8}$$

such that $|\varepsilon| \ll 1$. The linearised equations for the perturbation fields (Ψ, Θ) are solutions of the partial differential equations

$$\frac{\partial^2 \Psi}{\partial x^2} + \frac{\partial^2 \Psi}{\partial z^2} + R\,\frac{\partial \Theta}{\partial x} = 0\,,$$

$$\sigma\,\frac{\partial \Theta}{\partial t} + Pe\,\frac{\partial \Theta}{\partial x} + \frac{\partial \Psi}{\partial x} = \frac{\partial^2 \Theta}{\partial x^2} + \frac{\partial^2 \Theta}{\partial z^2}\,, \tag{9.9}$$

with the boundary conditions

$$z = 0\ :\quad \frac{\partial \Psi}{\partial x} = 0\,,\quad \frac{\partial \Theta}{\partial z} = 0\,,$$

$$z = 1\ :\quad \frac{\partial \Psi}{\partial x} = 0\,,\quad \Theta = 0\,. \tag{9.10}$$

We express the perturbations, (Ψ, Θ), through their Fourier transforms, $(\tilde{\Psi}, \tilde{\Theta})$, as exploited in Eq. (8.13), and we write

$$\tilde{\Psi} = f(z)\,\mathrm{e}^{\lambda(k)\,t}\,,\qquad \tilde{\Theta} = -\,\mathrm{i}\,k\,h(z)\,\mathrm{e}^{\lambda(k)\,t}\,. \tag{9.11}$$

Thus, the differential eigenvalue problem for the stability analysis is obtained from Eqs. (9.9) and (9.10) and reads

$$\left(\frac{\mathrm{d}^2}{\mathrm{d}\,z^2} - k^2\right) f + R\,k^2\,h = 0\,,$$

$$\left[\frac{\mathrm{d}^2}{\mathrm{d}\,z^2} - k^2 - \gamma(k)\right] h + f = 0\,,$$

$$z = 0\ :\quad f = 0\,,\quad \frac{\mathrm{d}\,h}{\mathrm{d}\,z} = 0\,,$$

$$z = 1\ :\quad f = 0\,,\quad h = 0\,, \tag{9.12}$$

where

$$\gamma(k) = \sigma\,\lambda(k) + \mathrm{i}\,k\,Pe\,. \tag{9.13}$$

Due to the boundary conditions prescribed for the eigenfunctions $(f\,, h)$, it is impossible to express the solution of Eq. (9.12) in terms of a simple sine function, as in the classical formulation of Prats problem with impermeable isothermal boundaries. In fact, a sine function, $\sin(n\,\pi\,z)$, fulfils the boundary conditions for f, but not those for h. Obviously, Eq. (9.12) can be solved analytically by employing the characteristic equation method, but this approach leads to an implicit dispersion relation, as described in Sect. 7.7.2. Then, there is no great advantage in tackling the stability analysis with this technique. A numerical solution is preferable.

Our focus is not a dispersion relation in the classical sense, but its differential counterpart, namely the eigenvalue problem (9.12).

9.1.2 Convective Instability

The convective instability analysis starts from the principle of exchange of stabilities. One can employ just the same reasoning provided in Sect. 7.7.1, the only difference is that γ appears in Eq. (9.12) instead of λ. Thus, we can prove that

$$\Im(\gamma)\, R k^2 \int_0^1 |h|^2 \, \mathrm{d}z = 0 \,, \tag{9.14}$$

by the same arguments employed for the proof of Eq. (7.115). Our conclusion is that $\Im(\gamma) = 0$. Since $\lambda = \eta - \mathrm{i}\,\omega$, on account of Eq. (9.13), we can write

$$\omega = \frac{k\, Pe}{\sigma} \,. \tag{9.15}$$

This is just the same conclusion drawn in Eq. (8.20) relative to the Prats problem with isothermal conditions at both boundaries $z = 0, 1$. It can be rephrased as $\gamma = \sigma\, \eta$. Then, the neutral stability condition ($\eta = 0$) is determined by the numerical solution of Eq. (9.12) with $\gamma = 0$,

$$\begin{gathered}
\left(\frac{\mathrm{d}^2}{\mathrm{d}\, z^2} - k^2\right) f + R k^2 h = 0 \,, \\
\left(\frac{\mathrm{d}^2}{\mathrm{d}\, z^2} - k^2\right) h + f = 0 \,, \\
z = 0 \,: \quad f = 0 \,, \quad \frac{\mathrm{d}\, h}{\mathrm{d}\, z} = 0 \,, \\
z = 1 \,: \quad f = 0 \,, \quad h = 0 \,.
\end{gathered} \tag{9.16}$$

This finding allows one to establish an important fact. The neutral stability condition, determined by the solution of Eq. (9.16), is independent of the Péclet number, Pe. Thus, one can determine such condition for the case $Pe = 0$. This special case is that examined in Sect. 7.7.2. In other words, the neutral stability curve, evaluated numerically, is that drawn in Fig. 7.11. The solution of Eq. (9.16) is employed to determine the numerical function $R(k)$, i.e. the neutral stability function. In other words, R is computed as the eigenvalue of Eq. (9.16), for every prescribed value of $k \in \mathbb{R}$. The result of this computation is provided in Fig. 7.11. This figure shows the point of minimum R along the neutral stability curve, i.e. the critical point for convective instability. The critical values of the wave number and of the Darcy–Rayleigh number are, in fact,

$$k_c = 2.32621 \,, \qquad R_c = 27.0976 \,. \tag{9.17}$$

Such behaviour is qualitatively the same found for the Prats problem with isothermal boundaries, studied in Sect. 8.2.3. The neutral stability condition is not affected by the basic horizontal flow, and the neutral stability curve is thus the same as for the case $Pe = 0$, namely for the limiting case where the Prats problem coincides with the Horton–Rogers–Lapwood problem.

9.1.3 Absolute Instability

The study of absolute instability relies on the steepest-descent approximation of the perturbation wave packets,

$$\Psi(x, z, t) = \frac{1}{\sqrt{2\pi}} \int_{-\infty}^{\infty} \mathrm{e}^{\lambda(k)\, t + \mathrm{i}\, k\, x} f(z)\, \mathrm{d}\, k \,,$$

$$\Theta(x, z, t) = -\frac{\mathrm{i}}{\sqrt{2\pi}} \int_{-\infty}^{\infty} k\, \mathrm{e}^{\lambda(k)\, t + \mathrm{i}\, k\, x} h(z)\, \mathrm{d}\, k \,. \tag{9.18}$$

Hence, the first step is the determination of the saddle points in the complex plane, $k = k_0 \in \mathbb{C}$, such that $\lambda'(k) = 0$. The threshold of absolute instability occurs when the prescribed value of R detects the condition of zero asymptotic growth, $\Re(\lambda(k_0)) = 0$. This threshold condition defines R_a.

The basis for the evaluation of R_a is still the eigenvalue problem (9.12), together with Eq. (9.13). However, the numerical solution of Eq. (9.12) must be approached with the specification that $k = k_r + \mathrm{i}\, k_i$ is a complex variable with real part k_r and imaginary part k_i. We assume Pe and R to be prescribed quantities. The fulfilment of the saddle-point condition can be automatically implemented by forcing the constraint $\lambda'(k) = 0$. One can implement this constraint by doubling the order of the differential problem (9.12). To this end, we define

$$\hat{f} = \frac{\partial f}{\partial k} \,, \qquad \hat{h} = \frac{\partial h}{\partial k} \,. \tag{9.19}$$

Then, we obtain the extended eigenvalue problem

$$\frac{\mathrm{d}^2 f}{\mathrm{d}\, z^2} - k^2 f + R\, k^2\, h = 0 \,,$$

$$\frac{\mathrm{d}^2 h}{\mathrm{d}\, z^2} - \left[k^2 + \sigma\, \lambda(k) + \mathrm{i}\, k\, Pe\right] h + f = 0 \,,$$

$$\frac{\mathrm{d}^2\hat{f}}{\mathrm{d}\,z^2} - k^2\,\hat{f} + R\,k^2\,\hat{h} - 2\,k\,f + 2\,R\,k\,h = 0\,,$$

$$\frac{\mathrm{d}^2\hat{h}}{\mathrm{d}\,z^2} - \left[k^2 + \sigma\,\lambda(k) + \mathrm{i}\,k\,Pe\right]\hat{h} + \hat{f} - (2\,k + \mathrm{i}\,Pe)\,h = 0\,,$$

$$z = 0\ :\quad f = 0\,,\quad \frac{\mathrm{d}\,h}{\mathrm{d}\,z} = 0\,,\quad \hat{f} = 0\,,\quad \frac{\mathrm{d}\,\hat{h}}{\mathrm{d}\,z} = 0\,,$$

$$z = 1\ :\quad f = 0\,,\quad h = 0\,,\quad \hat{f} = 0\,,\quad \hat{h} = 0\,, \tag{9.20}$$

where we took into account that $\gamma(k) = \sigma\,\lambda(k) + \mathrm{i}\,k\,Pe$ and that $\lambda'(k) = 0$. The notation seems a bit equivocal as, on writing Eq. (9.19), we intend $(f\,,h)$ as functions of k and z, while the extended eigenvalue problem is written by employing the symbol of ordinary derivatives with respect z, that is $\mathrm{d}/\mathrm{d}z$. This choice is made for internal consistency with the convention applied so far in this book, and because there are not reasonable possibilities to mistake the meaning of this notation. We finally note that there is no ambiguity as Eq. (9.20) involves only ordinary differential equations, as the only derivatives employed there are derivatives with respect to z.

The solution of Eq. (9.20) can be worked out by assuming an eigenvalue problem structure. In this sense, there is no formal difference with respect to the solution of Eq. (9.16). In the case of problem (9.20), the procedure is more complicated because the eigenfunctions are four, $(f\,,h,\hat{f}\,,\hat{h})$, instead of two, as in Eq. (9.16). Moreover, $(f\,,h,\hat{f}\,,\hat{h})$ are complex-valued, while the eigenfunctions $(f\,,h)$ of problem (9.16) are real-valued. These facts do not alter the intrinsic nature of Eq. (9.20), which is the same as that of Eq. (9.16). They are both ordinary differential eigenvalue problems. This means that the numerical technique for their solution is, in principle, just the same. For details, we refer the reader to Chap. 10, while for alternatives such as the compound matrix method or the Chebyshev tau method we mention the papers by Straughan and Walker [5] and by Dongarra et al. [2].

The strategy in the solution of Eq. (9.20) is based on the general characteristics of the saddle points $k_0 \in \mathbb{C}$ pertinent for the determination of the threshold value $R = R_\mathrm{a}$ for the transition from convective to absolute instability. These characteristics are the fulfilment of

$$\lambda'(k) = 0\,, \tag{9.21}$$

which is a built-in feature of the eigenvalue problem (9.20), and the requirement

$$\Re(\lambda(k)) = 0\,. \tag{9.22}$$

This requirement must be considered as an input datum, inasmuch as the value of Pe. The output constants to be determined, namely the eigenvalues, are

$$\Re(k)\,,\quad \Im(k)\,,\quad \Im(\sigma\,\lambda(k))\,,\quad R\,. \tag{9.23}$$

In order to check if this solution strategy is consistent, we reformulate Eq. (9.20) as an initial value problem, by introducing suitably defined unknown constants. We expand the conditions at the lower boundary so that now we have

$$z = 0 \; : \quad f = 0 \,, \quad \frac{\mathrm{d}f}{\mathrm{d}z} = 1 \,, \quad h = a_1 \,, \quad \frac{\mathrm{d}h}{\mathrm{d}z} = 0 \,,$$

$$\hat{f} = 0 \,, \quad \frac{\mathrm{d}\hat{f}}{\mathrm{d}z} = 0 \,, \quad \hat{h} = a_2 \,, \quad \frac{\mathrm{d}\hat{h}}{\mathrm{d}z} = 0 \,. \tag{9.24}$$

Setting $\mathrm{d}f/\mathrm{d}z = 1$ serves only to fix the, otherwise arbitrary, scale of the eigenfunctions $(f, h, \hat{f}, \hat{h})$. The condition $\mathrm{d}\hat{f}/\mathrm{d}z = 0$ is a consequence of this scale-fixing constraint. It is obtained from $\mathrm{d}f/\mathrm{d}z = 1$ by taking its derivative with respect to k and by employing Eq. (9.19). The complex constants a_1 and a_2 must be determined, together with the real variables listed in Eq. (9.23), by imposing the end conditions at the upper boundary,

$$z = 1 \; : \quad f = 0 \,, \quad h = 0 \,, \quad \hat{f} = 0 \,, \quad \hat{h} = 0 \,. \tag{9.25}$$

The end conditions are relative to complex eigenfunctions. Thus, they effectively correspond to eight real equations. They are enough to determine the four real variables given by Eq. (9.23) and the four real variables given by the real and imaginary parts of a_1 and a_2. We point out that the complex constants a_1 and a_2 are internal variables with no direct physical meaning. In fact, their values are a consequence of the condition $\mathrm{d}f/\mathrm{d}z = 1$ imposed to fix, in an arbitrary manner, the scale of the eigenfunctions. A change in this scale-fixing condition alters the values of a_1 and a_2, while it does not modify the values of the four real variables listed in Eq. (9.23).

We refer the reader to Chap. 10 for a more detailed description of the numerical algorithms employed and of their implementation. The framework for the evaluation of the variables given by Eq. (9.23) is, in fact, the shooting method. Its use is based on a root-finding technique in order to impose the end conditions (9.25). Finding numerically the roots of Eq. (9.25) is possible if one suitably initialises the procedure by prescribing guess values of the unknown variables to be determined. The efficient way to achieve this task is starting from a parametric condition where the solution is known, and then incrementing step by step the input value of Pe by small amounts, in order to track the change of the solution with the Péclet number. The guess values at a given step are the computed eigenvalues at the previous step. The smaller is the step, i.e. the smaller is the amount of the Pe increment, the better is the choice of the guess values.

In fact, a case where the value of R_a for a given Pe can be easily guessed is $Pe = 0$. In this case, one expects $R_\mathrm{a} = R_\mathrm{c} = 27.0976$. Consistently, in this case, one expects also

$$\Re(k_0) = \pm k_\mathrm{c} = \pm 2.32621 \,, \quad \Im(k_0) = 0 \,, \quad \Im(\sigma\,\lambda(k_0)) = 0 \,. \tag{9.26}$$

These predictions are grounded on the idea that the rest state ($Pe = 0$) is one where there is no parametric gap between convective and absolute instabilities, namely $R_a = R_c$. In fact, when there is no basic flow driving the perturbation downstream, the Fourier normal modes are non-travelling, so that they amplify or damp in place. This is a consequence of the principle of exchange of stabilities. In such situations, even a single Fourier mode which undergoes an exponential amplification is sufficient to induce an unbounded amplification, for large times, of the whole perturbation wave packet. Beyond this heuristic argument, the principle of exchange of stabilities ensures that, with $Pe = 0$, the critical values $k = \pm k_c$ and $R = R_c$ are the saddle points and their relative Darcy–Rayleigh number, R, yielding the threshold to absolute instability. In fact, the principle of exchange of stabilities proved in Sect. 7.7.1, namely for the case $Pe = 0$, ensures that $\Im(\lambda(k)) = 0$, while the condition of neutral stability provides the constraint $\Re(\lambda(k)) = 0$. Therefore, the neutral stability condition implies $\lambda(k) = 0$ and, hence, also $\lambda'(k) = 0$, which is the saddle point condition. Among the neutrally stable k modes, the critical values are selected because they correspond to the minimum condition $\partial R/\partial k = 0$. The latter condition is implicitly assumed on writing the absolute instability eigenvalue problem (9.20). We finally point out that the critical wave numbers are always two, having the same absolute value, while we generally identify k_c with the positive one. The reason is easily gathered from inspection of the convective instability eigenvalue problem (9.16) where k appears only through its square, k^2.

One can keep track of the gradual displacement of the saddle point starting from the real axis $k_0 = \pm 2.32621$, when $Pe = 0$, to the complex k plane when $Pe > 0$. Figure 9.1 displays the migration of the saddle points in the k plane as Pe increases above 0. This figure reveals that the imaginary part of k continuously decreases

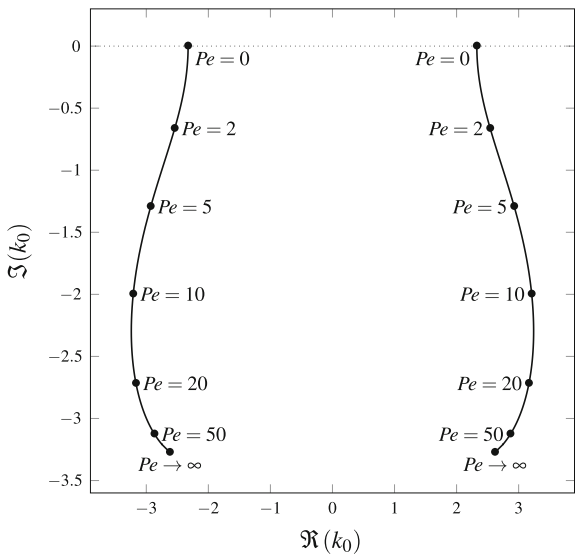

Fig. 9.1 Prats problem with isoflux lower boundary: migration of the pertinent saddle points, with increasing values of Pe, for the threshold to absolute instability

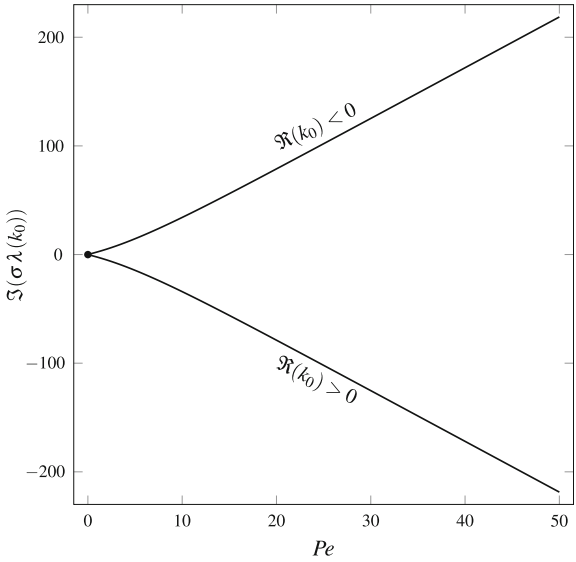

Fig. 9.2 Prats problem with isoflux lower boundary: plot of $\Im(\sigma\,\lambda(k_0))$ versus Pe for the saddle points k_0, at the threshold to absolute instability, with positive or negative $\Re(k_0)$

below 0, while the real part undergoes a non-monotonic trend. Figure 9.1 can be directly compared with Fig. 8.2, relative to the Prats problem with isothermal lower boundary. Figures 8.2 and 9.1 are indeed very similar, especially for large values of Pe. An interesting fact regards the behaviour for the limiting case $Pe \to \infty$. If one considers Eq. (9.20), the asymptotic behaviour for large Péclet numbers can be identified by writing

$$R = \xi\, Pe\ , \quad \sigma\,\lambda = \Lambda\, Pe\ , \quad f = f_{\mathrm{m}}\, Pe\ . \tag{9.27}$$

By substituting Eq. (9.27) into Eq. (9.12), by employing Eq. (9.13) and by keeping the leading terms for large Pe, one obtains

$$h = \frac{f_{\mathrm{m}}}{\Lambda + \mathrm{i}\,k}\ , \tag{9.28}$$

where the modified eigenfunction f_{m} must satisfy the differential equation

$$\left(\frac{\mathrm{d}^2}{\mathrm{d}\,z^2} - k^2 + \frac{\xi\,k^2}{\Lambda + \mathrm{i}\,k}\right) f_{\mathrm{m}} = 0\ , \tag{9.29}$$

with the boundary conditions

$$f_{\mathrm{m}}(0) = 0 = f_{\mathrm{m}}(1)\ . \tag{9.30}$$

Equations (9.29) and (9.30) are solved by writing

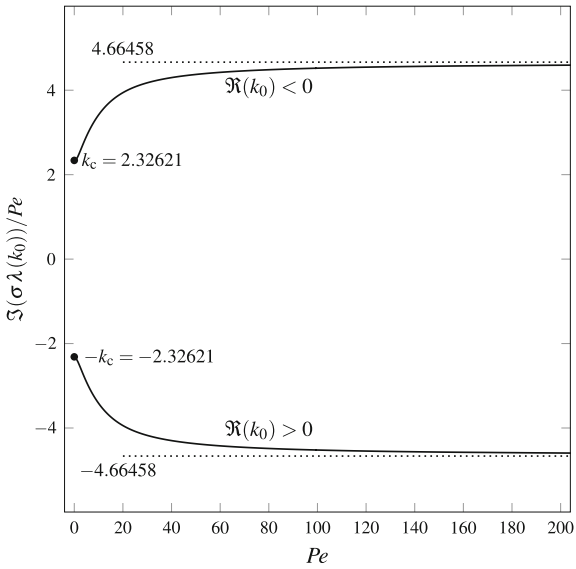

Fig. 9.3 Prats problem with isoflux lower boundary: plot of $\Im(\sigma\ \lambda(k_0)/Pe)$ versus Pe for the saddle points k_0, at the threshold to absolute instability, with positive or negative $\Re(k_0)$. The dotted lines display the asymptotic behaviour given by Eqs. (9.27) and (9.33)

$$f_{\mathrm{m}}(z) = \sin(n\,\pi\,z)\ , \qquad n = 1, 2, 3, \ \ldots\ , \tag{9.31}$$

provided that the dispersion relation

$$\Lambda = \frac{\xi\,k^2}{n^2\pi^2 + k^2} - \mathrm{i}\,k\ , \quad n = 1, 2, 3, \ \ldots \tag{9.32}$$

is satisfied.

Equation (9.32) coincides with Eq. (8.40). This means that the determination of the saddle points and the threshold value of ξ are exactly the same as for the Prats problem with isothermal lower boundary. Hence, the limiting regime $Pe \to \infty$ does not make any difference between the isoflux and isothermal conditions at the lower boundary. One may note that Eq. (9.28) marks an evident incompatibility between the eigenfunction h and the condition of a vanishing derivative $\mathrm{d}h/\mathrm{d}z$ at $z = 0$. This is a consequence of the stretching experienced by the eigenfunctions (f, h) when Pe unboundedly increases. This behaviour results in a singularity as evidenced by Eqs. (9.27) and (9.28). In fact, one can reckon that h becomes negligible with respect to f as $Pe \to \infty$, meaning that either f tends to infinity and h remains finite or f remains finite and h tends to zero. The sensible result is that the saddle points k_0 and the ratio R_{a}/Pe can still be approximated through Eqs. (8.42) and (8.43), if $Pe \gg 1$. In fact, Fig. 9.1 displays also the saddle points k_0 for the limiting case $Pe \to \infty$. As for the parameter Λ introduced in Eq. (9.27), its numerical estimate for $Pe \gg 1$ can be obtained directly from Eq. (9.32), namely

$$k_0 \approx \pm\,2.61941 - \mathrm{i}\,3.27327\ , \quad \Lambda \approx \mp\,\mathrm{i}\,4.66458\ . \tag{9.33}$$

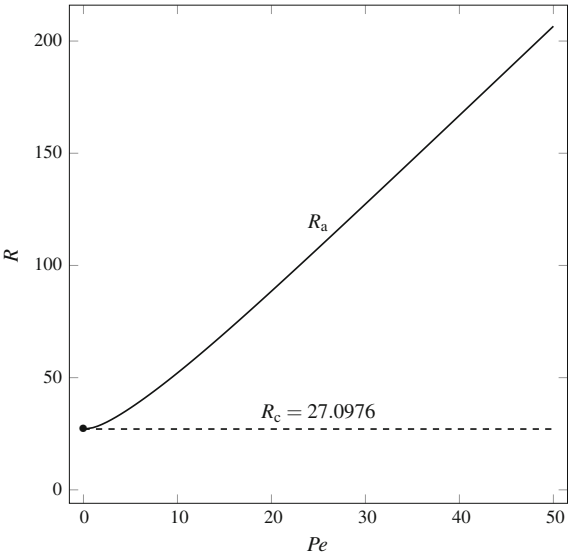

Fig. 9.4 Prats problem with isoflux lower boundary: plot of R_a (solid line) versus Pe, as compared with R_c (dashed line) which is independent of Pe

Equation (9.33) is obtained by substitution of k_0, evaluated for $n = 1$ through Eq. (8.42), as well as of $\xi = R_a/Pe$ given by Eq. (8.43), into Eq. (8.40).

Figure 9.2 shows that the imaginary part of $\sigma\,\lambda(k_0)$ continuously decreases from 0 as Pe increases, for the saddle points with $\Re(k_0) > 0$. The reverse occurs for the twin saddle points having $\Re(k_0) < 0$. The same numerical data over a larger range of Péclet numbers are reported in Fig. 9.3 as plots of $\Im(\sigma\,\lambda(k_0)/Pe)$ versus Pe, in order to illustrate the asymptotic behaviour described by Eqs. (9.27) and (9.33). We note that both $\Im(\sigma\,\lambda(k_0))$ and Pe tend to zero when $Pe \to 0$, while their ratio tends to a finite limit. This finite limiting value can be easily determined on the basis of Eq. (9.15) and on the equalities $k_0 = \pm k_c$, $R_a = R_c$, for $Pe \to 0$. In fact, we reckon that $\Im(\sigma\,\lambda(k_0)/Pe) = \Im(\sigma\,\lambda(\pm k_c)/Pe)$ tends to $\mp k_c = \mp 2.32621$.

The trend of the threshold value R_a for the onset of absolute instability is displayed in Fig. 9.4 as a function of Pe. The critical value R_c is shown for comparison as a dashed line. This figure clearly displays the asymptotic linear trend of R_a versus Pe when $Pe \gg 1$. A neat view of the asymptotic behaviour of R_a/Pe expressed by Eq. (8.43) is shown in Fig. 9.5, where the asymptote, $\xi = R_a/Pe \approx 3.99084$, is drawn as a dotted line. A comparison between Figs. 8.5 and 9.5 is useful. The differences are hardly discernible when $Pe > 10$. This observation is congruent with our previous findings regarding the poor influence on the transition to absolute instability of the thermal boundary condition at the lower boundary, when the horizontal through flow becomes more and more intense.

Figure 9.6 shows the isolines of $\Re(\sigma\,\lambda)$ in the complex k plane for the test case with $Pe = 20$ and $R = R_a = 88.5310$. This map of the lines $\Re(\lambda) = \lambda_r = \text{constant}$ serves as a check of the holomorphy requirement. The paths of steepest descent crossing the saddle points,

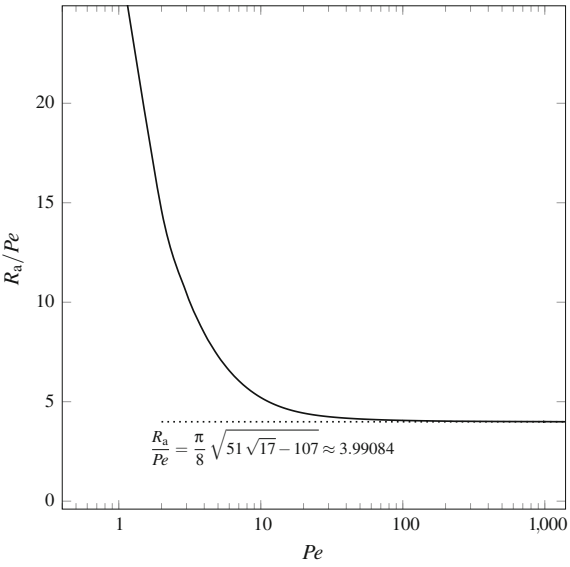

Fig. 9.5 Prats problem with isoflux lower boundary: plot of R_a/Pe (solid line) versus Pe, as compared with its asymptotic value $\xi = R_a/Pe \approx 3.99084$ (dotted line)

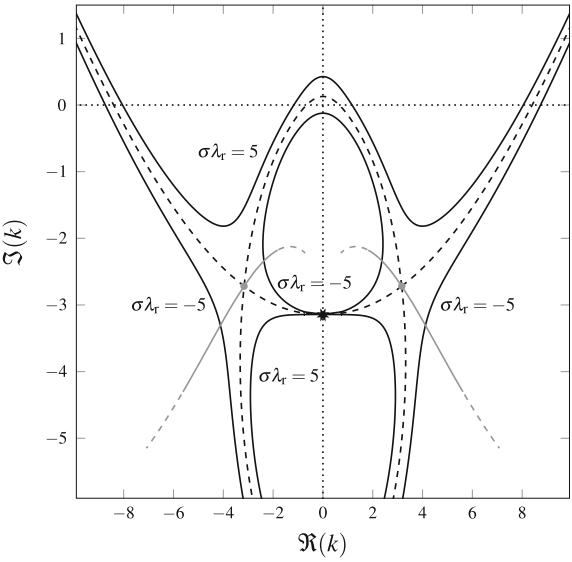

Fig. 9.6 Prats problem with isoflux lower boundary: map of the isolines of $\Re(\lambda) = \lambda_r$ (black solid lines) for $Pe = 20$ and $R = R_a = 88.5310$. The dashed black lines are for $\lambda_r = 0$. The grey dots are the saddle points, while the grey lines are the lines of steepest descent. The black asterisk denotes the singularity $k = -i\,\pi$

$$k_0 = \pm 3.16611 - i\,2.71779\,, \tag{9.34}$$

are drawn in this figure as grey lines. The lines of steepest descent are isolines of $\Im(\lambda)$. In this sample case, they correspond to $\Im(\sigma\,\lambda) = \mp 78.8420$. The map reported in Fig. 9.6 shows that, in fact, there exists a path, locally of steepest descent across the twin saddle points given by Eq. (9.34), that does not trap any singularity of $\Re(\lambda)$

in the region between such path and the real line $\Im(k) = 0$. A singularity is displayed at $k = -\mathrm{i}\,\pi$, thus marking a close analogy to the otherwise only qualitatively similar map reported in Fig. 8.3. The occurrence of such singularity was proved analytically for the Prats problem with isothermal lower boundary, as shown in Sect. 8.2.4. In the case examined in Fig. 9.6, the singularity at $k = -\mathrm{i}\,\pi$ emerges as an upshot of the numerical solution.

9.2 Thermal Instability in a Vertical Porous Channel

Up to this point, we have always investigated cases where the instability was driven by a mechanism of heating from below. However, there are situations such that the instability may occur even in a vertical porous layer, where the basic temperature gradient is the result of side heating.

A fairly simple example was proposed and analysed by Barletta [1]. In this paper, the study is focussed on the convective instability. In Barletta [1], the aim is to show that the classical proof presented by Gill [3] cannot be extended to the case where the porous layer is bounded by permeable planes instead of impermeable walls. The forthcoming analysis involves a situation where, unlike the cases examined by Gill [3] and Barletta [1], a vertical forced flow is present. This variant discloses the possibility of a transition from convective to absolute instability.

9.2.1 Problem Formulation

Let us consider a vertical porous slab bounded by two vertical and permeable planes at $x = \pm L/2$, kept at uniform temperatures T_1 and $T_2 < T_1$, respectively. We note that the generality of our analysis is not influenced in any way by the choice $T_2 < T_1$, as there is no physical difference between the left and right boundaries. On the other hand, when dealing with horizontal layers, it is quite evident that the direction of gravity makes a big physical difference between the lower boundary and the upper boundary.

A sketch of the vertical porous layer, of the coordinate frame and of the boundary conditions is given in Fig. 9.7. The permeable boundaries allow a perfect mechanical and thermal contact with external fluid reservoirs at temperatures T_1 and T_2. Therefore, the boundary pressure at $x = \pm L/2$ is imposed externally. More precisely, we assume that the boundary conditions allow an externally forced pressure gradient, $\partial P/\partial z$, along the vertical z-axis. Such gradient is considered as constant. We recall that P denotes the local difference between the fluid pressure and hydrostatic pressure.

According to all the previous examples, the x and y axes are horizontal with the x-axis perpendicular to the bounding planes, while the z-axis is vertical and upward oriented. We adopt a two-dimensional formulation with all the fields being invariant along the y-direction.

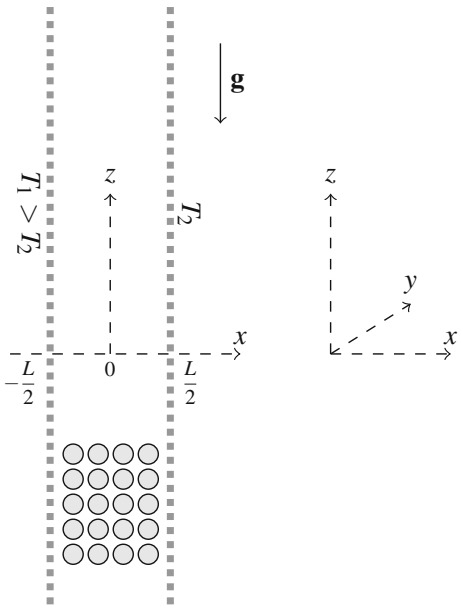

Fig. 9.7 A sketch of the vertical porous layer with permeable boundaries, of the (x, y, z) coordinate frame and of the boundary conditions

We adopt the Oberbeck–Boussinesq approximation and Darcy's law, together with the assumption of a negligible viscous dissipation. Thus, we arrange the dimensionless local balance of mass, momentum and energy in the pressure/temperature formulation according to the two-dimensional version of Eq. (8.79), namely

$$\frac{\partial^2 P}{\partial x^2} + \frac{\partial^2 P}{\partial z^2} - R\,\frac{\partial T}{\partial z} = 0\,,$$

$$\sigma\,\frac{\partial T}{\partial t} - \frac{\partial P}{\partial x}\,\frac{\partial T}{\partial x} - \left[\frac{\partial P}{\partial z} - R\,(T - r)\right]\frac{\partial T}{\partial z} = \frac{\partial^2 T}{\partial x^2} + \frac{\partial^2 T}{\partial z^2}\,, \tag{9.35}$$

where $r = (T_0 - T_2)/(T_1 - T_2)$ is the temperature ratio depending on the choice of the reference temperature, T_0, already introduced in Sect. 8.4, while the dimensionless quantities are scaled as defined by Eqs. (8.1) and (8.80). The Darcy–Rayleigh number, R, is given by Eq. (8.3).

We note that the dimensionless velocity components along the x and z directions are expressed through Darcy's law as

$$u = -\frac{\partial P}{\partial x}\,, \quad w = -\frac{\partial P}{\partial z} + R\,(T - r)\,. \tag{9.36}$$

The boundary conditions are expressed in a dimensionless form as

$$x = -\frac{1}{2}\ : \qquad \frac{\partial P}{\partial z} = -Pe\,, \quad T = 1\,,$$

$$x = \frac{1}{2} \; : \qquad \frac{\partial P}{\partial z} = -Pe \; , \quad T = 0 \; , \tag{9.37}$$

where Pe is the Péclet number associated with the externally forced pressure gradient along the z direction.

9.2.2 The Basic Solution

A stationary solution of Eqs. (9.35) and (9.37) is given by

$$\frac{\partial P_\mathrm{b}}{\partial x} = 0 \; , \quad \frac{\partial P_\mathrm{b}}{\partial z} = -Pe \; , \quad T_\mathrm{b} = \frac{1}{2} - x \; , \tag{9.38}$$

thus describing a vertical flow,

$$u_\mathrm{b} = 0 \; , \quad w_\mathrm{b} = Pe + R \left(\frac{1}{2} - r - x \right) \; , \tag{9.39}$$

where Eqs. (9.36) and (9.38) have been taken into account. The resulting vertical flow is the superposition of an externally forced uniform flow parametrised by the Péclet number, Pe, and a buoyancy-induced flow given by an x dependent linear velocity profile. The latter term depends on both R and r. We note that the net flow rate associated with the basic flow velocity, w_b, is given by

$$\int_{-1/2}^{1/2} w_\mathrm{b} \, \mathrm{d}x = Pe + R \left(\frac{1}{2} - r \right) \; . \tag{9.40}$$

Hence, there is a special value of r such that the buoyant flow term, proportional to R, yields a vanishing contribution to the net flow rate. This special value is $r = (T_0 - T_2)/(T_1 - T_2) = 1/2$ which, in dimensional terms, means a special choice of the reference temperature, i.e. $T_0 = (T_1 + T_2)/2$, the arithmetic mean of the two boundary temperatures, T_1 and T_2.

9.2.3 Stability Analysis

Small perturbations of the basic state (9.39) are defined as

$$P = P_\mathrm{b} + \varepsilon \, \Pi \; , \qquad T = T_\mathrm{b} + \varepsilon \, \Theta \; . \tag{9.41}$$

We substitute Eq. (9.41) into Eqs. (9.35) and (9.37) and neglect terms $O(\varepsilon^2)$. We thus obtain the governing equations for the perturbations,

$$\frac{\partial^2 \Pi}{\partial x^2} + \frac{\partial^2 \Pi}{\partial z^2} - R\,\frac{\partial \Theta}{\partial z} = 0\,,$$

$$\sigma\,\frac{\partial \Theta}{\partial t} + \frac{\partial \Pi}{\partial x} + \left[Pe + R\left(\frac{1}{2} - r - x\right)\right]\frac{\partial \Theta}{\partial z} = \frac{\partial^2 \Theta}{\partial x^2} + \frac{\partial^2 \Theta}{\partial z^2}\,, \tag{9.42}$$

with the boundary conditions

$$x = \pm\frac{1}{2} \;:\quad \frac{\partial \Pi}{\partial z} = 0\,, \quad \Theta = 0\,. \tag{9.43}$$

Equations (9.42) and (9.43) imply that the evolution of perturbations is influenced by the parameter r. This fact marks a deep difference with respect to what happens for the case of a horizontal channel, as pointed out in Sect. 8.4. In other words, for a vertical channel, the choice of the reference temperature T_0 in the formulation of the Oberbeck–Boussinesq approximation matters. One can adopt a twofold approach to this issue:

- Make a mindful choice of T_0 so that the first-order Taylor series expansion of $\rho(T)$, given by Eq. (5.57), is best satisfied. This choice is one where $\rho(T_0)$ is the average density of the fluid or, equivalently, T_0 is the average temperature. Thus, having in mind the base solution (9.38), T_0 is to be chosen as the arithmetic mean of the two boundary temperatures, T_1 and T_2, namely $T_0 = (T_1 + T_2)/2$. This implies that the parameter $r = (T_0 - T_2)/(T_1 - T_2)$ be equal to $1/2$.
- Rescale the Péclet number as

$$Pe^* = Pe + R\left(\frac{1}{2} - r\right)\,. \tag{9.44}$$

  By employing the scaled Péclet number, Pe^*, instead of Pe in Eqs. (9.42) and (9.43), the stability analysis becomes formally independent of r. This option does not imply any specific choice of T_0. On the other hand, this means a redefinition of the Péclet number so that it express the net flow rate along the channel, Pe^*, and not the strength of the vertical pressure gradient, Pe.

Whatever option is chosen, the stability analysis is just the same, being based on the differential problem

$$\frac{\partial^2 \Pi}{\partial x^2} + \frac{\partial^2 \Pi}{\partial z^2} - R\,\frac{\partial \Theta}{\partial z} = 0\,,$$

$$\sigma\,\frac{\partial \Theta}{\partial t} + \frac{\partial \Pi}{\partial x} + (Pe - R\,x)\,\frac{\partial \Theta}{\partial z} = \frac{\partial^2 \Theta}{\partial x^2} + \frac{\partial^2 \Theta}{\partial z^2}\,,$$

$$x = \pm\frac{1}{2} \; : \qquad \frac{\partial \Pi}{\partial z} = 0 \; , \quad \Theta = 0 \; . \tag{9.45}$$

Here, Pe denotes either the Péclet number with $r = 1/2$, or the scaled Péclet number (the asterisk is omitted for simplicity of notation), defined by Eq. (9.44), if we adopt the strategy of not fixing the value of r.

On seeking a solution for Eqs. (9.43) and (9.45) in terms of Fourier transforms, we take into account that the flow direction is the z-axis, so that we define

$$\tilde{\Pi}(k,x,t) = \frac{1}{\sqrt{2\pi}} \int_{-\infty}^{\infty} e^{-\mathrm{i}\,k\,z}\, \Pi(x,z,t)\, \mathrm{d}\,z \; ,$$

$$\Pi(x,z,t) = \frac{1}{\sqrt{2\pi}} \int_{-\infty}^{\infty} e^{\mathrm{i}\,k\,z}\, \tilde{\Pi}(k,x,t)\, \mathrm{d}\,k \; ,$$

$$\tilde{\Theta}(k,x,t) = \frac{1}{\sqrt{2\pi}} \int_{-\infty}^{\infty} e^{-\mathrm{i}\,k\,z}\, \Theta(x,z,t)\, \mathrm{d}\,z \; ,$$

$$\Theta(x,z,t) = \frac{1}{\sqrt{2\pi}} \int_{-\infty}^{\infty} e^{\mathrm{i}\,k\,z}\, \tilde{\Theta}(k,z,t)\, \mathrm{d}\,k \; , \tag{9.46}$$

where the dependence on t of $\tilde{\Pi}$ and $\tilde{\Theta}$ is factored out through exponential terms, namely

$$\tilde{\Pi} = f(x)\, \mathrm{e}^{\lambda(k)\,t} \; , \qquad \tilde{\Theta} = h(x)\, \mathrm{e}^{\lambda(k)\,t} \; . \tag{9.47}$$

By employing Eqs. (9.46) and (9.47), the Fourier transformed Eqs. (9.43) and (9.45) yield

$$\left(\frac{\mathrm{d}^2}{\mathrm{d}\,x^2} - k^2 \right) f - \mathrm{i}\,k\,R\,h = 0 \; ,$$

$$\left[\frac{\mathrm{d}^2}{\mathrm{d}\,x^2} - k^2 - \sigma\,\lambda(k) - \mathrm{i}\,k\,(Pe - R\,x) \right] h - \frac{\mathrm{d}\,f}{\mathrm{d}\,x} = 0 \; ,$$

$$x = \pm\frac{1}{2} \; : \qquad f = 0 \; , \quad h = 0 \; . \tag{9.48}$$

According to the usual procedure, we define the parameter

$$\gamma(k) = \sigma\,\lambda(k) + \mathrm{i}\,k\,Pe \; , \tag{9.49}$$

so that Eq. (9.48) is rewritten as

$$\left(\frac{\mathrm{d}^2}{\mathrm{d}\,x^2} - k^2\right) f - \mathrm{i}\,k\,R\,h = 0\,,$$

$$\left[\frac{\mathrm{d}^2}{\mathrm{d}\,x^2} - k^2 - \gamma(k) + \mathrm{i}\,k\,R\,x\right] h - \frac{\mathrm{d}\,f}{\mathrm{d}\,x} = 0\,,$$

$$x = \pm\frac{1}{2} \;:\quad f = 0\,,\quad h = 0\,. \tag{9.50}$$

9.2.4 Convective Instability

The study of convective instability is based on the eigenvalue problem (9.50). Where we have to set $\Re(\lambda) = 0$ in order to detect the zero growth rate modes, that is the neutrally stable Fourier modes. On account of Eq. (9.49), we have $\Re(\gamma) = 0$. Furthermore, since $\lambda = \eta - \mathrm{i}\,\omega$, we can write $\Im(\gamma) = -\sigma\,\omega + k\,Pe = -\sigma\,\omega_\mathrm{m}$, where ω_m happens to be a modified angular frequency. Hence, Eq. (9.50) reads

$$\left(\frac{\mathrm{d}^2}{\mathrm{d}\,x^2} - k^2\right) f - \mathrm{i}\,k\,R\,h = 0\,,$$

$$\left(\frac{\mathrm{d}^2}{\mathrm{d}\,x^2} - k^2 + \mathrm{i}\,\sigma\,\omega_\mathrm{m} + \mathrm{i}\,k\,R\,x\right) h - \frac{\mathrm{d}\,f}{\mathrm{d}\,x} = 0\,,$$

$$x = \pm\frac{1}{2} \;:\quad f = 0\,,\quad h = 0\,. \tag{9.51}$$

Evidently, $\omega_\mathrm{m} = \omega$ when the forced flow is switched off, i.e. when $Pe = 0$. When $Pe \neq 0$, the forced flow has no explicit influence on the mathematical solution of the eigenvalue problem (9.51) consistently with the $(k, R, \omega_\mathrm{m})$ parametrisation. This means that, if we solve Eq. (9.51) by setting k as input parameter, we can determine numerically the eigenvalue pair (R, ω_m), independently of the Péclet number. This is the reason why the convective instability analysis is influenced by the value of Pe only when it comes to the determination of ω from ω_m. On the other hand, the neutral stability curve in the (k, R) plane is just the same as that drawn for the special case $Pe = 0$, discussed by Barletta [1].

The numerical method described in Chap. 10 is employed to solve the eigenvalue problem (9.51) and thus to obtain the neutral stability function $R(k)$. The additional difficulty with respect to the case discussed in Sect. 9.1 is that, in this case, we do not have a formal proof regarding the principle of exchange of stabilities. In other words, we cannot prove rigorously that $\Im(\gamma) = -\sigma\,\omega_\mathrm{m} = 0$. In fact, this result comes out only through the output data of the numerical solution. The neutrally stable modes for any given k happen to display a zero modified angular frequency. This inductive origin of the result $\Im(\gamma) = -\sigma\,\omega_\mathrm{m} = 0$ implies a complication in the numerical

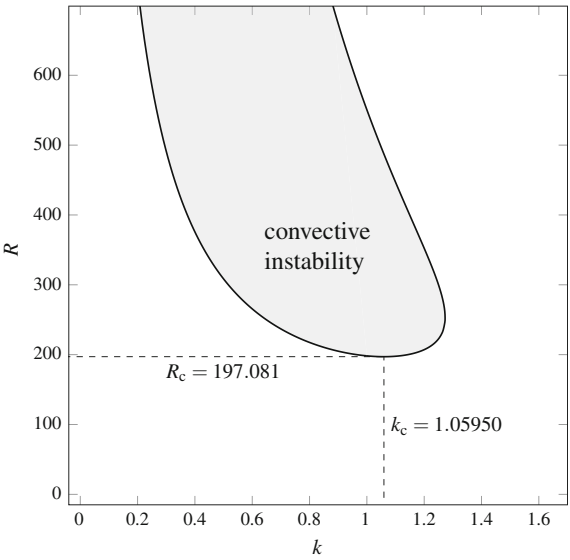

Fig. 9.8 Neutral stability curve for the vertical porous channel with isothermal and permeable boundaries

solution as we have to manage complex-valued eigenfunctions (f, h) and, hence, an effective doubled order for the differential eigenvalue problem to tackle. We have indeed to deal with a fourfold eigenfunction structure, $(\Re(f), \Im(f), \Re(h), \Im(h))$. This means a computationally heavier object to be treated numerically, but no effective difference in the algorithmic framework of the method.

Figure 9.8 displays the neutral stability curve and the convective instability region in the (k, R) plane. The shape of the curve is quite dissimilar from all that we encountered so far in the analysis of instability induced by heating from below. The neutral stability curve is not the plot of a single-valued function $R(k)$, as it happens for the Rayleigh–Bénard problem or the Horton–Rogers–Lapwood problem in their manifold variants. The neutral stability curve for the flow in a vertical porous channel has a droplike shape confining an internal region of convective instability. The point of minimum R along this curve defines the critical values k_c and R_c,

$$k_c = 1.05950\ , \qquad R_c = 197.081\ . \tag{9.52}$$

Another peculiar point along the neutral stability curve is that of maximum k, where

$$k_{max} = 1.27291\ , \qquad R_{max} = 253.340\ . \tag{9.53}$$

There was no such maximum wavelength in all our previous examples of convective instability. Its physical meaning is that Fourier modes with a wave number exceeding the maximum do not contribute to the onset of convective instability. In other terms, such large wavelength modes are ineffective in exciting an unstable response from the flow system. We mention that the numerical data used to draw the neutral

stability curve in Fig. 9.8 displayed values of σ $|\omega_{\mathrm{m}}|$ smaller than 10^{-10}. This provides inductive evidence that ω_{m} is effectively zero or, equivalently, that the relation

$$\omega = \frac{k\,Pe}{\sigma} \tag{9.54}$$

holds true for neutrally stable modes.

9.2.5 *Absolute Instability*

We now focus our analysis on the collective evolution at large times of perturbation wave packets, so that we aim to detect a possible transition from convective to absolute instability in the supercritical domain $R \geqslant R_{\mathrm{c}}$. As usual, the tool adopted to accomplish this task is the steepest-descent approximation of wave packet disturbances. This means starting from Eq. (9.48) in order to implement the saddle point condition $\lambda'(k) = 0$, with $k \in \mathbb{C}$. As in Sect. 9.1.3, we define

$$\hat{f} = \frac{\partial f}{\partial k}\,, \qquad \hat{h} = \frac{\partial h}{\partial k}\,, \tag{9.55}$$

so that the eigenvalue problem (9.48) doubles its differential order through a derivation of the differential equations and boundary conditions with respect to k, namely

$$\left(\frac{\mathrm{d}^2}{\mathrm{d}\,x^2} - k^2\right) f - \mathrm{i}\,k\,R\,h = 0\,,$$

$$\left[\frac{\mathrm{d}^2}{\mathrm{d}\,x^2} - k^2 - \sigma\,\lambda(k) - \mathrm{i}\,k\,(Pe - R\,x)\right] h - \frac{\mathrm{d}\,f}{\mathrm{d}\,x} = 0\,,$$

$$\left(\frac{\mathrm{d}^2}{\mathrm{d}\,x^2} - k^2\right) \hat{f} - \mathrm{i}\,k\,R\,\hat{h} - 2\,k\,f - \mathrm{i}\,R\,h = 0\,,$$

$$\left[\frac{\mathrm{d}^2}{\mathrm{d}\,x^2} - k^2 - \sigma\,\lambda(k) - \mathrm{i}\,k\,(Pe - R\,x)\right] \hat{h} - \frac{\mathrm{d}\,\hat{f}}{\mathrm{d}\,x} - [2\,k + \mathrm{i}\,(Pe - R\,x)]\,h = 0\,,$$

$$x = \pm\frac{1}{2}\ : \qquad f = 0\,, \quad h = 0\,, \quad \hat{f} = 0\,, \quad \hat{h} = 0\,, \tag{9.56}$$

where the condition $\lambda'(k) = 0$ has been taken into account.

The solution of the eigenvalue problem (9.56) is tackled by fixing as input data the values of Pe and $\Re(\sigma\,\lambda)$. In particular, in order to detect the threshold to absolute instability, we set $\Re(\sigma\,\lambda) = 0$. The output eigenvalues sought with the numerical

solution are $(k, R, \Im(\sigma\,\lambda))$. To this end, we employ the shooting method along the same lines discussed in Sect. 9.1.3.

There is a symmetry of the stability eigenvalue problem (9.48) which governs both the onset of convective instability and the transition to absolute instability. In fact, Eq. (9.48) is invariant under the transformation

$$x \to -x\,, \quad k \to -k\,, \quad R \to R\,, \quad Pe \to -Pe\,,$$
$$\lambda \to \lambda\,, \quad f \to -f\,, \quad h \to h\,. \tag{9.57}$$

The symmetry expressed by Eq. (9.57) ensures that the analysis of instability with a negative Péclet effectively means a reversed sign of k, but it does not imply any modification of the threshold values of R either for convective or absolute instability. This is physically not as obvious as for the instability in a horizontal layer. In fact, in the case of a vertical layer, the direction of the propagating disturbances is the vertical z-direction, where the positive or negative z-directions mean parallel or antiparallel directions with respect to gravity.

Further insights into the structure of the eigenvalue problem can be gathered by writing the complex conjugate of Eq. (9.48), namely

$$\left(\frac{\mathrm{d}^2}{\mathrm{d}\,x^2} - \bar{k}^2\right)\bar{f} + \mathrm{i}\,\bar{k}\,R\,\bar{h} = 0\,,$$
$$\left[\frac{\mathrm{d}^2}{\mathrm{d}\,x^2} - \bar{k}^2 - \sigma\,\bar{\lambda} + \mathrm{i}\,\bar{k}\,(Pe - R\,x)\right]\bar{h} - \frac{\mathrm{d}\,\bar{f}}{\mathrm{d}\,x} = 0\,,$$
$$x = \pm\frac{1}{2}\;: \qquad \bar{f} = 0\,, \quad \bar{h} = 0\,, \tag{9.58}$$

where, having in mind the transition to absolute instability, we allowed $k \in \mathbb{C}$. Both Eqs. (9.48) and (9.58) can be equivalently employed for detecting the relevant saddle points. The two eigenvalue problems coincide when we apply the transformation

$$k \to -\bar{k}\,, \quad \lambda \to \bar{\lambda}\,. \tag{9.59}$$

As a consequence, for every prescribed Pe and R, there is a pair of twin saddle points with opposite real parts and equal imaginary parts. Therefore, the values of λ for these twin saddle points have equal real parts and opposite imaginary parts. We reckon that just the same property of the pertinent saddle points for the threshold to absolute instability is implicitly reported in Figs. 9.1 and 9.2, relative to a different example. The existence of twin saddle points with opposite real parts is also displayed in Figs. 8.2 and 8.9. This situation suggests a general feature of the absolute instability analyses, even if a formal proof would require a characterisation of what a stability

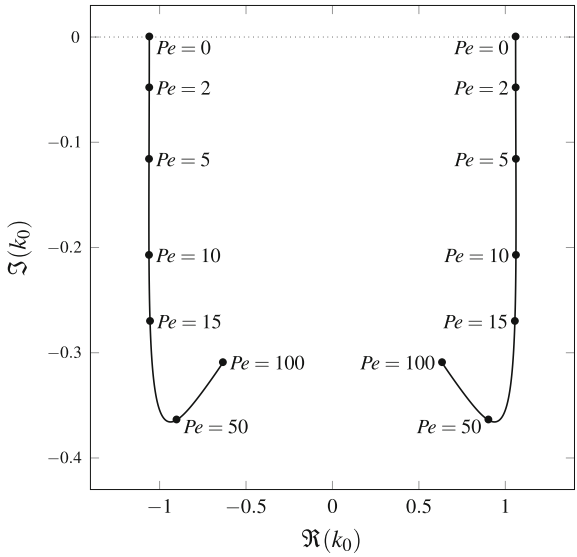

Fig. 9.9 Vertical porous channel with isothermal and permeable boundaries: migration of the pertinent saddle points, with increasing values of Pe, for the threshold to absolute instability

eigenvalue problem is meant to be. We do not aim to solve this formal conundrum here, and we focus again on our specific analysis.

On account of the above-mentioned mathematical properties of the stability eigenvalue problem, with no loss of generality, we will refer our forthcoming analysis to the case $Pe \geqslant 0$. The idea behind the search of the relevant saddle points for the transition to absolute instability is starting from $Pe = 0$ and then gradually increasing Pe. In fact, the case of no net average flow across the channel is one where we already ascertained, although inductively, that the principle of exchange of stabilities holds at neutral stability. Then, the condition of neutral stability is one where $\lambda(k) = 0$, so that we expect $R_a = R_c = 197.081$ and

$$\Re(k_0) = \pm k_c = \pm 1.05950 \,, \quad \Im(k_0) = 0 \,, \quad \Im(\sigma\,\lambda(k_0)) = 0 \,. \tag{9.60}$$

Starting from these data relative to $Pe = 0$, one can track the solution of Eq. (9.56) by gradually increasing Pe above 0. Figure 9.9 shows the migration of the twin saddle points with $Pe > 0$ originated from those given by Eq. (9.60). Figure 9.10 displays the threshold Darcy–Rayleigh number for the transition to absolute instability, R_a, plotted versus Pe and compared with the critical value $R_c = 197.081$. Once more, we see an ever- increasing gap $R_a - R_c$ as Pe increases. Furthermore, Fig. 9.11 displays the trend of $\Im(\sigma\,\lambda(k_0))$ versus Pe. Both Figs. 9.10 and 9.11 reveal some significant similarities with Figs. 9.4 and 9.2, respectively. However, there is an evident difference. The asymptotic regime for $Pe \gg 1$ where both R_a and $\Im(\sigma\,\lambda(k_0))$ are linear functions of Pe, widely discussed in Sect. 9.1.3, turns out to be unsuited to the plots reported in Figs. 9.10 and 9.11.

Another element of discrepancy emerges from Fig. 9.9. This figure appears to be dissimilar from Fig. 9.1 because there is no clue of k_0 attaining an asymptotic

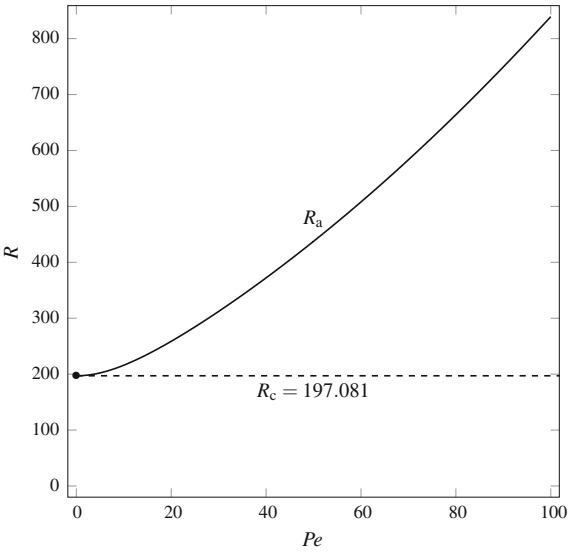

Fig. 9.10 Vertical porous channel with isothermal and permeable boundaries: plot of R_a (solid line) versus Pe, as compared with R_c (dashed line) which is independent of Pe

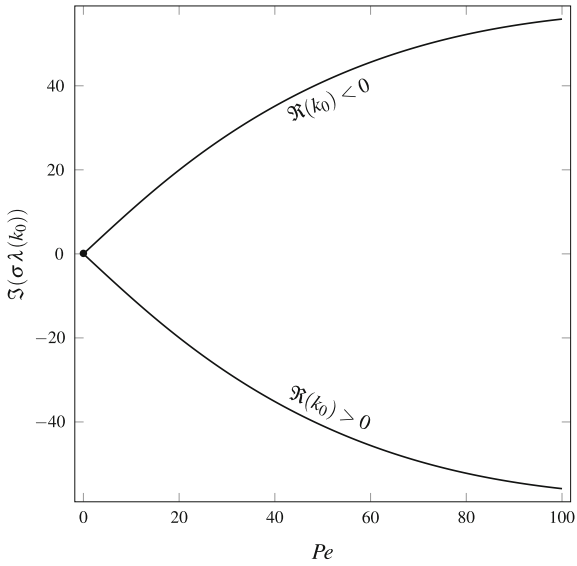

Fig. 9.11 Vertical porous channel with isothermal and permeable boundaries: plot of $\Im(\sigma\,\lambda(k_0))$ versus Pe for the saddle points k_0, at the threshold to absolute instability, with positive or negative $\Re(k_0)$

value for $Pe \to \infty$, despite the very wide range of values of Pe. In fact, we note that $Pe = 100$ is a very large value given that we are dealing with seepage flows in porous media.

An example where the fulfilment of the holomorphy requirement is satisfied is displayed in Fig. 9.12. In this figure, the test case where $Pe = 20$ and $R = R_a = 258.755$. This case corresponds to the threshold to absolute instability. The steepest-

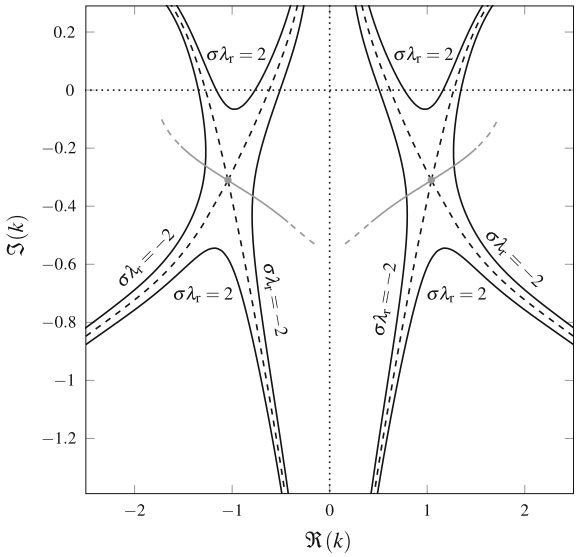

Fig. 9.12 Vertical porous channel with isothermal and permeable boundaries: map of the isolines of $\Re(\lambda) = \lambda_r$ (black solid lines) for $Pe = 20$ and $R = R_a = 258.755$. The dashed black lines are for $\lambda_r = 0$. The grey dots are the saddle points, while the grey lines are the lines of steepest descent

descent paths crossing the twin saddle points,

$$\Re(k_0) = \pm 1.04255\ , \quad \Im(k_0) = -0.311223\ ,$$

$$\Im(\sigma\,\lambda(k_0)) = \mp 19.9514\ , \tag{9.61}$$

are drawn as grey lines. It is evident from Fig. 9.12 that no singularities appear within the region of the k plane around the saddle points. Thus, one can devise a continuous deformation of the real axis, $\Im(k) = 0$, matching locally the steepest-descent paths. In other words, the holomorphy requirement can be considered as satisfied. Just the same conclusions can be drawn by considering Fig. 9.13 relative to the case where $Pe = 50$ and $R = R_a = 437.549$. Again, we are considering a threshold value of R for the onset of absolute instability, with the pertinent saddle points being, in this case,

$$\Re(k_0) = \pm 0.902055\ , \quad \Im(k_0) = -0.363949\ ,$$

$$\Im(\sigma\,\lambda(k_0)) = \mp 40.9155\ . \tag{9.62}$$

Such saddle points are denoted as grey dots in Fig. 9.13. We conclude that, in both the test cases examined in Figs. 9.12 and 9.13, the holomorphy requirement is satisfied.

We recall from Definition 4.2 and Eq. (4.50) that the transition to absolute instability is mathematically associated with a transition from a negative to a positive $\Re(\lambda(k_0))$. In fact, the numerical solution of Eq. (9.56) can be carried out, not only by setting $\Re(\lambda) = 0$, but also by prescribing any negative or positive value of $\Re(\lambda)$. This alternative serves to evaluate R versus Pe corresponding to negative or positive

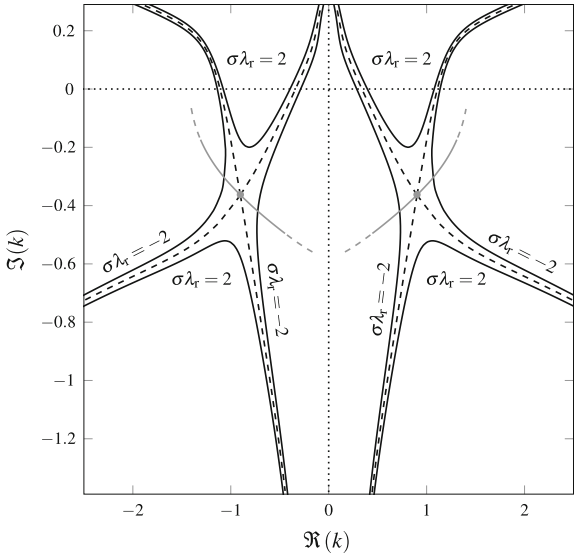

Fig. 9.13 Vertical porous channel with isothermal and permeable boundaries: map of the isolines of $\Re(\lambda) = \lambda_r$ (black solid lines) for $Pe = 50$ and $R = R_a = 437.549$. The dashed black lines are for $\lambda_r = 0$. The grey dots are the saddle points, while the grey lines are the lines of steepest descent

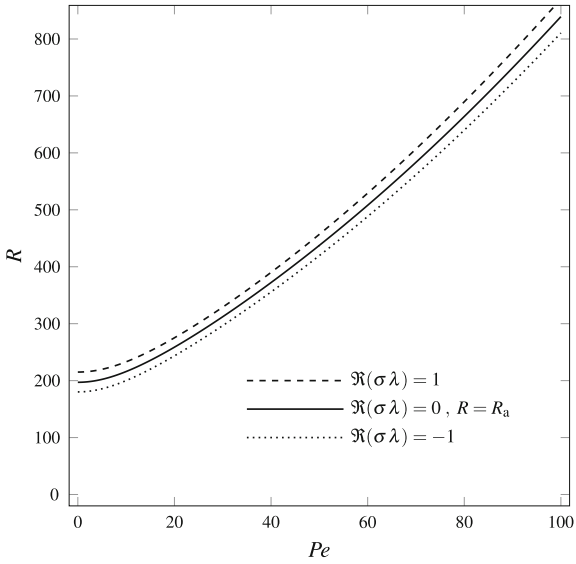

Fig. 9.14 Vertical porous channel with isothermal and permeable boundaries: plot of R_a (solid line) versus Pe, as compared with R versus Pe evaluated for negative and positive growth rates $\Re(\lambda)$ (dotted and dashed lines)

growth rates of the wave packet disturbances. The result is reported in Fig. 9.14 where the solid line showing the trend of R_a versus Pe is displayed together with the dotted line relative to an absolutely stable condition, $\Re(\sigma\,\lambda) = -1$, and the dashed line relative to an absolutely unstable condition, $\Re(\sigma\,\lambda) = 1$. As expected, these plots show that the absolutely unstable case, $\Re(\sigma\,\lambda) = 1$, corresponds to values of R larger than R_a, while the opposite occurs for the absolutely stable case, $\Re(\sigma\,\lambda) = -1$.

9.3 Concluding Remarks Regarding Numerical Solutions

We have seen the numerical method applied to the solution of absolute stability problems. One would have expected some intrinsic extra difficulty emerging when an analytical dispersion relation is not available or when it is too complicated to be practically preferable with respect to a numerical solution. In fact, the treatment of a numerical instance of absolute instability involves the solution of an ordinary differential eigenvalue problem. The order of such eigenvalue problem is doubled if compared with that involved in establishing the convective instability threshold. Moreover, the absolute instability eigenvalue problem involves complex eigenfunctions even if the neutral stability condition requires only real eigenfunctions. However, the algorithm for the numerical solution is not different from that employed for the convective instability analysis. Another important element is that, even when an analytical dispersion relation is available and it is expressed with simple rational functions, as it happens for the Prats problem discussed in Sect. 8.2, the evaluation of the saddle points needs the use of a numerical root-finding procedure. At least, this is what happens in general except for some very special cases. These considerations suggest that some numerical computation within the absolute instability analysis emerges in every case, even when the stability dispersion relation is expressed analytically. Our conclusion is that there is no true additional encumbrance, or limitation in the amount of results that can be gathered, when the stability analysis is to be carried out in a fully numerical framework.

References

1. Barletta A (2015) A proof that convection in a porous vertical slab may be unstable. J Fluid Mech 770:273–288
2. Dongarra JJ, Straughan B, Walker DW (1996) Chebyshev tau-QZ algorithm methods for calculating spectra of hydrodynamic stability problems. Appl Numer Math 22:399–434
3. Gill AE (1969) A proof that convection in a porous vertical slab is stable. J Fluid Mech 35:545–547
4. Prats M (1966) The effect of horizontal fluid flow on thermally induced convection currents in porous mediums. J Geophys Res 71:4835–4838
5. Straughan B, Walker DW (1996) Two very accurate and efficient methods for computing eigenvalues and eigenfunctions in porous convection problems. J Comput Phys 127:128–141

Chapter 10
Numerical Solution of Instability Problems

10.1 Numerical Solution of Instability Problems

There is a wide literature regarding the description of numerical methods for the analysis of the onset of instability in fluid systems. A very interesting analysis of this topic, mainly relative to the tau-method, has been carried out in the paper by Dongarra et al. [4]. A more general and comparative description of different numerical methods is available in the books by Straughan [9, 10]. The purpose of this chapter is to provide the presentation of a specific numerical method aimed to the solution of eigenvalue stability problems, namely the shooting method. This method is formulated to address the convective instability analysis of a flow problem, but it can be employed with little effort also in the solution of absolute instability problems. We describe how the shooting method works, and how it can be implemented within the open-source *Octave* environment [5]. The presentation of the method and of its code will be illustrated by a specific example. The fundamental steps are the reformulation of the differential eigenvalue problem as an initial value problem and the solution of the target conditions at the end of the interval where the eigenvalue problem is defined.

10.2 A Convective Instability Problem

We recall the differential problem defining the Rayleigh–Bénard instability in a horizontal fluid layer bounded by a pair of impermeable, rigid and isothermal boundaries, analysed in detail in Sect. 7.5. This problem is based on Eqs. (7.45)–(7.47), namely

$$\left(\frac{\eta}{Pr} - \frac{\mathrm{d}^2}{\mathrm{d}\,z^2} + k^2\right)\left(\frac{\mathrm{d}^2}{\mathrm{d}\,z^2} - k^2\right) f + Ra\,k^2\,h = 0\,,$$

$$\left(\eta - \frac{\mathrm{d}^2}{\mathrm{d}\,z^2} + k^2\right) h - f = 0\,,$$

A. Barletta, *Routes to Absolute Instability in Porous Media*,
https://doi.org/10.1007/978-3-030-06194-4_10

$$z = 0, 1 : \qquad f = 0 \,, \quad \frac{\mathrm{d}\, f}{\mathrm{d}\, z} = 0 \,, \quad h = 0 \,, \tag{10.1}$$

where we employed the equality $\lambda = \eta$ proved in Sect. 7.5.1. We recall that k, η, Pr and Ra are real parameters. By employing the notation with primes expressing the derivatives with respect to z, Eq. (10.1) can be rewritten as

$$f'''' - \left(2\,k^2 + \frac{\eta}{Pr}\right) f'' + \left(k^2 + \frac{\eta}{Pr}\right) k^2\, f - Ra\, k^2\, h = 0 \,,$$

$$h'' - \left(\eta + k^2\right) h + f = 0 \,,$$

$$z = 0, 1 : \qquad f = 0 \,, \quad f' = 0 \,, \quad h = 0 \,. \tag{10.2}$$

Equation (10.2) defines a real eigenvalue problem, meaning that both f and h are to be considered as real-valued functions. In fact, the ordinary differential equations are linear and homogeneous. The boundary conditions are linear and homogeneous as well. This means that if (f, h) is a solution of Eq. (10.2), then $(C\, f, C\, h)$ is also a solution of Eq. (10.2), for every constant $C \in \mathbb{R}$. In other words, Eq. (10.2) displays a scale invariance. The scale of the solution can be arbitrarily fixed by adding an extra boundary condition, say,

$$h'(0) = 1 \,. \tag{10.3}$$

The combined Eqs. (10.2) and (10.3) display a number of boundary conditions, i.e. seven, larger than the overall order of the differential equations, i.e. six. This circumstance allows one to solve Eqs. (10.2) and (10.3) by evaluating not only the unknowns, (f, h), but also one of the governing parameters $(k,\, Pr,\, Ra,\, \eta)$. In other words, these considerations mean that Eq. (10.2) defines an eigenvalue problem where (f, h) are the eigenfunctions and, say, Ra is the eigenvalue.

10.2.1 The Initial Value Problem

The formulation of the method described in this chapter starts with a reconfiguration of Eq. (10.2) as an initial value problem. In other words, we rewrite Eq. (10.2) as

$$f'''' - \left(2\,k^2 + \frac{\eta}{Pr}\right) f'' + \left(k^2 + \frac{\eta}{Pr}\right) k^2\, f - Ra\, k^2\, h = 0 \,,$$

$$h'' - \left(\eta + k^2\right) h + f = 0 \,,$$

$$f(0) = 0 \,, \quad f'(0) = 0 \,, \quad f''(0) = \xi \,, \quad f'''(0) = \zeta \,,$$

$$h(0) = 0 \,, \quad h'(0) = 1 \,, \tag{10.4}$$

where Eq. (10.3) has been employed, and the governing parameters,

$$\{k,\, Pr,\, Ra,\, \eta, \xi, \zeta\} \ ,$$

are considered as prescribed. In Eq. (10.4), there is a number of initial conditions coincident with the order of the system of differential equations. Thus, the system admits a unique solution, (f, h), for every given set of values of the governing parameters. This statement is grounded on the uniqueness theorem of initial value problems [1–3]. We now subdivide the governing parameters into a set of input parameters, whose value is to be considered known a priori,

$$\text{input parameters} \quad \Longrightarrow \quad \{k,\, Pr,\, \eta\} \ ,$$

and a set of unknown, or output, parameters,

$$\text{output parameters} \quad \Longrightarrow \quad \{Ra, \xi, \zeta\} \ .$$

This subdivision is motivated by having omitted in Eq. (10.4) the target, or end, conditions prescribed at $z = 1$. Such conditions are to be satisfied by the solution (f, h), as specified in Eq. (10.2). The imposed validity of the target conditions completes the shooting method, as it allows one to obtain the output parameters.

10.2.2 The Shooting Method

The target conditions indicated in Eq. (10.2) are

$$f(1) = 0 \ , \quad f'(1) = 0 \ , \quad h(1) = 0 \ . \tag{10.5}$$

In fact, there are three output parameters to be determined through the three equations (10.5).

The evaluation of the parameters $\{\xi, \zeta\}$ provides little interesting information, as these parameters have been introduced just to make the formulation of the initial value problem consistent. On the other hand, determining Ra is precisely the task we want to achieve with our numerical solver.

If we are able to implement the shooting method through a computer code, then we are virtually able to determine the output value Ra for every possible assignment of the input data $\{k,\, Pr,\, \eta\}$. In other terms, we are able to draw on the $(k,\, Ra)$ plane the regions where the growth rate of the normal modes, η, is negative, zero and positive. This means stability, neutral stability and instability, respectively. Obviously, drawing these regions in the $(k,\, Ra)$ plane requires a fixed value of Pr. An exception is the neutral stability curve, $\eta = 0$, that separates the stability and instability regions in the $(k,\, Ra)$ plane. One can immediately check from Eq. (10.2) that this curve is independent of Pr.

10.3 Implementation of the Numerical Solver

In order to build up the numerical code, the first step is transforming the higher-order differential equations given by Eq. (10.4) into a system of six first-order differential equations. This is an easy task if we define a vector function $X_n, n = 1, 2, 3, 4, 5, 6$, such that

$$X_1 = f\ , \quad X_2 = f'\ , \quad X_3 = f''\ , \quad X_4 = f'''\ , \quad X_5 = h\ , \quad X_6 = h'\ . \tag{10.6}$$

From Eq. (10.4), we infer that we need to solve the initial value problem

$$\begin{cases} \dfrac{\mathrm{d}\,X_1}{\mathrm{d}\,t} = X_2\ , \\ \dfrac{\mathrm{d}\,X_2}{\mathrm{d}\,t} = X_3\ , \\ \dfrac{\mathrm{d}\,X_3}{\mathrm{d}\,t} = X_4\ , \\ \dfrac{\mathrm{d}\,X_4}{\mathrm{d}\,t} = \left(2\,k^2 + \dfrac{\eta}{Pr}\right) X_3 - \left(k^2 + \dfrac{\eta}{Pr}\right) k^2\, X_1 + Ra\, k^2\, X_5\ , \\ \dfrac{\mathrm{d}\,X_5}{\mathrm{d}\,t} = X_6\ , \\ \dfrac{\mathrm{d}\,X_6}{\mathrm{d}\,t} = \left(\eta + k^2\right) X_5 - X_1\ , \\ X_1(0) = 0\ , \quad X_2(0) = 0\ , \quad X_3(0) = \xi\ , \\ X_4(0) = \zeta\ , \quad X_5(0) = 0\ , \quad X_6(0) = 1\ . \end{cases} \tag{10.7}$$

Here, we have chosen to denote with t, instead of z, the independent variable. Indeed, this is an unnecessary, but harmless, choice done just to follow the traditional notation for the evolution variable in initial value problems.

We aim to implement the numerical solver of the initial value problem defined in Eq. (10.7) by employing the open-source software *Octave* [5]. For this task, we have to declare a function:

```
function r = f1 (y,k)
NN = 2000;
Pr = 0.7;
eta = 0;
Ra = y(1); xi = y(2); zeta = y(3);
f = @(x, t) [x(2);
        x(3);
        x(4);
        (2*k^2+eta/Pr)*x(3)-(k^2+eta/Pr)*k^2*x(1)+Ra*k^2*x(5);
```

```
          x(6);
          (eta+k^2)*x(5)-x(1)];
  t = linspace (0, 1, NN)';
  lsode_options("absolute tolerance", 1e-16);
  lsode_options("relative tolerance", 1e-15);
  x = lsode (f, [0; 0; xi; zeta; 0; 1], t);
  r(1) = x(NN,1);
  r(2) = x(NN,2);
  r(3) = x(NN,5);
  endfunction
```

The function is called `f1`. It has two input variables, `y` and `k`. The former is an array with three components, corresponding to the constants `Ra`, `xi` and `zeta`. The unknown vector function $X_n(t)$ in the initial value problem given by Eq. (10.7) is denoted in the code through the array `x`, having six components. Within the code that defines function `f1`, we have a nested function definition relative to `f`. Function `f` yields the right-hand sides of the differential equations (10.7).

The variable `t` is defined, through the *Octave* built-in function `linspace`, as a row vector with `NN = 2000` linearly spaced elements in the interval $0 \leqslant t \leqslant 1$. Obviously, the larger is `NN`, the higher is the accuracy and, unavoidably, also the computational time. In the code reported above, we aim to evaluate the neutral stability data, `eta = 0`, which are independent of `Pr`, so that having set the value `0.7` is necessary but ineffective in this case.

The core part for the definition of function `f1` is the assignment of the output of function `lsode` to the variable `x`. The *Octave* built-in function `lsode` returns the solution of the system of first-order differential equations where the derivative of the unknowns functions $X_n(t)$ is equal to the array defined by the elements of `f`, the initial conditions are set to the values given by the array `[0; 0; xi; zeta; 0; 1]`, and the independent variable is the row vector `t`. The name of the built-in function `lsode` comes from the acronym LSODE, which stands for Livermore Solver for Ordinary Differential Equations described by Radhakrishnan and Hindmarsh [7]. This solver was developed by Hindmarsh as a *Fortran* subroutine based on the Adams method for non-stiff problems and the backward differentiation formula (BDF) for stiff problems [7]. The `lsode_options` are used to fix both the `absolute tolerance` and the `relative tolerance` parameters sought by the LSODE. The former parameter is smaller than the latter, with the `relative tolerance` providing a measure of the number of accurate significant figures in the numerical solution [7].

The variable `r` is the output of function `f1`, and its evaluation is the final part of the code where the three components `r(1)`, `r(2)` and `r(3)` are identified with $X_1(1)$, $X_2(1)$ and $X_5(1)$. In fact, the target conditions for the shooting method, expressed through Eq. (10.5), can be reformulated by employing Eq. (10.6) as

$$X_1(1) = 0\,, \quad X_2(1) = 0\,, \quad X_5(1) = 0\,. \tag{10.8}$$

This means that, in the end, `x(NN,1)`, `x(NN,2)` and `x(NN,5)`, that are identified with the three components of the output array `r`, must be zero.

The definition of function `f1` serves only to implement the solution of the initial value problem defined by Eq. (10.7). The second part of the code accomplishes the shooting method and, hence, the determination of Ra, ξ and ζ for given input values of k, Pr and η,

```
fileID1 = fopen(file1,'w');
kk = linspace(kmin,kmax,Nmax);
yy = [1708; 1; -1];
yyold = yy;
options=optimset('MaxIter',1e5,'TolFun',1e-16);
for ll = 1:Nmax
   k = kk(ll);
   yy = fsolve(@(y) f1(y,k),yyold,options);
   yyold = yy;
   format long;
   printf("k = %.15f\n", k);
   printf("Ra = %.15f\n", yy(1));
   fflush(stdout);
   fprintf(fileID1,'( %.10f , %.10f )\n', k, yy(1));
endfor
fclose(file1);
```

The objective is creating a file, named `file1`, where the neutral stability data $Ra(k)$ are stored. Here, the chosen output format for these data is `(k , Ra)`, but one can obviously adapt this format in compliance to the rules of the specific post-processing tool employed for drawing the neutral stability curve. At some point at the beginning of the *Octave* script, one must declare the variable `file1` by specifying the full path of the text output file. This file will contain several strings of data `(k , Ra)`, depending on how many values of `k` are directed to the solver function `f1`. At the beginning of the *Octave* script, one must assign specific values to the variables `kmin`, `kmax` and `Nmax`, say,

```
kmin = 3;
kmax = 6;
Nmax = 100;
```

meaning that we intend to span 100 values of $k \in [3, 6]$. In our code, the 100 points are equally spaced and assigned to the variable `kk` through the built-in function `linspace`. The array `yy` contains our guessed values for the unknown variables `Ra`, `xi`, `zeta`. This array is employed to initialise the variable `yyold`, that is updated at each iteration within the loop statement `for`. The core of the `for` loop statement is the function `fsolve` whose purpose is solving the target conditions given by

Eq. (10.8). This function is based on the *Fortran* subroutine library MINPACK, and it is aimed to solve systems of nonlinear equations [5]. Accuracy options for `fsolve` are assigned through the `optimset` statement and stored in the variable `options`. The first argument of function `fsolve` is an array of variables that is constrained to be zero through the optimisation algorithm. In our case, this array is the output of function `f1`. The three unknowns `Ra`, `xi` and `zeta` are evaluated by `fsolve` on the basis of the guess values assigned to `yyold` and, eventually, they are stored in the variable `yy`. The last code lines within the `for` loop are meant for updating the guess values `yyold` with the output values stored in `yy` and for processing the output instructions. These guess values are those employed in the next iteration, where the wave number `k` shifts to the next one of the `Nmax` values defined through the `linspace` function. The output generated is both visualised in the terminal and written in the text file whose path `file1` is to be assigned at the beginning of the *Octave* script.

Plots of the numerical values of Ra versus k are displayed in Fig. 10.1. Such data are relative to $Pr = 0.7$. This value of Pr influences only the position of the curves with $\eta = \pm 1$, but it does not affect the neutral stability curve, $\eta = 0$. The position of the curves with $\eta = \pm 1$ is consistent with the conclusion that the convective instability region lies above the neutral stability curve, while the region of stability lies below. Just the same qualitative behaviour is inferred through the analytical solution in the case where both boundaries are stress-free, as illustrated in Sect. 7.4.3.

By employing the above-described *Octave* script, one may note that the number of elements `NN`, set to 2000 in our code, yields only minor changes in the numerical results. On the other hand, the value of relative tolerance in the options of `lsode` is very important. The effect of different values assigned to the relative tolerance, given an absolute tolerance of 10^{-18}, is shown in Table 10.1.

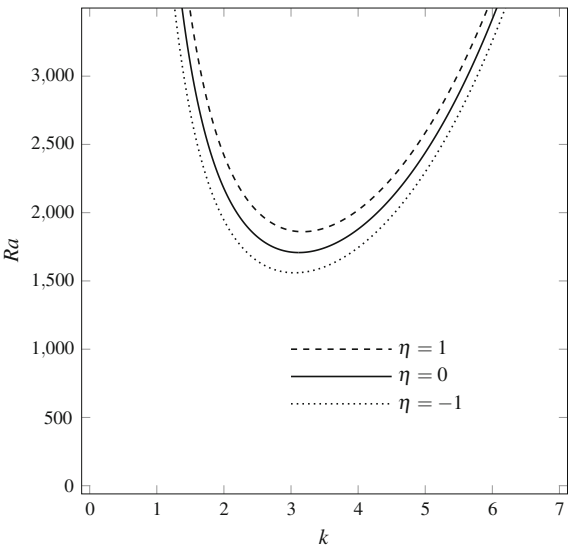

Fig. 10.1 Plots of Ra versus k, relative to the case $Pr = 0.7$, with $\eta = -1$ (stability), $\eta = 0$ (neutral stability), and $\eta = 1$ (convective instability), for the Rayleigh–Bénard problem with rigid and impermeable boundaries, Eq. (10.2)

Table 10.1 Solution of the eigenvalue problem given by Eq. (10.2) with $k = 3$ and $\eta = 0$: effect of a decreasing relative tolerance in the options of `lsode`

Relative tolerance	Ra	ξ	ζ
10^{-4}	1711.15227795	245.510186884	−1561.82037502
10^{-5}	1711.26143906	245.518156714	−1561.87849074
10^{-6}	1711.27597922	245.519402137	−1561.88611575
10^{-10}	1711.27714887	245.519544948	−1561.88677843
10^{-12}	1711.27714905	245.519545013	−1561.88677859
10^{-15}	1711.27714905	245.519545014	−1561.88677859

10.4 Determination of the Critical Values

In order to obtain the critical values k_c and Ra_c, we must detect the point of minimum Ra along the neutral stability curve in the (k, Ra) plane. This means that this point is one where the neutral stability function $Ra(k)$ has a zero derivative. There is a technique that allows one to evaluate directly the critical values k_c and Ra_c. This technique consists in doubling the differential order of the eigenvalue problem to be solved, in our case that defined by Eq. (10.2), by deriving each equation with respect to the wave number k. This technique is described, for instance, in Rees and Bassom [8]. If we consider Eq. (10.2), with $\eta = 0$, we can derive each differential equation and each boundary condition with respect to k, so that we obtain

$$f'''' - 2k^2 f'' + k^4 f - Ra\, k^2 h = 0 ,$$

$$h'' - k^2 h + f = 0 ,$$

$$\hat{f}'''' - 2k^2 \hat{f}'' + k^4 \hat{f} - Ra\, k^2 \hat{h} - 4k f'' + 4k^3 f - 2\, Ra\, k\, h = 0 ,$$

$$\hat{h}'' - k^2 \hat{h} + \hat{f} - 2k h = 0 ,$$

$$z = 0, 1 : \quad \begin{array}{lll} f = 0 , & f' = 0 , & h = 0 , \\ \hat{f} = 0 , & \hat{f}' = 0 , & \hat{h} = 0 . \end{array} \tag{10.9}$$

Here, we denoted with $\hat{f}$ and $\hat{h}$ the functions

$$\hat{f} = \frac{\partial f}{\partial k} , \qquad \hat{h} = \frac{\partial h}{\partial k} . \tag{10.10}$$

There is obviously no term containing $\partial Ra/\partial k$, in the third Eq. (10.9), because we are seeking the minimum of the neutral stability function $Ra(k)$. The solution of Eq. (10.9) allows one to determine the two eigenvalues k and Ra, without any input

parameter to be prescribed. Such eigenvalue pair, (k, Ra), yields in fact the critical values of k and Ra.

The numerical solution follows the procedure described in Sects. 10.2.1, 10.2.2 and 10.3. First, one has to complete the initial conditions in order to match the order of the system of differential equations (10.9),

$$\begin{gathered} f(0) = 0\,, \quad f'(0) = 0\,, \quad f''(0) = \xi\,, \quad f'''(0) = \zeta\,, \\ h(0) = 0\,, \quad h'(0) = 1\,, \\ \hat{f}(0) = 0\,, \quad \hat{f}'(0) = 0\,, \quad \hat{f}''(0) = \hat{\xi}\,, \quad \hat{f}'''(0) = \hat{\zeta}\,, \\ \hat{h}(0) = 0\,, \quad \hat{h}'(0) = 0\,. \end{gathered} \tag{10.11}$$

Here, parameters $\hat{\xi}$ and $\hat{\zeta}$ are defined as

$$\hat{\xi} = \frac{\partial \xi}{\partial k}\,, \qquad \hat{\zeta} = \frac{\partial \zeta}{\partial k}\,. \tag{10.12}$$

The shooting method is meant to determine the six unknown parameters, k, Ra, ξ, ζ, $\hat{\xi}$ and $\hat{\zeta}$, through the six target conditions included in Eq. (10.9), namely

$$\begin{gathered} f(1) = 0\,, \quad f'(1) = 0\,, \quad h(1) = 0\,, \\ \hat{f}(1) = 0\,, \quad \hat{f}'(1) = 0\,, \quad \hat{h}(1) = 0\,. \end{gathered} \tag{10.13}$$

One can easily generalise the *Octave* script described in Sect. 10.3 with reference to the doubled system of differential equations (10.9). The vector function X_n has now twelve components instead of six,

$$\begin{gathered} X_1 = f\,, \quad X_2 = f'\,, \quad X_3 = f''\,, \quad X_4 = f'''\,, \quad X_5 = h\,, \quad X_6 = h'\,, \\ X_7 = \hat{f}\,, \quad X_8 = \hat{f}'\,, \quad X_9 = \hat{f}''\,, \quad X_{10} = \hat{f}'''\,, \quad X_{11} = \hat{h}\,, \quad X_{12} = \hat{h}'\,. \end{gathered} \tag{10.14}$$

Then, function `f1` is defined through the piece of code,

```
function r = f1 (y)
NN = 2000;
k = y(1); Ra = y(2); xi = y(3); zeta = y(4);
xxi = y(5); zzeta = y(6);
f = @(x, t) [x(2);
   x(3);
   x(4);
   2*k^2*x(3)-k^4*x(1)+Ra*k^2*x(5);
   x(6);
```

```
    k^2*x(5)-x(1);
    x(8);
    x(9);
    x(10);
    2*k^2*x(9)-k^4*x(7)+Ra*k^2*x(11)+4*k*x(3) ...
    -4*k^3*x(1)+2*Ra*k*x(5);
    x(12);
    k^2*x(11)-x(7)+2*k*x(5)];
t = linspace (0, 1, NN)';
lsode_options("absolute tolerance", 1e-16);
lsode_options("relative tolerance", 1e-15);
x = lsode (f, [0; 0; xi; zeta; 0; 1; 0; 0; xxi;
zzeta; 0; 0], t);
r(1) = x(NN,1); r(2) = x(NN,2); r(3) = x(NN,5);
r(4) = x(NN,7); r(5) = x(NN,8); r(6) = x(NN,11);
endfunction
```

where we denoted with `xxi` and `zzeta` the variables corresponding to $\hat{\xi}$ and $\hat{\zeta}$. Then, the shooting method to solve the target conditions is coded as

```
yyold = [3; 1708; 1; -1; 1; -1];
options=optimset('MaxIter',1e5,'TolFun',1e-16);
yy = fsolve(@(y) f1(y),yyold,options);
zz = f1(yy);
format long;
printf("kc = %.15f\n", yy(1));
printf("Rac = %.15f\n", yy(2));
fflush(stdout);
```

The guess values for the six unknown parameters, k, Ra, ξ, ζ, $\hat{\xi}$ and $\hat{\zeta}$, are stored in the array `yyold` and determined through the built-in function `fsolve`. Running the *Octave* script yields output values corresponding to the six components of the array `yy`,

$$k_c = 3.11632355482\ , \quad Ra_c = 1707.76177710\ ,$$

$$\xi_c = 257.467534625\ , \quad \zeta_c = -1665.14952033\ ,$$

$$\hat{\xi}_c = 105.475318349\ , \quad \hat{\zeta}_c = -919.577067424\ . \tag{10.15}$$

Since choosing guess values to store in `yy` might have an influence on the accuracy of the solution produced by `fsolve`, we can rerun the script by employing Eq. (10.15) to produce the new guess values. Then, `yyold` is now defined as

```
yyold = [3.11632355482; 1707.76177710; 257.467534625;
-1665.14952033; 105.475318349; -919.577067424];
```

In fact, the output is almost left unchanged, at least within ten of the twelve significant figures reported in Eq. (10.15).

In order to have a comparison with accurate numerical results available in the literature, we can slightly alter our *Octave* script in order to obtain the critical values k_c and Ra_c relative to the case with an impermeable rigid lower boundary and a stress-free upper boundary, where the boundary conditions are given by Eq. (7.48) instead of Eq. (7.47). Glomski and Johnson [6] reported the results

$$\begin{aligned} k_c &= 2.6823217576934142448 4389 \,, \\ Ra_c &= 1100.64960688767678462749 \,. \end{aligned} \tag{10.16}$$

It must be mentioned that many more figures are given by these authors. On the other hand, if we run our *Octave* script, we obtain

$$\begin{aligned} k_c &= 2.68232175769 \,, \\ Ra_c &= 1100.64960689 \,. \end{aligned} \tag{10.17}$$

Within twelve significant figures, the agreement is perfect.

10.5 An Absolute Instability Problem

We now illustrate how the numerical method described in Sects. 10.2–10.4 can be adapted for use with absolute instability problems. To this end, we consider the eigenvalue problem examined in Sect. 9.1.3 and given by Eq. (9.20), namely

$$\begin{gathered} f'' - k^2 f + R k^2 h = 0 \,, \\ h'' - \left[k^2 + \sigma \lambda(k) + \mathrm{i}\, k\, \mathrm{Pe}\right] h + f = 0 \,, \\ \hat{f}'' - k^2 \hat{f} + R k^2 \hat{h} - 2 k f + 2 R k h = 0 \,, \\ \hat{h}'' - \left[k^2 + \sigma \lambda(k) + \mathrm{i}\, k\, \mathrm{Pe}\right] \hat{h} + \hat{f} - (2k + \mathrm{i}\, \mathrm{Pe})\, h = 0 \,, \\ z = 0 : \quad f = 0 \,, \quad h' = 0 \,, \quad \hat{f} = 0 \,, \quad \hat{h}' = 0 \,, \\ z = 1 : \quad f = 0 \,, \quad h = 0 \,, \quad \hat{f} = 0 \,, \quad \hat{h} = 0 \,. \end{gathered} \tag{10.18}$$

The implementation of the shooting method for the solution of the eigenvalue problem (10.18) features an important difference with respect to the analysis made in Sects. 10.2–10.4. In fact, the eigenfunctions $(f, h, \hat{f}, \hat{h})$ are complex-valued. Thus,

we have to consider the real and the imaginary parts of $(f, h, \hat{f}, \hat{h})$, hereafter denoted with "r" and "i" subscripts, so that we must deal with an eight-tuple of real functions, $(f_\mathrm{r}, f_\mathrm{i}, h_\mathrm{r}, h_\mathrm{i}, \hat{f}_\mathrm{r}, \hat{f}_\mathrm{i}, \hat{h}_\mathrm{r}, \hat{h}_\mathrm{i})$.

By separating the real and imaginary parts of the eigenfunctions, and by remembering that both k and λ are complex, we rewrite Eq. (10.18) as

$$
\begin{aligned}
f_\mathrm{r}'' &= \left(k_\mathrm{r}^2 - k_\mathrm{i}^2\right) f_\mathrm{r} - 2\,k_\mathrm{r}\,k_\mathrm{i}\,f_\mathrm{i} - R\left(k_\mathrm{r}^2 - k_\mathrm{i}^2\right) h_\mathrm{r} + 2\,k_\mathrm{r}\,k_\mathrm{i}\,R\,h_\mathrm{i}\,,\\
f_\mathrm{i}'' &= \left(k_\mathrm{r}^2 - k_\mathrm{i}^2\right) f_\mathrm{i} + 2\,k_\mathrm{r}\,k_\mathrm{i}\,f_\mathrm{r} - R\left(k_\mathrm{r}^2 - k_\mathrm{i}^2\right) h_\mathrm{i} - 2\,k_\mathrm{r}\,k_\mathrm{i}\,R\,h_\mathrm{r}\,,\\
h_\mathrm{r}'' &= \left(k_\mathrm{r}^2 - k_\mathrm{i}^2 + s_\mathrm{r} - k_\mathrm{i}\,Pe\right) h_\mathrm{r} - \left(2\,k_\mathrm{r}\,k_\mathrm{i} + s_\mathrm{i} + k_\mathrm{r}\,Pe\right) h_\mathrm{i} - f_\mathrm{r}\,,\\
h_\mathrm{i}'' &= \left(k_\mathrm{r}^2 - k_\mathrm{i}^2 + s_\mathrm{r} - k_\mathrm{i}\,Pe\right) h_\mathrm{i} + \left(2\,k_\mathrm{r}\,k_\mathrm{i} + s_\mathrm{i} + k_\mathrm{r}\,Pe\right) h_\mathrm{r} - f_\mathrm{i}\\
\hat{f}_\mathrm{r}'' &= \left(k_\mathrm{r}^2 - k_\mathrm{i}^2\right) \hat{f}_\mathrm{r} - 2\,k_\mathrm{r}\,k_\mathrm{i}\,\hat{f}_\mathrm{i} - R\left(k_\mathrm{r}^2 - k_\mathrm{i}^2\right) \hat{h}_\mathrm{r} + 2\,k_\mathrm{r}\,k_\mathrm{i}\,R\,\hat{h}_\mathrm{i}\\
&\quad + 2\,k_\mathrm{r}\,f_\mathrm{r} - 2\,k_\mathrm{i}\,f_\mathrm{i} - 2\,R\,k_\mathrm{r}\,h_\mathrm{r} + 2\,R\,k_\mathrm{i}\,h_\mathrm{i}\,,\\
\hat{f}_\mathrm{i}'' &= \left(k_\mathrm{r}^2 - k_\mathrm{i}^2\right) \hat{f}_\mathrm{i} + 2\,k_\mathrm{r}\,k_\mathrm{i}\,\hat{f}_\mathrm{r} - R\left(k_\mathrm{r}^2 - k_\mathrm{i}^2\right) \hat{h}_\mathrm{i} - 2\,k_\mathrm{r}\,k_\mathrm{i}\,R\,\hat{h}_\mathrm{r}\\
&\quad + 2\,k_\mathrm{i}\,f_\mathrm{r} + 2\,k_\mathrm{r}\,f_\mathrm{i} - 2\,R\,k_\mathrm{i}\,h_\mathrm{r} - 2\,R\,k_\mathrm{r}\,h_\mathrm{i}\,,\\
\hat{h}_\mathrm{r}'' &= \left(k_\mathrm{r}^2 - k_\mathrm{i}^2 + s_\mathrm{r} - k_\mathrm{i}\,Pe\right) \hat{h}_\mathrm{r} - \left(2\,k_\mathrm{r}\,k_\mathrm{i} + s_\mathrm{i} + k_\mathrm{r}\,Pe\right) \hat{h}_\mathrm{i} - \hat{f}_\mathrm{r}\\
&\quad + 2\,k_\mathrm{r}\,h_\mathrm{r} - \left(2\,k_\mathrm{i} + Pe\right) h_\mathrm{i}\,,\\
\hat{h}_\mathrm{i}'' &= \left(k_\mathrm{r}^2 - k_\mathrm{i}^2 + s_\mathrm{r} - k_\mathrm{i}\,Pe\right) \hat{h}_\mathrm{i} + \left(2\,k_\mathrm{r}\,k_\mathrm{i} + s_\mathrm{i} + k_\mathrm{r}\,Pe\right) \hat{h}_\mathrm{r} - \hat{f}_\mathrm{i}\\
&\quad + \left(2\,k_\mathrm{i} + Pe\right) h_\mathrm{r} + 2\,k_\mathrm{r}\,h_\mathrm{i}\,,
\end{aligned}
$$

$$
\begin{aligned}
z = 0\ :\quad & f_\mathrm{r} = 0\,,\quad h_\mathrm{r}' = 0\,,\quad \hat{f}_\mathrm{r} = 0\,,\quad \hat{h}_\mathrm{r}' = 0\,,\\
& f_\mathrm{i} = 0\,,\quad h_\mathrm{i}' = 0\,,\quad \hat{f}_\mathrm{i} = 0\,,\quad \hat{h}_\mathrm{i}' = 0\,,\\
z = 1\ :\quad & f_\mathrm{r} = 0\,,\quad h_\mathrm{r} = 0\,,\quad \hat{f}_\mathrm{r} = 0\,,\quad \hat{h}_\mathrm{r} = 0\,,\\
& f_\mathrm{i} = 0\,,\quad h_\mathrm{i} = 0\,,\quad \hat{f}_\mathrm{i} = 0\,,\quad \hat{h}_\mathrm{i} = 0\,.
\end{aligned}
\tag{10.19}
$$

We reconfigure Eq. (10.19) as an initial value problem by completing the conditions prescribed at $z = 0$, namely

$$
f_\mathrm{r}(0) = 0\,,\quad f_\mathrm{r}'(0) = 1\,,\quad f_\mathrm{i}(0) = 0\,,\quad f_\mathrm{i}'(0) = 0\,,
$$

$$
h_\mathrm{r}(0) = \xi_1\,,\quad h_\mathrm{r}'(0) = 0\,,\quad h_\mathrm{i}(0) = \xi_2\,,\quad h_\mathrm{i}'(0) = 0\,,
$$

$$\hat{f}_{\mathrm{r}}(0) = 0\,, \quad \hat{f}'_{\mathrm{r}}(0) = 0\,, \quad \hat{f}_{\mathrm{i}}(0) = 0\,, \quad \hat{f}'_{\mathrm{i}}(0) = 0\,,$$

$$\hat{h}_{\mathrm{r}}(0) = \hat{\xi}_1\,, \quad \hat{h}'_{\mathrm{r}}(0) = 0\,, \quad \hat{h}_{\mathrm{i}}(0) = \hat{\xi}_2\,, \quad \hat{h}'_{\mathrm{i}}(0) = 0\,. \tag{10.20}$$

In Eqs. (10.19) and (10.20), s_{r} and s_{i} denote the real and imaginary parts of $\sigma\ \lambda$, while the parameters $\hat{\xi}_1$ and $\hat{\xi}_2$ are defined as

$$\hat{\xi}_1 = \frac{\partial \xi_1}{\partial k}\,, \qquad \hat{\xi}_2 = \frac{\partial \xi_2}{\partial k}\,. \tag{10.21}$$

We mention that the constraints $f'_{\mathrm{r}}(0) = 1$ and $f'_{\mathrm{i}}(0) = 0$ define the scale fixing condition for the eigenfunctions and, in fact, it can be rewritten as $f'(0) = 1$. We recall that such a condition has been discussed in Sect. 10.2 and formulated in different terms through Eq. (10.3). For every prescribed set of values for the governing parameters,

$$\left\{k_{\mathrm{r}}, k_{\mathrm{i}}, Pe, R, s_{\mathrm{r}}, s_{\mathrm{i}}, \xi_1, \xi_2, \hat{\xi}_1, \hat{\xi}_2\right\}\,, \tag{10.22}$$

there is a unique solution of Eq. (10.19). In fact, the number of initial conditions (10.20) matches the differential order of the system of differential Eqs. (10.19). Our solution strategy is based on the definition of the input data, known a priori,

$$\text{input parameters} \quad \Longrightarrow \quad \{Pe, s_{\mathrm{r}}\}\,,$$

and output data, or unknown parameters,

$$\text{output parameters} \quad \Longrightarrow \quad \left\{k_{\mathrm{r}}, k_{\mathrm{i}}, R, s_{\mathrm{i}}, \xi_1, \xi_2, \hat{\xi}_1, \hat{\xi}_2\right\}\,.$$

The shooting method allows the evaluation of the eight output parameters by adopting a root finding algorithm for the solution of the eight target conditions

$$f_{\mathrm{r}}(1) = 0\,, \quad h_{\mathrm{r}}(1) = 0\,, \quad \hat{f}_{\mathrm{r}}(1) = 0\,, \quad \hat{h}_{\mathrm{r}}(1) = 0\,,$$

$$f_{\mathrm{i}}(1) = 0\,, \quad h_{\mathrm{i}}(1) = 0\,, \quad \hat{f}_{\mathrm{i}}(1) = 0\,, \quad \hat{h}_{\mathrm{i}}(1) = 0\,. \tag{10.23}$$

If the input parameter s_{i} is set equal to 0, the output value of R is expected to yield the threshold value R_{a} for the transition to absolute instability, while k_{r} and k_{i} yield the real and the imaginary parts of the saddle point $k_0 \in \mathbb{C}$. The output values of ξ_1, ξ_2, $\hat{\xi}_1$ and $\hat{\xi}_2$ have no direct physical meaning as they depend on our, arbitrary, choice of the scale fixing conditions, $f'_{\mathrm{r}}(0) = 1$ and $f'_{\mathrm{i}}(0) = 0$.

The implementation of the numerical solver through an *Octave* script follows the approach discussed in Sect. 10.3. We first define the vector function X_n, with $n = 1, 2, \ldots, 16$,

$$X_1 = f_\mathrm{r}\,, \quad X_2 = f_\mathrm{r}'\,, \quad X_3 = f_\mathrm{i}\,, \quad X_4 = f_\mathrm{i}'\,,$$

$$X_5 = h_\mathrm{r}\,, \quad X_6 = h_\mathrm{r}'\,, \quad X_7 = h_\mathrm{i}\,, \quad X_8 = h_\mathrm{i}'\,,$$

$$X_9 = \hat{f}_\mathrm{r}\,, \quad X_{10} = \hat{f}_\mathrm{r}'\,, \quad X_{11} = \hat{f}_\mathrm{i}\,, \quad X_{12} = \hat{f}_\mathrm{i}'\,,$$

$$X_{13} = \hat{h}_\mathrm{r}\,, \quad X_{14} = \hat{h}_\mathrm{r}'\,, \quad X_{15} = \hat{h}_\mathrm{i}\,, \quad X_{16} = \hat{h}_\mathrm{i}'\,. \tag{10.24}$$

Thus, the initial value problem based on Eqs. (10.19) and (10.20) can be rewritten in terms of a system of first-order ordinary differential equations. The core of the *Octave* script is the definition of function `f1` for the numerical solution of the initial value problem,

```
function r = f1 (y,Pe)
NN = 600;
sr = 0;
kr = y(1); ki = y(2); R = y(3); si = y(4);
xi1 = y(5); xi2 = y(6); xxi1 = y(7); xxi2 = y(8);
f = @(x, t) [x(2);
        (kr^2-ki^2)*x(1)-2*kr*ki*x(3)-R*(kr^2- ...
        ki^2)*x(5)+2*kr*ki*R*x(7);
        x(4);
        (kr^2-ki^2)*x(3)+2*kr*ki*x(1)-R*(kr^2- ...
        ki^2)*x(7)-2*kr*ki*R*x(5);
        x(6);
        (kr^2-ki^2+sr-ki*Pe)*x(5)-(2*kr*ki+si+kr*Pe)*x(7)-x(1);
        x(8);
        (kr^2-ki^2+sr-ki*Pe)*x(7)+(2*kr*ki+si+kr*Pe)*x(5)-x(3);
        x(10);
        (kr^2-ki^2)*x(9)-2*kr*ki*x(11)-R*(kr^2- ...
        ki^2)*x(13)+2*kr*ki*R*x(15)+2*kr*x(1)-2*ki*x(3)- ...
        2*R*kr*x(5)+2*R*ki*x(7);
        x(12);
        (kr^2-ki^2)*x(11)+2*kr*ki*x(9)-R*(kr^2- ...
        ki^2)*x(15)-2*kr*ki*R*x(13)+2*ki*x(1)+2*kr*x(3)- ...
        2*R*ki*x(5)-2*R*kr*x(7);
        x(14);
        (kr^2-ki^2+sr-ki*Pe)*x(13)-(2*kr*ki+si+kr*Pe)* ...
        x(15)-x(9)+2*kr*x(5)-(2*ki+Pe)*x(7);
        x(16);
```

```
        (kr^2-ki^2+sr-ki*Pe)*x(15)+(2*kr*ki+si+kr*Pe)* ...
        x(13)-x(11)+(2*ki+Pe)*x(5)+2*kr*x(7)];
t = linspace (0, 1, NN)';
lsode_options("absolute tolerance", 1e-16);
lsode_options("relative tolerance", 1e-15);
x = lsode (f, [0; 1; 0; 0; xi1; 0; xi2; 0; 0; 0; 0; 0; ...
xxi1; 0; xxi2; 0], t);
r(1) = x(NN,1); r(2) = x(NN,3); r(3) = x(NN,5);
r(4) = x(NN,7); r(5) = x(NN,9); r(6) = x(NN,11);
r(7) = x(NN,13); r(8) = x(NN,15);
endfunction
```

We note the use of the newline character "`...`" employed to continue a long statement to the next line. Once more, the independent variable is denoted as `t`, meaning the coordinate z. Such a variable is a row vector with `NN = 600` equally spaced nodes defined through the `linspace` function with `t` ranging from `0` to `1`. Function `f1` depends on the variables `y` and `Pe`, with `y` being an eight components array containing all the output parameters of the shooting method solution,

$$\{k_r, k_i, R, s_i, \xi_1, \xi_2, \hat{\xi}_1, \hat{\xi}_2\} ,$$

where $\hat{\xi}_1$ and $\hat{\xi}_2$ have been denoted as `xxi1` and `xxi2`. The input variable `sr` is set equal to `0` in order to detect the threshold value of `R` for the transition to absolute instability.

The initial conditions given by Eq. (10.20) and coded through the vector function X_n defined in Eq. (10.24), namely the array `x`, are provided as one of the arguments of function `lsode`. The latter is the function providing the numerical solution of the initial value problem obtained through the LSODE solver. The output of the function `f1` is the eight components array `r`. Such array serves to force compliance of the target conditions expressed by Eq. (10.23), by employing the coding given by Eq. (10.24). In the definition of `r`, the components of `x` are evaluated at node `NN`, that is at the end node of the interval, where `t` is equal to `1`. The target conditions expressed by Eq. (10.23) are fulfilled if all components of `r` are as close as possible to zero. This constraint is accomplished by employing function `fsolve` based on the *Fortran* subroutine library MINPACK,

```
fileID1 = fopen(file1,'w');
PP = linspace(Pemin,Pemax,Nmax);
yy = [2.3262145792; 0; 27.0976278778; 0; 1; 0; 1; 0];
yyold = yy;
options=optimset('MaxIter',1e5,'TolFun',1e-16);
for ll = 1:Nmax
   Pe = PP(ll);
   yy = fsolve(@(y) f1(y,Pe),yyold,options);
   zz = f1(yy,Pe);
```

```
    yyold = yy;
    format long;
    printf("Pe = %.15f\n", Pe);
    printf("R = %.15f\n", yy(3));
    fflush(stdout);
    fprintf(fileID1,'%.10f  %.10f  %.10f  %.10f  %.10f\n', ...
    Pe, yy(1), yy(2), yy(3), yy(4));
endfor
fclose(file1);
```

The file named `file1` contains the evaluated output variables `kr`, `ki`, `R` and `si` organised with rows labelled by the Péclet number, `Pe`. The value of `R` is the threshold R_a corresponding to the input `Pe`. The values of `Pe` and `R` are also displayed on the terminal at each iteration of the `for` loop. The loop stops after `Nmax` iterations, where the value of `Nmax` must be previously declared. The interval of Péclet numbers ranging from `Pemin` to `Pemax` must be previously declared as well.

The output data `kr`, `ki`, `R` and `si` are the first four elements of the array `y` employed by function `f1`. Function `fsolve` calls function `f1` in order to evaluate `y` so that the components of `r` are constrained to be zero. Function `fsolve` employs the array `yyold` as a guess for the array `y` to be determined. At each iteration of the `for` loop, the array `yyold` is updated by assigning the values of `y` obtained at the previous iteration. The initialisation is relative to an assumed `Pemin` equal to `0`, with the first four components of `yyold` given by their critical values, as declared in Sect. 9.1.3 on writing Eq. (9.26).

By analogy with Table 10.1, the effect of different relative tolerances for the `lsode` initial value solver is shown in Table 10.2. The output values reported in this table are obtained with an absolute tolerance of 10^{-16}. The test case examined is $Pe = 10$ with $s_r = 0$. Therefore, the values of k_r and k_i are the real and imaginary parts of the saddle point $k_0 \in \mathbb{C}$ pertinent for the transition to absolute instability, while the reported value of R is in fact R_a.

Table 10.2 Solution of the absolute instability eigenvalue problem given by Eq. (10.18) with $Pe = 10$ and $\Re(\sigma\,\lambda) = s_r = 0$: effect of a decreasing relative tolerance in the options of `lsode`

Relative tolerance	k_r	k_i	R	s_i
10^{-4}	3.2102790002	−1.9980466234	52.0998313332	−34.1531641659
10^{-5}	3.2102828920	−1.9980485749	52.0999155514	−34.1531956201
10^{-6}	3.2102845839	−1.9980494229	52.0999521699	−34.1532092950
10^{-10}	3.2102848043	−1.9980495336	52.0999569382	−34.1532110760
10^{-12}	3.2102848043	−1.9980495336	52.0999569391	−34.1532110763
10^{-15}	3.2102848043	−1.9980495336	52.0999569391	−34.1532110763

References

1. Arnold VI (1992) Ordinary differential equations. Springer, Berlin
2. Boyce WE, DiPrima RC (2012) Elementary differential equations and boundary value problems, 10th edn. Wiley, New York
3. Coddington A (1989) An introduction to ordinary differential equations. Dover, New York
4. Dongarra JJ, Straughan B, Walker DW (1996) Chebyshev tau-QZ algorithm methods for calculating spectra of hydrodynamic stability problems. Appl Numer Math 22:399–434
5. Eaton JW, Bateman D, Hauberg S, Wehbring R (2017) GNU octave, a high-level interactive language for numerical computations, 4th edn. www.gnu.org/software/octave/octave.pdf
6. Glomski M, Johnson MA (2012) A precise calculation of the critical Rayleigh number and wave number for the rigid-free Rayleigh-Bénard problem. Appl Math Sci 6:5097–5108
7. Radhakrishnan K, Hindmarsh AC (1993) Description and use of LSODE, the Livermore solver for ordinary differential equations. Lawrence Livermore National Laboratory, Report UCRL-ID-113855
8. Rees DAS, Bassom AP (2000) The onset of Darcy-Bénard convection in an inclined layer heated from below. Acta Mech 144:103–118
9. Straughan B (2004) The energy method, stability, and nonlinear convection, 2nd edn. Springer, New York
10. Straughan B (2008) Stability and wave motion in porous media. Springer, New York

Correction to: Instability of a Flow System

Correction to:
Chapter 4 in: A. Barletta, *Routes to Absolute Instability in Porous Media*,
https://doi.org/10.1007/978-3-030-06194-4_4

The original version of Chap. 4 was inadvertently published with errors in several equations and text that under come Sect. 4.4 which conflict with some of the conclusions. These errors have been corrected and the Fig. 4.9 has also been updated with relation to the corrected equation.

The correction chapter and the book have been updated with the change.

The updated version of this chapter can be found at
https://doi.org/10.1007/978-3-030-06194-4_4

A. Barletta, *Routes to Absolute Instability in Porous Media*,
https://doi.org/10.1007/978-3-030-06194-4_11

Appendix A
Separation of Variables

In this appendix, the separation of variables is illustrated using a couple of sample partial differential equations: the two-dimensional Laplace–Poisson equation and the diffusion equation. Finally, a three-dimensional example is presented and examined in detail.

A.1 Laplace–Poisson Equation

A well-known equation of applied mathematics is the *Laplace–Poisson equation*,

$$\nabla^2 \psi(\mathbf{x}) = q(\mathbf{x}) \,, \qquad \forall \mathbf{x} \in \mathscr{D} \,. \tag{A.1}$$

where ψ is the unknown function and q is a source function, known a priori. Examples of Laplace–Poisson equations in mathematical physics are the equation of the scalar electric potential in steady-state electromagnetism and the local energy balance equation in the theory of stationary heat conduction.

From the mathematical viewpoint, Eq. (A.1) is a second-order elliptic equation. Equation (A.1) is defined in a three-dimensional domain $\mathscr{D} \subseteq \mathbb{R}^3$ with a boundary surface $\partial\mathscr{D}$ where appropriate boundary conditions must be prescribed. Symmetries may be present in the geometry of $\mathscr{D}$, as well as in the form of the boundary conditions, such that the solution ψ of equation (A.1) is subject to an invariance.

For instance, if (x, y, z) is a set of Cartesian coordinates in $\mathscr{D}$, ψ may be invariant for arbitrary translation transformations along the z-direction.

This example suggests that physically significant cases may be reduced to a properly defined two-dimensional domain $\Omega \subseteq \mathbb{R}^2$ with boundary $\partial\Omega$. We will illustrate the separation of the variables with reference to these special cases, i.e. we will focus on the two-dimensional Laplace–Poisson equation, namely

A. Barletta, *Routes to Absolute Instability in Porous Media*,
https://doi.org/10.1007/978-3-030-06194-4

$$\frac{\partial^2 \psi(x,y)}{\partial x^2} + \frac{\partial^2 \psi(x,y)}{\partial y^2} = q(x,y) \; . \tag{A.2}$$

Different kinds of boundary conditions may be defined for the two-dimensional Laplace–Poisson equation. We will consider the Dirichlet, Neumann and Robin boundary conditions.

First Kind or Dirichlet Boundary Conditions

$$\psi(\mathbf{x}) = f(\mathbf{x}) \; , \qquad \forall \mathbf{x} \in \partial\Omega \; , \tag{A.3}$$

where $f(\mathbf{x})$ is any prescribed function defined on $\partial\Omega$.

Second Kind or Neumann Boundary Conditions

$$\frac{\partial \psi(\mathbf{x})}{\partial n} = f(\mathbf{x}) \; , \qquad \forall \mathbf{x} \in \partial\Omega \; , \tag{A.4}$$

where $\partial/\partial n$ is the normal derivative to the boundary line $\partial\Omega$. Usually, the preferred choice for the normal unit vector $\mathbf{n}$ is with the boundary line $\partial\Omega$ having an outward orientation.

Third Kind or Robin Boundary Conditions

$$\frac{\partial \psi(\mathbf{x})}{\partial n} + h\, \psi(\mathbf{x}) = f(\mathbf{x}) \; , \qquad \forall \mathbf{x} \in \partial\Omega \; , \tag{A.5}$$

where h is a prescribed constant parameter.

The adjective "homogeneous" is quite important for the characterisation of a partial differential equation or of its boundary conditions, but what does it mean? A partial differential equation, say the Laplace–Poisson equation, is homogeneous if its source term $q(\mathbf{x})$ vanishes $\forall \mathbf{x} \in \Omega$. In this case, the Laplace–Poisson equation is a linear partial differential equation meaning that any linear combination of two solutions is itself a solution. The boundary conditions given by Eqs. (A.3)–(A.5) are said to be homogeneous when $f(\mathbf{x})$ vanishes $\forall \mathbf{x} \in \partial\Omega$. In this case, the boundary conditions are linear in the same sense as described above.

We are interested in the solution of equation (A.2). We first note that the general solution of this partial differential equation can be expressed as

$$\psi(\mathbf{x}) = \hat{\psi}(\mathbf{x}) + \Psi(\mathbf{x}) \; , \tag{A.6}$$

where $\hat{\psi}(\mathbf{x})$ is a particular solution of equation (A.2), while $\Psi(\mathbf{x})$ is the general solution of the Laplace equation, namely

$$\frac{\partial^2 \Psi(x,y)}{\partial x^2} + \frac{\partial^2 \Psi(x,y)}{\partial y^2} = 0 \; . \tag{A.7}$$

There is no general rule for determining a particular solution of equation (A.2) and, obviously, no need to determine it if the partial differential equation (A.2) is homogeneous, i.e. if $q(\mathbf{x}) = 0$, $\forall \mathbf{x} \in \Omega$. In the homogeneous case, one can set $\hat{\psi}(\mathbf{x}) = 0$, $\forall \mathbf{x} \in \Omega$ and just focus the attention on the determination of $\Psi(\mathbf{x})$. The procedure is as follows:

- Equation (A.7) is linear, so that a linear combination of solutions is itself a solution;
- We choose as basic solutions the "separated" solutions, $\Psi(\mathbf{x}) = A(x)\,B(y)$;
- We combine linearly the separated solutions in order to express the general solution.

Then, we first set

$$\Psi(\mathbf{x}) = A(x)\,B(y)\,, \tag{A.8}$$

and substitute in Eq. (A.7), so that we obtain

$$B(y)\,A''(x) = -A(x)\,B''(y) \quad \Longrightarrow \quad \frac{1}{A(x)}\,A''(x) = -\frac{1}{B(y)}\,B''(y)\,, \tag{A.9}$$

where the primes denote differentiation with respect to the independent variable. In this case, the independent variable is either x or y. We obtain an equation where the left-hand side depends only on x, while the right-hand side depends only on y. Then, there must exist a constant $\lambda \in \mathbb{R}$ such that

$$A''(x) = -\lambda\,A(x)\,, \tag{A.10}$$

$$B''(y) = \lambda\,B(y)\,. \tag{A.11}$$

The separation constant λ is called the *eigenvalue*. It can be either positive, or negative, or zero. Whether λ must be non-negative or non-positive depends on the boundary conditions. This point will become clearer in the following. At this stage, it is not restrictive the assumption $\lambda \geqslant 0$. In this case, we call Eq. (A.10) the *eigenvalue equation* and $A(x)$ the *eigenfunction*.

We will now formulate a theorem without proving it. Among the many treatises on applied mathematics, for a proof of this theorem and a more extensive and rigorous survey of the eigenvalue problems involved in the separation of variables for partial differential equations we refer the reader, for instance, to Section 6.6 of the book by Herman [1].

Theorem A.1 (Sturm–Liouville) *A Sturm–Liouville eigenvalue problem is defined by the second-order differential equation*

$$\left[a(r)\,u'(r)\right]' + \left[b(r) + \lambda\,c(r)\right]u(r) = 0\,,$$

in the interval $r_1 \leqslant r \leqslant r_2$, *and by a pair of boundary conditions at* $r = r_1$ *and* $r = r_2$,

$$h_1\, u(r) + k_1\, u'(r) = 0 \quad \text{in} \quad r = r_1 \ ,$$

$$h_2\, u(r) + k_2\, u'(r) = 0 \quad \text{in} \quad r = r_2 \ ,$$

with prescribed real constants h_1, h_2, k_1 *and* k_2 *. The functions* $a(r)$, $b(r)$ *and* $c(r)$ *are known a priori, real-valued, differentiable and defined on the interval* $[r_1, r_2]$. *We assume that* $a(r) > 0$ *and* $c(r) > 0$ *for every* $r \in [r_1, r_2]$.

The following propositions hold:

- *the Sturm–Liouville eigenvalue problem admits non-trivial solutions only for special values of* λ *called eigenvalues; the corresponding non-trivial solutions are called eigenfunctions;*
- *the eigenvalues are infinite and can be structured in an increasing sequence* $\{\lambda_n\}$*;*
- *eigenfunctions* $u_m(r)$, $u_n(r)$ *corresponding to different eigenvalues* λ_m, λ_n *are orthogonal, meaning that*

$$\int_{r_1}^{r_2} c(r)\, u_m(r)\, u_n(r)\, \mathrm{d}r = 0 \ .$$

In the statement of this theorem, it is assumed that the functions $a(r)$, $b(r)$ and $c(r)$ are such that the second-order differential equation defines a well-posed eigenvalue problem. For instance, this assumption deals with the sign of the functions $a(r)$ and $c(r)$ within the interval $[r_1, r_2]$. In fact, a simple counter-example leading to an ill-posed eigenvalue problem can be obtained by the choice $a(r) = 1$, $b(r) = 0$ and $c(r) = -1$.

The adjective "orthogonal" used in the statement of the Sturm–Liouville theorem suggests that the space of the solutions of an eigenvalue problem can be endowed with an inner product operation as mathematicians do for a vector space. In fact, the inner product operation in a space of functions allows one to define a special kind of infinite-dimensional vector space called *Hilbert space*.

The separation of variables in Eq. (A.7) is allowed if Ω is a rectangle in the (x, y) plane, i.e. if

$$\Omega = [0, L] \times [0, H] \ . \tag{A.12}$$

The boundary of Ω is thus made of four sides

$$x = 0 \ , \quad x = L \ , \quad y = 0 \ , \quad y = H \ .$$

This means four boundary conditions to be prescribed for the solutions ψ of equation (A.2).

Remark A.1 The separation of variables can be applied if the associated Laplace equation (A.7) is endowed with four boundary conditions for Ψ such that not less than three are homogeneous. In fact, in this case, one can write the function Ψ as

$$\Psi(x, y) = \sum_n \eta_n \, A_n(x) \, B_n(y) \ , \tag{A.13}$$

where $A_n(x)$ and $B_n(y)$ are determined, up to an overall multiplicative constant, as solutions of equations (A.10) and (A.11), by employing the three homogeneous boundary conditions. These solutions are found together with suitable eigenvalues λ_n. On the other hand, the coefficients η_n form a sequence which can be determined by employing the inhomogeneous boundary condition.

We mention that the four boundary conditions for Ψ are obtained from those prescribed on ψ when the particular solution $\hat{\psi}$ has been chosen, i.e. by employing

$$\Psi = \psi - \hat{\psi} \ .$$

Then, following Remark A.1, the possibility of applying the separation of variables often depends on how clever was the choice of $\hat{\psi}$.

Remark A.2 In Eqs. (A.10) and (A.11), we can choose $\lambda \geqslant 0$ if the non-homogeneous boundary condition of Ψ is either on $y = 0$ or on $y = H$. We can choose $\lambda \leq 0$ if the non-homogeneous boundary condition of Ψ is either on $x = 0$ or on $x = L$.

Example A.1 We aim to solve the following problem

$$\frac{\partial^2 \psi}{\partial x^2} + \frac{\partial^2 \psi}{\partial y^2} = 1 \ ,$$

in the domain $\Omega = [0, L] \times [0, H]$, with the boundary conditions

$$\psi(0, y) = \psi(L, y) = \psi(x, 0) = \psi(x, H) = 0 \ .$$

We first seek the particular solution of the partial differential equation. Such solution can be conveniently chosen as

$$\hat{\psi}(x, y) = -\frac{1}{2} \, x \, (L - x) \ .$$

Then, the boundary conditions for Ψ are

$$\Psi(0, y) = \Psi(L, y) = 0, \quad \Psi(x, 0) = \Psi(x, H) = \frac{1}{2} \, x \, (L - x) \ .$$

There are two non-homogeneous boundary conditions, so that the separation of variables, according to Remark A.1, cannot be applied. In fact, we can if we first use the *superposition principle*, i.e. if we recognise that

$$\Psi(x, y) = \Psi_1(x, y) + \Psi_2(x, y) \ ,$$

where $\Psi_1(x, y)$ is the solution of

$$\text{Problem 1} \quad \begin{cases} \dfrac{\partial^2 \Psi_1}{\partial x^2} + \dfrac{\partial^2 \Psi_1}{\partial y^2} = 0 \,, \\ \Psi_1(0, y) = \Psi_1(L, y) = 0 \,, \\ \Psi_1(x, 0) = \dfrac{1}{2}\, x\,(L - x) \;\;, \quad \Psi_1(x, H) = 0 \,, \end{cases}$$

and $\Psi_2(x, y)$ is the solution of

$$\text{Problem 2} \quad \begin{cases} \dfrac{\partial^2 \Psi_2}{\partial x^2} + \dfrac{\partial^2 \Psi_2}{\partial y^2} = 0 \,, \\ \Psi_2(0, y) = \Psi_2(L, y) = 0 \,, \\ \Psi_2(x, 0) = 0 \,, \quad \Psi_2(x, H) = \dfrac{1}{2}\, x\,(L - x) \;. \end{cases}$$

One can easily show that

$$\Psi_2(x, y) = \Psi_1(x, H - y) \,, \quad \forall (x, y) \in [0, L] \times [0, H] \,.$$

Then, we have just to solve Problem 1 by the separation of variables. We solve Eq. (A.10) with $\lambda \geqslant 0$. Since the boundary conditions are

$$\Psi_1(0, y) = \Psi_1(L, y) = 0 \,,$$

we conclude that $A_n(0) = A_n(L) = 0$, so that

$$A_n(x) = \sin\left(x\sqrt{\lambda_n}\right) \;,$$

with

$$\sqrt{\lambda_n} = \frac{\pi\, n}{L} \,, \qquad \forall n \in \mathbb{N} \,.$$

We note that the eigenfunctions $A_n(x)$ are defined only up to an arbitrary overall constant scale factor. The functions $B_n(y)$ must be such that $B_n(H) = 0$, in order to satisfy the boundary condition $\Psi_1(x, H) = 0$. Then, by solving Eq. (A.11), we obtain

$$B_n(y) = \sinh\left[\frac{\pi\, n}{L}\,(H - y)\right] \,.$$

By expressing $\Psi_1(x, y)$ as a linear combination of all the products $A_n(x)\, B_n(y)$, we can write

$$\Psi_1(x, y) = \sum_{n=1}^{\infty} \eta_n \, \sin\left(\frac{\pi\, n}{L}\, x\right) \sinh\left[\frac{\pi\, n}{L}\,(H - y)\right] \,.$$

The arbitrary coefficients η_n can be determined by imposing the fourth boundary condition, i.e. the inhomogeneous one,

$$\Psi_1(x,0) = \frac{1}{2}\, x\,(L-x)\ ,$$

$$\frac{1}{2}\, x\,(L-x) = \sum_{n=1}^{\infty} \eta_n\, \sin\!\left(\frac{\pi\, n}{L}\, x\right)\, \sinh\!\left(\frac{\pi\, n\, H}{L}\right)\ .$$

We multiply both sides of this equation by an eigenfunction $A_m(x)$ and integrate with respect to x over the interval $[0, L]$, namely

$$\frac{1}{2} \int_0^L x\,(L-x)\, \sin\!\left(\frac{\pi\, m}{L}\, x\right) \mathrm{d}x$$

$$= \sum_{n=1}^{\infty} \eta_n\, \sinh\!\left(\frac{\pi\, n\, H}{L}\right) \int_0^L \sin\!\left(\frac{\pi\, m}{L}\, x\right)\, \sin\!\left(\frac{\pi\, n}{L}\, x\right) \mathrm{d}x\ .$$

On account of Theorem A.1, we can write the orthogonality condition,

$$\int_0^L \sin\!\left(\frac{\pi\, m}{L}\, x\right)\, \sin\!\left(\frac{\pi\, n}{L}\, x\right) \mathrm{d}x = 0\ , \qquad \forall m \neq n\ .$$

Moreover, one can easily show that

$$\int_0^L x\,(L-x)\, \sin\!\left(\frac{\pi\, m}{L}\, x\right) \mathrm{d}x = \frac{2\,[1-(-1)^m]\, L^3}{m^3 \pi^3}\ ,$$

$$\int_0^L \sin^2\!\left(\frac{\pi\, m}{L}\, x\right) \mathrm{d}x = \frac{L}{2}, \qquad \forall m \in \mathbb{N}\ .$$

We can deduce an expression for the generic η_n, namely

$$\eta_n = 0\ , \quad \forall n \in \mathbb{N}\ ,\ n = \text{even},$$

$$\eta_n = \frac{4\, L^2}{n^3\, \pi^3\, \sinh(\pi\, n\, H/L)}\ , \qquad \forall n \in \mathbb{N}\ ,\ n = \text{odd}\ .$$

The final expression of $\Psi_1(x, y)$ is

$$\Psi_1(x, y) = \sum_{\substack{n \in \mathbb{N} \\ n = \text{odd}}} \frac{4\,L^2}{n^3\,\pi^3\,\sinh(\pi\,n\,H/L)}\,\sin\left(\frac{\pi\,n}{L}\,x\right)\,\sinh\left[\frac{\pi\,n}{L}\,(H-y)\right] .$$

To conclude, the solution of the problem is given by

$$\begin{aligned}\psi(x, y) = &-\frac{1}{2}\,x\,(L-x) \\ &+ \sum_{\substack{n \in \mathbb{N} \\ n = \text{odd}}} \frac{4\,L^2}{n^3\,\pi^3\,\sinh(\pi\,n\,H/L)}\,\sin\left(\frac{\pi\,n}{L}\,x\right)\,\sinh\left[\frac{\pi\,n}{L}\,(H-y)\right] \\ &+ \sum_{\substack{n \in \mathbb{N} \\ n = \text{odd}}} \frac{4\,L^2}{n^3\,\pi^3\,\sinh(\pi\,n\,H/L)}\,\sin\left(\frac{\pi\,n}{L}\,x\right)\,\sinh\left(\frac{\pi\,n}{L}\,y\right) .\end{aligned}$$

A.2 Diffusion Equation

The diffusion equation can be expressed as

$$\nabla^2\psi(\mathbf{x}, t) + q(\mathbf{x}, t) = \frac{\partial\psi(\mathbf{x}, t)}{\partial t} . \tag{A.14}$$

Equation (A.14) is defined in a spatial domain $\mathscr{D} \subseteq \mathbb{R}^3$ with a boundary surface $\partial\mathscr{D}$ and in a time interval $[0, t_0]$.

The solution of Eq. (A.14) is possible if one specifies an initial condition,

$$\psi(\mathbf{x}, 0) = F(\mathbf{x}) , \quad \forall\mathbf{x} \in \mathscr{D} . \tag{A.15}$$

We must also specify boundary conditions that can be of the same kind as that defined for the Laplace–Poisson equation and given by Eqs. (A.3) and (A.5). Equation (A.14) can be solved by expressing the solution $\psi(\mathbf{x}, t)$ as

$$\psi(\mathbf{x}, t) = \hat{\psi}(\mathbf{x}, t) + \Psi(\mathbf{x}, t) , \tag{A.16}$$

where $\hat{\psi}(\mathbf{x}, t)$ is an arbitrarily chosen particular solution of Eq. (A.14), while $\Psi(\mathbf{x}, t)$ is the general solution of the associated homogeneous diffusion equation,

$$\nabla^2\Psi(\mathbf{x}, t) = \frac{\partial\Psi(\mathbf{x}, t)}{\partial t} . \tag{A.17}$$

Since there is no general method to obtain a convenient particular solution of Eq. (A.14), we will focus on the solution of Eq. (A.17) by the separation of variables. We follow the usual procedure. We first express $\Psi(\mathbf{x}, t)$ as the product

$$\Psi(\mathbf{x}, t) = A(\mathbf{x})\, B(t)\ . \tag{A.18}$$

By substituting Eq. (A.18) in Eq. (A.17), we obtain

$$\frac{1}{A(\mathbf{x})}\, \nabla^2 A(\mathbf{x}) = \frac{1}{B(t)}\, B'(t)\ . \tag{A.19}$$

The left-hand side of Eq. (A.19) depends only on $\mathbf{x}$, while the right-hand side depends only on t. Then, there must exist a separation constant such that

$$\nabla^2 A(\mathbf{x}) = -\,\alpha^2\, A(\mathbf{x})\ , \tag{A.20}$$

$$B'(t) = -\,\alpha^2\, B(t)\ . \tag{A.21}$$

In this case, we are not free to choose the sign of the separation constant. We have to choose, in fact, $\alpha^2 \geqslant 0$. The reason is that one of the two ordinary differential equations (A.20) and (A.21), is first order and, as such, it cannot give rise to an eigenvalue problem. Therefore, α^2 is the eigenvalue and $A(\mathbf{x})$ the corresponding eigenfunction.

It is quite important to point out that all this reasoning works well provided that the boundary conditions for $\Psi(\mathbf{x}, t)$ are all homogeneous.

Up to an arbitrary constant factor (that can be considered as part of the eigenfunction, with a proper normalisation), function $B(t)$ can be expressed as

$$B(t) = \mathrm{e}^{-\alpha^2 t}\ . \tag{A.22}$$

Since Eq. (A.17) is linear, any linear combination of solutions is itself a solution. Hence, we can express the general solution of Eq. (A.17) as

$$\Psi(\mathbf{x}, t) = \sum_{n=0}^{\infty} A_n(\mathbf{x})\, \mathrm{e}^{-\alpha_n^2 t}\ , \tag{A.23}$$

where we have assumed an infinite numerable sequence of eigenvalues $\alpha_0^2, \alpha_1^2, \ldots, \alpha_n^2, \ldots$.

Symmetries in the domain $\mathscr{D}$ and in the boundary conditions may imply that the solutions of the eigenvalue equation (A.20) are invariant by translations along two Cartesian axes, say y and z. In this case, the eigenfunctions depend only on x and Eq. (A.20) becomes an ordinary differential equation,

$$A''(x) = -\,\alpha^2\, A(x)\ . \tag{A.24}$$

The solution, provided that $\alpha \neq 0$, is given by

$$A(x) = \eta \cos(\alpha x) + \hat{\eta} \sin(\alpha x) , \tag{A.25}$$

where η and $\hat{\eta}$ are integration constants. As a consequence, Eq. (A.23) can be rewritten as

$$\Psi(x, t) = \sum_{n=0}^{\infty} \left[\eta_n \cos(\alpha_n x) + \hat{\eta}_n \sin(\alpha_n x)\right] \mathrm{e}^{-\alpha_n^2 t} . \tag{A.26}$$

The coefficients η_n and $\hat{\eta}_n$ are determined by employing the initial and boundary conditions.

A.3 On the Separation of Variables in Three Dimensions

The separation of variables is a powerful tool. We have just given some hints to understand what the method is like for the solution of the two-dimensional Laplace–Poisson equation or for the one-dimensional diffusion equation. What happens if we consider the three-dimensional Laplace–Poisson equation? What happens if we have to solve the two-dimensional or three-dimensional diffusion equation?

The general answer is that the method can still be used, but it becomes more complicated. More precisely, we must apply it several times, on separating one variable at a time.

Example A.2 We aim to solve the Laplace equation,

$$\frac{\partial^2 \psi(x, y, z)}{\partial x^2} + \frac{\partial^2 \psi(x, y, z)}{\partial y^2} + \frac{\partial^2 \psi(x, y, z)}{\partial z^2} = 0 ,$$

in the domain $[0, 1] \times [0, 1] \times [0, 1]$ with the six boundary conditions,

$$\psi(0, y, z) = 0 , \quad \psi(1, y, z) = 1 , \tag{A.27}$$

$$\psi(x, 0, z) = 0 , \quad \psi(x, 1, z) = 0 , \tag{A.28}$$

$$\psi(x, y, 0) = 0 , \quad \psi(x, y, 1) = 0 .$$

First of all, we write

$$\psi(x, y, z) = M(x, y)\, C(z) .$$

We substitute in the Laplace equation,

$$\frac{1}{M(x,\,y)}\,\left[\partial^2_{xx}M(x,\,y)+\partial^2_{yy}M(x,\,y)\right]=-\frac{1}{C(z)}\,C''(z)\;.$$

Both sides of this equation must coincide with a positive constant (α^2), so that we can split the equation into a pair of equations

$$\partial^2_{xx}M(x,\,y)+\partial^2_{yy}M(x,\,y)=\alpha^2\,M(x,\,y)\;,$$

$$C''(z)=-\,\alpha^2\,C(z)\;.$$

The boundary conditions $\psi(x,\,y,\,0)=0$ and $\psi(x,\,y,\,1)=0$ allow us to determine the eigenfunctions $C_n(z)$ and the eigenvalues (α_n^2). We obtain

$$C_n(z)=\sin(n\pi z)\;,\quad \alpha_n=n\,\pi\;,\quad n\in\mathbb{N}\;.$$

From the linearity of the Laplace equation, we can express $\psi(x,\,y,\,z)$ as a sum of separated solutions

$$\psi(x,\,y,\,z)=\sum_{n=1}^{\infty}M_n(x,\,y)\,\sin(n\pi z)\;.$$

We go ahead with the separation of variables relative to the partial differential equation,

$$\partial^2_{xx}M_n(x,\,y)+\partial^2_{yy}M_n(x,\,y)=(n\,\pi)^2\,M_n(x,\,y)\;,$$

We express $M_n(x,\,y)$ as a product

$$M_n(x,\,y)=A(x)\,B(y)\;.$$

We substitute in the partial differential equation so that we can write

$$\frac{1}{A(x)}\,A''(x)-(n\,\pi)^2=-\,\frac{1}{B(y)}\,B''(y)\;.$$

We obtained an equation where the left-hand side depends only on x, while the right-hand side depends only on y. Then, there must exist a constant $\mu^2\in\mathbb{R}$ such that

$$A''(x)=\left[\mu^2+(n\,\pi)^2\right]A(x)\;,$$

$$B''(y)=-\,\mu^2\,B(y)\;.$$

The boundary conditions $\psi(x, 0, z) = 0$ and $\psi(x, 1, z) = 0$ allow us to determine the eigenfunctions $B_m(y)$ and the eigenvalues μ_m^2. We obtain

$$B_m(y) = \sin(m\pi y), \quad \mu_m = m\,\pi, \quad m \in \mathbb{N}\,.$$

A solution of the ordinary differential equation for $A(x)$ compatible with the boundary condition $\psi(0, y, z) = 0$ is

$$A_{m,n}(x) = \sinh\left(\pi x\sqrt{m^2 + n^2}\right)\,.$$

Then, we may write

$$M_n(x, y) = \sum_{m=1}^{\infty} \eta_{m,n}\, \sinh\left(\pi x\sqrt{m^2 + n^2}\right) \sin(m\pi y)\,,$$

and, hence,

$$\psi(x, y, z) = \sum_{n=1}^{\infty}\sum_{m=1}^{\infty} \eta_{m,n}\, \sinh\left(\pi x\sqrt{m^2 + n^2}\right) \sin(m\pi y)\, \sin(n\pi z)\,.$$

The coefficients $\eta_{m,n}$ can be determined by imposing the non-homogeneous boundary condition $\psi(1, y, z) = 1$, namely

$$1 = \sum_{n=1}^{\infty}\sum_{m=1}^{\infty} \eta_{m,n}\, \sinh\left(\pi\sqrt{m^2 + n^2}\right) \sin(m\pi y)\, \sin(n\pi z)\,.$$

We multiply both sides of this equation by $\sin(p\pi y)\, \sin(q\pi z)$, where p and q are positive integers, and perform a double integration with respect to y and z in the domain $[0, 1] \times [0, 1]$. Then, we obtain

$$\begin{aligned}
&\int_0^1 \sin(p\pi y)\,\mathrm{d}y \int_0^1 \sin(q\pi z)\,\mathrm{d}z \\
&= \sum_{n=1}^{\infty}\sum_{m=1}^{\infty} \eta_{m,n}\, \sinh\left(\pi\sqrt{m^2 + n^2}\right) \int_0^1 \sin(p\pi y)\, \sin(m\pi y)\,\mathrm{d}y \\
&\qquad \times \int_0^1 \sin(q\pi z)\, \sin(n\pi z)\,\mathrm{d}z\,. \qquad \text{(A.29)}
\end{aligned}$$

Since $B_m(y) = \sin(m\pi y)$ and $C_n(z) = \sin(n\pi z)$ have been obtained by solving Sturm–Liouville eigenvalue problems, Theorem A.1 can be invoked. We can thus

write the orthogonality relationship

$$\int_0^1 \sin(p\pi y)\ \sin(m\pi y)\,\mathrm{d}y = \frac{1}{2}\,\delta_{mp}\ , \qquad \forall m,\, p \in \mathbb{N}\ .$$

Obviously, the result for $m = p$ (or $n = q$) is not a consequence of the Sturm–Liouville theorem, but it comes from a direct evaluation of the integral. Another useful integral formula is

$$\int_0^1 \sin(p\pi y)\,\mathrm{d}y = \frac{1-(-1)^p}{\pi p}\ , \quad \forall p \in \mathbb{N}\ .$$

We thus obtain the coefficients $\eta_{m,n}$,

$$\eta_{m,n} = \frac{4\,[1-(-1)^m]\,[1-(-1)^n]}{\pi^2\, m\, n\, \sinh\left(\pi\sqrt{m^2+n^2}\right)}\ .$$

To conclude, the solution of the problem is given by

$$\psi(x,\,y,\,z) = \frac{16}{\pi^2} \sum_{\substack{n\in\mathbb{N}\\ n=\text{odd}}} \sum_{\substack{m\in\mathbb{N}\\ m=\text{odd}}} \frac{\sinh\left(\pi x\sqrt{m^2+n^2}\right)}{m\, n\, \sinh\left(\pi\sqrt{m^2+n^2}\right)}\ \sin(m\pi y)\ \sin(n\pi z)\ .$$

Reference

[1] Herman RL (2013) A course in mathematical methods for physicists. CRC Press, Boca Raton

Appendix B
An Introduction to Tensors and to Einstein's Notation

For convenience, we denote the Cartesian coordinates as (x_1, x_2, x_3) instead of (x, y, z), and with $\mathbf{e}_1$, $\mathbf{e}_2$ and $\mathbf{e}_3$ the unit vectors along the three Cartesian axes.

Since Einstein's notation is useful when dealing with tensors, it is better to define precisely this concept. A *tensor* A in $\mathbb{R}^3$, where $\mathbb{R}$ is the set of real numbers, is an application,

$$A \,:\, \underbrace{\mathbb{R}^3 \times \mathbb{R}^3 \times \cdots \times \mathbb{R}^3}_{n \text{ times}} \,\rightarrow\, \mathbb{R}\,, \qquad A(\mathbf{u}_1, \mathbf{u}_2, \,\ldots\,, \mathbf{u}_n) \in \mathbb{R}\,, \tag{B.1}$$

that is linear with respect to each of its n arguments.

The linearity of A implies that, if we express the n vectors, $\mathbf{u}_1, \mathbf{u}_2, \,\ldots\,, \mathbf{u}_n$, through their components along the three Cartesian axes,

$$\mathbf{u}_1 = \sum_{i=1}^{3} u_{1i}\,\mathbf{e}_i\,, \quad \mathbf{u}_2 = \sum_{i=1}^{3} u_{2i}\,\mathbf{e}_i\,, \quad \ldots \quad \mathbf{u}_n = \sum_{i=1}^{3} u_{ni}\,\mathbf{e}_i\,, \tag{B.2}$$

the real value of $A(\mathbf{u}_1, \mathbf{u}_2, \,\ldots\,, \mathbf{u}_n)$ can be expressed as

$$A(\mathbf{u}_1, \mathbf{u}_2, \,\ldots\,, \mathbf{u}_n) = \sum_{i_1=1}^{3} \sum_{i_2=1}^{3} \cdots \sum_{i_n=1}^{3} u_{1i_1} u_{2i_2} \cdots u_{ni_n}\, A(\mathbf{e}_{i_1}, \mathbf{e}_{i_2}, \,\ldots\,, \mathbf{e}_{i_n})\,. \tag{B.3}$$

This expression highlights a fundamental aspect of tensors: their action on a n-tuple of vectors is uniquely determined by the numbers

$$A(\mathbf{e}_{i_1}, \mathbf{e}_{i_2}, \,\ldots\,, \mathbf{e}_{i_n}) = A_{i_1 i_2 \ldots i_n}\,. \tag{B.4}$$

This is the reason why a tensor, A, is often identified with an object endowed with n indices, $A_{i_1 i_2 \ldots i_n}$.

A. Barletta, *Routes to Absolute Instability in Porous Media*,
https://doi.org/10.1007/978-3-030-06194-4

The number n is called the *rank* of tensor A. A tensor of rank 1 is regarded as a vector $\mathbf{A}$, such that

$$A(\mathbf{u}) = \sum_{i=1}^{3} u_i \, A(\mathbf{e}_i) = \sum_{i=1}^{3} u_i \, A_i = \mathbf{u} \cdot \mathbf{A} \, . \tag{B.5}$$

In other words, the action of A on an arbitrary vector $\mathbf{u}$ yields the scalar product between $\mathbf{u}$ and $\mathbf{A}$. Similarly, a tensor of rank 2 is identified with a 3×3 matrix A_{ij}.

A quite important tensor of rank 2 is *Kronecker's delta*, δ. It is defined so that

$$\delta(\mathbf{u}, \mathbf{v}) = \mathbf{u} \cdot \mathbf{v} \, , \tag{B.6}$$

for every pair $(\mathbf{u}, \mathbf{v}) \in \mathbb{R}^3 \times \mathbb{R}^3$. As a consequence of its definition, we find out that $\delta_{ij} = 1$ if $i = j$ and $\delta_{ij} = 0$ if $i \neq j$. By definition, Kronecker's delta is a symmetric tensor, meaning that $\delta(\mathbf{u}, \mathbf{v}) = \delta(\mathbf{v}, \mathbf{u})$ or, equivalently, that $\delta_{ij} = \delta_{ji}$.

Another fundamental definition is the *Levi-Civita symbol*. It is a tensor of rank 3 denoted as ε and defined so that

$$\varepsilon(\mathbf{u}, \mathbf{v}, \mathbf{w}) = \mathbf{u} \cdot (\mathbf{v} \times \mathbf{w}) \, . \tag{B.7}$$

Its definition implies that

$$\varepsilon(\mathbf{e}_i, \mathbf{v}, \mathbf{w}) = (\mathbf{v} \times \mathbf{w})_i \, , \tag{B.8}$$

or, formulated differently,

$$(\mathbf{v} \times \mathbf{w})_i = \sum_{j=1}^{3} \sum_{k=1}^{3} \varepsilon_{ijk} \, v_j \, w_k \, . \tag{B.9}$$

From this equation, we obtain an important property of the Levi-Civita symbol $\varepsilon_{ijk} = 1$ if (i, j, k) is equal to $(1, 2, 3)$ or to any even[1] permutation of $(1, 2, 3)$, say $(2, 3, 1)$. Symbol $\varepsilon_{ijk} = -1$ if (i, j, k) is equal to any odd permutation of $(1, 2, 3)$, say $(1, 3, 2)$. Finally, $\varepsilon_{ijk} = 0$ if either $i = j$, or $j = k$, or $i = k$.

Another important property of the Levi-Civita symbol is the possibility to obtain an expression of the determinant of a 3×3 matrix,

$$M = \begin{pmatrix} M_{11} & M_{12} & M_{13} \\ M_{21} & M_{22} & M_{23} \\ M_{31} & M_{32} & M_{33} \end{pmatrix} \, . \tag{B.10}$$

[1] Let us consider the infinite string $123123123123 \cdots$. We call even permutation of $(1, 2, 3)$ any chunk of three neighbouring elements of this string ordered from left to right, namely $(1, 2, 3)$, $(2, 3, 1)$, or $(3, 1, 2)$. On the other hand, an odd permutation of $(1, 2, 3)$ is any chunk of three neighbouring elements of this string ordered from right to left, namely $(3, 2, 1)$, $(1, 3, 2)$, or $(2, 1, 3)$.

Obviously, we can write

$$\begin{aligned}\det(M) = M_{11}\,(M_{22}\,M_{33} - M_{32}\,M_{23}) \\ - M_{12}\,(M_{21}\,M_{33} - M_{31}\,M_{23}) \\ + M_{13}\,(M_{21}\,M_{32} - M_{31}\,M_{22})\ .\end{aligned} \tag{B.11}$$

By denoting the ith row vector of M as

$$\mathbf{M}^{(i)} = (M_{i1}, M_{i2}, M_{i3})\ , \tag{B.12}$$

we can rewrite Eq. (B.11) as

$$\det(M) = \mathbf{M}^{(1)} \cdot \left(\mathbf{M}^{(2)} \times \mathbf{M}^{(3)}\right)\ . \tag{B.13}$$

Therefore, by employing Eqs. (B.7), (B.12) and (B.13), we finally obtain

$$\det(M) = \varepsilon\left(\mathbf{M}^{(1)}, \mathbf{M}^{(2)}, \mathbf{M}^{(3)}\right) = \sum_{i=1}^{3}\sum_{j=1}^{3}\sum_{k=1}^{3} \varepsilon_{ijk}\, M_{1i}\, M_{2j}\, M_{3k}\ . \tag{B.14}$$

A useful tool for managing tensor algebra is *Einstein's notation*. As recalled above, the scalar product between two vectors **a** and **b** is defined as

$$\mathbf{a} \cdot \mathbf{b} = a_1\, b_1 + a_2\, b_2 + a_3\, b_3 = \sum_{i=1}^{3} a_i\, b_i\ . \tag{B.15}$$

We note that the sum over i is evaluated for the three values $i = 1, 2, 3$. This sum is referred to the expression $a_i b_i$ where the index i is repeated. Einstein's idea is a shorthand for such sums widely used in the vector and tensor analysis. The rule is the following: in a vector (or tensor) expression where the index i is repeated, the sum over i is implied. In other words,

$$a_i\, b_i$$

means, according to Einstein's notation,

$$\sum_{i=1}^{3} a_i\, b_i .$$

Obviously, Einstein's shorthand notation can be extended to expressions involving the sum over more than just one index. The convention was introduced by Einstein in 1916 on formulating the general theory of relativity. Later, Albert Einstein used to joke about that: "I have made a great discovery in mathematics; I have suppressed the

summation sign every time that the summation must be made over an index which occurs twice" [2].

Another interesting example, beyond the scalar product between two vectors, is the product of a second-rank tensor, *i.e.* a 3×3 matrix M, and a vector $\mathbf{a}$,

$$(M \cdot \mathbf{a})_i = M_{i1}\, a_1 + M_{i2}\, a_2 + M_{i3}\, a_3 = \sum_{j=1}^{3} M_{ij}\, a_j \ . \tag{B.16}$$

Einstein's notation is, in this case,

$$(M \cdot \mathbf{a})_i = M_{ij}\, a_j \ , \tag{B.17}$$

the sum over the repeated index j being implied.

Einstein's notation can be used also for representing the trace of a second-rank tensor and the divergence of a vector,

$$\mathrm{tr}(M) = M_{11} + M_{22} + M_{33} = \sum_{i=1}^{3} M_{ii} \ \Rightarrow \ \mathrm{tr}(M) = M_{ii} \ , \tag{B.18}$$

$$\boldsymbol{\nabla} \cdot \mathbf{a} = \frac{\partial a_1}{\partial x_1} + \frac{\partial a_2}{\partial x_2} + \frac{\partial a_3}{\partial x_3} = \sum_{i=1}^{3} \frac{\partial a_i}{\partial x_i} \ \Rightarrow \ \boldsymbol{\nabla} \cdot \mathbf{a} = \frac{\partial a_i}{\partial x_i} \ . \tag{B.19}$$

By adopting the Levi-Civita symbol, one can express the vector product,

$$(\mathbf{a} \times \mathbf{b})_i = \varepsilon_{ijk}\, a_j\, b_k \ , \tag{B.20}$$

the curl of a vector

$$(\boldsymbol{\nabla} \times \mathbf{b})_i = \varepsilon_{ijk}\, \frac{\partial b_k}{\partial x_j} \ , \tag{B.21}$$

and the determinant of a 3×3 matrix M,

$$\det(M) = \varepsilon_{ijk}\, M_{1i}\, M_{2j}\, M_{3k} \ . \tag{B.22}$$

There is an important fact about Einstein's notation. Its use is limited to products or to derivatives, so that the sum of the ith component of two vectors $\mathbf{a}$ and $\mathbf{b}$, written as

$$a_i + b_i \ ,$$

does not involve any implicit sum over the repeated index i. This simple fact must be always kept in mind when employing this notation, in order to avoid any possible confusion.

We introduced Kronecker's delta and the Levi-Civita symbol. There are interesting relationships that can be built between these tensors. Starting from the vector identity,

$$(\mathbf{a} \times \mathbf{b}) \cdot (\mathbf{u} \times \mathbf{v}) = (\mathbf{a} \cdot \mathbf{u})(\mathbf{b} \cdot \mathbf{v}) - (\mathbf{a} \cdot \mathbf{v})(\mathbf{b} \cdot \mathbf{u}) \ , \tag{B.23}$$

which can be proved straightforwardly on applying the definitions of scalar product and vector product, we can finally build up a relationship between the Levi-Civita symbol and Kronecker's delta. In fact, we can write

$$\varepsilon_{ijk}\, \varepsilon_{ilm}\, a_j\, b_k\, u_l\, v_m = (\delta_{jl}\, a_j\, u_l)(\delta_{km}\, b_k\, v_m) - (\delta_{jm}\, a_j\, v_m)(\delta_{kl}\, b_k\, u_l) \ , \tag{B.24}$$

and, by factoring the product $a_j\, b_k\, u_l\, v_m$, we obtain the identity

$$\varepsilon_{ijk}\, \varepsilon_{ilm} = \delta_{jl}\, \delta_{km} - \delta_{jm}\, \delta_{kl} \ . \tag{B.25}$$

Another interesting relationship is

$$\varepsilon_{ijk} = \det \begin{pmatrix} \delta_{i1} & \delta_{i2} & \delta_{i3} \\ \delta_{j1} & \delta_{j2} & \delta_{j3} \\ \delta_{k1} & \delta_{k2} & \delta_{k3} \end{pmatrix} = \begin{vmatrix} \delta_{i1} & \delta_{i2} & \delta_{i3} \\ \delta_{j1} & \delta_{j2} & \delta_{j3} \\ \delta_{k1} & \delta_{k2} & \delta_{k3} \end{vmatrix} \ . \tag{B.26}$$

This relationship can be proved by observing that both the left-hand side and the right-hand side are zero when any pair of indices within (i, j, k) are equal, as two rows of the determinant are equal. Moreover, any even permutation of (i, j, k) leaves unchanged both ε_{ijk} and the determinant, while any odd permutation of (i, j, k) changes the sign of both ε_{ijk} and of the determinant. If we apply the relationship to $(i, j, k) = (1, 2, 3)$, we obtain

$$\varepsilon_{123} = \begin{vmatrix} \delta_{11} & \delta_{12} & \delta_{13} \\ \delta_{21} & \delta_{22} & \delta_{23} \\ \delta_{31} & \delta_{32} & \delta_{33} \end{vmatrix} = \begin{vmatrix} 1 & 0 & 0 \\ 0 & 1 & 0 \\ 0 & 0 & 1 \end{vmatrix} = 1 \ , \tag{B.27}$$

and this completes the proof.

An important result of vector analysis is *Gauss' theorem* [1]. This theorem states that, given a vector field $\mathbf{A}$, a finite region V with a regular closed boundary ∂V having a unit outward normal $\mathbf{n}$, then the following equation holds:

$$\iint_{\partial V} \mathbf{A} \cdot \mathbf{n}\, \mathrm{d}S = \iiint_{V} \nabla \cdot \mathbf{A}\, \mathrm{d}V \ , \tag{B.28}$$

where $\mathrm{d}S$ and $\mathrm{d}V$ denote the measure for the surface and volume integrals, respectively. Equation (B.28) can be easily rewritten according to Einstein's notation,

$$\iint_{\partial V} A_j\, n_j\, \mathrm{d}S = \iiint_{V} \frac{\partial A_j}{\partial x_j}\, \mathrm{d}V \ . \tag{B.29}$$

In this form, one can easily extend the validity of Gauss' theorem relative to a tensor field of rank 2,

$$\iint_{\partial V} A_{ij}\, n_j \, \mathrm{d}S = \iiint_V \frac{\partial A_{ij}}{\partial x_j} \, \mathrm{d}V \ , \tag{B.30}$$

or, in general, to a tensor field of rank k,

$$\iint_{\partial V} A_{i_1 i_2 \ldots i_k}\, n_{i_k} \, \mathrm{d}S = \iiint_V \frac{\partial A_{i_1 i_2 \ldots i_k}}{\partial x_{i_k}} \, \mathrm{d}V \ . \tag{B.31}$$

References

[1] Apostol TM (1967) Calculus, vol 2: Multi-variable calculus and linear algebra with applications to differential equations and probability. Wiley, New York

[2] Pais A (2005) Subtle is the lord: The science and the life of Albert Einstein. Oxford University Press, Oxford

Index

A. Barletta, *Routes to Absolute Instability in Porous Media*,
https://doi.org/10.1007/978-3-030-06194-4